Regulation of ARTD1 by SET7/9-dependent Methylation

Dissertation

zur

Erlangung der naturwissenschaftlichen Doktorwürde

(Dr. sc. nat.)

vorgelegt der

Mathematisch-naturwissenschaftlichen Fakultät

der

Universität Zürich

von

Ingrid Kassner

aus

Deutschland

Promotionskomitee

Prof. Dr. Dr. Michael O. Hottiger

(Vorsitz und Leitung der Dissertation)

Prof. Dr. Matthias Peter

Prof. Dr. Alexander Bürkle

Prof. Dr. Primo Schär

Prof. Dr. Massimo Lopes

Zürich 2012

SUMMARY

Proteins are essential structural and functional components of cells and catalyze a multitude of biochemical reactions. Many proteins are subject to post-translational modifications in order to regulate their function and enzymatic activities. ADP-ribosylation of proteins is catalyzed by ADP-ribosyltransferases, which transfer one or more ADP-ribose molecules from their co-substrate NAD^+ to their target proteins. The best-studied mammalian ADP-ribosyltransferase is ARTD1 (also called PARP1), a nuclear enzyme, which binds to and is activated by damaged DNA and poly(ADP-ribosyl)ates itself and other proteins.

SET7/9 is a lysine methyltransferase that was initially identified as a mono-methyltransferase for H3K4, but also methylates many non-histone proteins such as p53 and DNMT1. SET7/9-dependent methylation has variable functional outcomes e.g. protein stabilization or crosstalk with other post-translational modifications.

In this thesis, ARTD1 and the linker histone H1 have been identified as new targets for SET7/9 and the influence of SET7/9 on their cellular functions has been characterized. We found *in vitro* and *in vivo* that SET7/9 methylates ARTD1 at K508. This modification was strongly inhibited by prior poly(ADP-ribosyl)ation of ARTD1, while the methylation did not inhibit the automodification of ARTD1 nor its acetylation by p300. In cells, H_2O_2-induced poly(ADP-ribose) formation was decreased after SET7/9 knockdown and increased after SET7/9 overexpression. Mutation of K508 to arginine reduced the activity of ARTD1 under certain conditions, indicating that direct methylation of ARTD1 by SET7/9 is involved in the regulation of its enzymatic activity.

Furthermore, we showed that SET7/9 methylates several lysine residues (K121, K129, K159, K171, K177 and K192) in the C-terminal domain of linker histone variant H1.4. Mutation of these residues, which are located at the terminal position of six KAK_{me} motifs, did not alter the nuclear distribution of H1.4. The functional consequence of H1 methylation by SET7/9 has to be further elucidated. Finally, we observed that ARTD1-dependent histone modifications shift the substrate specificity of SET7/9 from H3 to H1. This crosstalk supports a role of poly(ADP-ribosyl)ation as an additional component of the histone code.

Taken together, the identification of these two novel SET7/9 target proteins further underlines the important role of SET7/9 during the cellular stress response.

ZUSAMMENFASSUNG

Proteine verleihen Zellen ihre Struktur und Funktion und steuern alle biochemischen Prozesse. Viele Proteine werden posttranslational modifiziert, wodurch ihre Funktion und enzymatische Aktivität reguliert werden. Die ADP-Ribosylierung von Proteinen wird von ADP-Ribosyltransferasen katalysiert, welche ADP-Ribose von ihrem Coenzym NAD^+ auf ihre Zielproteine übertragen. Die bekannteste ist ARTD1 (auch PARP1), ein nukleäres Enzym, welches durch DNA-Schäden aktiviert wird und Polymere aus ADP-Ribose auf sich selbst und andere Proteine überträgt.

SET7/9 wurde ursprünglich als Monomethyltransferase für H3K4 entdeckt, aber methyliert auch Lysine von vielen Nicht-Histon-Proteinen wie p53 und DNMT1. Dies hat unterschiedliche Folgen für die Substrate, z. B. ihre Stabilisierung oder die Beeinflussung von anderen posttranslationalen Modifikationen.

In der vorliegenden Arbeit wurden ARTD1 und das Linkerhiston H1 als neue Substrate für SET7/9 identifiziert und der Einfluss der Methylierung auf deren Funktionen in der Zelle untersucht. Wir fanden *in vitro* und *in vivo*, dass SET7/9 ARTD1 an K508 methyliert. Dies wurde durch vorherige Poly(ADP-Ribosyl)ierung von ARTD1 stark gehemmt, während die Methylierung selbst weder die Automodifikation von ARTD1 noch seine Acetylierung durch p300 verringerte. In Zellen führte SET7/9-Knockdown zu verringerter Synthese von Poly(ADP-Ribose) nach H_2O_2-Behandlung, während SET7/9-Überexpression den gegenteiligen Effekt hatte. Auch Mutation von K508 zu Arginin verringerte die Aktivität von ARTD1 unter bestimmten Bedingungen, was darauf hindeutet, dass die Methylierung durch SET7/9 die enzymatische Aktivität von ARTD1 direkt beeinflusst.

Desweiteren haben wir gezeigt, dass SET7/9 mehrere Lysine (K121, K129, K159, K171, K177 and K192) im C-Terminus der Linkerhiston-Variante H1.4 methyliert. Alle sechs Lysine liegen am Ende der Konsensus-Sequenz KAK_{me} und ihre Mutation verändert die Verteilung von H1.4 im Zellkern nicht. Die genaue Funktion dieser H1-Methylierung muss noch erforscht werden. Interessanterweise methyliert SET7/9 nach ARTD1-abhängigen Histonmodifikationen bevorzugt H1 statt H3, was die Rolle der Poly(ADP-Ribosyl)ierung als Teil des Histoncodes untermauert.

Die Identifikation von zwei neuen SET7/9-Substraten in dieser Dissertation hebt die wichtige Rolle von SET7/9 in zellulären Stressreaktionen hervor.

TABLE OF CONTENTS

ABBREVIATIONS

3-AB	3-aminobenzamide
aa	amino acid(s)
ADP	adenosine diphosphate
AMD	automodification domain
AMP	adenosine monophosphate
AMPK	AMP-activated protein kinase
ARH	ADP-ribosyl hydrolase
ARTD	ADP-ribosyltransferase diphtheria toxin-like
ATP	adenosine triphosphate
bp	base pairs
BER	base excision repair
BRCT	BRCA1 C-terminus
CDK	cyclin-dependent kinase
CIP	calf intestinal alkaline phosphatase
ChIP	chromatin immunoprecipitation
CPT	camptothecin
CTD	carboxy-terminal domain
DAM-TIQ-A	2-dimethylaminomethyl-4H-thieno [2,3-c]isoquinolin-5-one
DAPI	4',6-diamidino-2-phenylindole
DBD	DNA binding domain
DDR	DNA damage response
DNA	deoxyribonucleic acid
DSB	DNA double-strand break
FAD	flavin adenine dinucleotide
GFP	green fluorescent protein
H_2O_2	hydrogen peroxide
HDAC	histone deacteylase
HIF	hypoxia inducible factor
HMG	high mobility group
HR	homologous recombination
IκB	NF-κB inhibitor
IKK	IκB kinase

IR	ionizing radiation
JmjC	Jumonji-C
KMT	lysine methyl transferase
LPS	lipopolysaccharide
LSD	lysine specific demethylase
MLFs	mouse lung fibroblasts
MMS	methyl methanesulfonate
NAD^+	nicotinamide adenine dinucleotide
NF-κB	nuclear factor κB
NTD	amino-terminal domain
PAR	poly(ADP-ribose)
PARG	poly(ADP-ribose) glycohydrolase
PARP	poly(ADP-ribose) polymerase
PARylation	poly(ADP-ribosyl)ation
PRMT	arginine methyl transferase
SAH	S-adenosyl homocysteine
SAM	S-adenosyl methionine
WGR	tryptophan-glycine-arginine motif
ZBD	zinc binding domain
ZF	zinc finger

INTRODUCTION

1. Chromatin

In eukaryotic cells, the genetic information is packaged into chromatin, a structure composed of DNA and a specialized group of proteins, mainly histones (reviewed in [1]). The assembly of the DNA into chromatin fulfills the remarkable task to fit a stretch of two meters of DNA into the cell nucleus that has a diameter of only a few microns. On the other hand, chromatin condensation is a natural obstacle for many DNA-based cellular processes like transcription, replication and DNA repair. In order to activate or repress genes according to the changing needs of a cell, chromatin architecture has to be tightly regulated. To this end, chromatin is divided into euchromatin and heterochromatin. Euchromatin comprises less condensed genomic regions that are usually transcriptionally active. Heterochromatin consists of more tightly packed DNA and usually stays condensed throughout the cell cycle. The gene-free regions at the centromeres and near the telomeres of the chromosomes are forms of constitutive heterochromatin. The formation of facultative heterochromatin, on the other hand, is often associated with developmental programs and X-chromosome inactivation in female mammalian cells.

1.1. Nucleosome structure

The smallest building unit of chromatin is the nucleosome, which consists of 147 bp of DNA wrapped approximately 1.7 times around an octamer of core histones. The octamer consists of a central H3-H4 tetramer capped by two H2A-H2B dimers. All core histones harbor a flexible N-terminal tail and a globular domain with a structurally conserved motif, the so-called histone fold. It consists of three alpha helices that are connected by short loops [2]. The N-terminal tails are highly enriched in basic amino acid residues and protrude from the nucleosome. The nucleosomes are connected by 20 to 80 bp of linker DNA and build the first level of compaction of the DNA (10nm fiber). This structure looks like “beads on a string” under an electron microscope.

The core histones and especially their N-terminal tails undergo many post-translational modifications that do not merely alter their affinity to the DNA but also

regulate the interaction with other proteins. These modifications allow a very shapeable chromatin structure, which is necessary to accommodate all cellular processes that take place at the DNA while retaining the ability to properly distribute the chromosomes to the daughter cells during cell division.

1.2. Linker histone H1

The linker histone H1 is responsible for further condensing the polynucleosomal fiber into a 30 nm fiber. It binds to the nucleosome at the DNA entry and exit sites and protects additional parts of the linker DNA (~ 20bp) from micrococcal nuclease digestion. The binding of H1 to nucleosomes induces the linker DNA to form a stem-loop structure [3], which enables the higher chromatin compaction into interphase chromosomes. During mitosis, further coiling leads to the highly condensed state of the metaphase chromosomes (Fig. 1).

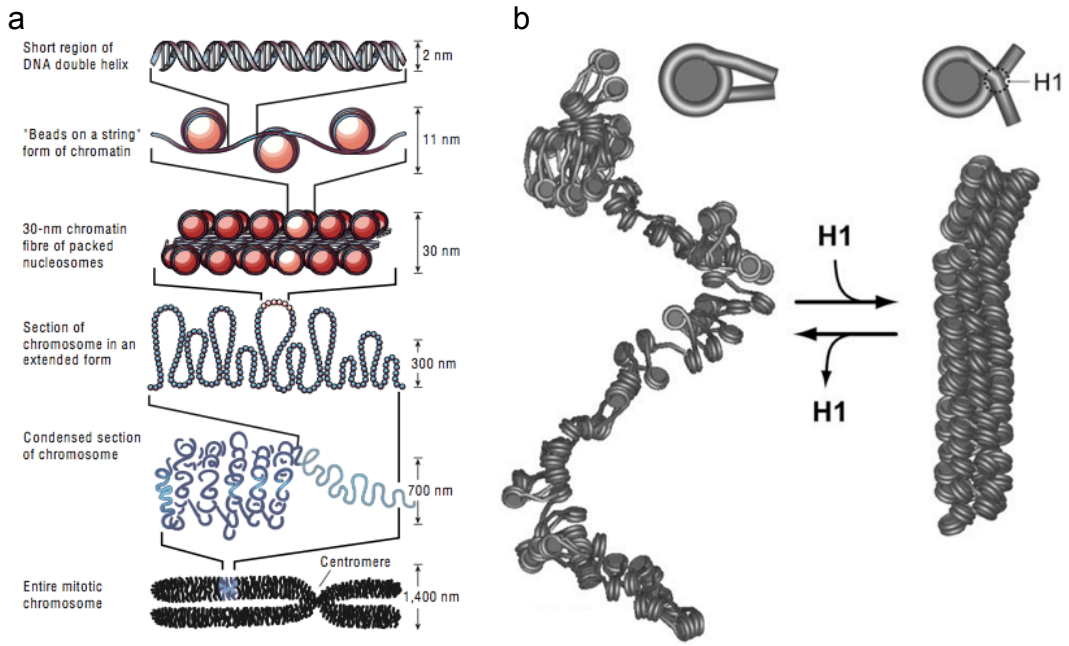

Figure 1. Chromatin structure and compaction by H1. (a) The DNA double helix is packaged into nucleosomes, further condensed into 30 nm fibers in presence of H1 and ultimately coiled into higher-order structures to form the metaphase chromosomes. Picture taken from [4]. (b) Binding of linker histone H1 to nucleosomes induces a more closed conformation of the linker DNA. Model from [5].

1.2.1. H1 structure

Linker histones exist in all multicellular organisms and some protists and histone H1-like proteins were even identified in some eubacteria, but not in archaebacteria [6].

The H1 from metazoans exhibits a tripartite structure composed of a central globular domain flanked by a short, flexible N-terminal tail and a long C-terminal tail rich in lysine residues. The globular domain of H1 is built by a winged helix motif [7] that is evolutionary unrelated to the histone fold of the core histones [6,7]. It is necessary for H1 function in chromatin condensation and involved in nucleosome binding [8,9]. While the globular domain is relatively well conserved between species, the C-terminal domain (CTD) is much more divergent. The CTD makes up almost half of the H1 protein (about 100 amino acid residues) and has a highly basic amino acid composition. It is the amino acid composition but not the primary sequence of the CTD that is important for its functions in chromatin condensation [10]. The predominant amino acid residues of the CTD are lysines (about 40%), followed by alanines and prolines, while serines, threonines, valines and glycines are much less abundant. The CTD is almost completely devoid of highly hydrophobic and negatively charged amino acids. Due to this particular amino acid composition, the CTD is thought to be intrinsically disordered [11]. This means it has molten globule-like properties in solution, but adopts a specific structure when associated with its macromolecular interaction partners [12]. Indeed, it was shown that the CTD does not exclusively function by neutralizing the negative charge of the linker DNA as previously assumed, but that the CTD can be subdivided into specific functional regions that are more or less important for DNA stem-loop formation and chromatin condensation, probably by adopting specific structural features [13]. Due to its high content of lysine and alanine residues, the CTD is predicted to form α-helices that might be initiated and interrupted by the proline residues [14,15].

Like the CTD, the N-terminal tail of H1 is less conserved than the globular domain and unstructured in aqueous solution [16]. It is much shorter than the CTD, not required for H1 function in chromatin condensation and is thought to influence H1-protein interactions [17] (e.g. with HP1 [18]).

1.2.2. H1 variants

The H1 family is the most divergent class of histone proteins [19]. To date, eleven different subtypes that are encoded by individual non-allelic genes were identified in mammals (reviewed in [20,21]). These H1 variants can be subgrouped based on different criteria such as their expression pattern or the localization of their genes on

different chromosomes. H1.1 to H1.5 are replication-dependent variants that are expressed in somatic cells during S phase of the cell cycle. In humans, these five H1 variants are located within a large histone gene cluster on chromosome 6 [21]. H1x is another variant that is ubiquitously expressed, but its expression is constant throughout the cell cycle and is not limited to S phase [22,23]. H1.0 is considered a replacement variant that is only expressed after terminal differentiation in specific cell types [24]. The expression of the residual four H1 variants (H1t, H1T2, Hils1, H1oo) is restricted to germ cells [21].

The H1 variants mainly differ in their N- and C-terminal extensions and originated from a common ancestral gene by gene duplication events. In mammals, the H1 paralogs within the same species often vary much more than the orthologs of an individual H1 variant in different species [25,26]. H1.2 and H1.4 are the predominant variants in most cell types, while H1.1 expression is rather low in most tissues [21,27]. The different somatic H1 subtypes also vary in their binding affinities to chromatin and their subnuclear localization. H1.4 and H1.5, for example, are mainly found in heterochromatic regions when overexpressed as GFP fusion proteins, while H1.0, H1.1, H1.2 and H1.3 are also present in euchromatic regions. Chromatin binding affinities of the H1 variants are generally correlated to the length of their CTD with H1.4 and H1.5 showing the highest affinity in FRAP studies. An exception is H1.0, which has the shortest CTD, but still exhibits moderate affinity for chromatin, probably due to the high content of basic amino acids within its CTD [28].

Despite the differences described above, none of the H1 variants seems to be essential in knockout studies in mice [29,30]. It is thus very likely that they have partially redundant functions and that the deletion of a single variant is compensated by increased expression of the others. Only the sequential knockout of three H1 genes (homologs of human H1.2, H1.3 and H1.4) in mice, which resulted in a 50% reduced H1 protein expression, was embryonically lethal [31]. In embryonic stem cells derived from these mice, the depletion of H1 resulted in a reduced H1/core histone ratio and reduced local chromatin compaction, but had only small effects on gene expression. This indicates that despite of its function in higher-order chromatin formation, H1 should not be regarded as a general repressor of transcription, but rather as a regulator of the expression of specific genes [32].

1.2.3. Post-translational modifications of H1

Like the core histones, linker histones undergo diverse post-translational modifications that regulate their affinity for chromatin and the interaction with other nuclear proteins [21,33-35]. An overview of some H1 modifications is given in Fig. 2. The most extensively studied modification of H1 is phosphorylation, which was discovered a long time ago [36]. H1 is phosphorylated at multiple serine and threonine residues within its N- and C-terminal tails. Most of the H1 phosphorylation sites lie within the CDK consensus motif (S/T)PX(K/R) which was also shown to be important for DNA binding of H1 [37]. The responsible kinases are CDK1 and CDK2 [37,38], which are counteracted by protein phosphatases [39]. H1 variants contain unequal total numbers of CDK motifs and these sites are differentially phosphorylated during the cell cycle with varying functional outcomes [40]. H1 phosphorylation progressively increases during the cell cycle with the lowest levels in G1 phase and the highest levels in late G2 phase and mitosis [41,42]. The phosphorylation of only few sites during the S-phase of the cell cycle leads to chromatin decondensation required for DNA replication [43], while extensive phosphorylation of H1 during mitosis is linked to chromosome condensation [44]. It was shown that unphosphorylated H1 binds more tightly to the DNA than the low-phosphorylated forms [45,46], which can be explained by the negative charges that are introduced by the phosphorylation and lead to electric repulsion of the DNA. H1 hyperphosphorylation during mitosis, however, induces structural changes in the CTD that finally lead to the opposite effect and induce the high compaction of the mitotic chromosomes [47].

Apart from this cell-cycle dependent regulation and function, H1 phosphorylation also seems to be involved in many other cellular processes such as apoptosis, DNA damage signaling and gene regulation. H1 phosphorylation is associated with transcription by RNA polymerase I and II and in this context mimics the effects of H1 removal and leads to chromatin relaxation [48,49].

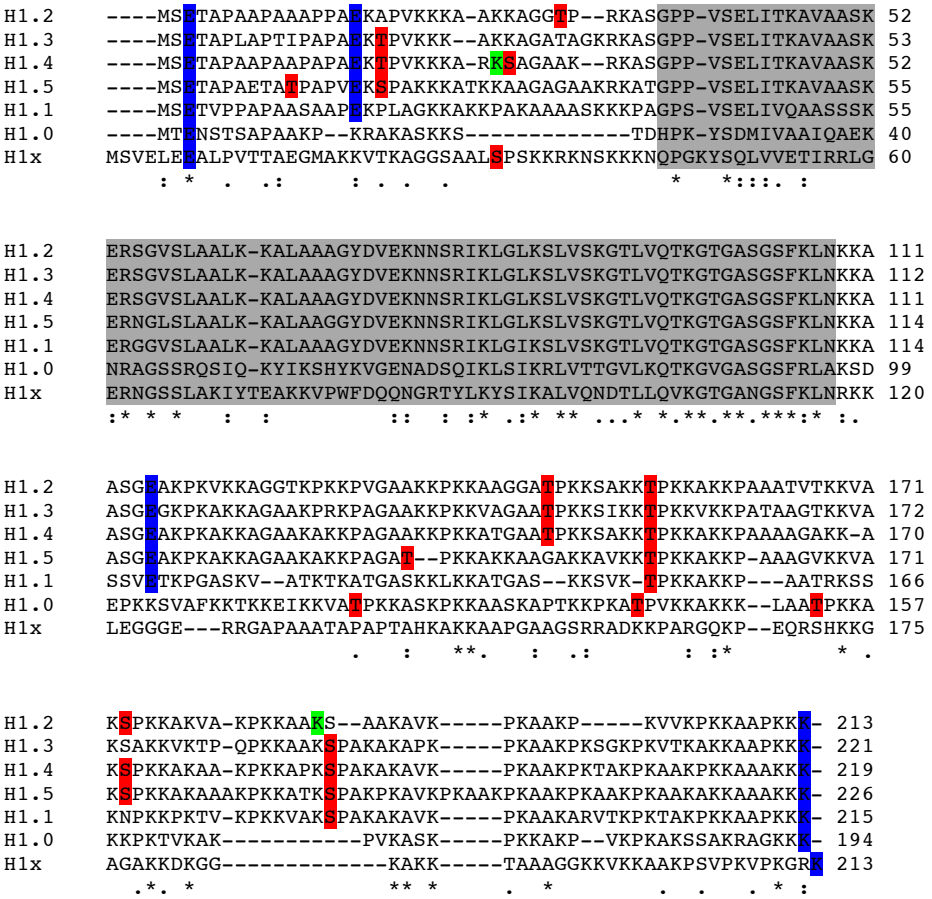

Figure 2. Post-translational modifications of the linker histones. Amino acid sequence alignment of the human somatic H1 variants (Gene bank accession numbers: H1.2: NM_005319, H1.3: NM_005320, H1.4: NM_005321, H1.5: NM_005322, H1.1: NM_005325, H1.0: NM_005318, H1x: NM_006026). The alignment was generated using ClustalW2 and similarity is indicated according to the ClustalW convention (asterisk: invariant, fully conserved residue; colon: highly similar residues; semi-colon: similar residues). The globular domain is marked by the box shaded in yellow. Residues described to be ADP-ribosylated are highlighted in blue, CDK phosphorylation sites in red and methylation sites in green.

Another post-translational modification of H1 that has been discovered very early is poly(ADP-ribosyl)ation (PARylation)(further explained in section 2). PARylation of polynucleosomes induces chromatin relaxation [50,51]. H1 was shown to be the main histone acceptor for poly(ADP-ribose) (PAR) *in vivo* [52] and it was described that the glutamates at positions 2, 14 and 116 and the carboxyl group of the C-terminal lysine residue can be modified by PAR [53].

Modern mass spectrometry technologies have been able to identify further post-translational modifications of H1 including acetylation, methylation, ubiquitination and N-formylation of lysine residues [54,55], but their exact role has to be determined. The first methylation described in H1 was the reversible di-methylation of K26 in

H1.4 by EZH2 and G9a [56-58], which serves as a docking site for HP1 and thereby induces transcriptional repression [18]. This methyl transferase (as well as the closely related enzyme GLP1) methylates H1 in a variant-specific manner [59]: While H1.4 is preferentially methylated in its NTD, H1.2, H1.3, H1.5 and H1.0 are methylated in their CTDs (K187 in H1.2). This variant-specific methylation of H1 also has different functional outcomes. Only the di-methylation of H1.4K26 but not the one of H1.2K187 can serve as a docking site for HP1 and be reversed by JMJD2/KDM4 proteins [58,59].

2. Poly(ADP-ribosyl)ation

ADP-ribosylation is an ancient post-translational modification of proteins during which the ADP-ribose moiety from the co-substrate nicotinamide adenine dinucleotide (NAD^+) is transferred onto specific amino acid side chains of acceptor proteins or attached to pre-existing protein-linked ADP-ribose units. The transfer of only one ADP-ribose unit is termed mono-ADP-ribosylation, whereas the attachment of linear or branched ADP-ribose polymers is termed PARylation. Mono-ADP-ribosylation is widely spread in eukaryotes, but it was originally identified as the mechanism of action of bacterial toxins such as the *Corynebacterium diphteriae* toxin, which ADP-ribosylates the unusual amino acid diphthamide in the eukaryotic elongation factor-2 and thereby inhibits host cell protein translation [60,61]. PARylation is common in higher eukaryotes, apart from yeast, and was also found in some archaebacteria and dinoflagellates [62,63].

2.1. Enzymatic mechanism of PARylation

NAD^+ is mainly known as a coenzyme for redox reactions in which it alternates between the two redox states NAD^+ and NADH, but it also serves as ADP-ribose donor during ADP-ribosylation of proteins. ADP-ribosyltransferases (ARTs) are the enzymes responsible for this post-translational modification. They cleave the high-energy bond between the nicotinamide and ADP-ribose moieties of NAD^+ and transfer the ADP-ribose unit to the acceptor protein, while nicotinamide is released as byproduct (Fig. 3). PARylation of proteins can be divided into at least three distinct reactions [64]: 1) the initiation, i.e. the attachment of the first ADP-ribose moiety to

the side chains of specific amino acids; 2) the elongation, i.e. the transfer of further ADP-ribose units to the pre-existing ones which generates linear ADP-ribose chains linked through glycosidic ribose-ribose bonds; 3) branching, i.e. the generation of branching points at irregular intervals. ADP-ribose chains vary in length and can reach 200 to 400 ADP-ribose units *in vitro* and *in vivo* [65]. Branching occurs on average every 20 to 50 ADP-ribose units [66].

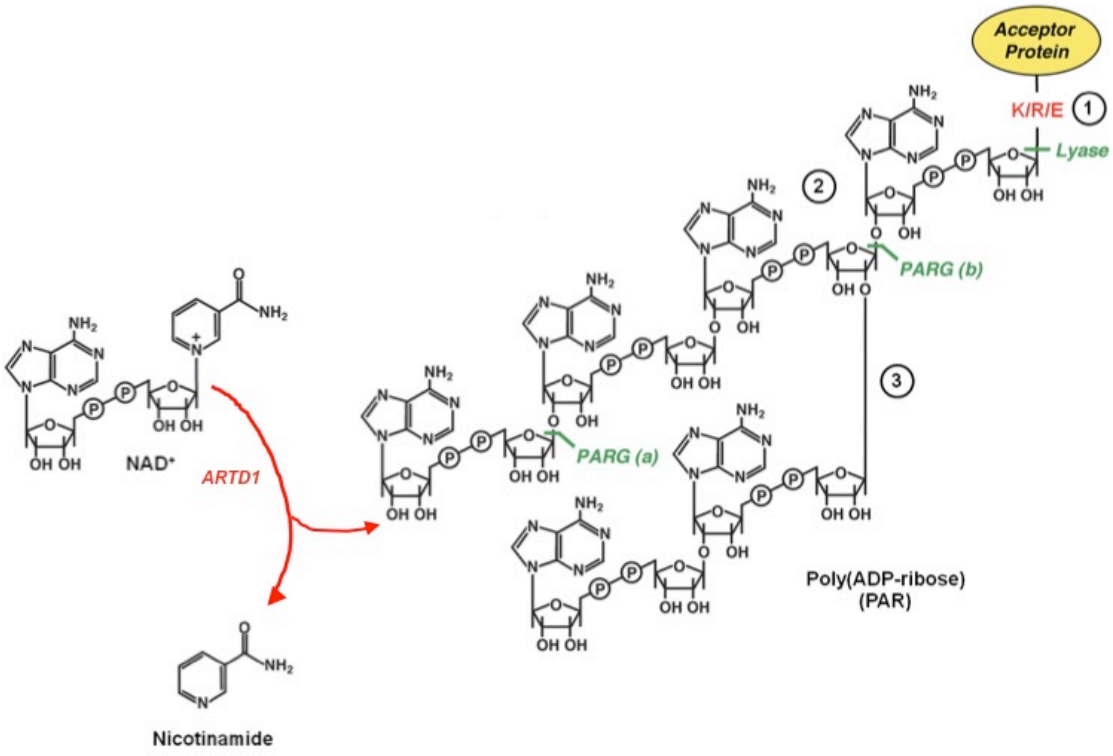

Figure 3. PARylation of proteins. ARTD1 and other members of the ARTD family successively transfer ADP-ribose units from their cofactor NAD^+ to lysine, arginine or glutamate residues of their target proteins thereby generating long linear and branched chains of ADP-ribose. This happens in three individual steps that create different chemical linkages: 1. Initiation 2. Elongation 3. Branching after every 20 to 50 ADP-ribose units. PARG degrades the ADP-ribose polymers with exoglysidic (a) and endoglycosidic (b) activity thereby creating free ADP-ribose monomers and free PAR, respectively. The most proximal ADP-ribose unit is removed by an ADP-ribosyl protein lyase. Distinct enzymes might be required for cleaving the bonds between ADP-ribose and the different amino acid side chains. Modified from [67].

In vivo, PARylation of proteins is transient as ARTs are counteracted by enzymes that cleave PAR. The extent of PARylation is thus determined by the equilibrium between enzymatic activities producing PAR and the ones degrading it. Poly(ADP-ribose) glycohydrolase (PARG) and ADP-ribosyl hydrolase 3 (ARH3) are able to hydrolyze the glycosidic bond between two ADP-ribose molecules [68,69]. PARG knockout leads to accumulation of PAR and thereby causes embryonic lethality in mice and *Drosophila* [70,71] indicating that PARG is the major PAR-degrading enzyme in

cells. The first ADP-ribose molecule is attached to the protein by different chemical linkages depending on the acceptor amino acids. ARH1 was shown to cleave off ADP-ribose molecules bound to arginine side chains [72] but it is currently not clear, which enzymes remove ADP-ribose moieties linked to lysine or glutamate residues [73].

As PAR is a very bulky and negatively charged polymer, the attachment of PAR to proteins often has a big impact on their structure, function or localization. In addition, many proteins also interact with PAR in a non-covalent manner. To this end, several conserved PAR binding modules have evolved including a short PAR-binding motif, which contains mainly basic and hydrophobic amino acid residues and is present in many DNA damage checkpoint proteins [74], a PAR-binding zinc finger domain [75] and the macrodomains [76].

2.2. ARTD family

Apart from the sirtuins, which are NAD^+-dependent deacetylases that partially also exhibit mono-ADP-ribosyltransferase activities, mammalian ARTs can be divided into two groups according to their similarity to the bacterial diphteria and cholera toxins - the ARTDs and ARTCs, respectively. The ARTDs were formerly known as poly(ADP-ribose) polymerases (PARPs). However, this name is inappropriate since the term polymerase usually refers to template-dependent enzymes such as RNA and DNA polymerases and because not all ARTDs have confirmed PARylation activities. In fact, it is likely that some of them merely act as mono-ADP-ribosyltransferases and others might be completely devoid of ADP-ribosyltransferase activity. Therefore, a new unified nomenclature with the family name ARTD for diphtheria toxin-like ART has been proposed [77].

In humans, 18 ARTD proteins have been identified so far [77]. ARTD1 (formerly known as PARP1) is the proto-type and best-studied member of the ARTD family. It is a nuclear, chromatin-associated enzyme that is very abundant (1×10^6 molecules on average per cell) and responsible for most (about 90%) of the cellular PAR generation [78,79]. ARTD1 is implicated in a huge number of cellular processes such as the DNA damage response, cell cycle regulation, gene expression, differentiation and aging. The major target of ARTD1 is ARTD1 itself, but it also modifies other nuclear proteins including core and linker histones, transcription factors and DNA repair

proteins. The enzymatic activity of ARTD1 is low under basal conditions, but it is greatly enhanced upon ARTD1 binding to DNA strand breaks. As a result, cellular PAR levels can increase 10 to 500 fold in response to DNA damage [80]. PAR formed upon genotoxic stress has a half-life in the range of few minutes [81]. This rapid turnover indicates that PAR-catabolizing enzymes like PARG immediately start to degrade DNA-damage induced PAR.

The other members of the ARTD family were identified through their "PARP signature", a highly conserved 50 amino acid motif within their catalytic domain that is responsible for NAD^+ binding [82]. ARTD2 shares the highest sequence homology with ARTD1 (40% identity between hARTD1 and hARTD2 catalytic domains) [83]. Similar to ARTD1, it is activated in a DNA-dependent manner and exhibits automodification activity [84].

PARylation activity of ARTDs is thought to depend on the presence of an evolutionary conserved H-Y-E catalytic triad, three amino acid residues critical for the mono-ADP-ribosylation and PARylation activities of ARTD proteins [77,85]. The catalytic glutamate residue in this motif (E988 in ARTD1) is required for ADP-ribose chain elongation [86,87], whereas chain initiation and thus mono-ADP-ribosylation is also possible without this residue. ARTD1 lacking an acidic amino acid residue at this position displays only weak mono-ADP-ribosylation but no polymerization activity. The histidine and tyrosine residues in this catalytic triad are involved in NAD^+ binding. According to the presence of these catalytic residues, ARTDs can be subdivided into three classes [85]: (1) enzymes with putative PARylation activity (ARTDs 1 to 6, which all contain the complete H-Y-E motif); (2) enzymes with putative mono-ADP-ribosyltransferase activity (all members lacking only the catalytic glutamate residue) and (3) catalytically inactive ARTD family members (ARTD9 and ARTD13, which lack the histidine and glutamate residue). Indeed, no auto-ADP-ribosylation of ARTD9 and ARTD13 has been described so far [88] and ARTD10 and ARTD8 displayed only mono-ADP-ribosylation activity [85], while synthesis of ADP-ribose oligomers and polymers has been confirmed for ARTDs 1, 2, 4 and 5 [84,89-91].

2.3. ARTD1 structure

ARTD1 is a ~113 kDa enzyme and composed of 1014 amino acids. It contains three major functional units: an N-terminal DNA-binding domain (DBD), a central automodification domain (AMD) and a C-terminal catalytic domain. The DBD harbors three zinc binding domains (ZFI, ZFII and ZBD III), which are required for the DNA-dependent activation of ARTD1, and a nuclear localization sequence (NLS). The automodification domain contains several confirmed automodification sites (K498, K521, K524) [89] and a BRCT motif (named after the C-terminal domain of breast cancer susceptibility protein 1 (BRCA1)), which promotes protein-protein interactions and is found in many proteins involved in the DNA damage response. The catalytic domain includes a WGR motif (named after the most conserved amino acid sequence in this motif) and an NAD^+ binding fold, which is required for the enzymatic activity of ARTD1. The structure of ARTD1 is depicted in Fig. 4.

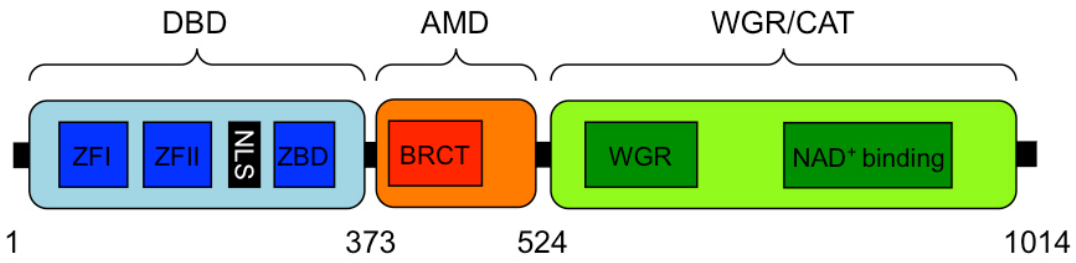

Figure 4. Scheme depicting the modular architecture of ARTD1. DBD: DNA binding domain; AMD: automodification domain; CAT: catalytic domain; ZFI and II: zinc finger I and II; NLS: nuclear localization signal; ZBD: zinc binding domain; BRCT: BRCA1 C-terminus.

2.4. Cellular functions of ARTD1

As mentioned above, ARTD1 is involved in many cellular functions such as NAD^+ metabolism, chromatin structure and gene expression, DNA damage signaling and repair, cell cycle regulation and cell death. On the physiological level, ARTD1 is implicated in processes like adipogenesis, aging, inflammatory responses and sensitivity to genotoxic agents.

ARTD1 knockout mice are viable and fertile but exhibit increased sensitivity to ionizing radiation and other genotoxic agents [92,93]. Interestingly, *ARTD1* gene disruption in mice conferred resistance to some oxidative stress-related disease models such as LPS-induced septic shock and streptozotocin-induced diabetes [94,95].

The relatively mild phenotype of *ARTD1* knockout in mice can be explained by functional redundancy with other ARTDs especially *ARTD2*, as *ARTD1/ARTD2* double-knockout is embryonically lethal in mice [96]. dARTD is essential in *Drosophila*, which possesses only two ARTD proteins (one ARTD1 homolog (dARTD) and tankyrase) [97].

2.4.1. Chromatin structure and transcription

As mentioned previously, core histones and linker histones are targets of ARTD1 and their PARylation induces decondensation of higher-order chromatin structures [50,51,98]. Further evidence that ARTD1 regulates chromatin structure comes from studies with *in vitro*-assembled chromatin, in which addition of ARTD1 induces chromatin compaction and transcriptional repression [99]. This effect is dependent on its DBD and catalytic domain and can be reversed by the addition of NAD^+, which leads to ARTD1 automodification and its subsequent release from nucleosomes [100]. In *Drosophila*, ARTD1 is required for local chromatin loosening during gene induction [101]. This is accompanied by accumulation of PAR at these sites. A role for ARTD1 in chromatin composition and gene regulation was further supported by the finding that ARTD1 is enriched at actively transcribed gene promoters and might serve to exclude H1 from these sites, as H1 showed a reciprocal chromatin binding pattern to ARTD1 and was increased at ARTD1-regulated genes upon ARTD1 depletion [102].

Apart from its function in chromatin modulation, ARTD1 also acts as a classical cofactor for diverse sequence-specific transcription factors such as nuclear factor κB (NF-κB), TATA-binding protein, hypoxia inducible factor 1 (HIF1) and nuclear receptors [103-106]. It can function as a transcriptional activator or repressor, depending on the cellular context and the genes analyzed [107]. In some cases, ARTD1 was shown to PARylate the corresponding transcription factor or other components of the transcriptional machinery [104,108,109], but the enzymatic activity of ARTD1 is not always required for its function as transcriptional coregulator [110,111]. The exact mechanism of gene-specific transcriptional regulation by ARTD1 is not clear and depends on the transcription factor with which it cooperates. The recruitment of ARTD1 to target promoters might occur via the interaction with the corresponding transcription factors. According to a study in

Drosophila, however, inactive dARTD is already present at the 5' end of the *Hsp70* locus before heat shock and becomes activated upon heat shock leading to its redistribution throughout the *Hsp70* locus [112]. Furthermore, it was shown that ARTD1 and PARG localize to promoters of both positively and negatively regulated target genes in the absence of a stimulus and regulate gene expression under basal conditions [113].

During hormone-regulated gene induction, topoisomerase IIβ was shown to induce a transient nucleosome-specific DNA double-strand break (DSB), which in turn activated the enzymatic activity of ARTD1, a requirement for subsequent H1/HMGB1 exchange and gene activation [114].

Finally, ARTD1 was also shown to PARylate the insulator protein CTCF and might thereby help to limit the activity of enhancers to discrete genomic regions and prevent the spread of heterochromatin [115].

2.4.2. DNA damage response

The cell is constantly threatened by diverse types of DNA damage, including DNA single and DSBs, chemical modification (e.g. oxidation and alkylation) of bases and base mismatches, generated by endogenous and exogenous sources. The term DNA damage response (DDR) summarizes all cellular processes necessary to detect, signal and remove DNA damage as well as the induction of the appropriate cell cycle checkpoint or apoptotic responses, if the DNA damage is too extensive to maintain genome integrity.

ARTD1 binds to a variety of aberrant DNA structures such as single and DSBs, cruciforms, crossovers and supercoils, which allosterically induce its enzymatic activity [116]. This is one of the reasons, why ARTD1 was mainly regarded as a DDR protein in the past. This was further supported by its rapid recruitment to sites of DNA damage *in vivo*, which is required for the accumulation of repair factors like XRCC1 and the MRN complex [117,118], and by its interactions with XRCC1 [119,120], DNA ligase IIIα [121], DNA polymerase β [122] and other proteins of the DNA repair machinery. Many DNA repair factors also possess PAR-binding domains and are thought to be recruited to DNA lesions in a PAR-dependent manner [74,75,123,124]. Thus, ARTD1 and PAR are implicated in diverse DNA repair pathways especially in base excision repair [122,125,126]. Other studies, however,

showed that DNA repair pathways are efficient in cells lacking ARTD1 [127-129]. This is supported by the finding that ARTD1 knockout mice are viable, fertile and display no increased predisposition to develop spontaneous tumors [92]. Thus, ARTD1 seems to be dispensable for DNA repair under normal physiological conditions and the exact role of ARTD1 in DNA damage signaling and repair has to be further elucidated in the future.

2.4.3. Cell death

Overactivation of ARTD1, e.g. in response to excessive oxidative stress, can deplete cellular NAD^+ and ATP levels and thereby promote cell-death [130,131]. It was proposed that ARTD1-mediated cell-death – known as parthanatos [132] – is initiated by the accumulation of PAR in the cytosol due to massive nuclear ARTD1 activity. Cytoplasmic PAR binds to apoptosis-inducing factor, which is subsequently released from the outer mitochondrial membrane and translocates to the nucleus, where it induces DNA fragmentation and caspase-independent cell-death [133].

During apoptosis, ARTD1 is cleaved by caspases, especially caspase 3, at their consensus motif DEVD after D214 [134,135]. This cleavage, which produces two ARTD1 fragments of 24 and 89 kDa, inactivates ARTD1 and is thought to be required to avoid overactivation of ARTD1 in response to apoptosis-induced DNA fragmentation to preserve cellular ATP levels [136]. This is important, as apoptosis is an ATP-dependent process. However, ARTD1 cleavage is not an absolute requirement for apoptosis because knockin mice harboring a caspase-resistant non-cleavable version of ARTD1 (D214N) develop normally [137]. Interestingly, these mice display a defect in NF-κB-dependent gene expression and are resistant to LPS-induced endotoxic shock and other inflammatory disease models indicating that ARTD1 cleavage, although a hallmark of apoptosis, has other non-apoptotic functions.

2.5. Post-translational modifications of ARTD1

One of the most important post-translational modifications of ARTD1 is its NAD^+-dependent automodification at certain residues within its DBD and AMD (K498, K521, K524) [89]. PARylation of ARTD1 induces its dissociation from DNA, probably due to electric repulsion between the negative charges of PAR and DNA. As

the interaction with damaged DNA induces ARTD1 enzymatic activity, PAR-dependent repulsion from the DNA creates a negative feedback loop that limits its activity to a certain extent.

However, ARTD1 is also subject to trans-modifications by other enzymes. It was, for example, shown that the mitogen-activated protein kinases ERK1/2 phosphorylate ARTD1 at the adjacent sites S372 and T373 and thereby potentiate its DNA damage-induced enzymatic activity [138]. Other kinases identified to phosphorylate ARTD1 at undefined sites are JNK1 (required for sustained ARTD1 activation during exposure to H_2O_2 [139]), AMPK (increased ARTD1 activity [140]) and protein kinase C (decreased ARTD1 DNA binding and enzymatic activity [141]). ARTD1 is also acetylated by p300/CBP, two components of transcriptional coactivator complexes, in response to inflammatory stimuli [142]. They acetylate ARTD1 at five different lysine residues within its AMD (K498, K505, K508, K521, K524), which is necessary for ARTD1 interaction with p50 and its coactivator function in NF-κB-dependent gene expression.

Apart from these small chemical modifications, ARTD1 is also subject to the covalent attachment of polypeptides such as small ubiquitin-like modifier (SUMO) and ubiquitin itself. SUMOylation of ARTD1 at K486 by the SUMO E3 ligase PIASγ restrains its coactivator function in HIF1-dependent gene expression [143] and, upon heat shock, is required for its subsequent ubiquitination by RNF4 and full *hsp70* transcriptional activation [144].

Notably, many of these post-translational modifications occur on the same or nearby residues within the AMD, thus creating a platform for vivid crosstalk. Acetylation of ARTD1, for example, affects three residues that are also important for its PARylation and therefore is likely to reduce its automodification.

2.6. ARTD inhibitors

Pharmacological inhibition of ARTDs was shown to induce synthetic lethality in homologous recombination (HR) deficient cell lines [145,146]. HR is an important error-free DSB repair mechanism and requires the tumor suppressor proteins BRCA1 and BRCA2. Mutation of BRCA1/2 underlies many cases of heritable ovarian, breast and prostate cancer and thus ARTD inhibitors are currently tested as single agents or in combination with chemotherapy to treat these and other types of cancers. It is

thought that ARTD1 inhibition interferes with single-strand break repair and thus leads to accumulation of endogenously generated single-strand breaks, which are converted to DSBs during replication. ARTD inhibitors would therefore be toxic for HR-deficient cancer cells as they cannot repair these DSBs in an appropriate manner, but not for normal HR-proficient cells. This hypothesis, however, is challenged by studies that show no increased formation of DNA strand breaks in ARTD inhibitor treated cells [147,148]. It is thus very likely that other mechanisms also contribute to the toxic effects of ARTD inhibitors e.g. their negative influence on NF-κB-dependent anti-apoptotic gene expression [149,150].

Another clinical application of ARTD inhibitors lies in a number of pathophysiological conditions where ARTD1 hyperactivation might have detrimental effects e.g. during cerebrial ischemia/reperfusion in patients suffering a stroke or in inflammatory disorders [151,152].

Most inhibitors of ARDT1 are analogs of its byproduct nicotinamide and thus also inhibit other NAD^+-dependent enzymes, especially other members of the ARTD family. Therefore, they should be called ARTD inhibitors and not ARTD1 inhibitors. 3-aminobenzamide (3-AB) was one of the earliest substances known to inhibit ARTD1 and used in many *in vitro* and *in vivo* studies to analyze the effects of ARTD1 inhibition. Its low potency and specificity, however, preclude its therapeutic utilization. During the last years, other ARTD inhibitors with increased potency and less off-target effects have been developed and several of them are presently analyzed in clinical trials [153]. These include, for example, olaparib (AstraZeneca) and ABT-888 (Abott), which have already completed several Phase II trials as single agents or potentiators of chemotherapy against different types of cancers.

3. Protein methylation

Protein methylation mainly targets lysine and arginine residues. While either one or two methyl groups can be transferred to the side chain of an arginine, resulting in mono- and symmetrically or assymetrically di-methylated arginine (depending on whether one methyl group is transferred to each of the terminal nitrogen atoms or two methyl groups are transferred to the same nitrogen), lysine methylation can take place in three different degrees: mono-, di- and trimethylation [154,155] (Fig. 5).

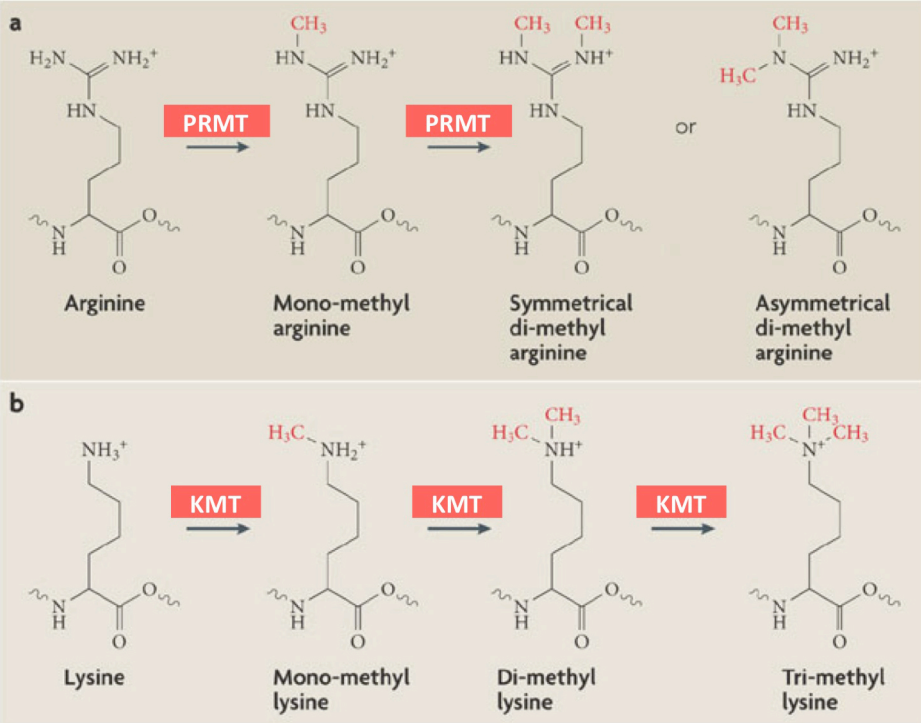

Figure 5. Arginine and lysine methylation. Arginines can be mono- or dimethylated while one to three methyl groups can be transferred to lysine residues. Picture modified from [156].

Unlike other post-translational modifications like acetylation and phosphorylation, methylation does not alter the overall charge of an amino acid and therefore cannot act through electro-static mechanisms. It does, however, change the size and hydrophobicity of the side chain in a manner proportional to the degree of the methylation. As a consequence, it can generate or destroy intra- and intermolecular binding sites and thereby influence the enzymatic activity, localization and interaction profile of a protein.

Protein methylation was most extensively studied on histone tails. While histone acetylation is generally linked to active transcription, histone methylation can either activate or repress gene expression, depending on the methylation state and residue that is modified. K4, K36 and K79 on H3 are methylation sites linked to active gene expression, whereas methylation of K9 and K27 on H3 and K20 on H4 is associated with transcriptionally silenced chromatin [157]. Due to the vast array of histone post-translational modifications that can act in a sequential and combinatorial manner, the histone code was proposed [158]. According to this hypothesis, distinct post-translational modifications on core histone tails operate alone or in combination to recruit other proteins (“readers”), which alter the chromatin structure and thereby promote or repress gene expression and other DNA-dependent processes.

Several protein interaction motifs that recognize specific methylated lysine residues on histone tails and other cellular proteins have been identified. These include the chromo- and tudor domains as well as the WD40 and MBT (malignant brain tumor) repeats [159,160]. These domains bind to methylated lysine residues within a certain amino acid context and are usually able to distinguish between different methylation states (mono-, di- or trimethylation), which increases the coding potential of this modification.

3.1. Enzymatic mechanism of protein methylation

The enzymes that carry out protein methylation in cells are termed arginine methyltransferases (PRMTs) and lysine methyltransferases (KMTs), depending on the residues, which they target. They catalyze the transfer of the methyl group from their cofactor S-adenosyl methionine (SAM) to the acceptor amino acid and thus generate a methylated arginine or lysine residue and the byproduct S-adenosyl homocysteine (SAH). The regeneration of SAM occurs via the hydrolysis of SAH to homocysteine and adenosine. Homocysteine is then remethylated to form methionine, which finally needs to be activated by methionine adenosyltransferase [161]. The metabolic cost for this cycle is high (12 ATP equivalents) [162]. Thus, reactions consuming SAM are much more expensive for the cell then e.g. protein phosphorylation which requires only one ATP molecule.

3.2. SET domain protein KMTs

Protein lysine methylation is carried out by SET domain containing enzymes (reviewed in [163-165]). The only exception known so far is Dot1 in yeast (and its homologs in other organisms), which is responsible for H3K79 methylation and does not harbor any domain structurally related to the SET domain [166]. The name of the SET domain is derived from the three *Drosophila melanogaster* proteins in which it was first identified, suppressor of variegation (Su(var)3-9) [167], enhancer of zeste (E(z)) [168] and trithorax [169].

The SET domain is a conserved sequence motif of about 130 amino acids and harbors the catalytically active site of the KMTs. The structures of several SET domains have been solved. They are not related to the active sites of other SAM-dependent enzymes

[170]. The SET domain is comprised of several small β-sheets that surround a knot-like structure [171]. The regions adjacent to the SET domain are called preSET (or N-SET) and postSET (or C-SET) domains, respectively, and are also required for enzymatic activity [172-174]. Together with the SET domain they form the peptide binding cleft and the SAM binding pocket, which are connected through a hydrophobic channel that accommodates the side chain of the target lysine and brings it in close proximity to the methyl donor to allow the methyl transfer [174-176]. The peptide binding cleft is responsible for substrate recognition by forming hydrogen bonds and other interactions with the amino acids flanking the target residue [177,178]. This explains the overall low sequence similarity between KMTs with different substrate specificities. The product specificity also lies within the SET domain. Certain residues that define the size and geometry of the narrow target lysine channel determine if one or several methyl groups can be transferred [175,179,180].
SET domain containing proteins have been found in all eukaryotes analyzed so far [164] and many of them are involved in chromatin regulation by methylating histones and other chromatin-associated proteins. In humans, more than ninety members of the SET domain protein family with diverse substrate and product specificities have been annotated [181], emphasizing the importance of lysine methylation as a mode of post-translational protein regulation in cells.

3.3. Identification and structure of the KMT SET7/9

SET7/9 (also SET7, SET9 or SETD7) was identified a decade ago independently by two groups as a mono-methyltransferase for H3K4 [182,183]. Both groups found that H3K4 methylation by SET7/9 inhibits subsequent H3K9 methylation by SUV39H1. SET7/9 was therefore linked to transcriptional activation, which was strengthened by the fact that H3K4 methylation by SET7/9 displaces the histone deacetylase NuRD complex [183] and promotes acetylation of H3 and H4 by p300 [182]. The KMT activity of SET7/9 towards H3 in nucleosomes, however, is weak, suggesting that other factors might be involved in SET7/9-dependent H3K4 methylation *in vivo* or that histone proteins are not the main substrates of SET7/9.
SET7/9 knockdown was shown to affect the expression of a subset of genes, which partially coincided with a decrease in local H3K4 methylation [184-186]. Depletion

of SET7/9 did not result in changes of global H3K4 levels, further indicating that H3 is not the main target of SET7/9 [187].

Several crystal structures of SET7/9, either free or in complex with its cofactor product SAH, were resolved in the presence and absence of substrate peptides [172,175,177,188,189]. These structures revealed that SET7/9 lacks the cysteine-rich pre- and postSET domains found in other methyltransferases such as the SUV39 family [164]. Nevertheless, the regions flanking the SET domain of SET7/9 are required for its enzymatic activity and especially the residues C-terminally to the SET domain are involved in the formation of the substrate binding cleft.

3.4. Non-histone targets of SET7/9

A few years after the discovery of the mono-methyltransferase activity towards H3K4, it became apparent that SET7/9 also modifies many non-histone proteins with diverse functional outcomes. TAF10, a component of the general transcription factor complex TFIID, was the first non-histone target shown to be methylated by SET7/9 [190], resulting in increased interaction with RNA polymerase II and elevated expression of some genes.

A comparison of known SET7/9 targets and a substrate specificity analysis based on peptide array methylation [191] showed that SET7/9 methylates the consensus motif [K>R][S>KYARTPN][K_{me}] and prefers lysine residues within net positively charged regions. SET7/9 mainly acts as a mono-methyltransferase, although dimethylation has been described in some cases [191,192]. Most of the substrate proteins of SET7/9 are transcription factors, nuclear receptors and other chromatin-associated proteins involved in gene regulation. Monomethylation by SET7/9 negatively or positively influences their stability and transcriptional activity, crosstalks with other post-translational modifications or regulates the interaction with other proteins (see table 1).

The most extensively studied non-histone substrate of SET7/9 is p53, which is methylated at K372 in response to DNA damage [193]. SET7/9-dependent methylation of p53 was shown to induce its subsequent acetylation and stabilization, a prerequisite for efficient p53-dependent gene expression and cell cycle arrest upon genotoxic stress [194,195]. However, these studies were performed in human cancer cell lines in which p53 is often deregulated. Kurash *et al.* confirmed the role of SET7/9 in p53 regulation and tumor suppression in SET7/9 knockout mice [195], but

in two other SET7/9 knockout mouse models, p53-mediated DNA damage response was not compromised [187,196]. Thus, it is controversial whether SET7/9-dependent methylation of p53 is important for p53 activity in nontransformed cells.

SET7/9 knockout mice (obtained by disruption of either exon 1 [196] or exon 5-8 [187]) were born at normal Mendelian ratios, survived to adulthood and displayed no obvious phenotypic abnormalities or increased tumor predisposition.

Substrate	Target site	Function of the methylation	Ref.s
TAF 10	K189	increased affinity to RNA polymerase II	[190]
p53	K372	increased acetylation, stability and transcriptional activity	[193-195]
ER	K302	increased stability and transcriptional activity	[197]
DNMT1	K142	decreased stability and DNA methylation	[198]
RelA	K314, K315	degradation of DNA-bound RelA	[199]
	K37	increased transcriptional activity	[200]
pRb	K873	stimulates HP1 binding, cell cycle arrest	[201]
	K810	prevents phosphorylation of pRb, cell cycle arrest	[202]
E2F1	K185	decreased stability	[203]
AR	K632	induces intramolecular interactions, enhanced transcriptional activity	[204]

Table 1. Human SET7/9 target proteins. Overview of identified SET7/9 substrates and their target lysine residues. The diverse functional outcomes of the methylation are indicated.

3.5. Reversal of lysine methylation

Histone methylation was regarded as a very stable or even irreversible epigenetic modification for a long time and it was thought that turnover of histone methyl marks mainly occurs via histone tail clipping or replacement of the whole histone [156,205]. Then it was shown that peptidyl arginine deiminase PAD4 antagonizes arginine methylation by converting methylated arginines to citrullin [206,207]. This does, however, not restore the original unmethylated state of the protein.

Only recently, enzymes that are able to reverse lysine methylation were identified, which demonstrates that, like other post-translational modifications, lysine methylation is a reversible, dynamic process (reviewed in [156,208]). Lysine demethylases can be divided into two different groups, the LSD family with only two members identified in humans so far (LSD1 and LSD2) and the Jumonji-C (JmjC) domain family. LSD1 and LSD2 are FAD-dependent amine oxidases that are only

able to demethylate mono- and dimethylated lysine residues [209,210]. JmjC domain containing demethylases are Fe^{2+}-dependent dioxygenases that use another catalytic mechanism involving the oxidative decarboxylation of α-ketoglutarate [211]. They are also able to demethylate trimethylated lysine residues. Both enzyme families create formaldehyde as a byproduct of the demethylation and exhibit a high substrate specificity for certain lysine residues and methyl states within the histone tails, which can shift upon interaction with different auxiliary factors [212-214]. Lysine demethylases are often affiliated with larger macromolecular complexes, which also contain other chromatin modifying enzymes such as histone deacetylases and methyl transferases.

Similar to lysine methylation, lysine demethylation reaches beyond histones. LSD1, for example, is able to demethylate p53 [215] and DNMT1 [216] as well.

3.6. Inhibitors of lysine methylation and demethylation

KMTs can be inhibited by compounds mimicking their cofactor SAM. These small-molecule inhibitors, however, often lack specificity, as they usually also inhibit other cellular SAM-dependent enzymes such as DNA and arginine methyl transferases [217]. The optimal inhibitor would not only have to be able to distinguish between KMTs and other SAM-dependent enzymes, but should also be selective among the various KMTs. Only few compounds with relatively narrow specificity have been described e.g. chaetocin, a mycotoxin selective for H3K9 specific KTMs like SUV39H1 and G9a [218]. For SET7/9, a bisubstrate-inhibitor was identified [219], but no SET7/9 specific inhibitors are commercially available yet.

LSD1 and LSD2 are related to other types of FAD-dependent amine oxidases such as the monoamine oxidases (MAO-A and MAO-B). It was thus not surprising that small-molecule inhibitors known to inhibit MAOs also exhibited activity towards LSDs. Two such molecules are tranylcypromine (TCP), which irreversibly inhibits LSD1 [220,221] and LSD2 [210], and - albeit with lower potency - pargyline [214].

4. Aim of the thesis

SET7/9 is a lysine mono-methyltransferase that modifies H3K4 as well as many non-histone proteins and regulates the activity of several proteins such as p53, pRb and E2F1 in response to DNA damage and other stresses. Based on these findings, we hypothesized that SET7/9 also methylates other nuclear proteins that are involved in the genotoxic stress response.

ARTD1 and the linker histone H1 are two chromatin-associated proteins that influence many DNA-related processes. It was the aim of this thesis to investigate if ARTD1 and H1 are methylated by SET7/9 *in vitro* and *in vivo* and how this modification affects their function.

RESULTS

5. Overview of published and submitted manuscripts

5.1. Set7/9-dependent methylation of ARTD1 at K508 enhances poly-ADP-ribose formation

Authors: **Ingrid Kassner**, Monika Fey, Martin Tomas, Elisa Ferrando-May, Michael O. Hottiger

Journal: manuscript submitted

Contribution: Planning, performing and evaluating the experiments. Preparation of the figures and revision of the manuscript. MT and EFM helped to plan and perform the laser irradiation experiments. MF helped with protein expression and purification and performed the experiment in Fig. 2B.

5.2. Crosstalk between Set7/9-dependent methylation and ARTD1-mediated ADP-ribosylation of histone H1.4

Authors: **Ingrid Kassner**, Marc Barandun, Monika Fey, Michael O. Hottiger

Journal: manuscript in preparation

Contribution: Planning, performing and evaluating the experiments. Preparation of the figures and revision of the manuscript. MB helped with cloning and protein expression and performed the experiments leading to figures 1B, 1D, 1E and supplementary figures S1B, S1C and S1D.

5.3. Sumoylation of poly(ADP-ribose) polymerase 1 inhibits its acetylation and restrains transcriptional coactivator function

Authors: Simon Messner, David Schuermann, Matthias Altmeyer, **Ingrid Kassner**, Darja Schmidt, Primo Schär, Stefan Müller and Michael O. Hottiger

Journal: FASEB J. 2009 Jul 31.

Contribution: Localization of SUMO2/3 and ARTD1 and detection of PAR upon H_2O_2 treatment by immunofluorescence (Suppl. Figure 4).

5.4. Inflammasome activated caspase 7 cleaves PARP1 to enhance the expression of a subset of NF-κB target genes

Authors: Süheda Erener, Virginie Petrilli, **Ingrid Kassner**, Roberta Minotti, Rosa Castillo, Raffaella Santoro, Paul O. Hassa, Jürg Tschopp and Michael O. Hottiger

Journal: Mol Cell. 2012 Mar 29.

Contribution: Planning, performing and evaluating the following experiments: preparation of nuclear and cytoplasmic extracts after LPS stimulation and detection of activated caspase 7 by Western blot (Figure 3B), determination of RelA localization after LPS stimulation by immunofluorescence (Suppl. Figures 2C and 4D), detection of caspase 3 activation upon LPS treatment (Suppl. Figure 3D). Preparation of the corresponding figures and proof-reading of the manuscript.

Set7/9-dependent methylation of ARTD1 at K508 enhances poly-ADP-ribose formation

Ingrid Kassner[1,2], Monika Fey[1], Martin Tomas[3,4], Elisa Ferrando-May[3], Michael O. Hottiger[1,*]

[1]Institute of Veterinary Biochemistry and Molecular Biology
University of Zurich, Winterthurerstrasse 190,
8057 Zurich, Switzerland
Email: hottiger@vetbio.uzh.ch

[2]Life Science Zurich Graduate School, Molecular Life Science Program,
University of Zurich

[3] Department of Biology, Bioimaging Center, University of Konstanz
Universitätsstrasse 10, 78464 Konstanz, Germany

[4]Department of Physics, Center for Applied Photonics, University of Konstanz
Universitätstrasse 10, 78464 Konstanz, Germany

*Corresponding author

ABSTRACT

ADP-ribosyltransferase diphtheria toxin-like 1 (ARTD1, formerly named PARP1) is localized in the nucleus, where it ADP-ribosylates specific target proteins. The post-translational protein modification (PTM) with a single ADP-ribose unit or with polymeric ADP-ribose (PAR) chains regulates protein function as well as protein-protein interactions and is implicated in many biological processes and diseases.

SET7/9 (also called Setd7 or KMT7) is a protein methyltransferase that catalyzes lysine monomethylation of histones, but also methylates many non-histone target proteins such as p53 or DNMT1.

Here, we identify ARTD1 as a new SET7/9 target protein that is methylated at K508 *in vitro* and *in vivo*. ARTD1 auto-modification inhibits its methylation by SET7/9, while auto-poly-ADP-ribosylation is not impaired by prior methylation of ARTD1. Moreover, ARTD1 methylation by SET7/9 enhances the synthesis of polymeric ADP-ribose (PAR) upon oxidative stress and stimulates the recruitment of ARTD1 to chromatin *in vivo*. Together, these results reveal a novel mechanism for the regulation of cellular ARTD1 activity by SET7/9 to assure efficient PAR formation upon cellular stress.

Running title: ARTD1 methylation at K508 by SET7/9

Key words: PARP-1, SET7/9, lysine methylation, poly-ADP-ribosylation, post-translational modification

INTRODUCTION

ADP-ribosyltransferase diphtheria toxin-like 1 (ARTD1, formerly named PARP1, [1]) is a nuclear protein that post-translationally modifies proteins by transferring the ADP-ribose moiety from NAD^+ to specific amino acid residues of target proteins. It is the best described member of the ADP-ribosyltransferase (ART) protein family, which currently comprises 22 human enzymes [1]. ARTD1 is not only the main nuclear ART, but also the primary acceptor for polymeric ADP-ribose (PAR). ARTD1 can be ADP-ribosylated at specific lysine residues and is also modified by acetylation and sumoylation between the amino acid residues 481 and 525 [2-4]. Protein modification with a single ADP-ribose unit or with PAR chains regulates protein function and is implicated in biological processes such as transcriptional control, cell differentiation or cell cycle regulation [5, 6]. Many cellular functions of ARTD1 are brought about by complex formation with partner proteins or the ADP-ribosylation of target proteins in the cell nucleus [5, 7]. For example, histones or transcription factors are poly-ADP-ribosylated by ARTD1, which causes concomitant changes in chromatin structure and DNA metabolism [8, 9].

Genotoxic and cellular stresses activate ARTD1 enzyme activity [10]. However, the detailed upstream mechanisms leading to the activation of ARTD1 and the involvement of PTMs modulating ARTD1 activity are little understood. *In vitro,* the DNA-dependent interaction between the amino-terminal DNA-binding domain and the catalytic domain of ARTD1 increased *Vmax* and decreased the *Km* for NAD^+ [4]. The amount of DNA in this study was kept at a saturating 1:1 ratio (DNA:ARTD1 dimer). It is currently not clear whether ARTD1 activity and the subsequent PAR formation under non-saturating DNA levels depends on additional regulatory mechanisms.

SET7/9 (also called Setd7 or KMT7) was discovered as a histone methyltransferase that causes mono-methylation of histone 3 lysine 4 (H3K4me1) [11] and is thereby involved in the regulation of euchromatic gene expression [12-14]. However, SET7/9 has only weak activity on nucleosomes [15], which implies that the main targets of the enzyme are non-histone proteins. In agreement with this hypothesis, numerous non-histone proteins such as Dnmt1 (reduction in stability), p53 (activation and stabilization), TAF10 (increased affinity for polymerase II), estrogen receptor α (activation and

stabilization), pRb, p65, MyoD and Tat protein of HIV1 are methylated by SET7/9[16-24]. In addition, a recent study identified up to 90 new non-histone SET7/9 target peptides and a strong methylation of free H2A and H2B tails [25]. This promiscuous targeting of SET7/9 to different substrates suggests a low specificity of the enzyme. Set7/9 knockout mice are viable and fertile and loss of Set7/9 does not seem to impair p53-dependent cell-cycle arrest or apoptosis following DNA damage [26, 27], although Set7/9 was originally thought to regulate p53 activity in human cells [17]. SET7/9 preferentially modifies positively charged amino acid regions and methylates the last lysine residue in the motif [K>R] [S>KYARTPN] [K] [25]. Peptides that do not perfectly match this sequence can be methylated to a lesser extent. In cells, a strong interaction of acceptor proteins with the SET7/9 methyltransferase might stimulate the transfer of a methyl group to weak target sites. Hence, a weaker methylation does not have to imply a lower biological importance [25].

SET7/9 mediated monomethylation is a reversible PTM that can be removed by demethylases such as the lysine specific demethylase 1 (LSD1) and its homolog LSD2. Both proteins are flavin-dependent demethylases that are specific for mono- and di-methylated lysines and which are part of histone modification complexes that control cell specific gene expression [28, 29].

The study presented here identifies ARTD1 as a new SET7/9 target protein that is methylated at K508, which enhances synthesis of PAR especially at low DNA concentrations. These results add an additional regulator element to cellular ADP-ribosylation, which affects ARTD1 enzymatic activity under oxidative stress conditions.

RESULTS

ARTD1 activity is regulated by SET7/9 activity *in vivo*

In order to test the hypothesis that SET7/9 regulates the enzymatic activity of ARTD1, we first confirmed that both enzymes are localized in the nucleus of U2OS cells (Figure S1A). Moreover, SET7/9 was knocked down in U2OS cells (Figure S1A, B) and PAR formation following oxidative stress by H_2O_2 was determined. Indeed, siSET7/9 treated cells formed less PAR than cells transfected with a control siRNA (Figure 1A, B), suggesting that SET7/9 regulates PAR formation *in vivo*. To further analyze the influence of SET7/9 on ARTD1 enzymatic activity in cells, nuclear extracts from siRNA treated U2OS cells (control siRNA or siRNA directed against SET7/9 or ARTD1) were prepared and auto-ADP-ribosylation of ARTD1 was tested *in vitro* in the presence or absence of exogenous DNA. Down-regulation of SET7/9 reduced the basal ARTD1 activity to levels only slightly above those in siARTD1 cells (in absence of exogenous DNA, Figure 1C, D). This effect was also seen, but to a lesser extent, when ARTD1 activity was stimulated by an excess of exogenous DNA (Figure1 C, D). In agreement with these findings, overexpression of Flag-tagged wildtype (WT) SET7/9 enhanced PAR formation upon H_2O_2 treatment and even in unstimulated cells, while the enzymatically inactive SET7/9 mutant H297A did not show this effect (Figure 1E, F). Finally, we monitored PAR formation in live cells via time-lapse imaging of the recruitment of GFP-labeled macroH2A to laser microirradiated sites [30]. Down-regulation of SET7/9 resulted in a significant reduction of macroH2A-specific signal at the irradiated region, indicative of reduced PAR synthesis (Figure S1D). Together, these results suggest that SET7/9 stimulates ARTD1-dependent PAR formation in U2OS cells in a manner that depends on the methylation of proteins.

ARTD1 is methylated *in vitro* and *in vivo* at K508 by SET7/9

To determine whether SET7/9 stimulates ARTD1 activity and PAR formation by direct methylation of ARTD1, *in vitro* methylation assays were performed. SET7/9 methylated the known substrate histone H3 as well as full-length ARTD1 *in vitro*, while neither GST nor ARTD2, another member from the ARTD family, were modified (Figure 2A). To localize the modification site, purified

ARTD1 fragments covering the whole amino acid sequence were methylated by SET7/9 *in vitro* (Figure 2B). The potential SET7/9 modification site(s) in ARTD1 could be narrowed down to the automodification domain (AD) consisting of amino acids 373-524, which was strongly methylated *in vitro*, while all other tested ARTD1 fragments (containing the DBD, WGR or CAT domain) were not methylated (Figure 2B). *In silico* analysis identified lysine 508 (K508) as the putative target site as it was the only lysine residue within this region matching the published [KR] [STA] [K(me)] consensus motif for SET7/9-dependent methylation[18]. Mutation of K508 to arginine (K508R) indeed abolished SET7/9-dependent methylation in the ARTD1 automodification domain of the full-length ARTD1 (Figure 2C). SET7/9-dependent methylation of ARTD1 K508 was confirmed by mass spectrometric analysis of recombinant ARTD1 (373-524) that was incubated with SET7/9 in presence or absence of SAM as methyl donor (Figure S2A, B). To confirm the methylation of ARTD1 K508 *in vivo*, a polyclonal antibody against a synthetic ARTD1 peptide containing the mono-methylated K508 was generated. The anti-meARTD1 antibody specifically detected *in vitro* the modified peptides (Figure S2C) and SET7/9-mediated methylation of full-length ARTD1 at K508 (Figure S2D), while the methylation deficient K508R mutant was not detected (Figure 2D). Moreover, upon overexpression of SET7/9 the same antibody specifically detected the methylation of ARTD1 *in vivo* (Figure 2E and F). Together, these results indicated that ARTD1 is methylated *in vitro* and *in vivo* by SET7/9 and identified K508 as the main target site for SET7/9-dependent methylation of ARTD1.

ARTD1 auto-modification inhibits its methylation by SET7/9

Interestingly, the SET7/9 target residue K508 lies within a heavily modified region (aa 486-524) of the ARTD1 automodification domain that comprises five acetylation and three ADP-ribosylation sites as well as one lysine residue that becomes sumoylated (Figure S3A). Modification of ARTD11 with SUMO did not affect its ADP-ribosylation activity but completely abrogated p300-mediated acetylation of ARTD1, revealing an intriguing crosstalk of sumoylation and acetylation on ARTD1. Crosstalk between different PTMs of the same modified amino acid residue has been documented in particular for modifications comprising the histone code[31-33]. It was thus tested whether there is crosstalk between SET7/9-dependent methylation, PARylation and acetylation of ARTD1 *in vitro*.

Prior stimulation of recombinant ARTD1 with DNA in the presence of NAD^+ and subsequent auto-modification completely inhibited methylation by SET7/9 (Figure 3A). Inhibition of ADP-ribosylation by 3-aminobenzamide from the beginning (3-AB; +) reverted this effect on ARTD1 methylation, while 3-AB addition after the auto-modification but before methylation (3-AB; ±) did not abolish methylation *per se* (Figure 3A). Consequently, these experiments suggested that auto-ADP-ribosylation of ARTD1, but not a possible ADP-ribosylation of SET7/9 by ARTD1, prevented subsequent methylation. The sharp band of methylated ARTD1 running at the height of unmodified ARTD1 strengthened the conclusion that SET7/9 only methylated ARTD1 that was not ADP-ribosylated.

In contrast, auto-poly-ADP-ribosylation of ARTD1 was not impaired by prior methylation of ARTD1 as indicated by the smear of methylated ARTD1 upon incubation with radiolabelled NAD^+ and DNA (Figure 3B). Similarly, methylation of the 373-524 ARTD1 fragment by SET7/9 did not affect subsequent acetylation by p300 (Figure 3C, left panel). The experiment was controlled with the enzymatically inactive H297A SET7/9 mutant and methylation of ARTD1 was confirmed in a parallel experiment using ^{14}C-SAM (Figure3C, right panel).

These results suggested that SET7/9-dependent methylation of ARTD1 is subject to crosstalk with ARTD1 auto-modification, while neither PARylation itself nor acetylation are impaired by the methyl-modification of K508.

SET7/9-dependent methylation of ARTD1 as K508 regulates ADP-ribosylation *in vivo*

To elucidate whether SET7/9-dependent methylation of ARTD1 at K508 is directly responsible for the observed influence of SET7/9 on ARTD1-dependent PAR formation *in vivo* (Figure 1), *ARTD1-/-* MLFs were stably genetically complemented with WT ARTD1 or with the two methylation deficient mutants (K508A and K508R), which were comparably expressed and only detected in the nucleus (NE, Figure 4A). Nuclear extracts containing WT or mutant ARTD1 were incubated with radioactively labeled NAD^+, but without exogenous DNA, and ARTD1 auto-ADP-ribosylation was assessed. The methylation deficient ARTD1 mutants K508A and K508R exhibited markedly reduced activity in comparison to the WT control (Figure 4B and S3B). Upon addition of excess DNA, the

methylation deficient ARTD1 proteins K508A and K508R still exhibited reduced enzymatic activity, but the effect was less pronounced as compared to conditions without exogenous DNA (Figure 4C and S3C). This indicated that the methylation deficient ARTD1 mutants (K508A and K508R) are enzymatically less active and provided further evidence that SET7/9-dependent methylation of ARTD1 affects its activity.

Mutation of K508 affects ARTD1 recruitment to chromatin

The results described above suggested that the methylation of ARTD1 at K508 mainly affects its enzymatic activity by regulating its stimulation by DNA (Figure 1C and 4B). This should consequently lead to a more efficient recruitment of WT ARTD1 to sites of DNA damage within the nucleus as compared to the methylation deficient ARTD1 mutant. We thus first analyzed whether the affinity of ARTD1 to chromatin would be affected under normal (non-genotoxic stress) conditions. ARTD1 affinity was not affected by SET7/9 down-regulation and could thus not have caused this effect (Figure S3C). In order to study if ARTD methylation affected the recruitment of ARTD1 to sites of DNA damage, cells expressing EGFP-tagged WT and methylation deficient ARTD1 were analyzed by localized femtosecond laser irradiation [34]. This method allows studying the kinetics of the recruitment of proteins to sites of DNA damage. The nature of the lesion can be influenced via the irradiation wavelength: At 775 nm, both DNA strand breaks and UV photoproducts are generated, while at 1050 nm mainly DNA strand breaks are produced [34]. Interestingly, recruitment of the K508R mutant ARTD1 was lower than of WT ARTD1 if cells were irradiated with femtosecond pulses at λ = 775 nm (Figure 4D). [34]. On the other hand, irradiation at a wavelength of 1050 nm caused similar recruitment of WT and K508R ARTD1 (Figure S3D). The kinetics of release of WT and K508R ARTD1 from the irradiated sites was comparable (data not shown). These results strongly suggest that SET7/9 regulates the recruitment of ARTD1 to damaged DNA in a DNA lesion-specific manner.

DISCUSSION

The results presented here suggest that SET7/9 methylates ARTD1 *in vivo* and *in vitro* at lysine K508. The K508 was identified as the target site for SET7/9-dependent methylation by site-directed mutagenesis and mass spectrometry as well as with a specific polyclonal antibody raised against this methylated site. Methylation of ARTD1 by SET7/9 did not prevent its consecutive ADP-ribosylation, but affected ARTD1 recruitment to sites of local DNA damage *in vivo*. Prior auto-ADP-ribosylation of ARTD1 impaired its methylation by SET7/9. Knockdown of SET7/9 or the expression of methylation deficient ARTD1 in cells lacking WT ARTD1 caused reduced PAR formation *in vitro* and *in vivo*. Moreover, overexpression of SET7/9, but not its enzymatic inactive mutant enhanced PAR formation in untreated (basal) and H_2O_2 treated cells. These findings define a new SET7/9 methylation target and reveal a previously unknown mechanism for the regulation of ARTD1 activity in cells.

The effect of ARTD1 methylation on PAR formation was most apparent if no exogenous DNA was added to the reactions using lysates of cells with either knockdown of SET7/9 or genetically complemented with a methylation deficient ARTD1 mutant (the cell lysate did contain low amounts of DNA). The effect was much weaker under conditions of saturating DNA concentrations (1:1 ration DNA:ARTD1 dimer), which may hint at a regulatory effect on ARTD1 activation by DNA. We have already provided evidence that DNA double strand breaks are recognized and bound by the DBD of ARTD1, which subsequently binds to the CAT domain to induce structural changes within the catalytic cleft in order to increase the affinity for NAD^+ and stabilize reaction intermediates [4]. The identified SET7/9-dependent methylation site at K508 of ARTD1 lies within the central automodification domain [4]. It is at first glance surprising that ARTD1 is methylated in the AD and not in one of the zinc fingers of the DNA binding domain or in the catalytic domain of ARTD1, but nevertheless affected in its enzymatic activity. However, the AD harbours the ADP-ribose acceptor sites indicating that this domain has to enter the catalytic cleft of ARTD1 to be subsequently modified. SET7/9-dependent methylation may sensitize ARTD1 for automodification by stabilizing the automodification domain in the catalytic domain of ARTD1 under non-genotoxic conditions or in the presence of minimal DNA damage (fewer DNA lesions compared to ARTD1 molecules).

Alternatively, methylation might induce structural changes, which affect the binding of the DBD to the CAT and thus sensitise the enzyme for a special type of DNA damage (see below). Likewise, methylated ARTD1 could exhibit higher affinity for its substrate NAD^+ and therefore show increased catalytic activity. Based on this hypothesis, methylation of ARTD1 at K508 by SET7/9 serves as a sensitization step that assures basal ARTD1 activity under low-stress conditions.

The AD represents a PTM hotspot that is also modified by ADP-ribosylation, acetylation and sumoylation [2-4]. Interestingly, prior auto-modification of recombinant ARTD1 inhibited subsequent methylation by SET7/9 most likely through steric hindrance (Figure 3A), which is in agreement with earlier studies providing evidence that the adjacent lysines 498, 521 and 524 are the acceptor sides for ADP-ribose [4]. However, the SET7/9-mediated methylation of ARTD1 did not influence the auto-ADP-ribosylation, indicating that the methylation would not affect the positioning of this domain into the catalytic domain. The functional relevance of this crosstalk needs to be further defined. It is intriguing to speculate that ARTD1 automodification would hamper K508 methylation to avoid an additional enhancement of its activity through this modification. Moreover, this could explain the inefficiency of SET7/9-dependent methylation to further activate already stimulated ARTD1 and hints again at a sensitization function of SET7/9 for ARTD1 under non-stimulatory conditions.

The overall affinity of K508R mutant ARTD1 for (undamaged) chromatin *in vivo* was not affected. In contrast, different recruitment of WT and K508R ARTD1 to sites of local damage in the nucleus was observed *in vivo*. Interestingly, WT and K508R ARTD1 showed similar recruitment upon irradiation at a wavelength of 1050 nm, while a clear reduction was observed for the mutant after treatment with laser pulses at 775 nm (Figures 4D and S3D). This effect was likely due to differences in the number of lesions induced by 775 nm vs. 1050 nm irradiation. The latter wavelength is specific for the induction of DNA strand breaks but achieves a lower overall damage than 775 nm at the irradiation conditions employed here [34]. Alternatively, a higher affinity for a certain type of lesion or chromatin alteration (qualitative difference) of the methylated ARTD1 protein, as compared to the unmethylated or the non-methylatable mutant, could also contribute to this behaviour.

Based on the results described here, SET7/9-dependent methylation of ARTD1 at K508 is proposed as a mechanism to sensitize ARTD1 and thus assure the efficient activation under genotoxic stress.

However, the factors and conditions regulating the enzymatic activity of SET7/9 are currently not known.

ARTD1 methylation at K508 could be detected in extracts of cells overexpressing SET7/9, while neither treatment with LPS or TNF nor induction of DNA damage by topoisomerase inhibitors could enhance ARTD1 methylation as discernible by the antibody (data not shown). This indicates either low endogenous levels of ARTD1 K508 methylation or further di- and trimethylation at this residue by other methyl transferases. Here, SET7/9 strongly affected ARTD1 activity in the presence of low amounts of DNA and upon stimulation by H_2O_2, although we do not know whether this was due to oxidative damage of the DNA. Whether SET7/9 is similarly required for the response to other signals (e.g. MNNG or PMA) remains to be investigated. The fact that SET7/9 is not required for cell cycle arrest or p53 stabilization suggests that the methylation-dependent stimulation of PAR formation is not required for these aspects but serves for other, yet to be identified, signalling pathways. Most importantly, the results presented here may indicate DNA-damage independent induction of ARTD1 activity *in vivo* and suggest that ARTD1 methylation stimulates ADP-ribosylation in response to other cellular stresses that do not necessarily involve DNA damage [5].

MATERIAL and METHODS

Plasmids and protein expression

pGEX-SET7/9 (52-366) and pcDNA3-SET7/9 (full-length/WT and H297A) were kindly provided by D. Reinberg (Howard Hughes Medical Institute, NYU School of Medicine, New York, USA). pcDNA4-Flag-HA-SET7/9 was created by subcloning SET7/9 into pcDNA4. pCMV-HA-PARP1 and pRRL-vectors were described previously [2]. All point mutations were inserted by site-directed mutagenesis. The construct encoding macroH2A-EGFP was kindly provided by A. Ladurner (Department of Physiological Chemistry, Ludwig-Maximilians-Universität (LMU) Munich, Munich, Germany).

The baculovirus expression vector BacPak8 (Clontech, Mountain View, CA, USA) was used for the expression of recombinant proteins in Sf21 insect cells, as described previously [35]. Recombinant GST-tagged proteins were expressed in *E.coli*. All recombinant proteins were purified by a one step affinity chromatography using ProBond resin (Invitrogen, Zug, Switzerland) for His-tagged and glutathione sepharose (GE Healthcare, Zurich, Switzerland) for GST-tagged proteins, according to the manufacturer‘s recommendations.

Antibodies and siRNAs

The following antibodies were used for immunoblotting: rabbit PARP-1 (H-250, Santa Cruz, Heidelberg, Germany); rabbit poly(ADP-ribose) (LP96-10, BD Biosciences, Allschwil, Switzerland); rabbit SET7/9 (#2815, Cell Signaling); mouse Flag (M2, Sigma-Aldrich, Buchs, Switzerland); mouse tubulin (T6199, Sigma); rabbit PARP (mono methyl K508) (ab92986) was generated in collaboration with Abcam (Cambridge, UK) using a synthetic ARTD1 peptide containing the methylated lysine residue (LSKKSK(me1)GQVKE).

The following FlexiTube siRNAs (QIAGEN, Hombrechtikon, Switzerland) were used in RNAi experiments: AllStars Negative Control, Hs_SET7_3 and Hs_PARP1_6.

Tissue culture and transfections

U2OS cells were cultured in Dulbecco's modified eagle medium (PAA Laboratories, Pasching, Austria) supplemented with 10% FCS and penicillin/streptomycin. MLFs were cultured in the same medium supplemented in addition with non-essential amino acids (Gibco/Invitrogen). Transfections with the indicated plasmids were performed with TransIT®-LT1 (Mirus Bio, Madison, WI, USA) according to the manufacturer's instructions and cells were harvested after 48 hrs. Knockdown was achieved by reverse transfection of 16 nM siRNA using RNAiMAX (Invitrogen) according to the manufacturer's protocol. Cells were harvested after three days. Cells were treated with 1 mM H_2O_2 in PBS containing 1 mM $MgCl_2$ for 10 min and with 0.5 μM Adr in normal medium.

Complementation of ARTD1 knockout MLFs was achieved by retroviral transduction with pRRL-myc-PARP1 vectors containing a blasticidine resistance marker or the corresponding empty vector. Generation of viruses and transduction of cells was done as described earlier [36].

***In vitro* methylation assays**

1 μg substrate protein was incubated with 1 μg bacterially purified GST-SET7/9 in presence of 0.03 μCi [^{14}C]-SAM (PerkinElmer) or 0.8 mM cold SAM (Sigma-Aldrich) in methylation buffer (50 mM Tris-HCl pH8.0, 50 mM NaCl, 10% glycerol, 1 mM PMSF, 1 mM DTT) or PAR buffer (see section below) for 1 h at 30° C. Reactions were stopped by boiling in 10X SDS-loading buffer and separated by SDS-PAGE. Gels were stained with Coomassie Blue, incubated in 1 M sodium salicylate for 20 min, dried, and exposed on X-ray films at -80° C. For mass spectrometric analysis, ARTD1 fragment 373-524 was methylated as described above, separated by SDS-PAGE, excised from the gel and digested with Glu-C. Peptides were analyzed by MALDI-MS.

Sequential *in vitro* modification assays

Sequential ADP-ribosylation and methylation assays were performed in PAR buffer (50 mM Tris-HCl, 4 mM $MgCl_2$, 250 μM DTT, 1 mg/ml pepstatin, 1 mg/ml bestatin, 1 mg/ml leupeptin). 10 pmol recombinant ARTD1 was methylated with 1 μg recombinant GST-SET7/9 as described above. The ADP-ribosylation was then started by addition of 5 pmol activating DNA and 400 μM cold NAD+

(Sigma, after methylation with [^{14}C]-SAM) or 100 µM NAD^+ spiked with [^{32}P]-NAD^+ (Perkin Elmer, after methylation with cold SAM). ADP-ribosylation reactions were incubated for 5 min at 30° C, stopped by addition of 10X SDS-loading buffer and proteins were separated by SDS-PAGE. Hot methylation/ADP-ribosylation was assayed by autoradiography of the Coomassie stained, dried gels, while cold modifications were controlled by immunoblotting with the indicated antibodies.

In the reverse experiment, 10 pmol ARTD1 was first incubated with activating DNA and 100 µM NAD^+ for 5 min on ice. 3-AB (Sigma-Aldrich) was added in a concentration of 8 mM to stop the ADP ribosylation before the methylation was started by addition of 1 µg SET7/9 and [^{14}C]-SAM. The activating DNA used in all assays was an annealed double-stranded oligomer (5'-GGAATTCC-3'). For sequential methylation/acetylation, 1 µg ARTD1 fragment (373-524) was methylated as described above. Acetylation was then started by addition of 20 µl HAT reaction mix (50 mM Tris-HCl pH 8.0, 50 mM NaCl, 10% glycerol, 1 mM DTT, 1 mM sodium butyrate, 1 mM PMSF, 0.5 µg p300, 75 µM [^{14}C]-AcCoA) and allowed to proceed for 1 h at 30°C.

Cellular extracts and ARTD1 activity assays

Whole cell extracts were prepared in lysis buffer (50 mM Tris-HCl pH7.5, 400 mM NaCl, 1%Triton, 25 mM NaF). Chromatin fractions were prepared as described elsewhere [37].

Nuclear extracts from U2OS cells and complemented MLFs were generated as described earlier [38, 39]. 5 µg nuclear extracts were incubated in 30 µl reaction buffer (50 mM Tris-HCl, 4 mM $MgCl_2$, 1 mg/ml pepstatin, 1 mg/ml bestatin, 1 mg/ml leupeptin, 250 nM [^{32}P]-NAD^+) in absence or presence of 5 pmol activating DNA for 20 min at 30°C. Proteins were separated by SDS-PAGE and ADP-ribosylation was analyzed by autoradiography. Quantifications were done using the software ImageQuant.

Induction of local DNA damage and imaging setup

Local DNA damage was induced by femtosecond laser irradiation and recruitment of fluorescently tagged proteins was recorded as described previously using a LSM 5 Pascal confocal microscope [34, 40]. Briefly, cells were irradiated with femtosecond laser pulses through a 40x oil immersion lens with a

numerical aperture of 1.3 (EC-Plan-Neo-Fluar, Carl Zeiss) along a 6 μm track within the nucleus, followed by fluorescence imaging at 488 nm. The maximum peak irradiance in the focal plane was 330 GW/cm^2 (pulse duration 200 fs, repetition rate 40 MHz) for excitation at 775 nm and 1200 GW/cm^2 (pulse duration 85 fs, repetition rate 107 MHz) at 1050 nm. Time series of fluorescence images were quantified with ImageJ (http://rsb.info.nih.gov/ij) as described [40, 41].

SUPPLEMENTAL DATA

Supplemental material includes 3 supplementary figures.

ACKNOWLEDGEMENTS

We thank Danny Reinberg (Howard Hughes Medical Institute, NYU School of Medicine, New York, USA) for providing SET7/9 plasmids. S. Flott from Abcam is acknowledged for support during the generation of the anti-meARTD1 antibody. We are grateful to Florian Freimoser and all the members of the Institute of Veterinary Biochemistry and Molecular Biology (University of Zurich, Switzerland) for helpful advice and discussions. The Functional Genomics Center Zurich (FGCZ) is acknowledged for mass spectrometric analyses. This work was supported Swiss National Science Foundation Grants 31003A-122421 and 310030B-138667 (to MOH) and the Kanton of Zurich (to MOH).

AUTHOR CONTRUBUTIONS

IK and MOH designed the experiments; IK, MF and MT performed experiments; MOH designed and supervised the study. IK and MOH wrote the manuscript. All the authors read and agreed with the manuscript. The authors declare that they have no conflict of interest.

REFERENCES

1 Hottiger M, Hassa P, Lüscher B, Schüler H, Koch-Nolte F. Toward a unified nomenclature for mammalian ADP-ribosyltransferases. *Trends Biochem Sci* 2010; **35**:208-219.

2 Messner S, Schuermann D, Altmeyer M *et al.* Sumoylation of poly(ADP-ribose) polymerase 1 inhibits its acetylation and restrains transcriptional coactivator function. *FASEB J* 2009; **23**:3978-3989.

3 Hassa P, Haenni S, Buerki C *et al.* Acetylation of poly(ADP-ribose) polymerase-1 by p300/CREB-binding protein regulates coactivation of NF-kappaB-dependent transcription. *J Biol Chem* 2005; **280**:40450-40464.

4 Altmeyer M, Messner S, Hassa P, Fey M, Hottiger M. Molecular mechanism of poly(ADP-ribosyl)ation by PARP1 and identification of lysine residues as ADP-ribose acceptor sites. *Nucleic Acids Res* 2009; **37**:3723-3738.

5 Hassa P, Haenni S, Elser M, Hottiger M. Nuclear ADP-ribosylation reactions in mammalian cells: where are we today and where are we going? *Microbiol Mol Biol Rev* 2006; **70**:789-829.

6 Ji Y, Tulin A. The roles of PARP1 in gene control and cell differentiation. *Current Opinion in Genetics & Development* 2010.

7 Schreiber V, Dantzer F, Ame J-C, De Murcia G. Poly(ADP-ribose): novel functions for an old molecule. *Nat Rev Mol Cell Biol* 2006; **7**:517-528.

8 D'Amours D, Desnoyers S, D'Silva I, Poirier G. Poly(ADP-ribosyl)ation reactions in the regulation of nuclear functions. *Biochem J* 1999; **342**:249-268.

9 Ueda K, Kawaichi M, Okayama H, Hayaishi O. Poly(ADP-ribosy)ation of nuclear proteins. Enzymatic elongation of chemically synthesized ADP-ribose-histone adducts. *J Biol Chem* 1979; **254**:679-687.

10 Luo X, Kraus WL. On PAR with PARP: cellular stress signaling through poly(ADP-ribose) and PARP-1. *Genes Dev* 2012; **26**:417-432.

11 Wang H, Cao R, Xia L *et al.* Purification and functional characterization of a histone H3-lysine 4-specific methyltransferase. *Mol Cell* 2001; **8**:1207-1217.

12 Brasacchio D, Okabe J, Tikellis C *et al.* Hyperglycemia induces a dynamic cooperativity of histone methylase and demethylase enzymes associated with gene-activating epigenetic marks that coexist on the lysine tail. *Diabetes* 2009; **58**:1229-1236.

13 Deering TG, Ogihara T, Trace AP, Maier B, Mirmira RG. Methyltransferase Set7/9 maintains transcription and euchromatin structure at islet-enriched genes. *Diabetes* 2009; **58**:185-193.

14 Li Y, Reddy MA, Miao F *et al.* Role of the histone H3 lysine 4 methyltransferase, SET7/9, in the regulation of NF-kappaB-dependent inflammatory genes. Relevance to diabetes and inflammation. *J Biol Chem* 2008; **283**:26771-26781.

15 Wang H, Huang Z, Xia L *et al.* Methylation of histone H4 at arginine 3 facilitating transcriptional activation by nuclear hormone receptor. *Science* 2001; **293**:853-857.

16 Chuikov S, Kurash JK, Wilson JR *et al.* Regulation of p53 activity through lysine methylation. *Nature* 2004; **432**:353-360.

17 Kurash J, Lei H, Shen Q *et al.* Methylation of p53 by Set7/9 mediates p53 acetylation and activity in vivo. *Mol Cell* 2008; **29**:392-400.

18 Couture JF, Collazo E, Hauk G, Trievel RC. Structural basis for the methylation site specificity of SET7/9. *Nature Structural & Molecular Biology* 2006; **13**:140-146.

19 Ea C, Baltimore D. Regulation of NF-{kappa}B activity through lysine monomethylation of p65. *Proc Natl Acad Sci USA* 2009.

20 Munro S, Khaire N, Inche A, Carr S, La Thangue N. Lysine methylation regulates the pRb tumour suppressor protein. *Oncogene* 2010.

21 Pagans S, Kauder S, Kaehlcke K *et al.* The Cellular lysine methyltransferase Set7/9-KMT7 binds HIV-1 TAR RNA, monomethylates the viral transactivator Tat, and enhances HIV transcription. *Cell Host Microbe* 2010; **7**:234-244.

22 Kouskouti A, Scheer E, Staub A, Tora L, Talianidis I. Gene-specific modulation of TAF10 function by SET9-mediated methylation. *Mol Cell* 2004; **14**:175-182.

23 Subramanian K, Jia D, Kapoor-Vazirani P *et al.* Regulation of estrogen receptor alpha by the SET7 lysine methyltransferase. *Mol Cell* 2008; **30**:336-347.

24 Tao Y, Neppl RL, Huang ZP *et al.* The histone methyltransferase Set7/9 promotes myoblast differentiation and myofibril assembly. *J Cell Biol* 2011; **194**:551-565.

25 Dhayalan A, Kudithipudi S, Rathert P, Jeltsch A. Specificity Analysis-Based Identification of New Methylation Targets of the SET7/9 Protein Lysine Methyltransferase. *Chemistry & Biology* 2011; **18**:111-120.

26 Lehnertz B, Rogalski JC, Schulze FM *et al.* p53-Dependent Transcription and Tumor Suppression Are Not Affected in Set7/9-Deficient Mice. *Mol Cell* 2011; **43**:673-680.

27 Campaner S, Spreafico F, Burgold T *et al.* The Methyltransferase Set7/9 (Setd7) Is Dispensable for the p53-Mediated DNA Damage Response In Vivo. *Mol Cell* 2011; **43**:681-688.

28 Karytinos A, Forneris F, Profumo A *et al.* A novel mammalian flavin-dependent histone demethylase. *J Biol Chem* 2009; **284**:17775-17782.

29 Shi Y, Lan F, Matson C *et al.* Histone demethylation mediated by the nuclear amine oxidase homolog LSD1. *Cell* 2004; **119**:941-953.

30 Timinszky G, Till S, Hassa P *et al.* A macrodomain-containing histone rearranges chromatin upon sensing PARP1 activation. *Nat Struct Mol Biol* 2009; **16**:923-929.

31 Lee JS, Smith E, Shilatifard A. The language of histone crosstalk. *Cell* 2010; **142**:682-685.

32 van Attikum H, Gasser SM. Crosstalk between histone modifications during the DNA damage response. *Trends Cell Biol* 2009; **19**:207-217.

33 Yang X-J, Seto E. Lysine acetylation: codified crosstalk with other posttranslational modifications. *Mol Cell* 2008; **31**:449-461.

34 Trautlein D, Deibler M, Leitenstorfer A, Ferrando-May E. Specific local induction of DNA strand breaks by infrared multi-photon absorption. *Nucleic Acids Res* 2010; **38**:e14.

35 Hassa P, Buerki C, Lombardi C, Imhof R, Hottiger M. Transcriptional coactivation of nuclear factor-kappaB-dependent gene expression by p300 is regulated by poly(ADP)-ribose polymerase-1. *J Biol Chem* 2003; **278**:45145-45153.

36 El-Andaloussi N, Valovka T, Toueille M *et al.* Arginine methylation regulates DNA polymerase beta. *Mol Cell* 2006; **22**:51-62.

37 Todorov IT, Attaran A, Kearsey SE. BM28, a human member of the MCM2-3-5 family, is displaced from chromatin during DNA replication. *J Cell Biol* 1995; **129**:1433-1445.

38 Felzien LK, Woffendin C, Hottiger MO, Subbramanian RA, Cohen EA, Nabel GJ. HIV transcriptional activation by the accessory protein, VPR, is mediated by the p300 co-activator. *Proc Natl Acad Sci USA* 1998; **95**:5281-5286.

39 Perkins ND, Agranoff AB, Duckett CS, Nabel GJ. Transcription factor AP-2 regulates human immunodeficiency virus type 1 gene expression. *Journal of virology* 1994; **68**:6820-6823.

40 Camenisch U, Trautlein D, Clement FC *et al.* Two-stage dynamic DNA quality check by xeroderma pigmentosum group C protein. *EMBO J* 2009; **28**:2387-2399.

41 Clement FC, Kaczmarek N, Mathieu N *et al.* Dissection of the xeroderma pigmentosum group C protein function by site-directed mutagenesis. *Antioxidants & redox signaling* 2011; **14**:2479-2490.

FIGURE LEGENDS

Figure 1. ARTD1 activity is influenced by SET7/9 *in vivo*. U2OS cells were transfected with scrambled siRNA (scr) or siRNA targeting SET7/9. (A) Three days after knockdown, the cells were treated with or without 1mM H_2O_2 for 5 min and PAR formation was analyzed by Western blot. (B) Quantification of (A). (C) ARTD1 activity was analyzed in nuclear extracts from U2OS cells after knockdown of SET7/9 and ARTD1 for three days by radioactive ADP-ribosylation assays. Upper panels: autoradiographies, lower panels: Coomassie stained gels. (D) Quantification of (C). (E) H_2O_2-induced PAR formation was analyzed after overexpression of Flag-SET7/9 WT or H297A as in (A). (F) Quantification of (E).

Figure 2. ARTD1 is methylated at K508 by SET7/9 *in vitro* and *in vivo*. (A) GST, ARTD1, ARTD2 and H3 were incubated with SET7/9 and ^{14}C-labeled SAM in an *in vitro* methylation assay, separated by SDS-PAGE and analyzed by autoradiography. (B) Full-length ARTD1 and fragments covering the whole protein were incubated in an *in vitro* methylation assay and analyzed by autoradiography. (C) Decreasing amounts of WT ARTD1 and K508R ARTD1 were methylated by SET7/9 and analyzed by autoradiography. Left: ARTD1 automodification domain (aa 373-524), right: full length WT or methylation deficient K508 ARTD1 mutant (D) *In vitro* methylation of WT and K508R ARTD1 was assessed in cells overexpressing SET7/9 (+) with an anti-meARTD1 antibody. (E) U2OS cells were transfected with scrambled siRNA (scr) or siRNA directed against ARTD1. One day, later cells were transfected with an empty vector or with a plasmid containing WT *SET7/9*. Whole cell extracts were analyzed by Western blot at day 3 after knockdown using an antibody directed against a peptide carrying the methylated lysine residue of ARTD1. (F) U2OS cells were co-transfected with HA-ARTD1 (WT or K508R) and EGFP or Flag-HA-SET7/9 (WT or H297A). After immunoprecipitation (IP) with an anti-HA antibody, whole cell extracts and IP samples were analyzed by Western blotting with the indicated antibodies.

Figure 3. ARTD1 methylation by SET7/9 does not influence its PARylation or acetylation but is inhibited by ARTD1 automodification. (A) Recombinant ARTD1 was methylated by SET7/9 after

ADP-ribosylation in presence or absence of DNA and 3AB. ±: 3-AB was added after the ADP-ribosylation reaction. (B) ARTD1 was first incubated with SET7/9 in presence or absence of ^{14}C-SAM and afterwards incubated with activating DNA and cold NAD^+ to allow automodification. (C) ARTD1 (373-524) was first incubated with WT SET7/9 or an enzymatic dead mutant (H297A) in presence of cold SAM and afterwards acetylated with p300 and ^{14}C-AcCoA (left). Methylation was controlled with ^{14}C-SAM (right).

Figure 4. ARTD1 recruitment to chromatin and enzymatic activity after SET7/9 knockdown and K508 mutation.

(A) ARTD1 knockout MLFs were stably complemented with WT ARTD1 or two methylation deficient mutants. Cells were then fractionated and cytoplasmic (CE) and nuclear extracts (NE) were analyzed by Western blot. (B) ARTD1 activity in NE from (A) was analyzed by radioactive PAR assay. (C) ARTD1 activity in NE from complemented MLFs as in (A) but in presence of 5 pmol activating DNA. (D) Recruitment of WT and K508R ARTD1 to sites of local DNA damage induced by femtosecond laser irradiation a λ = 775 nm.

LEGENDS OF SUPPLEMENTARY FIGURES

Figure S1. (A) U2OS cells expressing GFP-tagged SET7/9 and mCherry-tagged ARTD1 were analyzed by fluorescence microscopy. (B) U2OS cells were transfected with scrambled siRNA (scr) or siRNA targeting SET7/9. (C) Effect of SET7/9 depletion with three different siRNAs on mRNA levels. (D) Recruitment of macroH2A-EGFP to sites of local DNA damage induced by femtosecond laser irradiation at λ = 1050 nm.

Figure S2. (A) Mass spectrometric analysis of recombinant ARTD1 (373-524) incubated with SET7/9 in presence and absence of SAM. (B) MS/MS scan of ion with m/z 3119.72 according to ARTD1 peptide 485 – 514 identifying lysine 508 as the methylated residue. (C) Dot blot with non methylated (nm) and methylated (met) ARTD1 peptides at the indicated concentrations. Two different antibody batches were tested. (D) Validation of a peptide specific antibody directed against the methylated K508 in ARTD1. A specific signal for K508 ARTD1 methylation was observed upon *in vitro* methylation with WT SET7/9.

Figure S3. (A) Schematic representation of the ARTD1 domain structure and the important methylation, sumoylation, acetylation and ADP-ribosylation sites in the automodification domain of ARTD1. (B-C) ARTD1 knockout MLFs were stably complemented with WT ARTD1 or two methylation deficient mutants. Cells were then fractionated and cytoplasmic (CE) and nuclear extracts (NE) were analyzed by Western blot. (B) Quantification of ARTD1 activity in NE of complemented MLFs (shown in Figure 4B). (C) Quantification of ARTD1 activity in NE from complemented MLFs in presence of 5 pmol activating DNA (shown in Figure 4C). (D) Recruitment of WT and K508R ARTD1 to sites of local DNA damage induced by femtosecond laser irradiation at λ = 1050 nm.

Fig.1 Kassner et al.

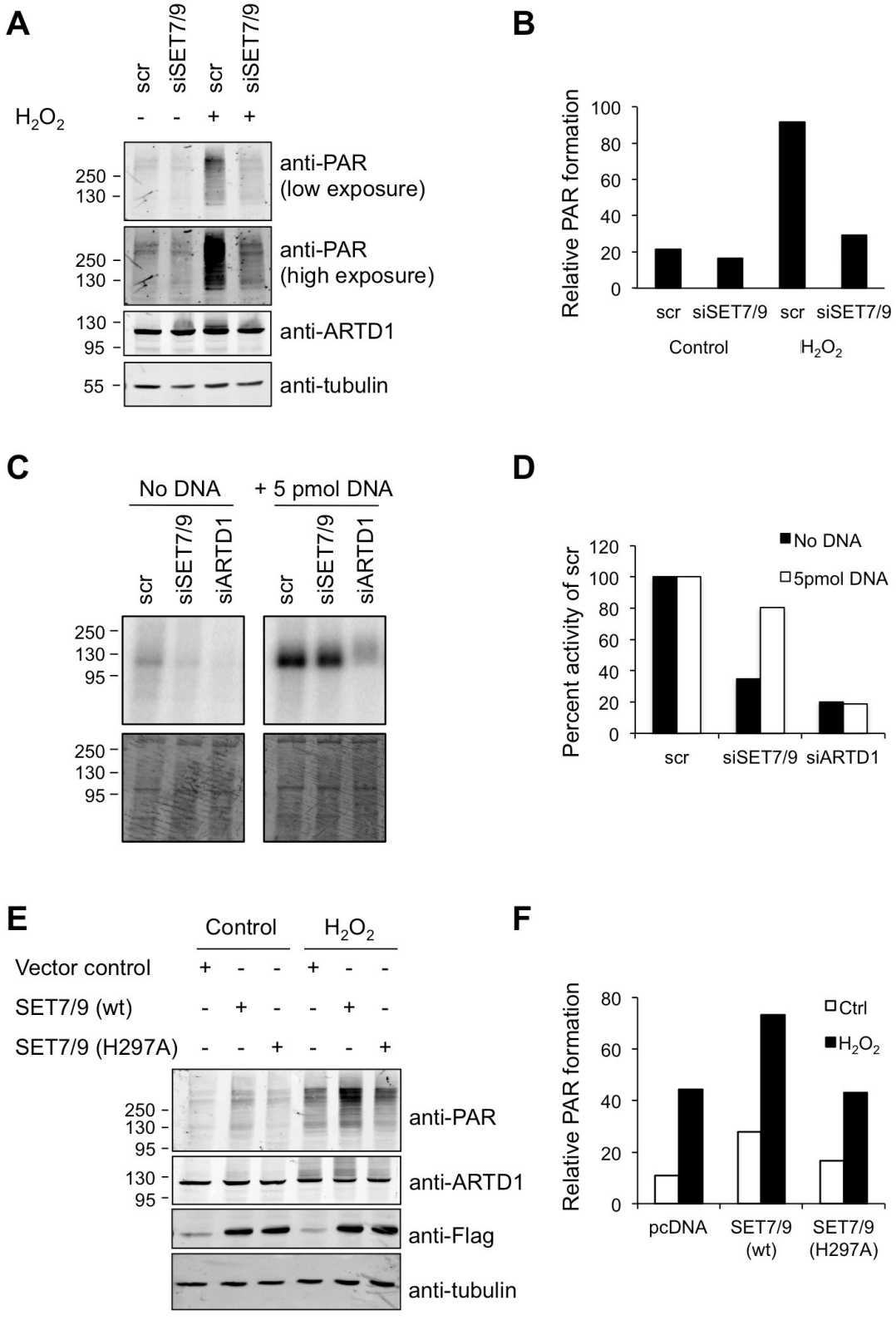

Fig.2 Kassner et al.

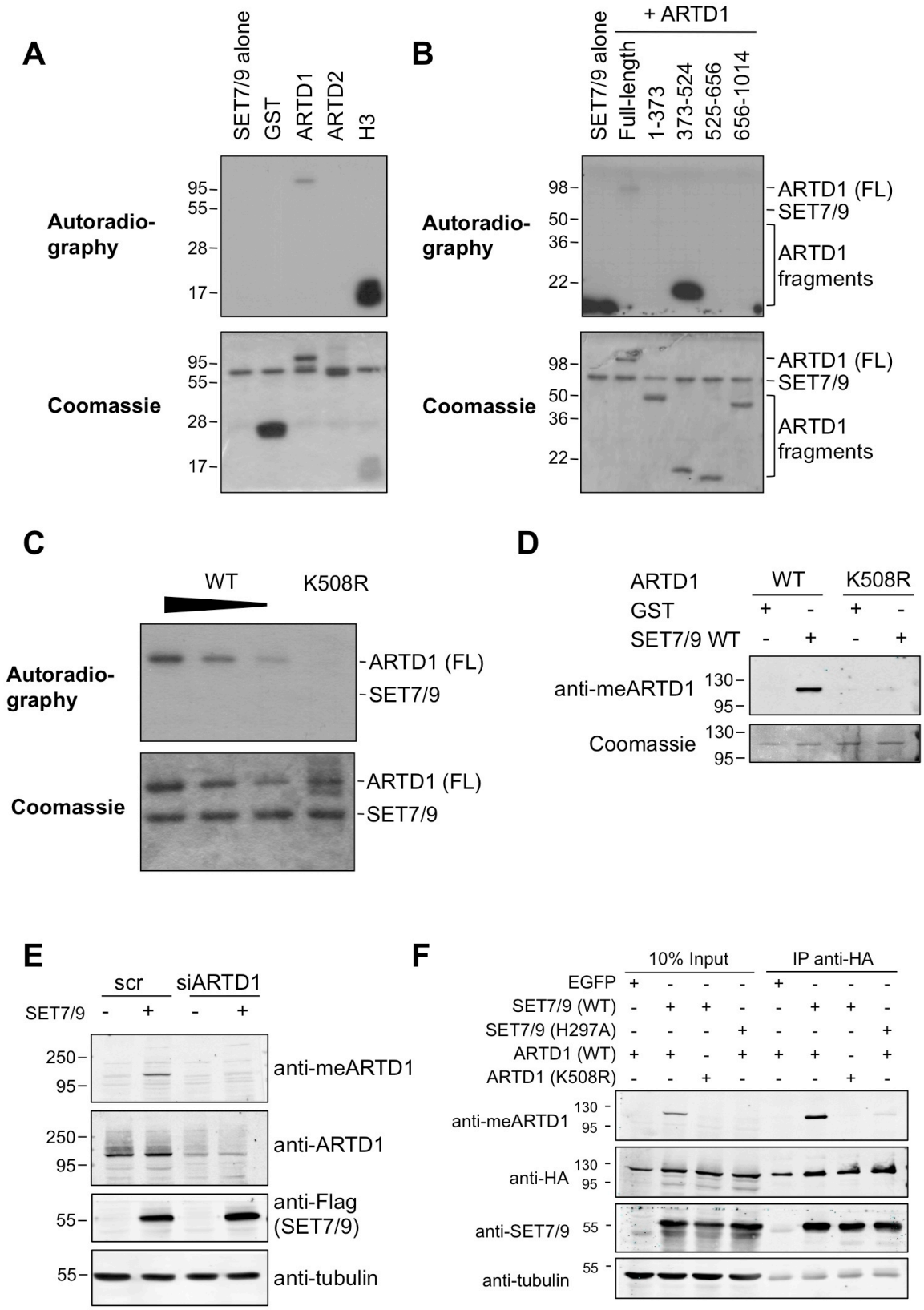

Fig.3 Kassner et al.

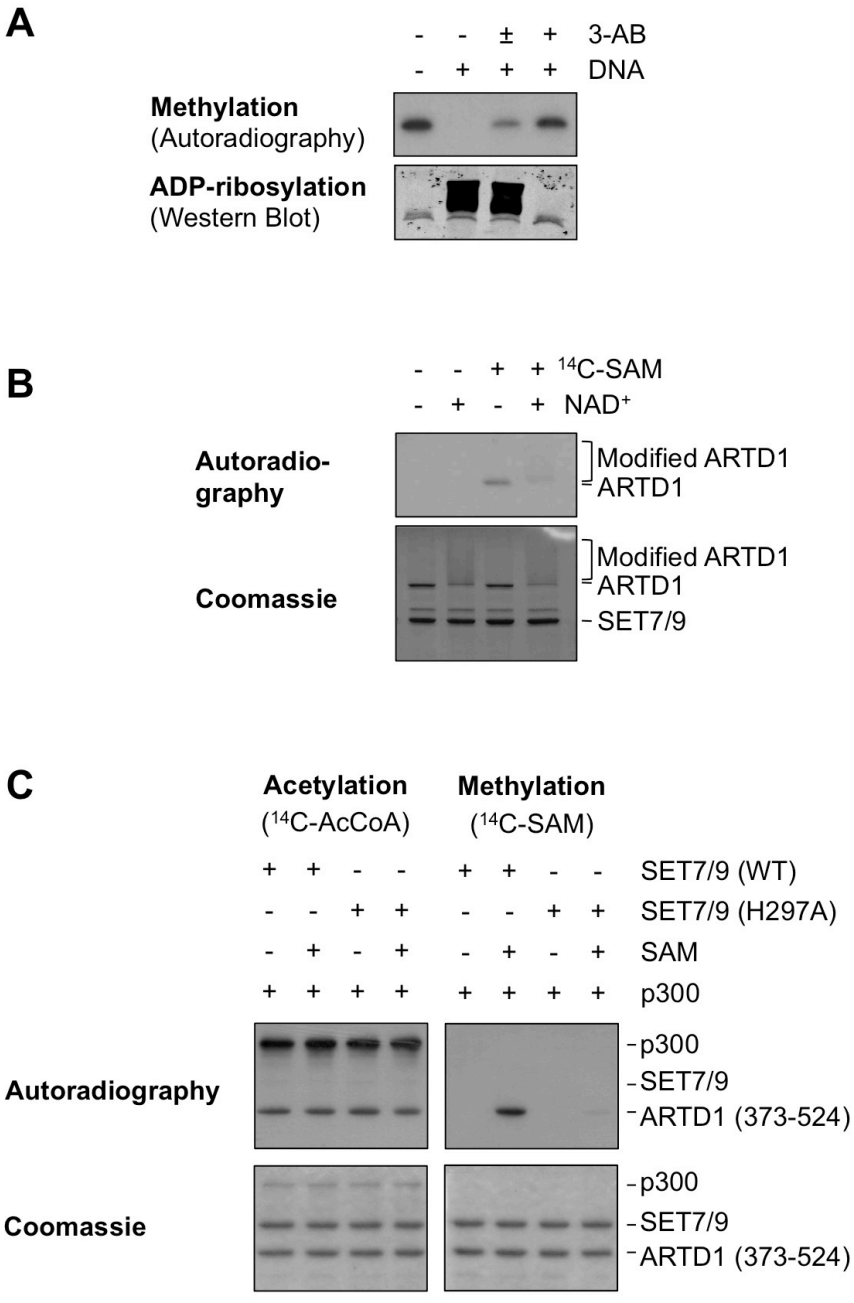

Fig.4 Kassner et al.

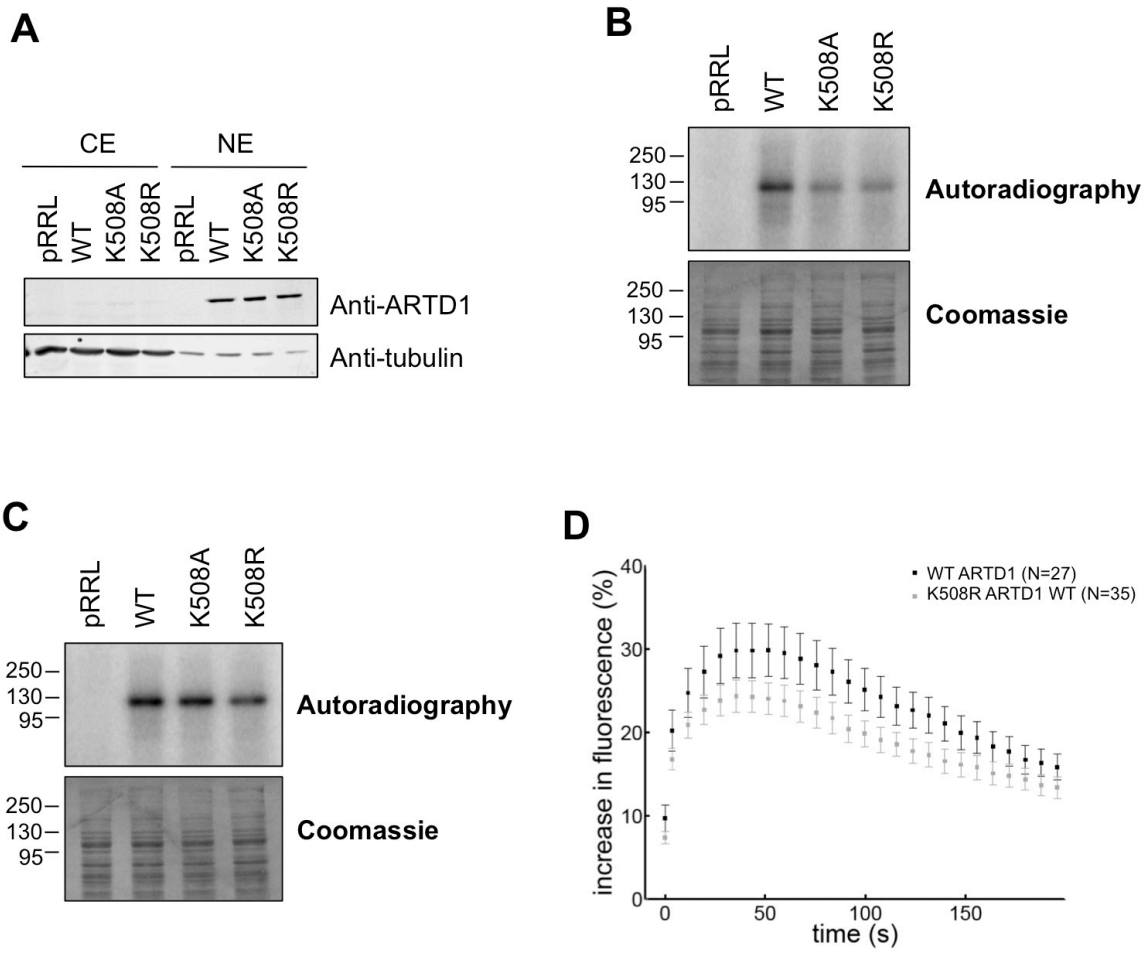

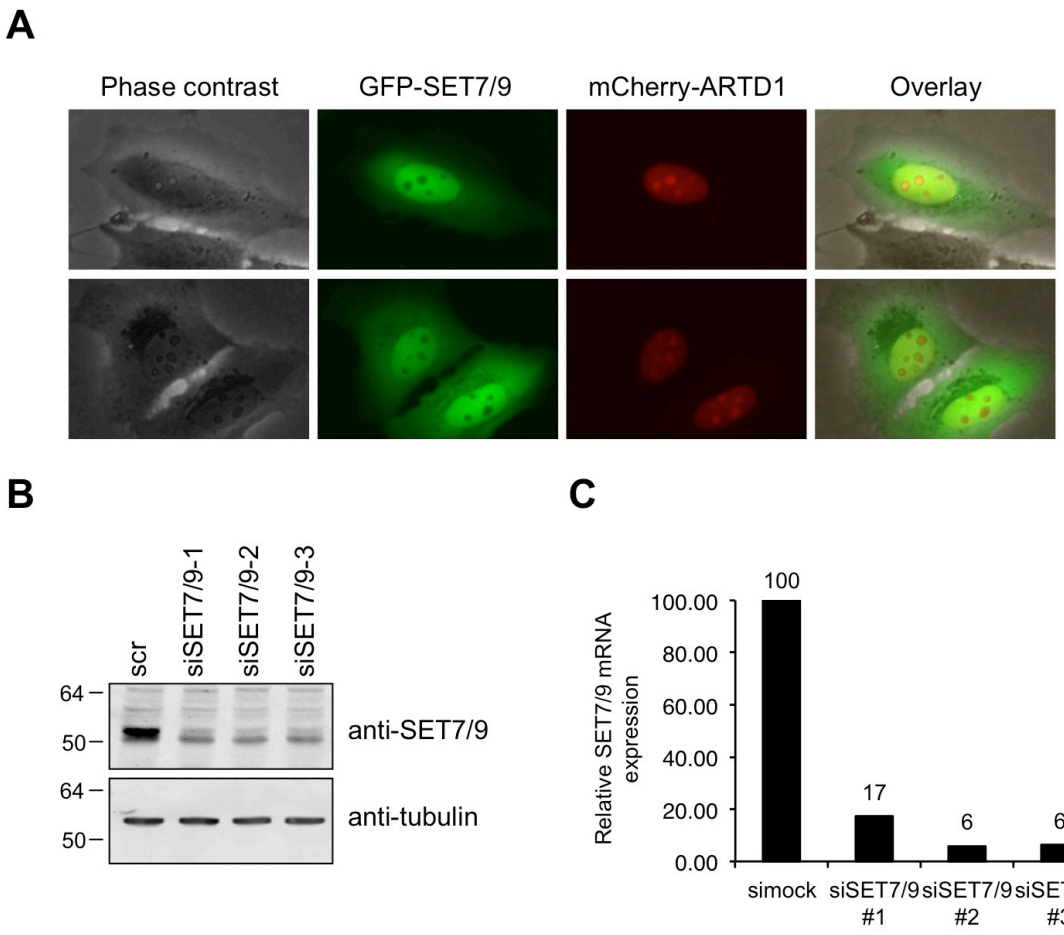
A
Phase contrast
GFP-SET7/9
mCherry-ARTD1
Overlay
B
scr
siSET7/9-1
siSET7/9-2
siSET7/9-3
64
50
anti-SET7/9
64
50
anti-tubulin
C
Relative SET7/9 mRNA expression
100.00
80.00
60.00
40.00
20.00
0.00
100
17
6
6
simock
siSET7/9 #1
siSET7/9 #2
siSET7/9 #3
D
increase in fluorescence (%)
40
30
20
10
0
control (N=45)
siSET7/9 (N=32)
0
50
100
150
time (s)

A

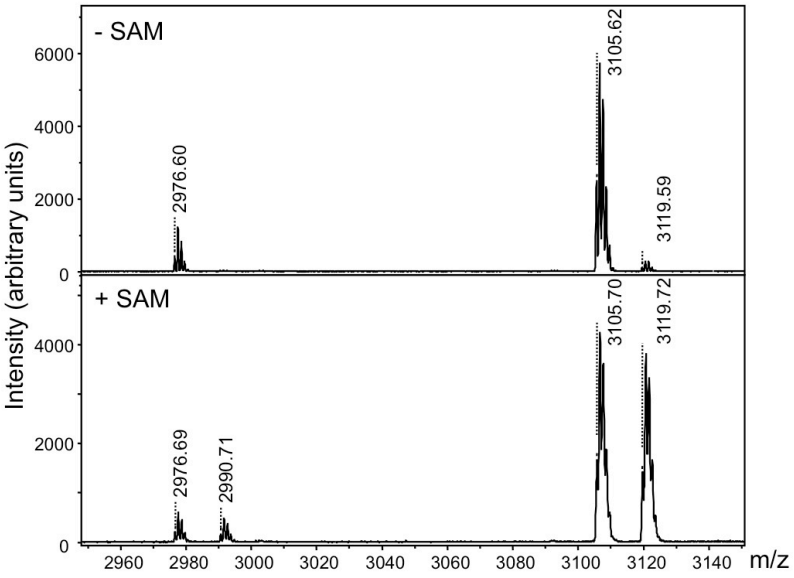

B

485 V K A E P V E V V A P R G K S G A A L S K K S K * G Q V K E E 514

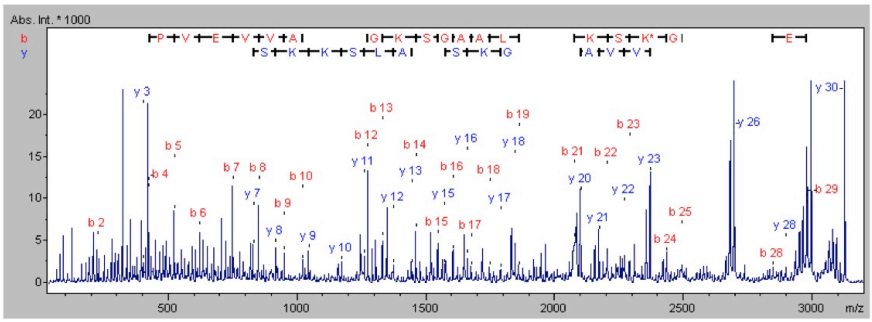

C

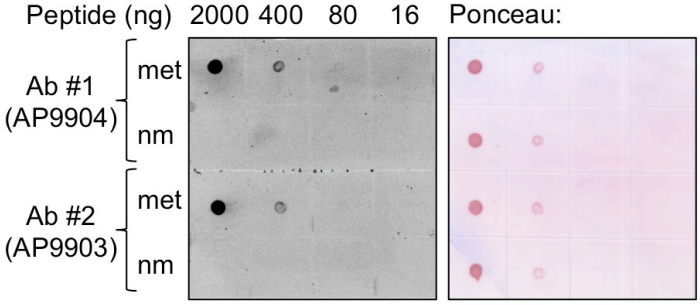

D

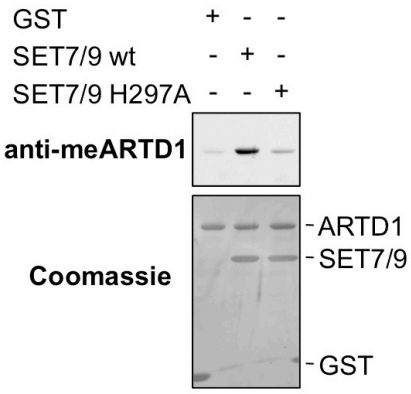

Fig.S3 Kassner et al.

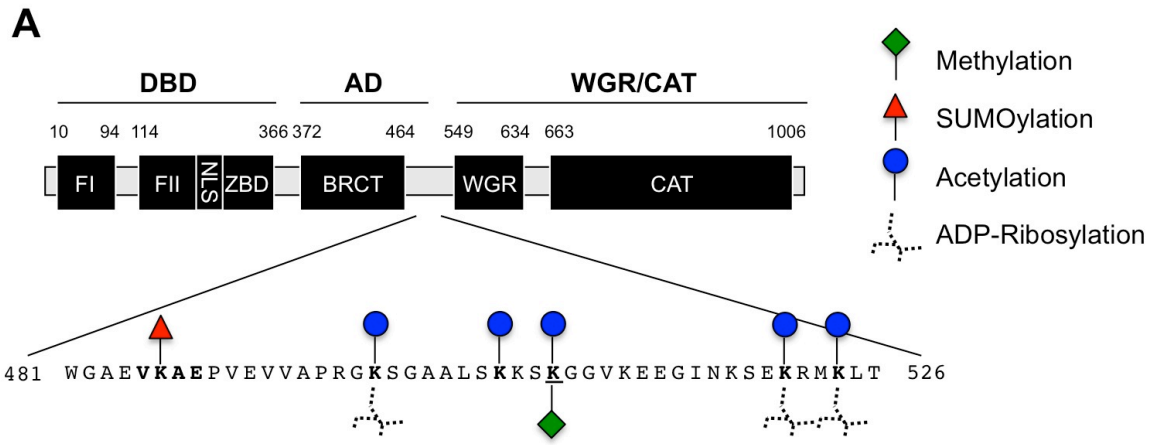

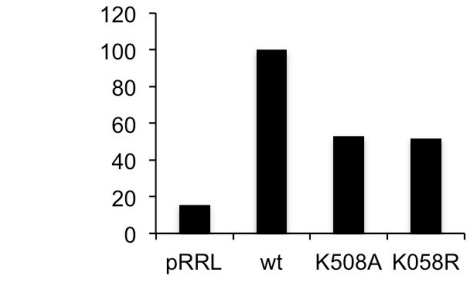

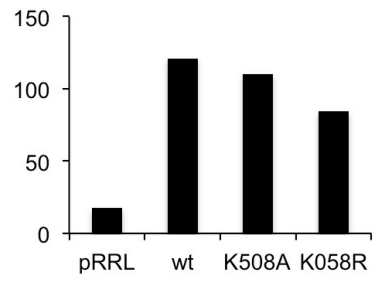

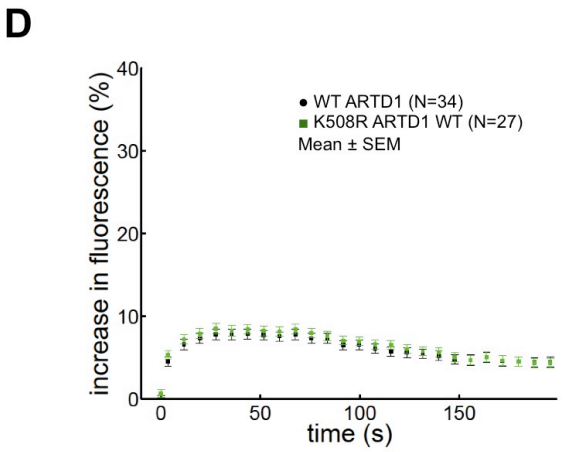

Crosstalk between Set7/9-dependent methylation and ARTD1-mediated ADP-ribosylation of histone H1.4

Ingrid Kassner[1,2], Marc Barandun[1], Monika Fey[1], Michael O. Hottiger[1,*]

[1]Institute of Veterinary Biochemistry and Molecular Biology

University of Zurich, Winterthurerstrasse 190

8057 Zurich, Switzerland

Email: hottiger@vetbio.uzh.ch

[2]Life Science Zurich Graduate School, Molecular Life Science Program,

University of Zurich

*Corresponding author

Running title: Methylation and ADP-ribosylation of linker histone H1.4

ABSTRACT

Crosstalk between different histone post-translational modifications (PTMs) fine-tunes and regulates the cellular response to different external signals. ADP-ribose modification by cellular ADP-ribosyltransferases such as ARTD1 was recently added as a PTM of the histone code. All 5 histone proteins were described to be ADP-ribosylated *in vitro* and *in vivo*. However, the crosstalk of ADP-ribosylation with other modifications is little understood. Here, we identified histone H1.4 as a new target for SET7/9, which is methylated at the last lysine residues of the six KAK motifs in the C-terminal domain (K121, K129, K159, K171, K177 and K192). Interestingly, H1 competed with histone H3, a known SET7/9 target protein, for SET7/9-dependent methylation. Using isolated histones it was found that H3 is preferably ADP-ribosylated, which allowed subsequent methylation of H1. Extended poly-ADP-ribosylation (PARylation) of histones (including H1) by ARTD1 prevented the methylation of H1 by SET7/9, suggesting an interesting mechanism by which ARTD1 activity and the level of histone PARylation influence methylation and potentially other chromatin-associated processes.

Together, these findings illustrate a new function and target for SET7/9-dependent methylation and support the role of ADP-ribosylation as an element of the histone code, which likely regulates chromatin-responses.

Key words: PARP-1, SET7/9, lysine methylation, poly-ADP-ribosylation, post-translational modification

INTRODUCTION

Histones are highly alkaline proteins found in cell nuclei that package and order the DNA into structural units called nucleosomes (Campos & Reinberg, 2009). Five major families of histones exist: H1 (H5), H2A, H2B, H3, and H4. Two copies of the core histones H2A, H2B, H3 and H4 form the octameric nucleosome core particles (Kornberg & Lorch, 1999). Unlike the other histones, only one copy of the linker histone H1 is present and thus stabilizes the DNA, which is wrapped around the core nucleosome (Annunziato, 2008). The H1 linker histone binds to both, the nucleosome and the "linker DNA" (approximately 20-80 nucleotides in length) region between nucleosomes. Many experiments addressing H1 function have been performed with purified, processed chromatin under low-salt conditions, but the *in vivo* role of H1 is less certain. Cellular studies have shown that overexpression of H1 can cause aberrant nuclear morphology and chromatin structure and that depending on the gene H1 can serve as both a positive and negative regulator of transcription (Shen & Gorovsky, 1996). Similar to the core histones, H1 is also composed of three domains (Ramakrishnan et al, 1993). The N-terminus is a short, flexible segment rich in basic amino acids, the central domain exhibits a globular structure composed of a winged helix motif (Ramakrishnan et al, 1993) and the C-terminus is predominantly composed of lysine, alanine and proline residues and is the main determinant for the H1 binding to chromatin (Hendzel et al, 2004). The interaction of H1 with the nucleosome and additional DNA stretches at the entry/exit of the nucleosome forms the chromatosome and leads to higher order chromatin structure (Happel & Doenecke, 2009). Among the five histones of the nucleosome, the linker histone H1 is the least conserved. In the human genome, 11 genes encoding H1 variants have been identified and are transcribed either ubiquitously or in a cell type specific manner (Happel & Doenecke, 2009; Izzo et al, 2008). The study described here focuses on histone H1.4, which represents a histone variant that is expressed in somatic cells during S phase.

Together with H1.2 it is the predominant histone variant in most cell types. Similar to the core histones, linker histones are subject to extensive post-translational modifications (PTMs), including phosphorylations, methylations and acetylations (Raghuram et al, 2009).

SET7/9 (also SET7, SET9, SETD7 or KMT7) is a mono-methyltransferase for lysine at position 4 of histone H3 (H3K4) (Nishioka et al, 2002; Wang et al, 2001) that was linked to transcriptional activation. It methylates the consensus motif [K>R][S>KYARTPN][K_{me}] and prefers lysine residues within positively charged regions (Dhayalan et al, 2011). However, SET7/9 exhibits only weak lysine methyltransferase activity towards H3 in nucleosomes, suggesting that other factors might be involved in SET7/9-dependent H3K4 methylation *in vivo* or that histone proteins are not the main substrates of SET7/9. Lysine methylation can be reversed by demethylases of the LSD family or the Jumonji-C domain family of proteins (Klose & Zhang, 2007; Mosammaparast & Shi, 2010).

In contrast to the canonical PTMs of the histone code such as methylation, ADP-ribosylation is much less studied. ADP-ribosylation comprises the transfer of the ADP-ribose moiety from the co-substrate nicotinamide adenine dinucleotide (NAD^+) onto specific amino acid side chains of acceptor proteins or to pre-existing protein-linked ADP-ribose units by ADP-ribosyltransferases (ARTs). Mammalian ARTs can be divided into two groups according to their similarity to the bacterial diphteria and cholera toxins - the ARTDs and ARTCs, respectively. The ARTDs were formerly known as poly(ADP-ribose) polymerases (PARPs) (Hottiger et al, 2010). ARTD1 (PARP1) is the best-studied member of the ARTD family and represents a highly abundant (on average 1 x 10^6 molecules per cell), nuclear, chromatin-associated enzyme that is responsible for most (about 90%) of the cellular PAR generation (D'Amours et al, 1999; Yamanaka et al, 1988). It is implicated in many and different cellular processes such as the DNA damage response, cell cycle regulation, gene expression, differentiation and aging. The major target of ARTD1 is ARTD1 itself, but it also modifies

other nuclear proteins including all five histone proteins *in vitro* and *in vivo* (Hottiger, 2011). In native chromatin, histone H1 is the main ADP-ribose acceptor, but depending on the chromatin composition and the accessibility of different histones, the ADP-ribosylation pattern of histones varies (Adamietz & Hilz, 1976; Huletsky et al, 1989). The identity of the ADP-ribose acceptor sites has been debated extensively and different amino acids have been put forward as ADP-ribose acceptors. More recently glutamate and lysine residues were identified as ADP-ribose acceptor sites based on mass spectrometry (Altmeyer et al, 2009; Tao et al, 2009). Importantly, mass spectrometry and electron-transfer dissociation (ETD) identified for the first time, lysine K13 of histone H2A, K30 of H2B, K27 and K37 of H3 as well as K16 of H4 as ADP-ribose acceptor sites (catalysed by ARTD1) (Messner et al, 2010). Crosstalk between different PTMs occurs directly by competition for acceptor sites or indirectly by changes in the accessibility of chromatin for modifying enzymes. The observation that specific lysine residues serve as ADP-ribose acceptors is important because the same amino acid residues are potential acetylation and methylation sites (Kouzarides, 2007). It is therefore likely that competition for acceptor sites between different histone PTMs such as ADP-ribosylation, acetylation, methylation and phosphorylation causes crosstalk (Hottiger, 2011). This has been demonstrated by the finding that acetylation of lysine residue K16 of histone H4 inhibits ADP-ribosylation *in vitro* (Messner et al, 2010), which suggests that different crosstalk likely exists *in vivo* as well. Similarly, H1.4 K26 dimethylation and AuroraB-mediated phosphorylation of S27 have been reported to interfere with each other (Hergeth et al, 2011). Whether or not other modifications of the histone code such as methylations or phosphorylation also crosstalk with ADP-ribosylation has not been studied before.

Here, we define the linker histone H1.4 as a novel target of SET7/9-dependent methylation, identify lysines K121, K129, K159, K171, K177 and K192 as methyl acceptor sites and

describe crosstalk between H1.4 methylation and ADP-ribosylation as well as competition with histone H3 methylation.

RESULTS

The C-terminus of linker histone H1.4 is methylated by SET7/9

In vitro methylation experiments with the histone H3 methyltransferase SET7/9 and ADP-ribosylated histones as acceptors revealed that linker histone H1 was unexpectedly strongly methylated (Figure 1A). Therefore, SET7/9-dependent methylation of the new target H1 was characterized in more detail. Interestingly, full-length histone H1.4 was not methylated in the presence of plasmid DNA, while a H1.4 variant lacking the C-terminus (ΔCT) was not methylated at all (Figure 1B). These results suggested that H1.4 is methylated at the CTD, which was described to bind to DNA, and that SET7/9 likely methylates soluble H1.4 that is not part of the chromatin structure. In order to locate the methylation site in histone H1.4, recombinant, C-terminally truncated, HIS-tagged H1.4 fragments as well as short fragments of the C-terminal domain (CTD) were analyzed (Figure 1C). Full length H1.4 (aa 1-219) was strongly methylated, while partial truncation of the CTD (1-189 or 1-156) caused reduced SET7/9-dependent methylation (Figure 1D). Deletion of the entire CTD (ΔCTD, aa 1-113) completely abolished H1.4 methylation (Figure 1D). To further pinpoint the methylation sites in the H1.4 CTD, three H1.4 fragments covering the whole CTD were expressed as GST-fusion proteins (aa 114-144, 145-189, 190-219, Figure 1C), purified and used in methylation assays. All three fragments were methylated by SET7/9, albeit to different degree (Figure 1E). Fragment 190-219 showed the strongest methylation, while the fragment from amino acids 114-144 showed only weak methylation, suggesting that multiple SET7/9-dependent methylation sites are present in the CTD of H1.4. These results clearly demonstrated that the linker histone H1.4 is methylated by SET7/9 *in vitro*. The differences in the degree of SET7/9-dependent methylation of different H1.4 fragments indicated multiple methylation sites in the H1.4 CTD.

Linker histone H1.4 is methylated at six lysine residues of the C-terminal domain

In order to define all SET7/9 methylation sites of the H1.4 CTD, the three fragments (114-144, 145-189, 190-219) were further mutagenized. Since the strongest methylation was seen for fragments 145-189 and 190-219, these peptides were subjected to a cluster mutation approach. Seven sequence clusters that comprised all potential lysine methylation sites were defined and in each of these seven clusters all lysines were mutated to arginines (Figure S1A). Of the seven cluster mutants, methylation of the cluster 4 and cluster 6 mutant proteins was comparable to the wildtype protein (Figure S1B), which indicated that the lysine residues located in these two clusters are not methylated by SET7/9. The remaining clusters 1, 2, 3, 5 and 7, as well as the fragment 114-144 were computationally analyzed in order to identify putative SET7/9 target site matching the [KR][STA]K consensus motif for SET7/9-dependent methylation (Couture et al, 2006). This *in silico* analysis identified six lysines at positions 121, 129, 159, 171, 177 and 192, which all represented the last lysine of the KAK* motif (Figure S1A).

Only the mutation of all three lysines (K159, K171, K177) of the fragment 145-189 completely abolished methylation of the protein fragment (Figure S1C). Similarly, the K192R mutation abrogated the SET7/9-dependent methylation of the fragment 190-219 (Figure S1D). Interestingly, combination of the K159R, K171R, K177R and K192R mutations in full-length H1.4 did not completely prevent its methylation (Figure 2). Only upon the additional mutation of K121 and K129 of the fragment 114-144 to arginines, SET7/9-dependent methylation of full-length H1.4 could no longer be observed (Figure 2). The mapping of the methylation sites in the H1.4 CTD thus identified the KAK* motif and the six lysines K121, K129, K159, K171, K177 and K192 as the targets for SET7/9-dependent methylation of this linker histone variant.

Poly-ADP-ribosylation of histones prevents methylation by SET7/9

Besides its originally described target histone H3, SET7/9 also methylates H1.4 and non histone proteins. Interestingly, ARTD1 is methylated at lysine K508 by SET7/9, which enhances its enzymatic activity and which is inhibited by ARTD1 auto-PARylation (Kassner et al). It was therefore tested if PARylation of core histones also impairs consecutive SET7/9-dependent methylation. Calf histones were PARylated for different time periods and then subjected to methylation assays with SET7/9 and radio-labelled S-adenosyl-L-[methyl-^{14}C]methionine (^{14}C-SAM) as methyl donor. In the absence of PARylation, mainly core histones were methylated, while only a faint signal was observed for the linker histone H1 (Figure 3A). A short PARylation reaction strongly reduced the consecutive methylation of core histones, while H1 methylation was drastically increased. More extensive PARylation (> 2 min) prevented methylation of both, core and linker histones. These results confirmed that core and linker histones are methylated by SET7/9 and suggested strong crosstalk and competition between methylation and PARylation and between core and linker histones.

SET7/9 was described as a specific histone H3 methyltransferase (Nishioka et al, 2002; Wang et al, 2001). In order to elucidate the nature of the competition and crosstalk described above, PARylation and methylation of the histones H3 and H1 were therefore studied in more detail. Recombinant H3 or a mixture of H1 was incubated with ARTD1, NAD^+ and with or without DNA (to stimulate ARTD1) and 3-AB (to inhibit ARTD1). Both, H3 and H1 were methylated if ARTD1 was inactive due to the lack of stimulation by DNA (lane 1) or because of inhibition by 3-AB (lane 4) (Figure 3B, C). PARylation of SET7/9 was not the cause for this effect, because the methyltransferase was only added after the PARylation reaction and addition or omission of 3-AB did not affect the result (Figure 3C, lanes 2 and 3). The addition of previously PARylated ARTD1 to H1 methylation reactions did not inhibit SET7/9 activity (Figure 3D). These results suggested that H1.4 and H3 are only methylated by SET7/9 in the

absence of PARylation and that ARTD1-dependent PARylation might modulate which histone protein is methylated. To test this hypothesis, *in vitro* competition experiments with or without PARylation of H1.4 and H3 were performed. As shown before (Figure 3B, C), H1 and H3 were strongly methylated by SET7/9 if present alone (Figure 4, lanes 1 and 5). However, H1 and H3 competed with each other when present in the same reaction and thus lead to a reduced methylation signal (lanes 2-4). Prior PARylation of histone H3 completely abolished its competing activity for SET7/9-dependent H1 methylation (lanes 6-7).

It was thus concluded that PARylation of H1 and H3 by ARTD1 abolishes consecutive SET7/9-dependent methylation and that non-PARylated H1.4 and H3 compete for SET7/9. These results suggest that differential PARylation of histone proteins by ARTD1 can indirectly influence histone methylation and thus the histone code by determining which target proteins are modified.

DISCUSSION

This study describes the linker histone H1.4 as a new target for the H3K4 mono-methyltransferase SET7/9. Full-length histone H1.4 was methylated by SET7/9 at the lysine residues K121, K129, K159, K171, K177 and K192 of the KAK motifs of the CTD, which suggests a strong preference of SET7/9 for this recognition sequence. However, some of the KAK motifs seemed preferentially methylated, which may indicate a sequential modification of the different acceptor sites or indicate differences in the accessibility of the different methylation sites.

The addition of plasmid DNA abolished SET7/9-dependent methylation of target proteins, indicating that incorporation into the nucleosome structure and DNA binding may prevent methylation. This could be explained by DNA-induced conformational changes of the H1 CTD and by charge neutralization through DNA, as SET7/9 is known to prefer lysine residues in a positively charged context. Likewise, methylation may directly influence the binding of H1 to DNA and its function in chromatin compaction, especially as the six lysine residues targeted by SET7/9 all reside in the CTD of H1.4, which is important for chromatin binding (Caterino & Hayes, 2011). These findings may indicate that the SET7/9-dependent methylation regulates free histones and possibly their turnover and exchange, which extends the scope of the histone code outside of the chromatin realm.

Covalent histone modifications can alter chromatin structure and thereby define transcriptionally active or inactive states of chromatin (Jenuwein & Allis, 2001). Compared with core histones, little is known about the modifications and the corresponding modifiers of the linker histones. One possible function of H1 methylation by SET7/9 might thus be the stimulation or repression of other post-translational modifications. Crosstalk between K26 dimethylation and AuroraB-mediated phosphorylation of S27 has been reported previously (Hergeth et al, 2011). In addition, the H1.4 CTD is the target of acetylation, ADP-

ribosylation and phosphorylation (Ogata et al, 1980; Wisniewski et al, 2007). Interestingly, the four last KAK motifs, which displayed the strongest methylation in *in vitro* methylation assays with SET7/9, are located in close proximity to well-known CDK phosphorylation sites and two acetylated lysine residues (Figure 5A), which suggests the potential for significant crosstalk between acetylation, methylation and phosphorylation. Two of the sites in this region, S172 and S187, are not exclusively phosphorylated during mitosis and their phosphorylation in interphase correlated with transcription and chromatin relaxation (Zheng et al, 2010). These results indicate that significant crosstalk between different histone modifications of H1.4 may fulfill important functions. However, in most cases the modifying enzymes are currently not known and thus the biological and cellular functions of these modifications have not been elucidated in detail yet.

ARTD1 and histone ADP-ribosylation were previously suggested as components of the histone code (Hottiger, 2011; Messner & Hottiger, 2011). The results described here provide a further line of evidence for this hypothesis. We show that ARTD1-dependent PARylation of histones influences their subsequent methylation by SET7/9. Compared to phosphorylation, which strongly reduces methylation if in proximity of SET7/9 target lysine residues (Dhayalan et al, 2011), PARylation is a much more bulky modification with more negative charges and therefore also inhibited histone methylation by SET7/9. Based on our experiments, we know that SET7/9 methylates both, H1 and H3. Yet, when both histones are present, H3 is preferred over H1. Strikingly, PARylation did not merely inhibit SET7/9-dependent methylation of histones, but completely shifted its substrate-specificity from H3 to H1 (Figure 5B). These observations could be explained by sequential PARylation events, where ARTD1 modifies H3 before H1. PARylation of H3 would then inhibit its subsequent methylation by SET7/9 and its competition as a SET7/9 target with H1.

This ARTD1-dependent regulation of the substrate specificity of another histone modifying enzyme may be an exciting mechanism to explain how ARTD1 influences chromatin-associated processes such as transcription. It is also important to note that progressive PARylation of histones also inhibited the methylation of H1, documenting that different outcomes for SET7/9-dependent histone methylation can occur depending on the extent of ARTD1 activity.

The complexity of ARTD1-dependent histone modifications is increased by the facts that (1) ARTD1 can modify all core histones and the linker histones (Messner et al, 2010) and (2) the size and quality (e.g. branching or length) of the polymers may differ under varying conditions and depending on the substrate histone. Therefore, future studies should not merely focus on the influence of ARTD1 and PARylation on other histone modifications but also on how ARTD1-dependent histone methylation itself is regulated. In this regard, it will also be interesting to investigate if SET7/9-dependent ARTD1 methylation may influence its substrate choice and trans-PARylation activities.

MATERIAL and METHODS

Plasmids and protein expression

pGEX-SET7/9 (52-366) and pET28b-H1.4 (fl) bacterial expression vectors were kind gifts from D. Reinberg and R. Schneider, respectively. H1.4 full-length and deletions mutants were subcloned into pET-28a to add the N-terminal His-tag. C-terminal H1.4 fragments were cloned into pGEX6P1. All point mutations were inserted by site-directed mutagenesis. Cluster mutants were created by overlapping PCR with the corresponding primers.

The baculovirus expression vector BacPak8 (Clontech, Mountain View, CA, USA) was used for the expression of recombinant ARTD1 in Sf21 insect cells, as described previously (Hassa et al, 2003). GST- and His-tagged histone proteins were expressed in *E.coli*. All recombinant proteins were purified by a one step affinity chromatography using ProBond resin (Invitrogen) for His-tagged and glutathione sepharose (GE Healthcare) for GST-tagged proteins, according to the manufacturer‘s recommendations. His-H1.4(fl) proteins were purified as described elsewhere (Weiss et al, 2010).

Reagents

Lyophilized histones or H1 mix from calf thymus was purchased from Roche and resolubilized in water. Recombinant H3 was a kind gift from T. J. Richmond. 3-AB (Sigma-Aldrich) was prepared freshly in water.

In vitro methylation assays

If not stated otherwise, approximately 1 µg histone proteins were incubated with 1 µg bacterially purified GST-SET7/9 in presence of 0.03 µCi [^{14}C]-SAM (PerkinElmer) in methylation buffer (50 mM Tris-HCl pH8.0, 50 mM NaCl, 10% glycerol, 1 mM PMSF, 1 mM DTT) for 10 to 60 min at 30°C in a 25µl reaction. For DNA inhibition assays, histones

were preincubated with or without 0.5 µg plasmid DNA (pcDNA) and then methylated for 15 min. Reactions were stopped by addition of 10X SDS-loading buffer, boiled and separated by SDS-PAGE. Gels were stained with Coomassie Blue, incubated in 1 M sodium salicylate for 20 min, dried, and exposed on X-ray films at -80° C.

Sequential ADP-ribosylation and methylation assays

Sequential modification assays were performed in PAR buffer (50 mM Tris-HCl, 50 mM NaCl, 4 mM $MgCl_2$, 250 µM DTT, 1 mg/ml pepstatin, 1 mg/ml bestatin, 1 mg/ml leupeptin). 10 pmol ARTD1 was incubated with or without 2.5 µg histone mix or 1 µg individual histones in presence or absence of 5 pmol activating DNA and 160 µM NAD^+ (Sigma-Aldrich) for 15 min at 30°C. 8 mM 3-AB (Sigma-Aldrich) or 0.2 mM PJ-34 were added to inhibit ARTD1 activity either before the ADP-ribosylation or afterwards where indicated. The methylation was then started by addition of 1 µg SET7/9 and 0.03 µCi [^{14}C]-SAM and allowed to proceed for 1hr at 30°C. Autoradiography was performed as described above. The activating DNA used in all assays was an annealed double-stranded oligomer (5'-GGAATTCC-3').

SUPPLEMENTAL DATA

Supplemental material includes 3 supplementary figures.

ACKNOWLEDGEMENTS

We thank Danny Reinberg (Howard Hughes Medical Institute, NYU School of Medicine, New York, USA) for providing SET7/9 and Robert Schneider (Max-Planck Institute of Immunobiology and Epigenetics, Freiburg, Germany) for helpful advice. We are grateful to Florian Freimoser and all the members of the Institute of Veterinary Biochemistry and

Molecular Biology (University of Zurich, Switzerland) for helpful advice and discussions. This work was supported Swiss National Science Foundation Grants 31003A-122421 and 310030B-138667 (to MOH) and the Kanton of Zurich (to MOH).

AUTHOR CONTRUBUTIONS

IK and MOH designed the experiments; IK and MB performed experiments; MOH designed and supervised the study. IK and MOH wrote the manuscript. All the authors read and agreed with the manuscript. The authors declare that they have no conflict of interest.

REFERENCES

Adamietz P, Hilz H (1976) Poly(adenosine diphosphate ribose) is covalently linked to nuclear proteins by two types of bonds. *Hoppe-Seyler's Z Physiol Chem* **357:** 527-534

Altmeyer M, Messner S, Hassa P, Fey M, Hottiger M (2009) Molecular mechanism of poly(ADP-ribosyl)ation by PARP1 and identification of lysine residues as ADP-ribose acceptor sites. *Nucleic Acids Res* **37:** 3723-3738

Annunziato AT (2008) DNA packaging: Nucleosomes and chromatin. *Nature Education* **1(1)**

Campos E, Reinberg D (2009) Histones: Annotating Chromatin. *Annu Rev Genet*

Caterino TL, Hayes JJ (2011) Structure of the H1 C-terminal domain and function in chromatin condensation. *Biochemistry and cell biology = Biochimie et biologie cellulaire* **89:** 35-44

Couture JF, Collazo E, Hauk G, Trievel RC (2006) Structural basis for the methylation site specificity of SET7/9. *Nature Structural & Molecular Biology* **13:** 140-146

D'Amours D, Desnoyers S, D'Silva I, Poirier GG (1999) Poly(ADP-ribosyl)ation reactions in the regulation of nuclear functions. *The Biochemical journal* **342 (Pt 2):** 249-268

Dhayalan A, Kudithipudi S, Rathert P, Jeltsch A (2011) Specificity Analysis-Based Identification of New Methylation Targets of the SET7/9 Protein Lysine Methyltransferase. *Chemistry & Biology* **18:** 111-120

Happel N, Doenecke D (2009) Histone H1 and its isoforms: contribution to chromatin structure and function. *Gene* **431:** 1-12

Hassa P, Buerki C, Lombardi C, Imhof R, Hottiger M (2003) Transcriptional coactivation of nuclear factor-kappaB-dependent gene expression by p300 is regulated by poly(ADP)-ribose polymerase-1. *J Biol Chem* **278:** 45145-45153

Hendzel MJ, Lever MA, Crawford E, Th'ng JP (2004) The C-terminal domain is the primary determinant of histone H1 binding to chromatin in vivo. *J Biol Chem* **279:** 20028-20034

Hergeth SP, Dundr M, Tropberger P, Zee BM, Garcia BA, Daujat S, Schneider R (2011) Isoform-specific phosphorylation of human linker histone H1.4 in mitosis by the kinase Aurora B. *J Cell Sci* **124:** 1623-1628

Hottiger M, Hassa P, Lüscher B, Schüler H, Koch-Nolte F (2010) Toward a unified nomenclature for mammalian ADP-ribosyltransferases. *Trends Biochem Sci* **35:** 208-219

Hottiger MO (2011) ADP-ribosylation of histones by ARTD1: An additional module of the histone code? *FEBS letters* **585:** 1595-1599

Huletsky A, de Murcia G, Muller S, Hengartner M, Ménard L, Lamarre D, Poirier G (1989) The effect of poly(ADP-ribosyl)ation on native and H1-depleted chromatin. A role of poly(ADP-ribosyl)ation on core nucleosome structure. *J Biol Chem* **264:** 8878-8886

Izzo A, Kamieniarz K, Schneider R (2008) The histone H1 family: specific members, specific functions? *Biological chemistry* **389:** 333-343

Jenuwein T, Allis CD (2001) Translating the histone code. *Science* **293:** 1074-1080

Kassner I, Fey M, Tomas M, Ferrando-May E, Hottiger MO SET7/9-dependent methylation of ARTD1 at K508 enhances DNA-mediated poly-ADP-ribose formation. **submitted for publication**

Klose RJ, Zhang Y (2007) Regulation of histone methylation by demethylimination and demethylation. *Nature reviews Molecular cell biology* **8:** 307-318

Kornberg RD, Lorch Y (1999) Twenty-five years of the nucleosome, fundamental particle of the eukaryote chromosome. *Cell* **98:** 285-294

Kouzarides T (2007) Chromatin modifications and their function. *Cell* **128:** 693-705

Messner S, Altmeyer M, Zhao H, Pozivil A, Roschitzki B, Gehrig P, Rutishauser D, Huang D, Caflisch A, Hottiger M (2010) PARP1 ADP-ribosylates lysine residues of the core histone tails. *Nucleic Acids Res* **38:** 6350-6362

Messner S, Hottiger MO (2011) Histone ADP-ribosylation in DNA repair, replication and transcription. *Trends Cell Biol* **21:** 534-542

Mosammaparast N, Shi Y (2010) Reversal of histone methylation: biochemical and molecular mechanisms of histone demethylases. *Annual review of biochemistry* **79:** 155-179

Nishioka K, Chuikov S, Sarma K, Erdjument-Bromage H, Allis CD, Tempst P, Reinberg D (2002) Set9, a novel histone H3 methyltransferase that facilitates transcription by precluding histone tail modifications required for heterochromatin formation. *Genes & Development* **16:** 479-489

Ogata N, Ueda K, Kagamiyama H, Hayaishi O (1980) ADP-ribosylation of histone H1. Identification of glutamic acid residues 2, 14, and the COOH-terminal lysine residue as modification sites. *J Biol Chem* **255:** 7616-7620

Raghuram N, Carrero G, Th'ng J, Hendzel MJ (2009) Molecular dynamics of histone H1. *Biochemistry and cell biology = Biochimie et biologie cellulaire* **87:** 189-206

Ramakrishnan V, Finch JT, Graziano V, Lee PL, Sweet RM (1993) Crystal structure of globular domain of histone H5 and its implications for nucleosome binding. *Nature* **362:** 219-223

Shen X, Gorovsky MA (1996) Linker histone H1 regulates specific gene expression but not global transcription in vivo. *Cell* **86:** 475-483

Tao Z, Gao P, Liu H (2009) Identification of the ADP-Ribosylation Sites in the PARP-1 Automodification Domain: Analysis and Implications. *J Am Chem Soc*

Wang H, Cao R, Xia L, Erdjument-Bromage H, Borchers C, Tempst P, Zhang Y (2001) Purification and functional characterization of a histone H3-lysine 4-specific methyltransferase. *Mol Cell* **8:** 1207-1217

Weiss T, Hergeth S, Zeissler U, Izzo A, Tropberger P, Zee BM, Dundr M, Garcia BA, Daujat S, Schneider R (2010) Histone H1 variant-specific lysine methylation by G9a/KMT1C and Glp1/KMT1D. *Epigenetics Chromatin* **3:** 7

Wisniewski JR, Zougman A, Kruger S, Mann M (2007) Mass spectrometric mapping of linker histone H1 variants reveals multiple acetylations, methylations, and phosphorylation as well as differences between cell culture and tissue. *Molecular & cellular proteomics : MCP* **6:** 72-87

Yamanaka H, Penning CA, Willis EH, Wasson DB, Carson DA (1988) Characterization of human poly(ADP-ribose) polymerase with autoantibodies. *The Journal of biological chemistry* **263:** 3879-3883

Zheng Y, John S, Pesavento JJ, Schultz-Norton JR, Schiltz RL, Baek S, Nardulli AM, Hager GL, Kelleher NL, Mizzen CA (2010) Histone H1 phosphorylation is associated with transcription by RNA polymerases I and II. *J Cell Biol* **189:** 407-415

FIGURE LEGENDS

Figure 1. Linker histones are methylated by SET7/9. (A) Calf histone mix was first ADP-ribosylated by ARTD1 for 1 min. Then, after addition of PARP inhibitor PJ-34, histones were incubated with SET7/9 in presence of methyl donor [^{14}C]-SAM. Proteins were separated by SDS-PAGE, stained with Coomassie blue (lower panel) and methylation was analyzed by autoradiography (upper pannel). The asterisk marks the shift of automodified ARTD1. (B) His-tagged H1.4 FL and a deletion mutant without the CTD (ΔCTD) were *in vitro* methylated by SET7/9 in the presence or absence of plasmid DNA. (C) Schematic depiction of H1.4 WT protein and constructs. NTD: N-terminal domain, GD: globular domain, CTD: C-terminal domain, ΔCT: H1.4 construct completely lacking the C-terminus. (D) Recombinant His-tagged H1.4 full-length (FL) and deletion mutants were *in vitro* methylated by SET7/9 and analyzed as described in A. (E) H1.4 C-terminal fragments were expressed as GST fusion proteins and *in vitro* methylated by SET7/9. Methylation was analyzed by autoradiography as in A.

Figure 2. Full-length H1.4 is methylated at six lysine residues by SET7/9. Mutation of the four lysine residues K159, K171, K177 and K192 (K4R) in WT H1.4 reduces SET7/9-dependent methylation. The additional mutation of K121 and K129 (K6R) abolishes methylation of full-length H1.4 by SET7/9. The lower panel shows the Coomassie stained gel and methylation is visualized by autoradiography in the upper panel. Of each sample, two elutions were analyzed.

Figure 3. Poly-ADP-ribosylated histones are not methylated by SET7/9. (A) Calf histone mix was first ADP-ribosylated by ARTD1 for the indicated times. Then, after addition of PARP inhibitor PJ-34, histones were incubated with SET7/9 in presence of methyl donor

[^{14}C]-SAM. Proteins were separated by SDS-PAGE, stained with Coomassie blue (bottom) and methylation was analyzed by autoradiography (top). The asterisk marks the shift of automodified ARTD1. (B) H3 was incubated with ARTD1 and 160 μM NAD^+. Activating DNA and PARP inhibitor 3-AB were present during the reaction as indicated. Methylation was then started by addition of SET7/9 and ^{14}C-SAM. ±: 3-AB was added directly before addition of SET7/9 after the PAR reaction. (C) Influence of ARTD1 on H1 methylation as in B. (D) Presence of ADP-ribose polymers or nicotinamide does not disturb H1 methylation by SET7/9. ARTD1 was automodified for the indicated times and then inhibited by addition of 3-AB. H1 was then methylated by SET7/9 in presence of the PAR reactions and ^{14}C-SAM.

Figure 4. H3 and H1 compete for methylation by SET7/9. H1 was methylated in presence of the indicated molar ratios of H3. In lanes 6 and 7, H3 was incubated with ARTD1 and NAD^+ in presence or absence of 3-AB before addition of H1 and the methylation reaction.

Figure 5. (A) Summary of known post-translational modification sites of H1.4. (B) Model of sequential ADP-ribosylation of histone H3 and H1 by ARTD1.

LEGENDS OF SUPPLEMENTARY FIGURES

Figure S1. H1.4 CTD is methylated at KAK* motifs. (A) Amino acid sequences of C-terminal H1.4 fragments. Boxes represent the lysine clusters which were mutated to arginines in B. Grey boxes mark the clusters that markedly influence methylation. KAK* motifs are highlighted in dark grey and the methylated lysines are bold. (B) Cluster mutant approach to identify methylation sites in H1.4 CTD, which contains 43 lysine residues as potential target sites. Clusters were mutated one by one in the corresponding C-terminal fragment and methylation efficiency by SET7/9 was tested *in vitro*. (C) Methylation of C-terminal fragments by SET7/9 was tested *in vitro* after mutation of single lysine residues in KAK* motifs. (D) Methylation of H1.4 (145-189) double and triple mutants by SET7/9.

Fig.1 Kassner et al.

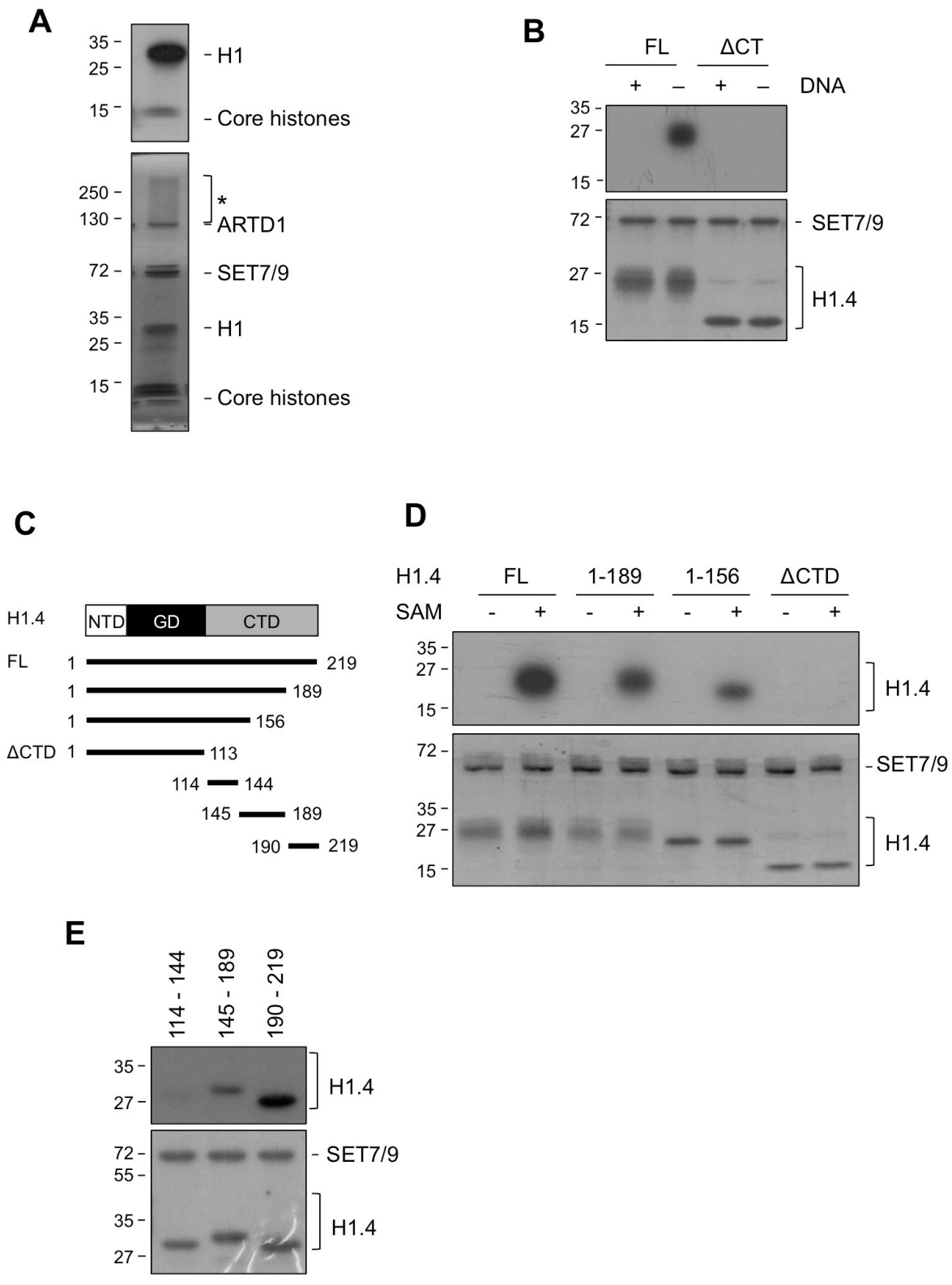

Fig. 2 Kassner et al.

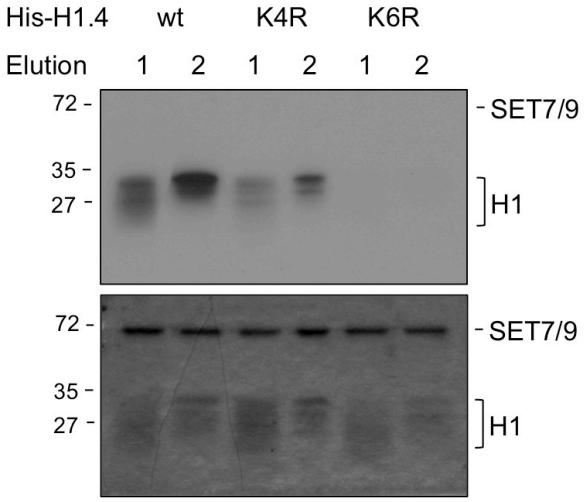

Fig. 3 Kassner et al.

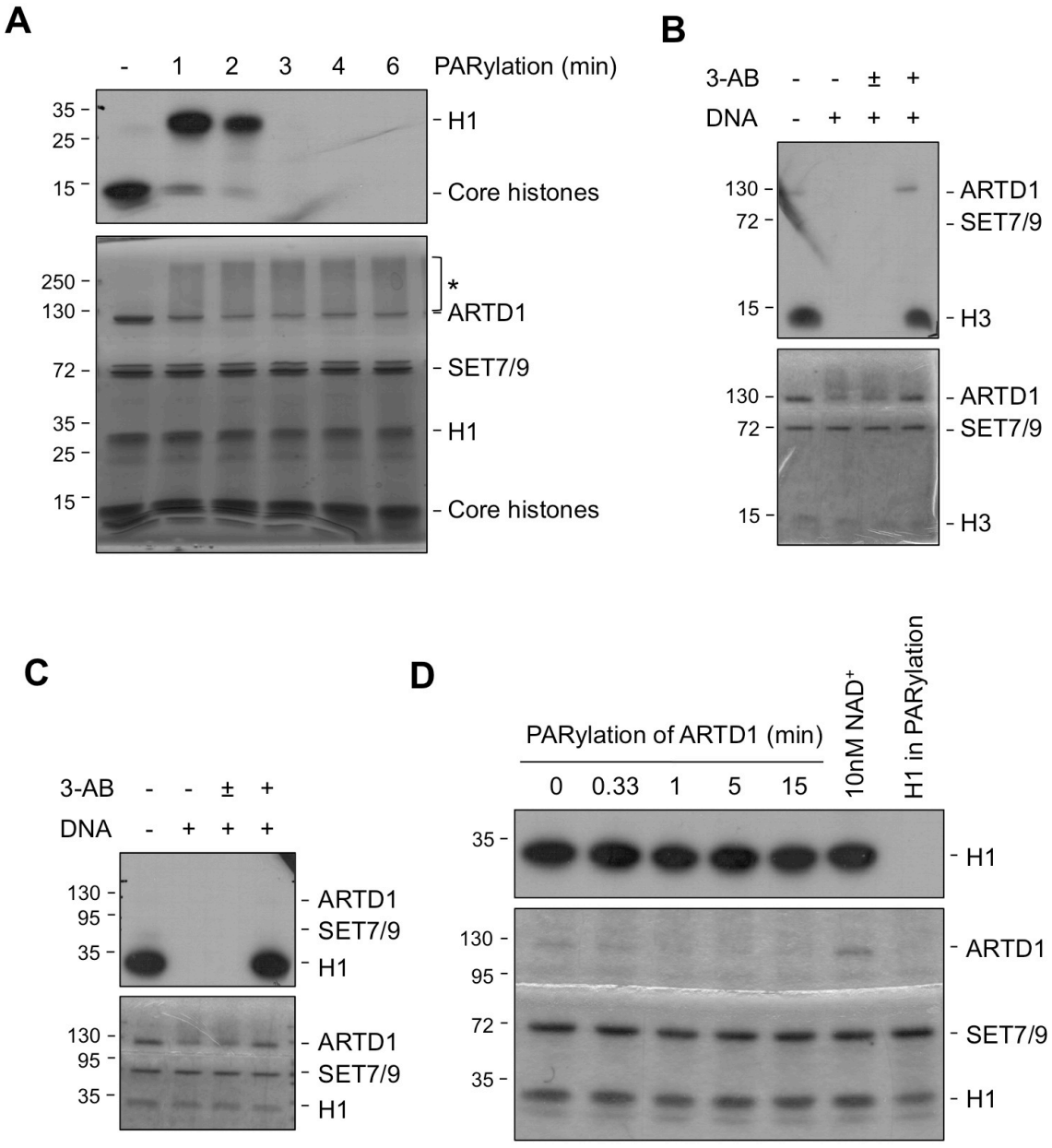

Fig.4 Kassner et al.

A

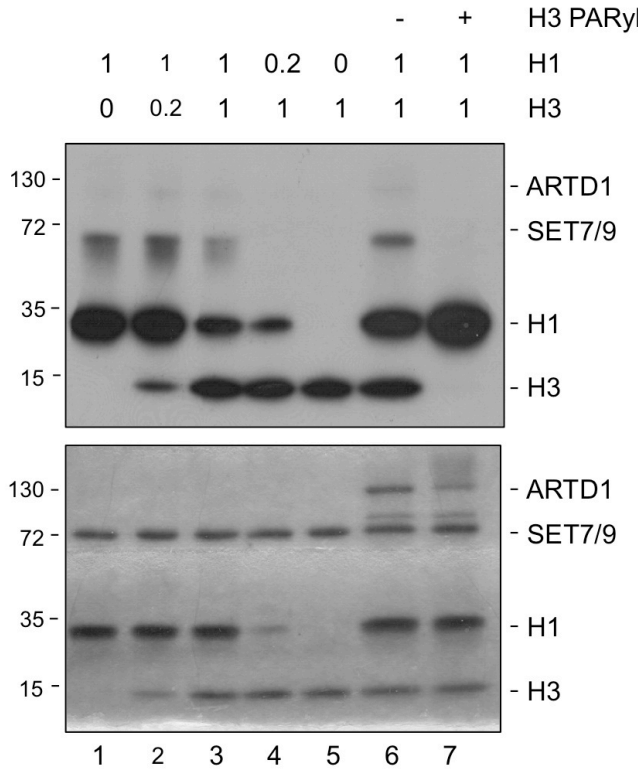

Fig. 5 Kassner et al.

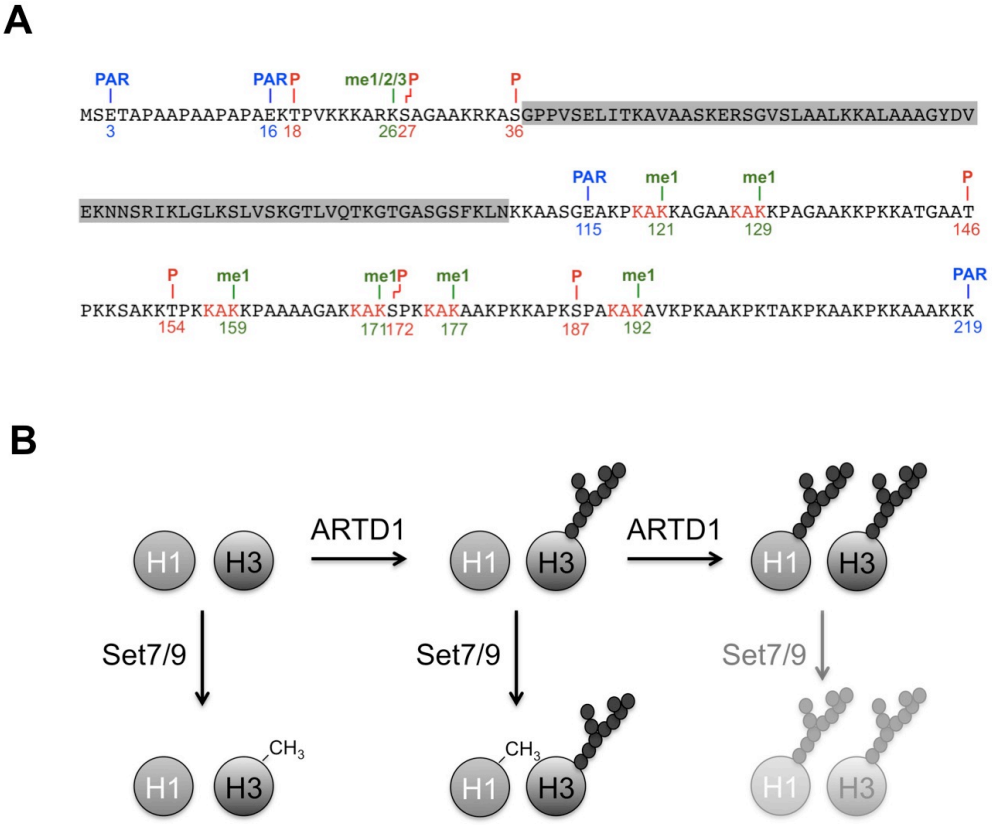

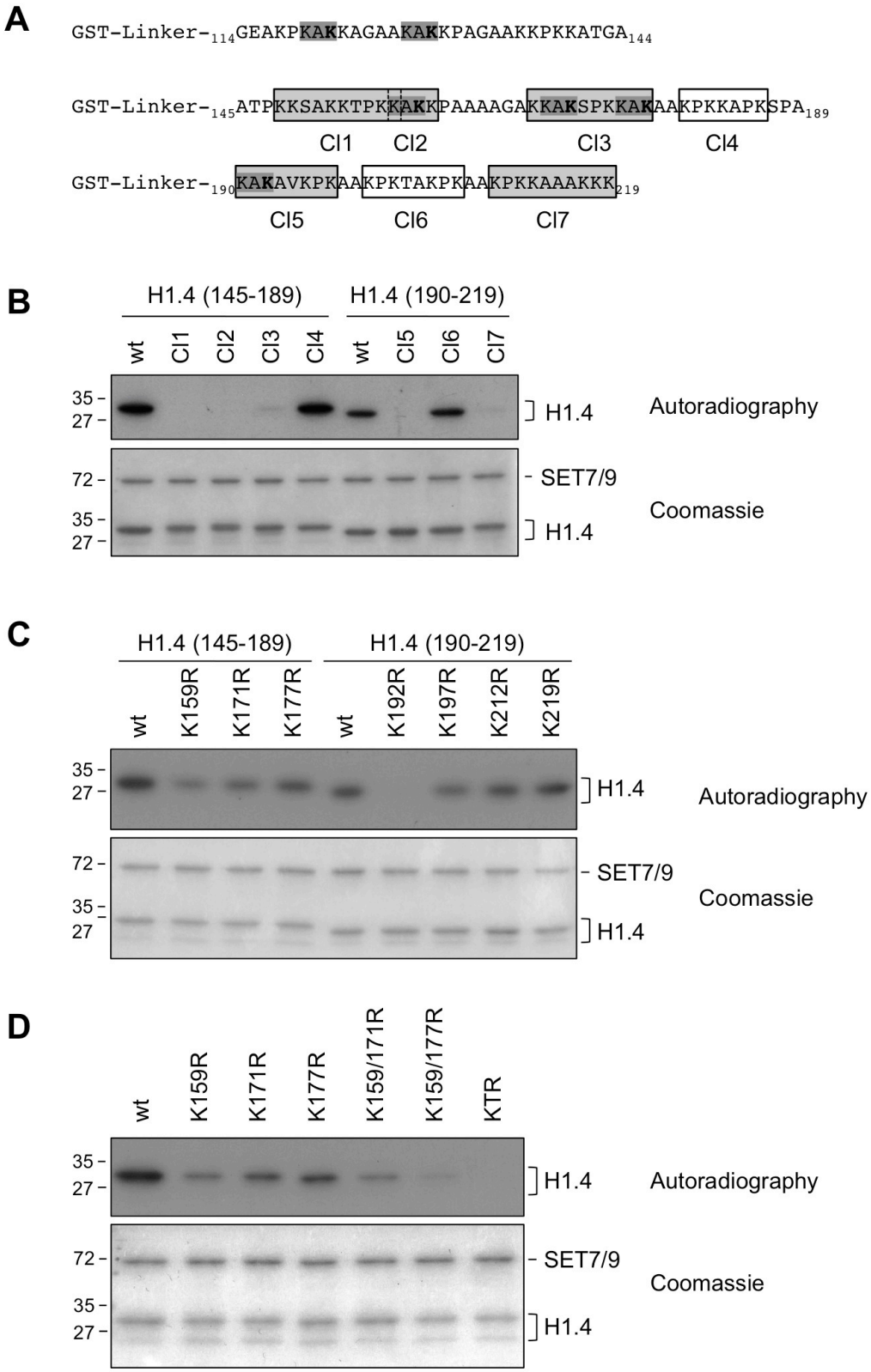
A
GST-Linker-114GEAKPKAKKAGAAKAKKPAGAAKKPKKATGA144
GST-Linker-145ATPKKSAKKTPKKAKKPAAAAGAKKAKSPKKAKAAKPKKAPKSPA189
Cl1
Cl2
Cl3
Cl4
GST-Linker-190KAKAVKPKAAKPKTAKPKAAKPKKAAAKKK219
Cl5
Cl6
Cl7
B
H1.4 (145-189)
H1.4 (190-219)
wt
Cl1
Cl2
Cl3
Cl4
wt
Cl5
Cl6
Cl7
35
27
H1.4
Autoradiography
72
SET7/9
35
27
H1.4
Coomassie
C
H1.4 (145-189)
H1.4 (190-219)
wt
K159R
K171R
K177R
wt
K192R
K197R
K212R
K219R
35
27
H1.4
Autoradiography
72
SET7/9
35
27
H1.4
Coomassie
D
wt
K159R
K171R
K177R
K159/171R
K159/177R
KTR
35
27
H1.4
Autoradiography
72
SET7/9
35
27
H1.4
Coomassie

The FASEB Journal article fj.09-137695. Published online July 21, 2009.
The FASEB Journal • Research Communication

Sumoylation of poly(ADP-ribose) polymerase 1 inhibits its acetylation and restrains transcriptional coactivator function

Simon Messner,[*,†] David Schuermann,[‡] Matthias Altmeyer,[*,†] Ingrid Kassner,[*,†] Darja Schmidt,[§] Primo Schär,[‡] Stefan Müller,[§] and Michael O. Hottiger[*,1]

[*]Institute of Veterinary Biochemistry and Molecular Biology and [†]Life Science Zurich Graduate School, Molecular Life Science Program, University of Zurich, Zurich, Switzerland; [‡]Institute of Biochemistry and Genetics, Department of Biomedicine, University of Basel, Basel, Switzerland; and [§]Department of Molecular Cell Biology, Max Planck Institute of Biochemistry, Martinsried, Germany

ABSTRACT **Poly(ADP-ribose) polymerase 1 (PARP1) is a chromatin-associated nuclear protein and functions as a molecular stress sensor. At the cellular level, PARP1 has been implicated in a wide range of processes, such as maintenance of genome stability, cell death, and transcription. PARP1 functions as a transcriptional coactivator of nuclear factor κB (NF-κB) and hypoxia inducible factor 1 (HIF1). In proteomic studies, PARP1 was found to be modified by small ubiquitin-like modifiers (SUMOs). Here, we characterize PARP1 as a substrate for modification by SUMO1 and SUMO3, both *in vitro* and *in vivo*. PARP1 is sumoylated at the single lysine residue K486 within its automodification domain. Interestingly, modification of PARP1 with SUMO does not affect its ADP-ribosylation activity but completely abrogates p300-mediated acetylation of PARP1, revealing an intriguing crosstalk of sumoylation and acetylation on PARP1. Genetic complementation of PARP1-depleted cells with wild-type and sumoylation-deficient PARP1 revealed that SUMO modification of PARP1 restrains its transcriptional coactivator function and subsequently reduces gene expression of distinct PARP1-regulated target genes. Messner, S., Schuermann, D., Altmeyer, M., Kassner, I., Schmidt, D., Schär, P., Müller, S., and Hottiger, M. O. Sumoylation of poly(ADP-ribose) polymerase 1 inhibits its acetylation and restrains transcriptional coactivator function. *FASEB J.* 23, 000–000 (2009). www.fasebj.org**

Key Words: NAD · SUMO · hypoxia

Poly(ADP-ribose) polymerase 1 (PARP1) is an abundant nuclear chromatin-associated multifunctional enzyme found in higher eukaryotes that belongs to a family of 5 "*bona fide*" PARP enzymes (1). PARP1 has an amino-terminal DNA-binding domain (DBD) containing 3 zinc finger motifs, as well as a central automodification domain (AMD), which functions as a target of direct covalent automodification. The carboxyl-terminal catalytic domain polymerizes linear or branched chains of ADP-ribose from the donor nicotinamide adenine dinucleotide (NAD^+). ADP-ribose is mainly attached on PARP1, but also other proteins are modified (2). Together, the DBD and the automodification domain allow PARP1 to interact with genomic DNA and chromatin. Although originally characterized as a key factor in DNA single strand-break repair, a wealth of studies over the past decade have demonstrated a role of PARP1 in the regulation of gene expression under basal, signal-activated, and stress-activated conditions (1, 3). Recent studies have highlighted the role of PARP1 in distinct modes of transcriptional regulation and provided novel insight into the cellular signaling systems that interface with PARP1 in the nucleus (4).

The basal enzymatic activity of PARP1 is very low, but it is stimulated dramatically under conditions of cellular stress (2, 3). Activation of PARP1 results in the synthesis of poly(ADP-ribose) (PAR) from NAD^+ and the release of nicotinamide as a reaction by-product (1). Following PARP1 activation, intracellular PAR levels can rise 10- to 500-fold (1), caused by a mechanism that remains to be resolved. Very recently, we identified 3 lysine residues in the automodification domain of PARP1 as acceptor sites for auto-ADP-ribosylation (5). PARP1 is the main acceptor for poly(ADP-ribosyl)ation *in vivo*, and automodification of PARP1 abolishes its affinity for NAD^+ and DNA (5). Remarkably, the same 3 ribosylated lysines (K498, K521, K524) were previously identified as targets for acetylation by the histone acetyltransferase p300 (6). Acetylation of PARP1 has been reported to be important for its transactivation activity (6). Recently, we also highlighted the role of PARP1 as a transcriptional coactivator of hypoxia inducible factor 1-α (HIF1-α). On hypoxic induction of cells, PARP1 was shown to interact with HIF1-α and to regulate the transcriptional activity of HIF1-α-dependent genes (7).

[1] Correspondence: Institute of Veterinary Biochemistry and Molecular Biology, University of Zurich, Winterthurerstrasse 190, 8057 Zurich, Switzerland. E-mail: hottiger@vetbio.uzh.ch
doi: 10.1096/fj.09-137695

Another post-translational protein modification in response to cellular stresses is the conjugation of small ubiquitin-like modifiers (SUMOs) (8). SUMOs regulate diverse cellular processes, including cell-cycle progression, genome stability, intracellular trafficking, and transcription (9, 10). In many cases, SUMO conjugation alters localization and/or activity of the substrate by providing a new protein-protein interaction interface. However, in certain cases, SUMO modification can also prevent distinct protein-protein interactions. Mammalian cells express three SUMO paralogs: SUMO2 and SUMO3, which are 96% identical and only differ by three N-terminal residues, and SUMO1, which is 45% identical to SUMO2/3. Moreover, SUMO2/3 proteins are able to form chains, which SUMO1 cannot (11). Although virtually all of the SUMO1 is engaged in conjugates, there is a free pool of the more abundant SUMO2/3 that is utilized when cells are stressed by heat shock or ethanol exposure (12). It is clear that proteins can be modified selectively by SUMO1 and SUMO2/3. Growing evidence suggests that SUMO2/3 and SUMO1 have some unique biological functions (12–14).

SUMO family proteins are conjugated to target lysines *via* a cascade of the E1-activating enzyme (SAE1/SAE2), the E2-conjugating enzyme Ubc9, and E3 SUMO ligases (8, 10). The SUMO E2 protein Ubc9 often recognizes the consensus sequence ΨKxE/D (where Ψ is a large hydrophobic amino acid, such as isoleucine or valine, and x is any amino acid) in the target protein and catalyzes SUMO conjugation (8). Generally, sumoylation with SAE1/SAE2 and Ubc9 only is rather inefficient, and additional proteins known as SUMO E3 ligases are often required to accelerate this reaction (10). A family of deconjugation enzymes, SENPs, is responsible for the removal of SUMO from target lysines (15), which accounts for the transient nature of this modification. In human cells, six members of this family (SENP1-3 and SENP5-7) have been identified. Importantly distinct members exhibit paralog specificity and show a characteristic subcellular localization, indicating that spatial control is an important regulatory concept of SENP activity.

Several proteomic studies to identify substrates for SUMO conjugation have been reported (16–18). In this context, PARP1 was detected to be sumoylated in HEK293 cells and in K562 cells. SUMO modification of proteins that regulate transcription has been associated with dynamic regulation of gene expression (9, 19). A large number of transcriptional regulators, including transcription factors, cofactors, and chromatin-modifying enzymes, have been found to be substrates of SUMO modification. Generally, a SUMO-modified factor exists in a dynamic distribution between the SUMO-modified and unmodified forms, and although the SUMO-modified form of a protein is often difficult to detect, it can have a great impact on transcriptional activation (9, 10). Sumoylation of transcription factors has generally been correlated with transcriptional repression (9, 10). The specific effects, however, have to be determined experimentally for each case.

In this study, we characterize the modification of PARP1 through SUMO1 and SUMO3. The modification primarily occurs at a lysine residue within the automodification domain of PARP1. The attachment site is close to hotspots of other post-translational modifications of PARP1, such as ADP-ribosylation and acetylation. This proximity led us to investigate a potential crosstalk of these modifications. Sumoylation of PARP1 inhibits its acetylation through p300, and correspondingly, a sumoylation-deficient PARP1 mutant has a higher acetylation status than wild-type PARP1. In addition, a PARP1 sumoylation-deficient cell line exhibits increased transcriptional activity of genes under the control of transcription factor HIF1-α.

MATERIALS AND METHODS

Chemicals and antibodies

Protein G sepharose and glutathione sepharose 4B were purchased from GE Healthcare (Les Ulis, France), ^{32}P-NAD$^+$ and ^{35}S-methionine were from PerkinElmer (Boston, MA, USA). NAD$^+$, trichostatin A (TSA), acetyl-coenzyme A, 3AB, ATP, anti-tubulin, and anti-Flag (M2) were obtained from Sigma-Aldrich (Milan, Italy). Anti-p300 (C20) was obtained from Santa Cruz Biotechnology (Santa Cruz, CA, USA) and anti-HA antibody 16B12 from Covance (Evansville, IL, USA). Anti-myc antibody (9E10) was purchased from Roche (Basel, Switzerland), SUMO2/3 (18H8) was obtained from Cell Signaling (Beverly, MA, USA), and His antibody was from Qiagen (Valencia, Spain). Monoclonal CAIX antibody supernatant from hybridoma was a gift from D. Stiehl (University of Zurich, Zurich, Switzerland). Anti-PARP1 was produced in this laboratory; anti-acetyl-PARP1 was generated in collaboration with the monoclonal antibody core facility at the EMBL Monterotondo (Monterotondo, Italy).

Cell culture and transfection

HEK293T and K562 cells were grown under standard conditions. Transfections were carried out with the calcium phosphate method. Whole-cell extracts were prepared as described previously (20) with 10 mM NEM and/or HDAC inhibitors (2 μM TSA, 5 mM NAM, 1 mM Na-butyrate). Nuclear extracts were prepared as described previously (6).

Plasmids

The baculovirus expression vectors pQE-TriSystem (Qiagen) and BacPak8 (Clontech, Mountain View, CA, USA) were used for the expression of recombinant proteins in Sf21 insect cells, as described previously (21). pcDNA-myc-SUMO1, myc-SUMO3, and myc-Ubc9 expression plasmids were kindly provided by R. T. Hay (University of Dundee, Dundee, UK). PARP1 was cloned into a pCMV-HA vector with *Nhe*I/*Not*I restriction enzymes. pCU vector with Ubc9 was a kind gift from R. Niedenthal (Hannover Medical School, Hannover, Germany). PARP1 was cloned into pCU with *Nhe*I/*Sma*I restriction enzymes, generating a 15-aa linker between PARP1 and Ubc9. pCMV-Flag-p300 was used for expression in mammalian cells. Plasmids for SUMO proteases SENP1-6 were in

pCI-Flag backbone. Short hairpin RNA was cloned and expressed in pSUPER vector.

Cloning, expression, and purification of recombinant proteins

Wild-type hPARP1 (National Center for Biotechnology Information ID: BC037545) was cloned and expressed as amino-terminal HA-tagged and carboxyl-terminal His-tagged protein. HA-PARP1, HA-PARP1 K486R, p300, SUMO1, SUMO3, and Ubc9 proteins were purified by 1-step affinity chromatography using ProBond resin, according to the manufacturer's recommendations (Invitrogen, Carlsbad, CA, USA). GST-SUMO3, SUMO3, SENP2 (aa 364-569), and SENP2 (aa 364-569 C548S) were cloned in pGEX-vectors, expressed and purified with glutathione sepharose, according to the manufacturer's recommendations (GE Healthcare). The double-tagged heterodimeric human E1-activating enzyme was expressed from the pGEX-E1H6 vector and purified by sequential GST beads and nickel beads; GST-cleavage was performed through thrombin, and the recombinant protein was loaded and eluted from nickel beads using standard protocols.

***In vitro* sumoylation assay**

The reaction was carried out in standard SUMO reaction buffer (50 mM Tris-HCl, pH 8.0; 50 mM NaCl; 5 mM $MgCl_2$; 10% glycerol; and 0.5 mM DTT). 5 mM ATP was added to start the reaction. Incubation time was 30 min at 30°C, unless otherwise indicated. The final concentration of proteins was 100 nM for SAE1/SAE2, 500 nM Ubc9, 5 μM SUMO1/SUMO3, and 500 nM HA-PARP1.

Purification of sumoylated PARP1

The sumoylation reaction was 15× scaled up, and the incubation time was increased to 120 min at 30°C. Instead of SUMO3, a GST-tagged SUMO3 at a final concentration of 10 μM was used. After sumoylation, the sample was diluted with 2× the volume with SUMO-purification buffer (50 mM Tris-HCl, pH 7.5; 150 mM NaCl; 1 mM EDTA; and 1 mM DTT) and bound to glutathione sepharose beads. After 60 min of incubation on rolls at 4°C, the supernatant was washed away with the same buffer, and 2 U of PreScission protease was added to the beads and incubated 16 h at 4°C. The supernatant was used for experiments with sumoylated PARP1.

Desumoylation of PARP1 *in vitro*

Purified sumoylated PARP1 was subjected to active recombinant SENP2 (aa 364-569) or inactive SENP2 (aa 364-569 C548S) treatment in SUMO-purification buffer (50 mM Tris-HCl, pH 7.5; 150 mM NaCl; 1 mM EDTA; and 1 mM DTT) for 15 min at 30°C with a concentration of 10 ng SENP2/μl.

^{32}P-NAD automodification

Sumoylated or desumoylated PARP1 in SUMO-purification buffer (50 mM Tris-HCl, pH 7.5; 150 mM NaCl; 1 mM EDTA; and 1 mM DTT) was supplemented with 4 mM $MgCl_2$ and 5 pmol of annealed double-stranded oligomer (5′-GGAATTCC-3′). The reaction was started by adding ^{32}P-NAD^+ at a final concentration of 100 nM NAD^+. Automodification was allowed for 5 min at 30°C. Reactions were stopped by the addition of SDS-PAGE-loading buffer and boiling for 5 min at 95°C. Samples were subjected to SDS-PAGE, followed by detection of automodification by autoradiography.

PAR detection by silver staining

Following synthesis of PAR in the presence of 400 μM NAD^+ and 5 pmol *Eco*RI-linker DNA for 20 min, PAR chains were purified and separated by modified DNA-sequencing gel electrophoresis, as described previously (22).

Immunoprecipitation and nickel-NTA pulldown

Sumoylated or desumoylated PARP1 was bound to protein G sepharose beads with anti-HA antibody in SUMO-purification buffer. The beads were washed and adjusted to IP buffer (50 mM Tris-HCL, pH 8.0; 100 mM NaCl; 0.25% Nonidet P-40; and 1 μg/ml protease inhibitors). Recombinant p300 (2 μg) was added to the beads and incubated for 2 h at 4°C on rolls. Washing of the beads with the same buffer removed unbound p300. Immunoprecipitation of nuclear extracts was done with HA antibody with IP-binding buffer (20 mM HEPES, 150 mM NaCl, and 0.25% Nonidet P-40; 1 μg/ml), protease inhibitors, and HDAC inhibitors (2 μM TSA, 5 mM NAM, 1 mM Na-butyrate). The salt concentration was increased with 50 mM KCl for washing steps. Elution of bound proteins was done with SDS-PAGE loading buffer and boiled for 5 min at 95°C. Nickel-NTA pulldown was done as described previously (23).

HAT Assay

Sumoylated or desumoylated PARP1 was subjected to *in vitro* acetylation assay with recombinant p300 as described elsewhere (24).

Knockdown and complementation of PARP1 in K562 cells

Generation of viruses and transduction of cells was done as described earlier (25). shRNA was cloned into pRDI vector and transduced to K562 cells. The short hairpin RNA was designed against 5′UTR region of PARP1 mRNA. Transduced cells were selected through puromycine resistance gene. Complementation of cells was done with pRRL-myc-PARP1 vectors containing a blasticidine resistance marker and subsequently selected with this antibiotic.

RNA preparation

Total RNA was isolated from 3 biological replicates of complemented K562 cells with the Total RNA Isolation kit (Agilent Technologies, Santa Clara, CA, USA). Reverse transcription was achieved with the High-Capacity cDNA Reverse Transcription kit (Applied Biosystems, Foster City, CA, USA).

Quantitative PCR

Total reverse-transcribed cDNA from untreated or treated K562 cells was used for q-PCR with primers against carbonic anhydrase IX, LOXL2, and Pdk1. Amplification products were analyzed by SYBR Green (Quantace, London, UK), and ribosomal protein L28 was used to normalize for differences in RNA input. Rotor-Gene3000A (Qiagen, Basel, Switzerland) was used to perform the real-time PCR reactions.

RESULTS

PARP1 is sumoylated *in vivo*

Because PARP1 was identified as a SUMO modification target in proteomic studies, we aimed to confirm that PARP1 is indeed sumoylated *in vivo*. HA-tagged PARP1 was coexpressed with myc-tagged SUMO1 or SUMO3 in HEK293T cells, and extracts were analyzed by Western blot. Ectopic expression of SUMO1 or SUMO3 *per se* induced the modification of a multitude of proteins (**Fig. 1*A***, bottom). Expression of SUMO induced a higher molecular form of PARP1 (depicted as Su-PARP1), which was more prominent in the presence of SUMO3 as compared to SUMO1, suggesting that PARP1 is preferentially conjugated with SUMO3 (Fig. 1*A*). Expressing His-tagged SUMO, we could enrich an anti-PARP1-reactive species on Ni-NTA beads, thus validating that the higher molecular form corresponds, indeed, to a covalent SUMO-PARP1 conjugate (Fig. 1*B*). Only one distinctive band of sumoylated PARP1 was detected, suggesting that PARP1 is monosumoylated at a single lysine residue under the tested conditions. Similar results were obtained when PARP1 was expressed as fusion protein with Ubc9/E2 conjugation protein, although the overall modification rate was clearly enhanced (Supplemental Fig. 1*A*). Mutation of the catalytic cysteine of the fused Ubc9 resulted in a strong reduction of the modification, indicating that the Ubc9 fused to PARP1 catalyzes the sumoylation of PARP1 (Supplemental Fig. 1*B*). Immunoprecipitation of this fusion protein in extracts of cells expressing myc-tagged SUMO3 and subsequent Western blot analysis using an anti-myc antibody revealed SUMO moieties on PARP1, providing additional evidence for covalent modification of PARP1 with SUMO (Supplemental Fig. 1*C*). To test whether PARP1 would bind to SUMO noncovalently *via* a SUMO-interacting motif (SIM), GST pulldowns were performed with conjugation-deficient SUMO1-4 and RelA/p65 as a positive control (Supplemental Fig. 2*A–C*). Although PARP1 was able to interact with RelA/p65, no interaction was detectable with GST or all tested SUMOs. Thus, we conclude that PARP1 is covalently modified by SUMO.

SENP1 and SENP3 are able to desumoylate PARP1

SUMO proteases are known to reverse sumoylation of proteins. To test whether SUMO proteases act on

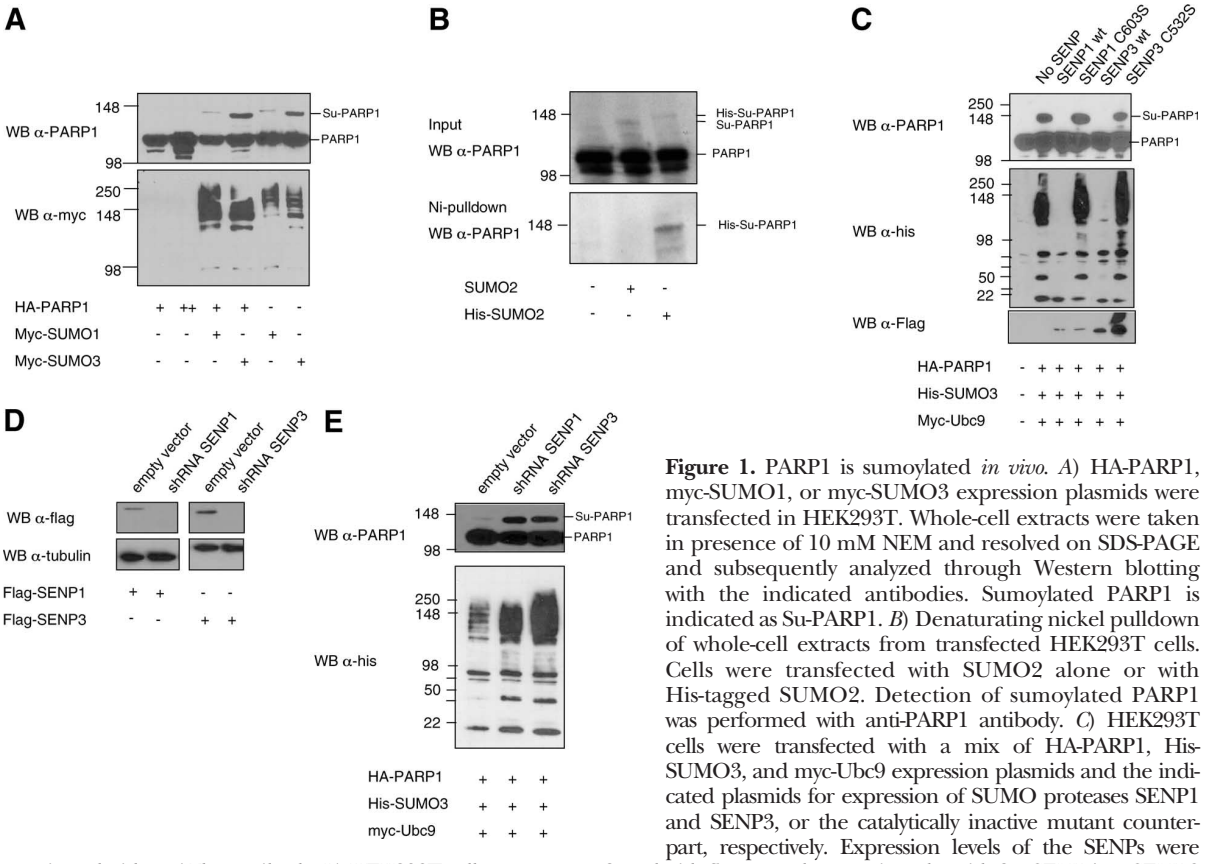

Figure 1. PARP1 is sumoylated *in vivo*. *A*) HA-PARP1, myc-SUMO1, or myc-SUMO3 expression plasmids were transfected in HEK293T. Whole-cell extracts were taken in presence of 10 mM NEM and resolved on SDS-PAGE and subsequently analyzed through Western blotting with the indicated antibodies. Sumoylated PARP1 is indicated as Su-PARP1. *B*) Denaturating nickel pulldown of whole-cell extracts from transfected HEK293T cells. Cells were transfected with SUMO2 alone or with His-tagged SUMO2. Detection of sumoylated PARP1 was performed with anti-PARP1 antibody. *C*) HEK293T cells were transfected with a mix of HA-PARP1, His-SUMO3, and myc-Ubc9 expression plasmids and the indicated plasmids for expression of SUMO proteases SENP1 and SENP3, or the catalytically inactive mutant counterpart, respectively. Expression levels of the SENPs were monitored with anti-Flag antibody. *D*) HEK293T cells were cotransfected with flag-tagged expression plasmids for SENP1 or SENP3 and pSUPER vector with shRNAs against SENPs. Knockdown efficiency after 28-h expression was examined with anti-Flag antibody. *E*) Knockdown of SENP1 and SENP3 was achieved as in *D*, but in addition, a mix of HA-PARP1, His-SUMO3, and myc-Ubc9 was cotransfected in HEK293T cells. Cell extracts were prepared and examined with the anti-PARP1 and anti-His antibodies.

SUMO-modified PARP1, we coexpressed wild-type or catalytically inactive SENP1 and SENP3 with PARP1 and SUMO3 in HEK293T cells (Fig. 1*C*). This showed that coexpression of catalytically active SENP1 and SENP3 deconjugated SUMO3 from PARP1 (Fig. 1*C*). Correspondingly, knockdown of SENP1 and SENP3 with transiently transfected shRNAs (Fig. 1*D*) resulted in the accumulation of sumoylated PARP1, as compared to the control (Fig. 1*E*), indicating that SENP1 and SENP3 can act on PARP1-SUMO conjugates at physiological expression levels. Taken together, our results illustrate that PARP1 is preferably modified by SUMO3 and desumoylated by the isopeptidases SENP1 and SENP3. Furthermore, sumoylation of PARP1 seems thus to be a transient and reversible modification.

PARP1 is sumoylated at K486 *in vitro* and *in vivo*

The consensus sumoylation site sequence is ΨKxE/D (8). As determined by the SUMOsp analysis program (http://sumosp.biocuckoo.org), the highest score matched to lysine 486 in human PARP1 (**Fig. 2*A***), which is located in proximity to previously described sites of acetylation and ADP ribosylation. To confirm PARP1 sumoylation *in vitro* and to map the modification site, we established an *in vitro* sumoylation system reconstituted with recombinant human E1 (SAE1/SAE2 heterodimer), E2 (Ubc9), wild-type SUMO1, or SUMO3 and wild-type PARP1 (Fig. 2*B*). PARP1 sumoylation was efficiently reconstituted *in vitro* with purified proteins: reactions containing all components produced slower migrating PARP1 forms, consistent with conjugated SUMO moieties. Attachment of a single moiety was detected with low E2 concentrations (running at ~140 kDa), whereas multiple SUMO moieties were attached only at higher E2 concentrations (Fig. 2*B*). One additional band between 120 and 140 kDa was observed at elevated Ubc9 concentrations and likely represents the modification of a degradation product of PARP1 by SUMO3. To test for putative sumoylation sites in PARP1, lysine 486 of PARP1 was substituted with arginine (PARP1 K486R) and analyzed *in vitro*. Substitution did completely prevent the sumoylation of PARP1 *in vitro* with SUMO1, SUMO3, or GST-tagged SUMO3, as monitored by Western blot analysis (Fig. 2*C, D*), indicating that K486 is the major SUMO acceptor site of PARP1.

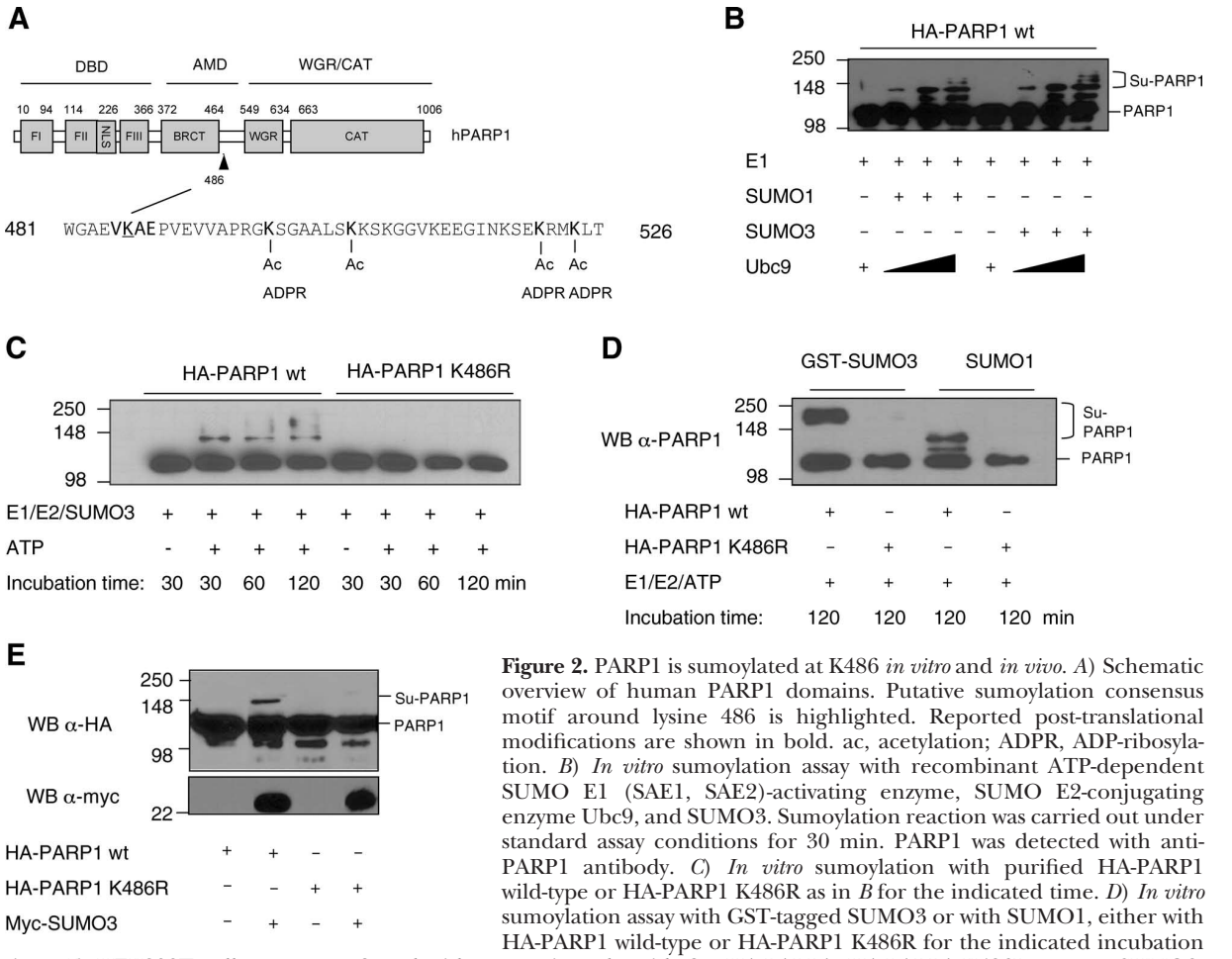

Figure 2. PARP1 is sumoylated at K486 *in vitro* and *in vivo*. *A*) Schematic overview of human PARP1 domains. Putative sumoylation consensus motif around lysine 486 is highlighted. Reported post-translational modifications are shown in bold. ac, acetylation; ADPR, ADP-ribosylation. *B*) *In vitro* sumoylation assay with recombinant ATP-dependent SUMO E1 (SAE1, SAE2)-activating enzyme, SUMO E2-conjugating enzyme Ubc9, and SUMO3. Sumoylation reaction was carried out under standard assay conditions for 30 min. PARP1 was detected with anti-PARP1 antibody. *C*) *In vitro* sumoylation with purified HA-PARP1 wild-type or HA-PARP1 K486R as in *B* for the indicated time. *D*) *In vitro* sumoylation assay with GST-tagged SUMO3 or with SUMO1, either with HA-PARP1 wild-type or HA-PARP1 K486R for the indicated incubation time. *E*) HEK293T cells were transfected with expression plasmids for HA-PARP1, HA-PARP1 K486R, or myc-SUMO3, respectively. Whole-cell extracts were analyzed with anti-HA antibody and anti-myc antibody. Saturated levels of unbound myc-SUMO3 were detected in the control Western blot.

To verify sumoylation of PARP1 at K486 *in vivo*, we coexpressed wild-type or the K486R mutant of PARP1 with myc-tagged SUMO3. Sumoylation of wild-type PARP1 could be detected but not of the K486R mutant (Fig. 2*E*), confirming K486 as the main sumoylated residue *in vivo*.

Sumoylation of PARP1 does not affect its ADP ribosylation activity

To explore a potential interplay of PARP1 sumoylation with PARP1 function, we modified the established *in vitro* sumoylation system to purify sumoylated PARP1. A large-scale sumoylation reaction was performed with GST-tagged SUMO3, E1–E2 enzymes, and HA-PARP1, followed by GST affinity purification and subsequent protease digestion to remove the GST tag and to purify Su-PARP1, specifically modified at K486 (**Fig. 3*A***). On purification, only Su-PARP1 could be detected, indicating that no unmodified PARP1 was in the purified complex (Fig. 3*B*). Because PARP1 was described to form a homodimer, this result suggests that both subunits are equally accessible for SUMO-conjugation. PARP1 was also efficiently sumoylated in the presence of double-stranded DNA ends, suggesting that binding of PARP1 to DNA does not affect its sumoylation *in vitro* (Supplemental Fig. 3*A*). Similarly, Su-PARP1 was still able to bind specifically to DNA fragments that mimic damaged DNA (Supplemental Fig. 3*B*).

To determine whether sumoylation regulates the intrinsic ADP-ribosylation activity of PARP1, mono-ADP-ribosylation of purified Su-PARP1 was measured using an *in vitro* ADP-ribosylation assay in the presence of 100 nM ^{32}P-NAD$^+$. Sumoylation of PARP1 still allows its mono-ADP-ribosylation activity (Fig. 3*B*, lane 1). To compare the extent of ADP ribosylation, Su-PARP1 was either desumoylated by recombinant SENP2 (aa 364-569) before or after ADP ribosylation took place (Fig. 3*B*, lanes 2 and 3). Quantification of the detected radioactivity confirmed that both proteins were modified to the same extent. Similar experiments were repeated with 400 μM NAD$^+$, a concentration that allows detection of poly(ADP-ribosyl)ation of PARP1. PAR polymers synthesized by Su-PARP1 and desumoylated PARP1 were isolated and analyzed with silver-stained PAGE (Fig. 3*C*). Neither the amount nor the distribution of freshly synthesized PAR was altered by sumoylated PARP1, indicating that SUMO modification neither alters the ability of PARP1 to initiate nor to extend PAR synthesis. In addition, overexpression of SUMO3 in HEK293T cells *per se* did not stimulate PAR formation (Supplemental Fig. 4*A*), although PARP1 is sumoylated under these conditions (see Fig. 1*A*, last lane). Furthermore, H_2O_2-treated cells showed PAR formation (Supplemental Fig. 4*B*), which was independent of SUMO3 levels, indicating that SUMO modification of PARP1 does not enhance its poly(ADP-ribosyl)ation activity. To test the possibility of differential localization of PARP1 upon sumoylation, we overex-

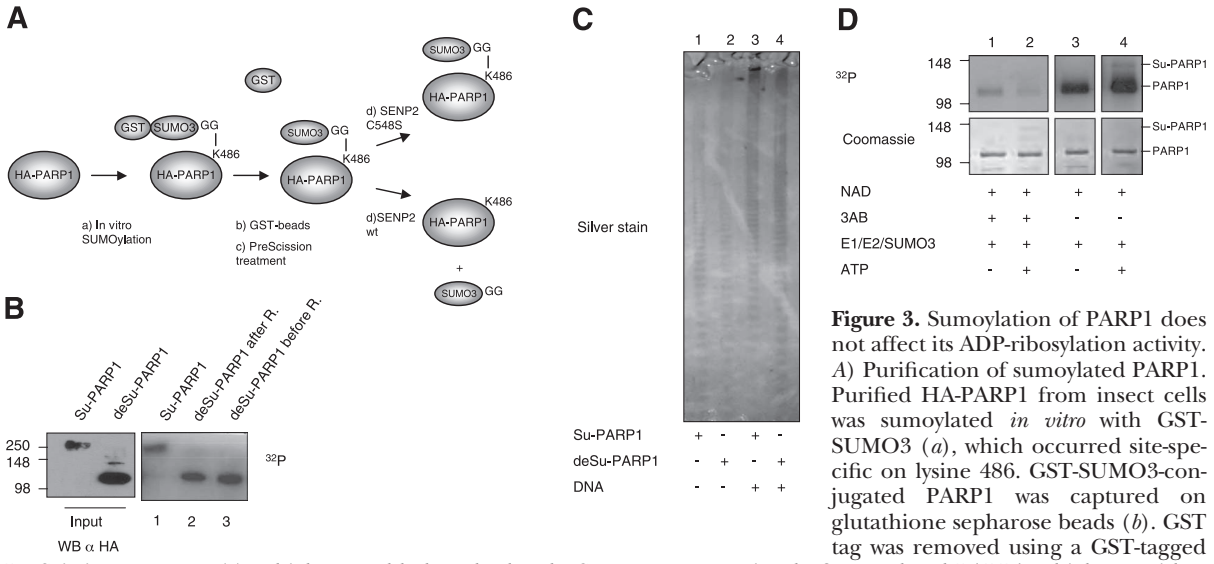

Figure 3. Sumoylation of PARP1 does not affect its ADP-ribosylation activity. *A*) Purification of sumoylated PARP1. Purified HA-PARP1 from insect cells was sumoylated *in vitro* with GST-SUMO3 (*a*), which occurred site-specific on lysine 486. GST-SUMO3-conjugated PARP1 was captured on glutathione sepharose beads (*b*). GST tag was removed using a GST-tagged PreScission protease (*c*), which was added to the beads. Supernatant consisted of sumoylated PARP1, which was either incubated with active recombinant SENP2 fragment (aa 364-569) or the inactive mutant SENP2 C548S. *B*) Sumoylated PARP1 (lanes 1 and 2) or desumoylated PARP1 (lane 3) was incubated with 100 nM radiolabeled ^{32}P-NAD$^+$ and 5 pmol *Eco*RI-linker DNA. Reaction was stopped with PARP-inhibitor 3AB, and active SENP2 was added to deconjugate SUMO3 from PARP1 (lane 2), thus generating free PARP1. Mono(ADP-ribosyl)ation was monitored with autoradiography. *C*) Silver stain of isolated PAR generated by sumoylated PARP1 (lanes 1 and 3) or by desumoylated PARP1 (lanes 2 and 4). Reaction was carried out in the absence (lanes 1 and 2) or in the presence (lanes 3 and 4) of *Eco*RI-linker DNA at 400 μM NAD$^+$. *D*) Mono(ADP-ribosyl)ation of PARP1 in the presence or absence of PARP-inhibitor 3AB with 100 nM NAD$^+$. Each sample was supplemented with E1, E2, and SUMO3 proteins. Reaction was stopped after a 5-min incubation time with 3AB (lanes 3 and 4), and ATP was added (lanes 2 and 4). After the sumoylation reaction, proteins were separated by SDS-PAGE and analyzed by autoradiography.

pressed SUMO3 in cells and monitored PARP1 localization by immunofluorescence. However, we did not observe differential localization of PARP1 within the nucleus upon ectopic SUMO3 expression (Supplemental Fig. 4*C*).

We recently reported that PARP1 is auto-ADP-ribosylated at several lysines adjacent to the identified sumoylation site (26). To exclude that ADP-ribosylation would affect sumoylation, we mono-ADP-ribosylated PARP1 *in vitro* with radioactive NAD^+ and subsequently sumoylated the labeled PARP1 fraction (Fig. 3*D*). PARP1 was sumoylated in an ATP-dependent manner independent of its ADP-ribosylation. Consistently, *in vivo* treatment of cells with the PARP inhibitor 3-amino-benzamide (3AB) did not affect sumoylation (data not shown). Taken together, this suggests that although the sumoylated and ADP-ribosylated lysines are rather close within the PARP1 amino acid sequence, their modifications do not interfere with each other.

Sumoylation counteracts p300-induced acetylation of PARP1

As p300 is critical for PARP1 transcriptional coactivation and acetylates PARP1 at distinct lysines (6), we first examined whether acetylated PARP1 would still be sumoylated *in vitro*. Acetylation of PARP1 was monitored with a specific anti-acetyl PARP1 (E4) antibody (Supplemental Fig. 5*A*), while sumoylation was assessed by the migration difference between unmodified PARP1 and Su-PARP1. Acetylation with the indicated control and subsequent addition of sumoylation enzymes, followed by the sumoylation reaction, revealed that similar to the mono-ADP-ribosylated PARP1, acetylated PARP1 could also be efficiently modified with SUMO (**Fig. 4*A***, lane 4).

Moreover, we tested whether sumoylation of PARP1 would affect acetylation. Purified Su-PARP1 or desumoylated PARP1 by recombinant SENP2 was both incubated with p300 and acetyl-CoA *in vitro*. Western blot analysis using the specific anti-acetyl PARP1 (E4) antibody revealed that PARP1 is acetylated only when PARP1 was desumoylated prior to acetylation (Fig. 4*B*, lane 2), suggesting that the SUMO-modification inhibits p300-mediated PARP1 acetylation. To substantiate this, we examined protein interactions with p300, PARP1, or Su-PARP1. p300 could interact efficiently with PARP1 but not with Su-PARP1, as demonstrated by coimmunoprecipitation of p300 (Fig. 4*C*). Thus, the absence of detectable acetylation of Su-PARP1 (see Fig. 4*B*) suggests that SUMO modification at K486 prevents p300-mediated acetylation of PARP1, likely because of steric hindrance of the bulky SUMO conjugate blocking p300 binding and acetylation at the adjacent lysine residues. To explore whether the inhibitory effect of PARP1 sumoylation on acetylation is also observed *in vivo*, we coexpressed wild-type PARP1 or the sumoylation-deficient PARP1 mutant (K486R) with p300 and monitored acetylation with the E4 antibody on Western blots. This revealed lower levels of acetylation for the wild-type PARP1 compared to the sumoylation-defi-

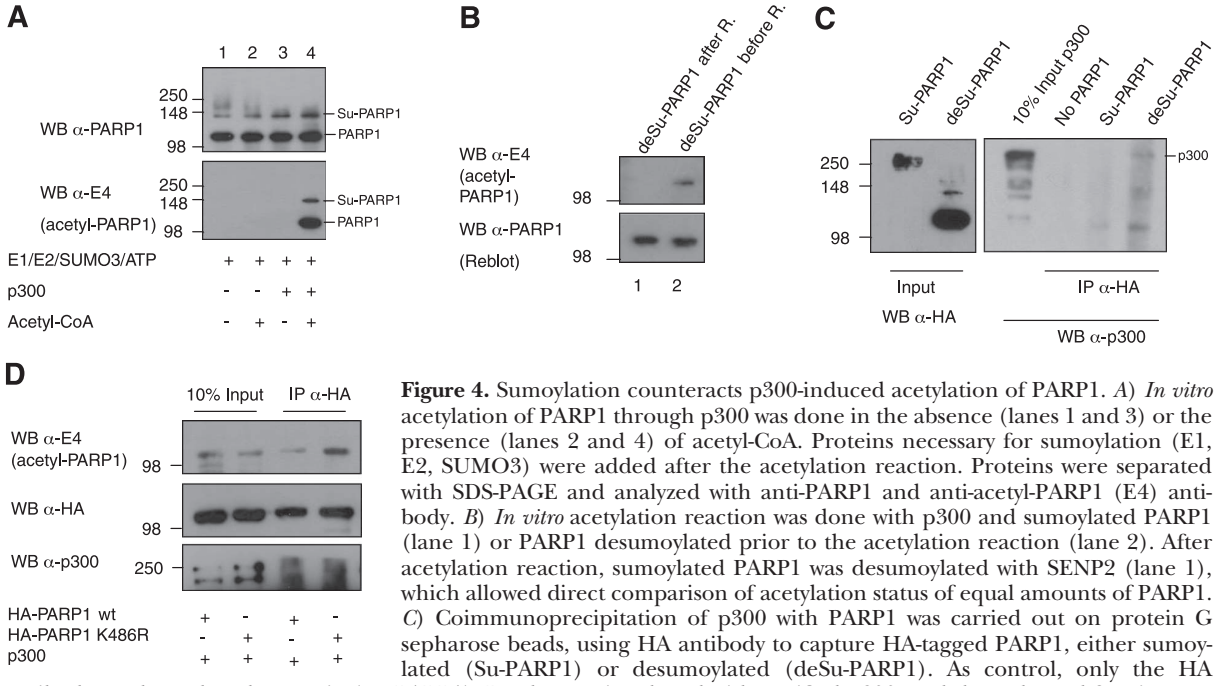

Figure 4. Sumoylation counteracts p300-induced acetylation of PARP1. *A*) *In vitro* acetylation of PARP1 through p300 was done in the absence (lanes 1 and 3) or the presence (lanes 2 and 4) of acetyl-CoA. Proteins necessary for sumoylation (E1, E2, SUMO3) were added after the acetylation reaction. Proteins were separated with SDS-PAGE and analyzed with anti-PARP1 and anti-acetyl-PARP1 (E4) antibody. *B*) *In vitro* acetylation reaction was done with p300 and sumoylated PARP1 (lane 1) or PARP1 desumoylated prior to the acetylation reaction (lane 2). After acetylation reaction, sumoylated PARP1 was desumoylated with SENP2 (lane 1), which allowed direct comparison of acetylation status of equal amounts of PARP1. *C*) Coimmunoprecipitation of p300 with PARP1 was carried out on protein G sepharose beads, using HA antibody to capture HA-tagged PARP1, either sumoylated (Su-PARP1) or desumoylated (deSu-PARP1). As control, only the HA antibody was bound to the matrix (no PARP1). Beads were incubated with purified p300, and the unbound fraction was removed by extensive washing. *D*) HEK293T cells were transfected with either HA-PARP1 wt or HA-PARP1 K486R mutant along with p300 expression plasmid. Cells were incubated with HDAC inhibitors 2 h prior to lysis, and HDAC inhibitors were present at all steps of manipulation. Nuclear extracts were taken and subjected to immunoprecipitation using an HA antibody. After SDS-PAGE, proteins were detected by anti-acetyl-PARP1 (E4), anti-HA, or anti-p300 antibody.

cient PARP1 mutant (Fig. 4*D*). Together, these results provide evidence for a crosstalk between these modifications.

The sumoylation-deficient K486R PARP1 mutant exhibits higher coactivator function compared to wild-type PARP1

To explore a possible mechanism by which sumoylation affects PARP1-dependent transcriptional coactivator function *in vivo*, we first knocked down endogenous PARP1 protein levels in K562 cells with an shRNA approach directed against the untranslated region of PARP1's mRNA and subsequently complemented these cells with wild-type or sumoylation-deficient K486R PARP1 mutant (**Fig. 5*A, B***). The expression levels of the complemented cells were comparable to the endogenous wild-type counterpart. Hypoxia treatment of these cells for 28 h and subsequent profiling of the gene expression of defined hypoxia-inducible genes revealed that certain genes, such as CAIX, LOXL2 or Pdk1, are dependent on PARP1, but only a subset was affected by the sumoylation-deficient K486R mutation (Fig. 5*C*). Similar results were obtained when PARP1$^{-/-}$ mouse lung fibroblasts were complemented with wild-type or sumoylation-deficient K486R PARP1 mutant and stimulated by the hypoxia-mimicking drug ciclopirox olamine (Supplemental Fig. 5*B*). Sumoylation-deficient K486R PARP1 mutant not only enhanced CAIX mRNA levels in K562 cells, but also CAIX protein levels *in vivo* (Fig. 5*D*). Furthermore, hypoxia treatment of K562 cells very strongly correlated with protein sumoylation and enhanced SUMO modification of PARP1 in HEK293T cells (Supplemental Fig. 5*C, D*). Thus, we conclude that sumoylation of PARP1 reduces its coactivator activity and thus regulates gene expression *in vivo*.

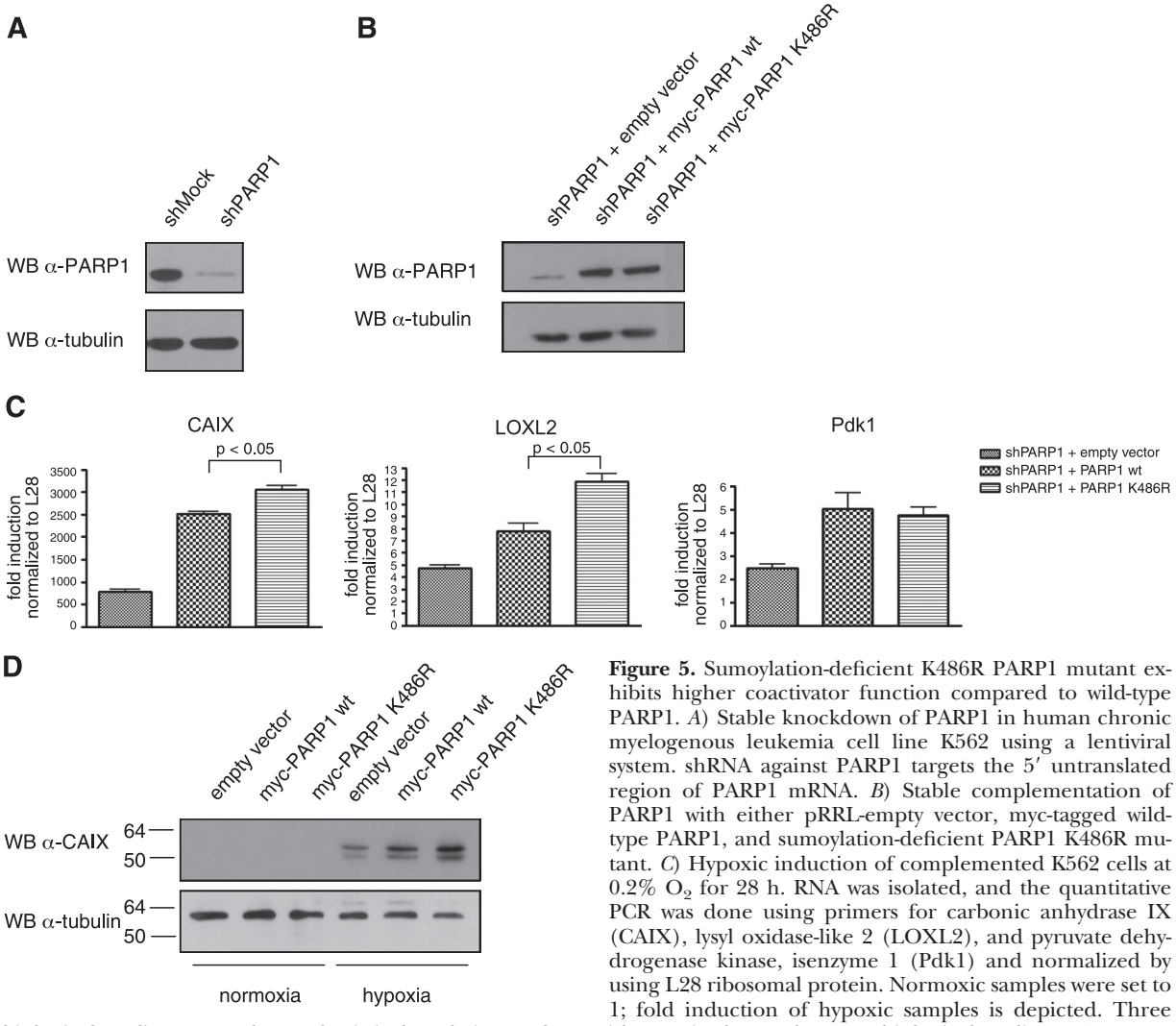

Figure 5. Sumoylation-deficient K486R PARP1 mutant exhibits higher coactivator function compared to wild-type PARP1. *A*) Stable knockdown of PARP1 in human chronic myelogenous leukemia cell line K562 using a lentiviral system. shRNA against PARP1 targets the 5′ untranslated region of PARP1 mRNA. *B*) Stable complementation of PARP1 with either pRRL-empty vector, myc-tagged wild-type PARP1, and sumoylation-deficient PARP1 K486R mutant. *C*) Hypoxic induction of complemented K562 cells at 0.2% O_2 for 28 h. RNA was isolated, and the quantitative PCR was done using primers for carbonic anhydrase IX (CAIX), lysyl oxidase-like 2 (LOXL2), and pyruvate dehydrogenase kinase, isenzyme 1 (Pdk1) and normalized by using L28 ribosomal protein. Normoxic samples were set to 1; fold induction of hypoxic samples is depicted. Three biological replicates are shown. Statistical analysis was done with unpaired *t* test between biological replicates. Data are represented as means ± SE. *D*) Complemented K562 cells were exposed for 29 h to 0.2% O_2 hypoxia. Whole-cell extracts were prepared and Western blotted with monoclonal anti-CAIX antibody and anti-tubulin antibody.

DISCUSSION

The aim of this study was to characterize and investigate the role of PARP1 sumoylation in the cellular context. We provide biochemical and cellular evidence for SUMO modification of PARP at lysine 486 within its automodification domain. Mutation of K486 enhances the transcriptional activity of PARP1, suggesting that sumoylation restrains its transcriptional activity.

PARP1 is covalently sumoylated

Noncovalent interactions of proteins can occur through SUMO interaction motifs (SIMs) (27). Proteins like the DNA repair enzyme TDG and the tumor suppressor PML were shown to interact with SUMOs *via* SIMs, and such interactions were associated with important biological activities (28–30). Although PARP1 exhibits several putative SIMs, we did not observe any direct noncovalent interaction of PARP1 with SUMOs, indicating that the interaction of PARP1 with SUMO is exclusively covalent. Pulldown experiments of sumoylated PARP1 under denaturating conditions and site-directed mutagenesis revealed that sumoylation of PARP1 is indeed a covalent and site-specific modification. A possible involvement of SUMO E3 ligases for the sumoylation of PARP1 needs further investigations. Although PIAS family members are attractive candidates, overexpression of different PIAS proteins did not enhance PARP1 sumoylation (data not shown).

Notably, we observed only monosumoylation of PARP1 *in vivo*, but do not exclude that under specific conditions, PARP1 may also be polysumoylated. In support of this idea, heat shock has been reported to induce a pattern of PARP1 sumoylation, which would be consistent with polysumoylation (18). Understanding the balance between monosumoylation and polysumoylation of PARP1, as well as their functional differences will remain an exciting issue.

Crosstalk between sumoylation and other post-translational modifications

The crosstalk of post-translational modification systems is an emerging concept (31). Sumoylation of target proteins can be regulated through crosstalks with other post-translational modification events. Phosphorylation, for instance, was shown to regulate SUMO conjugation through a highly conserved motif, which is called phosphorylation-dependent sumoylation motif (PDSM) (32). The PDSM motif, which contains a SUMO consensus site and an adjacent proline-directed phosphorylation site (ΨKxExxSP, where Ψ represents large hydrophobic residue and x is any amino acid), regulates phosphorylation-dependent sumoylation of multiple transcription factors (33–35). Lysine residues are targeted by several other post-translational modifications, including ubiquitination, acetylation, methylation, and ADP-ribosylation. It has been documented that SUMO conjugation can occur on the same lysine residue as ubiquitination or acetylation in some proteins. For example, the competition between sumoylation and ubiquitination of the same lysine regulates the stability of IκBα (36), whereas in other cases, sumoylation acts as a recognition signal for a ubiquitin ligase (37). An interplay between sumoylation and acetylation has been observed in the regulation of proteins, such as MEF2, the core histones, and hypermethylation in cancer 1 (HIC1) (38, 39). In the case of MEF2, the sumoylation-acetylation switch is regulated by phosphorylation (40). These studies demonstrate the importance of signaling crosstalk in the regulation of protein sumoylation.

Mechanisms of SUMO-mediated repression of PARP1 coactivator function

First, sumoylation may directly affect PARP1's binding to DNA by promoting its dissociation from specific chromatin regions. This possibility seems unlikely, since sumoylation of PARP1 did not alter its ability to recognize and bind damaged DNA *in vitro*. Second, SUMO modification could also affect enzymatic activities of PARP1, which is important for gene expression. Also, this seems unlikely, since we have shown that SUMO modification of PARP1 does not interfere with DNA-dependent ADP-ribosylation activity *in vitro*. In addition, increased SUMO3 levels do not correspond to elevated poly(ADP-ribosyl)ation in cells on hydrogen peroxide-induced DNA damage, suggesting that sumoylation of PARP1 does not have a stimulatory effect on its enzymatic activity. However, it was shown that poly(ADP-ribosyl)ation is not required for NF-κB-dependent gene expression (41). Neither the enzymatic activity of PARP1 nor its binding to DNA was required for full activation of NF-κB in response to various stimuli *in vivo* when tested on transiently transfected reporter plasmids (21, 42). Consistently, the enzymatic activity of PARP1 was not required for full transcriptional activation of NF-κB in the presence of the histone acetyltransferase p300 (6). Because sumoylation of PARP1 inhibits its acetylation at adjacent lysine residues and because these residues are also targets of ADP-ribosylation, a potential acetylation-ADP-ribosylation switch, which is controlled through sumoylation of PARP1, is very likely. Third, the SUMO modification could promote or inhibit protein-protein interactions through protein complex formation. This scenario seems to be the most relevant for PARP1, since the interaction of PARP1 with p300 and subsequent PARP1 acetylation was impaired after sumoylation of PARP1 at K486. This lysine residue lies within the domain of PARP1, which contributes to most protein-protein interactions such as XRCC1 (6). However, we did not observe a general SUMO-dependent inhibition of protein interactions in this region since HIF1-α and XRCC1 binding does not seem to be affected by sumoylation of PARP1 (Supplemental Fig. 5*E* and unpublished results). In addition to the inhibition of p300

binding, SUMO modification of PARP1 may facilitate the recruitment of a transcriptional corepressor. Currently, several chromatin-modifying enzymes and chromatin-binding proteins have been implicated as effectors of SUMO-mediated repression. For example, SUMO modification of the transcription factor Elk-1 promotes recruitment of HDAC2, associated with histone deacetylation and transcriptional repression of the c-fos promoter (43). Very recently, CoREST1 and Mi2 were identified as SUMO-dependent corepressors, and evidence was provided that CoREST1 binds directly and noncovalently to SUMO2/3, but not to SUMO1 (44, 45). Notably, the aforementioned interaction of PARP1 with PIAS family members could contribute to gene silencing.

Desumoylation of PARP1 by SENP1 and SENP3

We observed that SENP1 and SENP3 are able to catalyze PARP1's SUMO deconjugation. The nucleoplasmic SENP1 relieves SUMO-dependent repression of Ets1, c-Jun, and the androgen receptor, the latter effect being through desumoylation of histone deacetylase 1 (46). Recent data also implicate the nucleolus in dynamic cycles of sumoylation and desumoylation. For example, nucleolar SENP3 is able to catalyze desumoylation of various proteins in this compartment, with specificity to SUMO2/3 (15, 46). In addition, it seems that SENPs regulate SUMO paralog preference of substrate proteins by deconjugation of specific SUMOs, as shown for RanGAP1 (47). This could also explain the higher steady-state level of SUMO3-modified than SUMO1-modified PARP1.

Only a subset of PARP1-dependent genes are affected by sumoylation

Analyses of the role of SUMO in transcriptional regulation have mainly relied on the use of protein overexpession and transiently transfected reporter genes, which may not give a true reflection of the physiological situation. Therefore, we have established a system where we complement cells depleted from endogenous PARP1 with sumoylation deficient PARP1 or wild-type PARP1 and analyzed the expression of endogenous target genes. Known HIF1-α dependent genes with a high induction upon hypoxia were tested. Of these, CAIX and LOXL2 showed increased transcript levels in sumoylation deficient K486R mutant cell line, whereas other genes were solely dependent on PARP1, but not on its sumoylation. Consistent with the qPCR data, the expression levels of CAIX were increased in cells expressing sumoylation-deficient PARP1. Previous studies on PARP1's coactivator function revealed that this function is heavily dependent on its acetylation through p300. Here, we showed that acetylation is abrogated if the SUMO moiety is present on PARP1. Consistently, the sumoylation-deficient mutant showed a higher acetylation status, which corresponded to higher gene expression status for some genes. Collectively, these data support the mechanistic studies performed *in vitro*, unraveling an important role of sumoylation in regulating PARP1-dependent transcriptional coactivation through regulation of its acetylation. It is largely accepted that post-translational modifications fine tune and regulate the requirement of certain transcriptional cofactors for gene expression by transcription factors and might thus influence only a subset of genes (48).

Hypoxia-induced gene expression is affected by PARP1 sumoylation

The role of sumoylation in the regulation of hypoxia-induced gene expression and HIF-1α stability is controversial (49). Hypoxia can induce the expression of SUMO1 (50) and an RWD-containing sumoylation enhancer (RSUME) that functions as a promoter of protein sumoylation (51). RSUME expression is induced by hypoxia, which leads to the enhanced sumoylation and stabilization of HIF-1α. Alternatively, a recent study indicates that the hypoxia-induced sumoylation of HIF-1α targets HIF-1α for degradation through the von Hippel–Lindau (VHL) protein-mediated ubiquitin-proteasome pathway (37). Clearly, further studies are needed to clarify these controversial findings on the role of sumoylation in the regulation of HIF-1α stability during hypoxia. In this study, we have investigated the regulation of the known HIF1-α-dependent genes CAIX and LOXL2 and provide novel insights to understand the complex transcriptional regulation of these emerging tumor markers. The expression of these genes is restrained through SUMO modification of the transcriptional coactivator PARP1, indicating that sumoylation of PARP1 dampens HIF1-α signaling for these genes. Thus, this pathway may have an important regulatory role in the regulation of intracellular pH and hypoxia-induced metastasis (52, 53). Moreover, it remains to be elucidated whether sumoylation of PARP1 is also affecting transcription mediated by other transcription factors and whether SUMO modification is associated with the role of PARP1 in several pathophysiological disease models. Further studies of the sumoylation of PARP1 will determine the role of SUMO modification/deconjugation in these pathological states. FJ

We are grateful to L. Sistonen and H. A. Blomster (University of Turku, Turku, Finland) for support and scientific insight. We thank G. Poirier and D. Gauvin (Laval University Medical Research Center, Laval University, Quebec, QC, Canada), D. Stiehl and R. Wenger (University of Zurich, Zurich, Switzerland), S. Pastorekova (Slovak Academy of Sciences, Bratislava, Slovak Republic), R. T. Hay (University of Dundee, Dundee, UK), and R. Niedenthal (Hannover Medical School, Hannover, Germany) for generously providing reagents. We are grateful to T. Valovka (University of Innsbruck, Innsbruck, Austria) and P. O. Hassa, M. Fey, and other members of the Institute of Veterinary Biochemistry and Molecular Biology (University of Zurich) for their critical and constructive comments on the manuscript. This work was

supported in part by the Deutsche Forschungsgemeinschaft (to S. Müller), the Swiss National Science Foundation (grants 31-109315.05 and 31-122421/1 to M.O.H.), and the Kanton of Zurich (to M.O.H.).

REFERENCES

1. Hassa, P. O., Haenni, S. S., Elser, M., and Hottiger, M. O. (2006) Nuclear ADP-ribosylation reactions in mammalian cells: where are we today and where are we going? *Microbiol. Mol. Biol. Rev.* **70,** 789–829
2. D'Amours, D., Desnoyers, S., D'Silva, I., and Poirier, G. G. (1999) Poly(ADP-ribosyl)ation reactions in the regulation of nuclear functions. *Biochem. J.* **342,** 249–268
3. Kim, M. Y., Zhang, T., and Kraus, W. L. (2005) Poly(ADP-ribosyl)ation by PARP-1: 'PAR-laying' NAD+ into a nuclear signal. *Genes Dev.* **19,** 1951–1967
4. Kraus, W. L. (2008) Transcriptional control by PARP-1: chromatin modulation, enhancer-binding, coregulation, and insulation. *Curr. Opin. Cell Biol.* **20,** 294–302
5. Altmeyer, M., Messner, S., Hassa, P. O., Fey, M., and Hottiger, M. O. (2009) Molecular mechanism of poly(ADP-ribosyl)ation by PARP1 and identification of lysine residues as ADP-ribose acceptor sites. *Nucleic Acids Res.* **37,** 3723–3738
6. Hassa, P. O., Haenni, S. S., Buerki, C., Meier, N. I., Lane, W. S., Owen, H., Gersbach, M., Imhof, R., and Hottiger, M. O. (2005) Acetylation of poly(ADP-ribose) polymerase-1 by p300/CREB-binding protein regulates coactivation of NF-κB-dependent transcription. *J. Biol. Chem.* **280,** 40,450–40,464
7. Elser, M., Borsig, L., Hassa, P. O., Erener, S., Messner, S., Valovka, T., Keller, S., Gassmann, M., and Hottiger, M. O. (2008) Poly(ADP-ribose) polymerase 1 promotes tumor cell survival by coactivating hypoxia-inducible factor-1-dependent gene expression. *Mol. Cancer Res.* **6,** 282–290
8. Johnson, E. S. (2004) Protein modification by SUMO. *Annu. Rev. Biochem.* **73,** 355–382
9. Gill, G. (2004) SUMO and ubiquitin in the nucleus: different functions, similar mechanisms? *Genes Dev.* **18,** 2046–2059
10. Hay, R. T. (2005) SUMO: a history of modification. *Mol. Cell.* **18,** 1–12
11. Tatham, M. H., Jaffray, E., Vaughan, O. A., Desterro, J. M., Botting, C. H., Naismith, J. H., and Hay, R. T. (2001) Polymeric chains of SUMO-2 and SUMO-3 are conjugated to protein substrates by SAE1/SAE2 and Ubc9. *J. Biol. Chem.* **276,** 35,368–35,374
12. Saitoh, H., and Hinchey, J. (2000) Functional heterogeneity of small ubiquitin-related protein modifiers SUMO-1 versus SUMO-2/3. *J. Biol. Chem.* **275,** 6252–6258
13. Ayaydin, F., and Dasso, M. (2004) Distinct in vivo dynamics of vertebrate SUMO paralogues. *Mol. Biol. Cell* **15,** 5208–5218
14. Vertegaal, A. C., Andersen, J. S., Ogg, S. C., Hay, R. T., Mann, M., and Lamond, A. I. (2006) Distinct and overlapping sets of SUMO-1 and SUMO-2 target proteins revealed by quantitative proteomics. *Mol. Cell. Proteomics* **5,** 2298–2310
15. Mukhopadhyay, D., and Dasso, M. (2007) Modification in reverse: the SUMO proteases. *Trends Biochem. Sci.* **32,** 286–295
16. Vertegaal, A. C., Ogg, S. C., Jaffray, E., Rodriguez, M. S., Hay, R. T., Andersen, J. S., Mann, M., and Lamond, A. I. (2004) A proteomic study of SUMO-2 target proteins. *J. Biol. Chem.* **279,** 33,791–33,798
17. Rosas-Acosta, G., Russell, W. K., Deyrieux, A., Russell, D. H., and Wilson, V. G. (2005) A universal strategy for proteomic studies of SUMO and other ubiquitin-like modifiers. *Mol. Cell. Proteomics* **4,** 56–72
18. Blomster, H. A., Hietakangas, V., Wu, J., Kouvonen, P., Hautaniemi, S., and Sistonen, L. (2009) Novel proteomics strategy brings insight into the prevalence of SUMO-2 target sites. *Mol. Cell. Proteomics* **8,** 1382–1390
19. Girdwood, D. W., Tatham, M. H., and Hay, R. T. (2004) SUMO and transcriptional regulation. *Semin. Cell. Dev. Biol.* **15,** 201–210
20. Dadke, S., Cotteret, S., Yip, S. C., Jaffer, Z. M., Haj, F., Ivanov, A., Rauscher, F., 3rd, Shuai, K., Ng, T., Neel, B. G., and Chernoff, J. (2007) Regulation of protein tyrosine phosphatase 1B by sumoylation. *Nat. Cell Biol.* **9,** 80–85
21. Hassa, P. O., Buerki, C., Lombardi, C., Imhof, R., and Hottiger, M. O. (2003) Transcriptional coactivation of nuclear factor-κB-dependent gene expression by p300 is regulated by poly(ADP)-ribose polymerase-1. *J. Biol. Chem.* **278,** 45,145–45,153
22. Fahrer, J., Kranaster, R., Altmeyer, M., Marx, A., and Burkle, A. (2007) Quantitative analysis of the binding affinity of poly(ADP-ribose) to specific binding proteins as a function of chain length. *Nucleic Acids Res.* **35,** e143
23. Muller, S., Berger, M., Lehembre, F., Seeler, J. S., Haupt, Y., and Dejean, A. (2000) c-Jun and p53 activity is modulated by SUMO-1 modification. *J. Biol. Chem.* **275,** 13,321–13,329
24. Haenni, S. S., Hassa, P. O., Altmeyer, M., Fey, M., Imhof, R., and Hottiger, M. O. (2008) Identification of lysines 36 and 37 of PARP-2 as targets for acetylation and auto-ADP-ribosylation. *Int. J. Biochem. Cell Biol.* **40,** 2274–2283
25. El-Andaloussi, N., Valovka, T., Toueille, M., Steinacher, R., Focke, F., Gehrig, P., Covic, M., Hassa, P. O., Schar, P., Hubscher, U., and Hottiger, M. O. (2006) Arginine methylation regulates DNA polymerase beta. *Mol. Cell* **22,** 51–62
26. Altmeyer, M., Messner, S., Hassa, P. O., Fey, M., and Hottiger, M. O. (2009) Molecular mechanism of poly(ADP-ribosyl)ation by PARP1 and identification of lysine residues as ADP-ribose acceptor sites. *Nucleic Acids Res.* **37,** 3723–3738
27. Kerscher, O. (2007) SUMO junction-what's your function? New insights through SUMO-interacting motifs. *EMBO Rep.* **8,** 550–555
28. Baba, D., Maita, N., Jee, J. G., Uchimura, Y., Saitoh, H., Sugasawa, K., Hanaoka, F., Tochio, H., Hiroaki, H., and Shirakawa, M. (2005) Crystal structure of thymine DNA glycosylase conjugated to SUMO-1. *Nature* **435,** 979–982
29. Takahashi, H., Hatakeyama, S., Saitoh, H., and Nakayama, K. I. (2005) Noncovalent SUMO-1 binding activity of thymine DNA glycosylase (TDG) is required for its SUMO-1 modification and colocalization with the promyelocytic leukemia protein. *J. Biol. Chem.* **280,** 5611–5621
30. Shen, T. H., Lin, H. K., Scaglioni, P. P., Yung, T. M., and Pandolfi, P. P. (2006) The mechanisms of PML-nuclear body formation. *Mol. Cell* **24,** 331–339
31. Hunter, T. (2007) The age of crosstalk: phosphorylation, ubiquitination, and beyond. *Mol. Cell* **28,** 730–738
32. Hietakangas, V., Anckar, J., Blomster, H. A., Fujimoto, M., Palvimo, J. J., Nakai, A., and Sistonen, L. (2006) PDSM, a motif for phosphorylation-dependent SUMO modification. *Proc. Natl. Acad. Sci. U. S. A.* **103,** 45–50
33. Hietakangas, V., Ahlskog, J. K., Jakobsson, A. M., Hellesuo, M., Sahlberg, N. M., Holmberg, C. I., Mikhailov, A., Palvimo, J. J., Pirkkala, L., and Sistonen, L. (2003) Phosphorylation of serine 303 is a prerequisite for the stress-inducible SUMO modification of heat shock factor 1. *Mol. Cell. Biol.* **23,** 2953–2968
34. Gregoire, S., Tremblay, A. M., Xiao, L., Yang, Q., Ma, K., Nie, J., Mao, Z., Wu, Z., Giguere, V., and Yang, X. J. (2006) Control of MEF2 transcriptional activity by coordinated phosphorylation and sumoylation. *J. Biol. Chem.* **281,** 4423–4433
35. Tremblay, A. M., Wilson, B. J., Yang, X. J., and Giguere, V. (2008) Phosphorylation-dependent sumoylation regulates estrogen-related receptor-alpha and -gamma transcriptional activity through a synergy control motif. *Mol. Endocrinol.* **22,** 570–584
36. Desterro, J. M., Rodriguez, M. S., and Hay, R. T. (1998) SUMO-1 modification of IκBα inhibits NF-κB activation. *Mol. Cell* **2,** 233–239
37. Cheng, J., Kang, X., Zhang, S., and Yeh, E. T. (2007) SUMO-specific protease 1 is essential for stabilization of HIF1α during hypoxia. *Cell* **131,** 584–595
38. Gregoire, S., and Yang, X. J. (2005) Association with class IIa histone deacetylases upregulates the sumoylation of MEF2 transcription factors. *Mol. Cell. Biol.* **25,** 2273–2287
39. Stankovic-Valentin, N., Deltour, S., Seeler, J., Pinte, S., Vergoten, G., Guerardel, C., Dejean, A., and Leprince, D. (2007) An acetylation/deacetylation-SUMOylation switch through a phylogenetically conserved psiKXEP motif in the tumor suppressor HIC1 regulates transcriptional repression activity. *Mol. Cell. Biol.* **27,** 2661–2675
40. Shalizi, A., Gaudilliere, B., Yuan, Z., Stegmuller, J., Shirogane, T., Ge, Q., Tan, Y., Schulman, B., Harper, J. W., and Bonni, A.

(2006) A calcium-regulated MEF2 sumoylation switch controls postsynaptic differentiation. *Science* **311,** 1012–1017
41. Hassa, P. O., and Hottiger, M. O. (2002) The functional role of poly(ADP-ribose)polymerase 1 as novel coactivator of NF-κB in inflammatory disorders. *Cell. Mol. Life Sci.* **59,** 1534–1553
42. Hassa, P. O., Covic, M., Hasan, S., Imhof, R., and Hottiger, M. O. (2001) The enzymatic and DNA binding activity of PARP-1 are not required for NF-κB coactivator function. *J. Biol. Chem.* **276,** 45,588–45,597
43. Yang, S. H., and Sharrocks, A. D. (2004) SUMO promotes HDAC-mediated transcriptional repression. *Mol. Cell* **13,** 611–617
44. Stielow, B., Sapetschnig, A., Kruger, I., Kunert, N., Brehm, A., Boutros, M., and Suske, G. (2008) Identification of SUMO-dependent chromatin-associated transcriptional repression components by a genome-wide RNAi screen. *Mol. Cell* **29,** 742–754
45. Ouyang, J., Shi, Y., Valin, A., Xuan, Y., and Gill, G. (2009) Direct binding of CoREST1 to SUMO-2/3 contributes to gene-specific repression by the LSD1/CoREST1/HDAC complex. *Mol. Cell* **34,** 145–154
46. Kim, J. H., and Baek, S. H. (2009) Emerging roles of desumoylating enzymes. *Biochim. Biophys. Acta* **1792,** 155–162
47. Zhu, S., Goeres, J., Sixt, K. M., Bekes, M., Zhang, X. D., Salvesen, G. S., and Matunis, M. J. (2009) Protection from isopeptidase-mediated deconjugation regulates paralog-selective sumoylation of RanGAP1. *Mol. Cell* **33,** 570–580
48. Buerki, C., Rothgiesser, K. M., Valovka, T., Owen, H. R., Rehrauer, H., Fey, M., Lane, W. S., and Hottiger, M. O. (2008) Functional relevance of novel p300-mediated lysine 314 and 315 acetylation of RelA/p65. *Nucleic Acids Res.* **36,** 1665–1680
49. Liu, B., and Shuai, K. (2008) Regulation of the sumoylation system in gene expression. *Curr. Opin. Cell Biol.* **20,** 288–293
50. Comerford, K. M., Leonard, M. O., Karhausen, J., Carey, R., Colgan, S. P., and Taylor, C. T. (2003) Small ubiquitin-related modifier-1 modification mediates resolution of CREB-dependent responses to hypoxia. *Proc. Natl. Acad. Sci. U. S. A.* **100,** 986–991
51. Carbia-Nagashima, A., Gerez, J., Perez-Castro, C., Paez-Pereda, M., Silberstein, S., Stalla, G. K., Holsboer, F., and Arzt, E. (2007) RSUME, a small RWD-containing protein, enhances SUMO conjugation and stabilizes HIF-1α during hypoxia. *Cell* **131,** 309–323
52. Kaluz, S., Kaluzova, M., Liao, S. Y., Lerman, M., and Stanbridge, E. J. (2009) Transcriptional control of the tumor- and hypoxia-marker carbonic anhydrase 9: A one transcription factor (HIF-1) show? *Biochim. Biophys. Acta* **1795,** 162–172
53. Peinado, H., Moreno-Bueno, G., Hardisson, D., Perez-Gomez, E., Santos, V., Mendiola, M., de Diego, J. I., Nistal, M., Quintanilla, M., Portillo, F., and Cano, A. (2008) Lysyl oxidase-like 2 as a new poor prognosis marker of squamous cell carcinomas. *Cancer Res.* **68,** 4541–4550

Received for publication May 18, 2009.
Accepted for publication July 2, 2009.

Supplementary Methods:

DNA binding assay

For *in vitro* DNA binding assays a biotinylated oligonucleotide (5′-GCTGTGGACCCTGCTGTGGGCTGGAGAACAAGGTGATCTGCG-3′) was annealed with a fully complementary oligonucleotide 5′-CGCAGATCACCTCCAGCCCACAGCAGGGTCCACAGC-3′ (control a). To mimic nicked or gapped DNA the biotinylated oligonucleotide was annealed with the oligonucleotide 5′-CGCAGATCACCTTGTTCTCCA-3′ and either 5′-GCGCACAGCAGGGTCCACAGC-3′ (control b, nicked fragment) or 5′-CGCAGATCACCTTGTTCT-P (gapped fragment). Biotinylated oligonucleotides were captured on Streptavidin Agarose beads (Novagen).

Immunofluorescence

For detection of proteins by immunofluorescence, HEK293T cells were fixed with freshly prepared Methanol:Acetic acid (3:1) mix for 5 min on ice, and washed with PBS. Unspecific binding sites were blocked with 0.05% Tween20 and 5% non-fat dry milk in PBS for 30 min at room temperature prior to staining with primary and FITC-conjugated secondary antibodies in the presence of blocking buffer. Pictures were taken with standard fluorescence microscope (Olympus Mx51, 40x, NA 1.3).

Reporter gene Assay

Mouse $PARP1^{+/+}$ or $PARP1^{-/-}$ mouse lung fibroblasts (MLF) cells were isolated from 129S/EV-PARP1+/+ and 129S/EV-PARP1−/− mice (Wang, Morrison, 1997). Only cell passages 2 to 10 were used for experiments. MLF were grown in DMEM Glutamax-I (Invitrogen) containing 4.5 g/L glucose, supplemented with 10% FCS (Invitrogen), 50 units/mL penicillin, 50 µg/mL streptomycin (Sigma), and α-naphthylacetic acid (Invitrogen). Cells were grown in 5% CO2 at 37°C in a humidified incubator. MLF were transfected with polyethylenimine as previously described. Because of differences in transfection efficiencies, an expression plasmid of CMV driven Renilla luceriferase was cotransfected as a transfection efficiency control, and luciferase activities were normalized based on Renilla light units. Luciferase activity was measured with the pSG5C-CA9 reporter gene (described in Kopacek J, et al. (2005). Biochim Biophys Acta 1729: 41-49).

Plasmids

Human HIF1-α (aa 365-805) was amplified from pENTR-d hHIF1-α (aa 5-805) and cloned into a pGEX6P3 vector with BamHI and XhoI restriction enzymes.

Protein purification

GST-hHIF1-α (aa 365-805) was expressed in bacteria and purified according to standard protocols using glutathione sepharose 4B (GE healthcare).

Immunoprecipitation

Sumoylated PARP1 was purified as described in the material and methods section. Either sumoylated HA-PARP1 or desumoylated HA-PARP1 was incubated on protein G sepharose beads (GE healthcare) together with anti-HA antibody. After 1.5 h incubation time, the beads were washed and 5 ug of purified GST-HIF1-α (aa 365-805) was added for 2h. The beads were washed with IP-buffer (50 mM Tris pH 8.0, 170 mM NaCl, 0.5% NP-40, Protease inhibitors) and subjected to SDS-PAGE, followed by western blot analysis.

Supplementary Figures:

Supplementary Figure 1:

(A) HA-PARP1-Ubc9 fusion protein was ectopically expressed with either myc-SUMO1 or myc-SUMO3 in HEK293T. Cell extracts were examined with anti-HA and anti-myc antibody. (B) HA-PARP1-Ubc9 or HA-PARP1-Ubc9 C93S were transfected along with myc-SUMO3 into HEK293T cells. Whole cell extracts were taken and analyzed with anti-HA antibody (C) Immunoprecipitation of ectopically expressed HA-PARP1-Ubc9 fusion protein, expressed in HEK293T with or without myc-SUMO3. Cell extracts were examined with anti-HA and anti-myc antibody.

Supplementary Figure 2:

(A) GST-pulldown with GST alone, conjugation deficient GST-SUMO-AA, or GST-p65 against whole cell extracts from HEK293T. Detection of PARP1-binding was done with PARP1 western blot. GST was used as negative control, GST-p65 as positive control for PARP1 interaction. A coomassie stain of the western blot membrane is shown. (B) GST-pulldown as in (A), but with purified PARP1. (C) GST-pulldown with more stringent conditions than in (B), but with recombinant purified TDG as positive control for non-covalent interaction.

Supplementary Figure 3:

(A) An *in vitro* sumoylation assay with purified PARP1 was carried out without or with EcoRI-linker DNA in the reaction. (B) Three different biotin-tagged oligonucleotides were bound to *in vitro* translated ^{35}S-Methionine labeled and sumoylated PARP1. Precipitation of the oligonucleotides was performed with Streptavidin-Agarose. Bound proteins were separated through SDS-PAGE and detected with autoradiography.

Supplementary Figure 4:

(A) Immunofluorescence staining of untransfected or with myc-SUMO3 transfected HEK293T cells. The cells were fixed 28 h after transfection and stained with the anti-SUMO2/3 (18H8) or anti-PAR (10H) antibody. (B) Immunofluorescence staining of untransfected or with myc-SUMO3 transfected HEK293T cells. The cells were treated with 0.5 mM H_2O_2 for 10 min, fixed and stained with the anti-SUMO2/3 (18H8) or anti-PAR (10H) antibody. (C) Immunofluorescence staining of untransfected or with myc-SUMO3

transfected HEK293T cells. Cells were fixed 28 h after transfection and stained with anit-PARP1 (H250) or anti-myc (9E10) antibody.

Supplementary Figure 5:

(A) *In vitro* acetylation assay with PARP1 wild-type or with acetylation-deficient PARP1 KQR (K498R, K505R, K521R, K524R) mutant. Western blot was done with monoclonal E4 antibody and anti-PARP1 antibody. The antibody was generated against an acetylated peptide corresponding to residues K498, K505 and K508 in human PARP1 sequence. Control of equal inputs of PARP1 was done through coomassie stain of the western blot membrane. (B) CAIX reporter plasmid is induced with SUMOylation deficient PARP1. Primary mouse lung fibroblasts (MLF) were transfected with HA-PARP1 wt or HA-PARP1 K486R along with CAIX reporter plasmids and Renilla-Luciferase for normalization. Cells were induced with hypoxia mimicking drug Ciclopirox-olamine for 8h. (C) SUMO2/3 conjugation is induced after hypoxia. K562 whole cell extracts were examined with SUMO 2/3 antibody after hypoxic induction for 28h at 0.2% O_2. (D) HEK293T cells were transfected with HA-PARP1 and myc-SUMO3 expression plasmids. 20 hours after transfection, cells were exposed to hypoxia (0.2%O_2) for 28 h. Whole cell extracts were examined by western blot using anti-myc and anti-PARP1 antibodies. (E) HA-PARP1 was sumoylated (Su-PARP1) or desumoylated (deSu-PARP1) *in vitro* as described in Fig. 3A, and subsequently immunoprecipitated using anti-HA antibody. As control, only beads with the anti-HA antibody was used (no protein). After extensive washing, beads were incubated with purified GST-HIF1-α (aa 365-805). Co-immunoprecipitated GST-HIF1-α was detected by western blot using an anti-GST antibody.

A

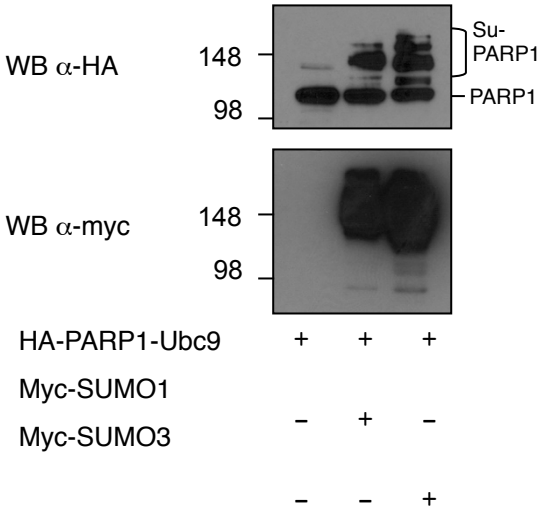
WB α-HA
148
98
Su-
PARP1
PARP1
WB α-myc
148
98
HA-PARP1-Ubc9 + + +
Myc-SUMO1
Myc-SUMO3 – + –
– – +

B

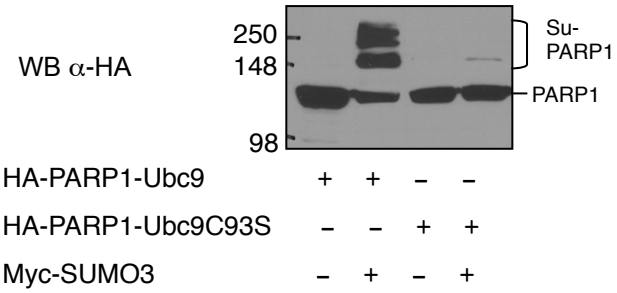
WB α-HA
250
148
98
Su-
PARP1
PARP1
HA-PARP1-Ubc9 + + – –
HA-PARP1-Ubc9C93S – – + +
Myc-SUMO3 – + – +

C

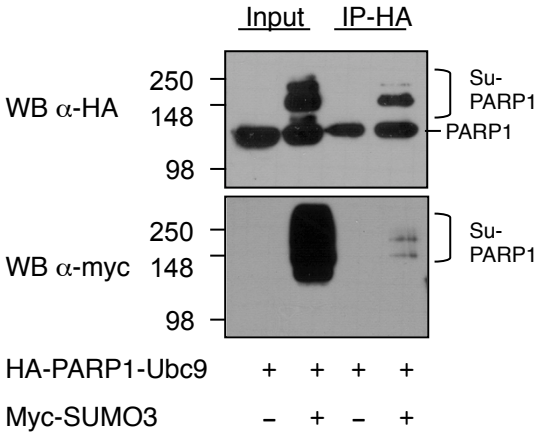
Input IP-HA
WB α-HA
250
148
98
Su-
PARP1
PARP1
WB α-myc
250
148
98
Su-
PARP1
HA-PARP1-Ubc9 + + + +
Myc-SUMO3 – + – +

Supplementary Fig. 2

Messner et al.

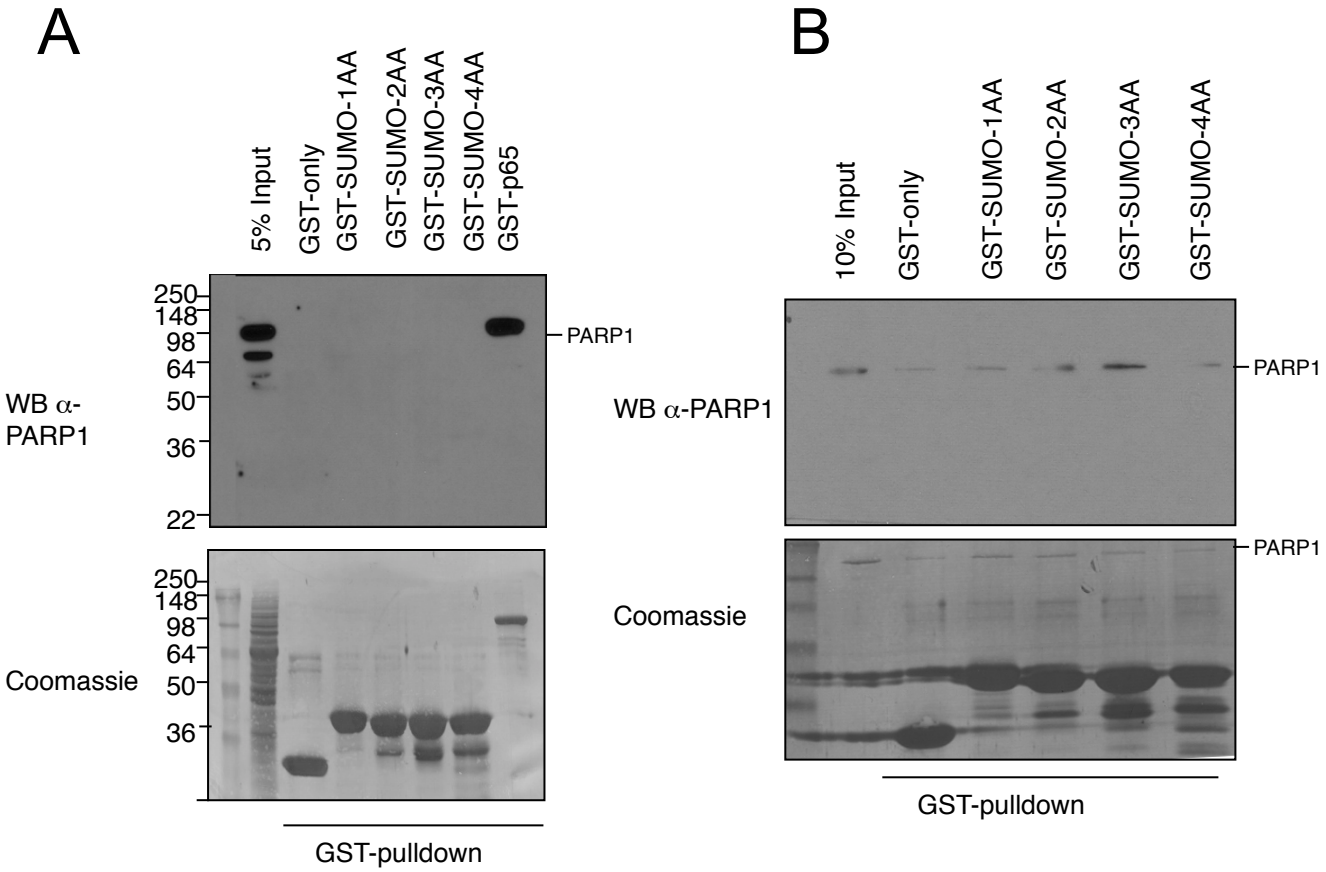

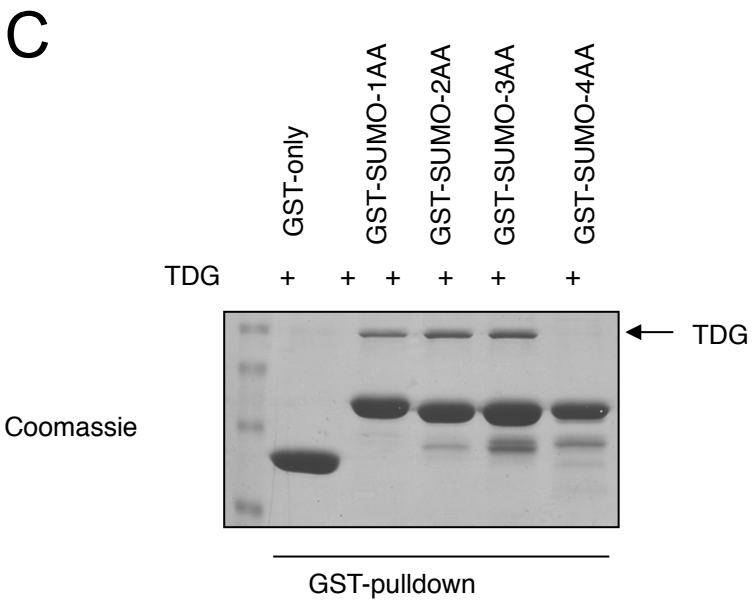

A

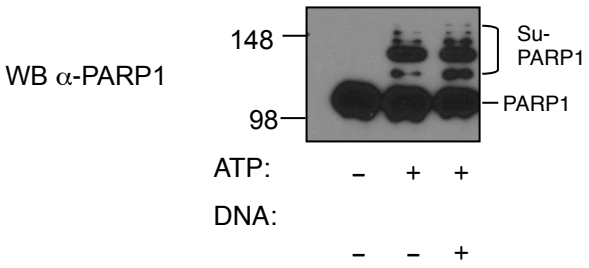
WB α-PARP1
148
98
Su-
PARP1
PARP1
ATP: – + +
DNA: – – +

B

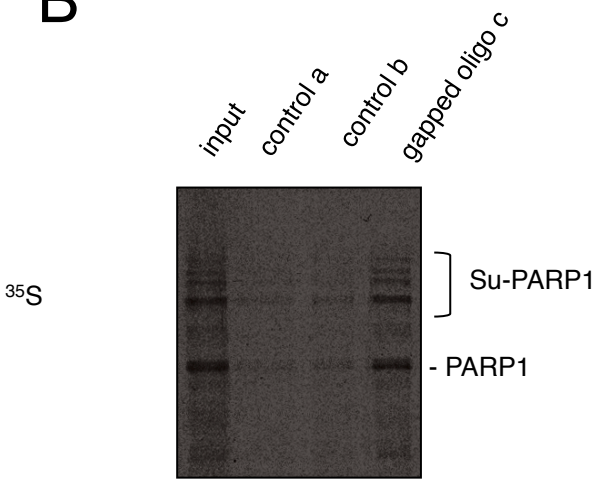
input
control a
control b
gapped oligo c
35S
Su-PARP1
- PARP1

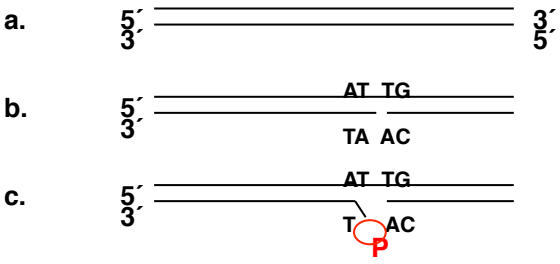
a.
5´
3´
3´
5´
b.
AT TG
TA AC
c.
AT TG
T AC
P

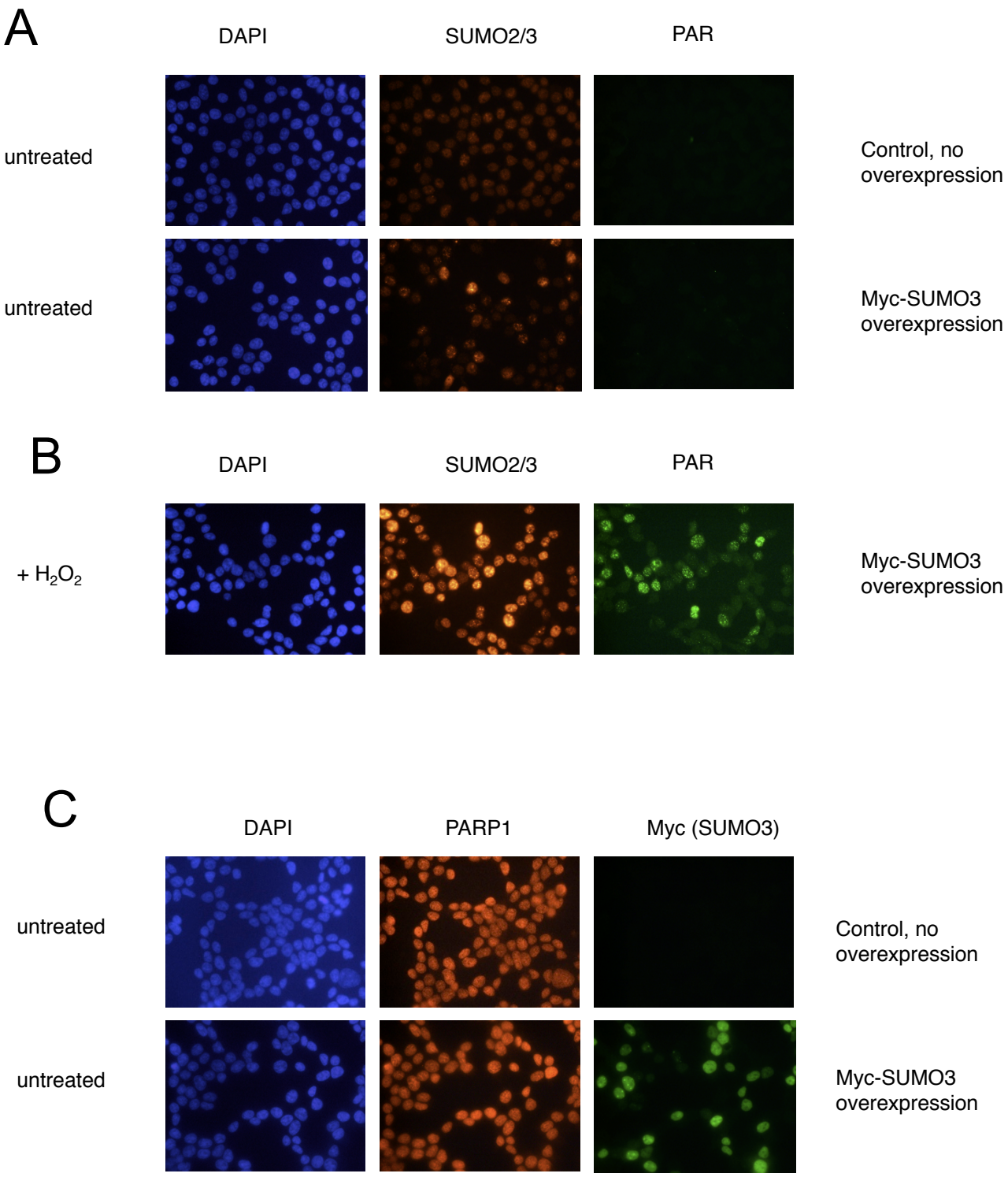
A
DAPI
SUMO2/3
PAR
untreated
Control, no overexpression
untreated
Myc-SUMO3 overexpression
B
DAPI
SUMO2/3
PAR
+ H_2O_2
Myc-SUMO3 overexpression
C
DAPI
PARP1
Myc (SUMO3)
untreated
Control, no overexpression
untreated
Myc-SUMO3 overexpression

A

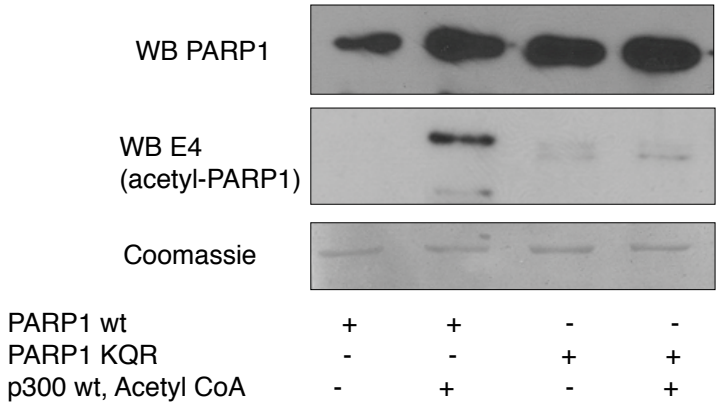
WB PARP1
WB E4
(acetyl-PARP1)
Coomassie
PARP1 wt + + - -
PARP1 KQR - - + +
p300 wt, Acetyl CoA - + - +

B

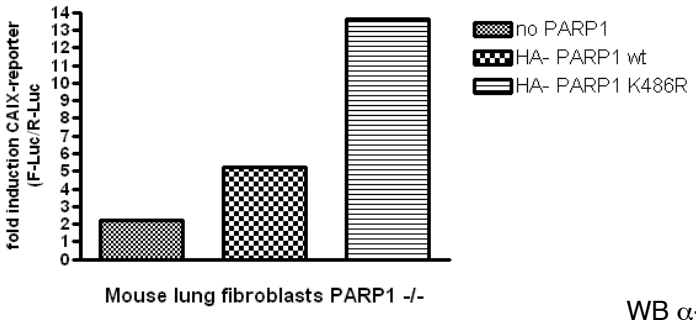
fold induction CAIX-reporter (F-Luc/R-Luc
0 1 2 3 4 5 6 7 8 9 10 11 12 13 14
no PARP1
HA- PARP1 wt
HA- PARP1 K486R
Mouse lung fibroblasts PARP1 -/-

C

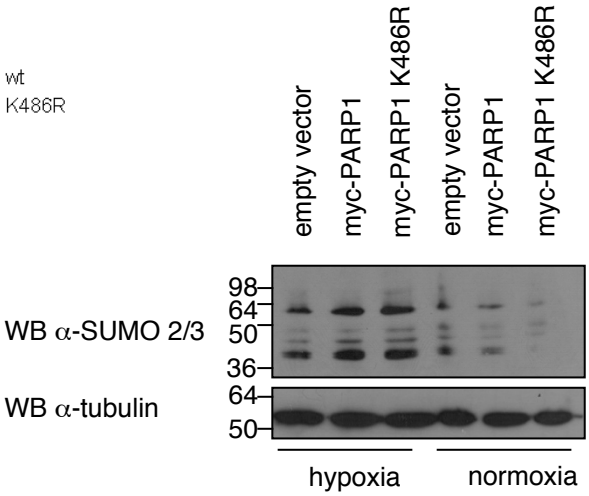
empty vector
myc-PARP1
myc-PARP1 K486R
empty vector
myc-PARP1
myc-PARP1 K486R
WB α-SUMO 2/3
98
64
50
36
WB α-tubulin
64
50
hypoxia
normoxia

Please cite this article in press as: Erener et al., Inflammasome-Activated Caspase 7 Cleaves PARP1 to Enhance the Expression of a Subset of NF-κB Target Genes, Molecular Cell (2012), doi:10.1016/j.molcel.2012.02.016

Molecular Cell
Article

Inflammasome-Activated Caspase 7 Cleaves PARP1 to Enhance the Expression of a Subset of NF-κB Target Genes

Süheda Erener,[1,2] Virginie Pétrilli,[3,4] Ingrid Kassner,[1,2] Roberta Minotti,[1] Rosa Castillo,[3] Raffaella Santoro,[1] Paul O. Hassa,[1] Jürg Tschopp,[3] and Michael O. Hottiger[1,*]
[1]Institute of Veterinary Biochemistry and Molecular Biology
[2]Molecular Life Science Program, Life Science Zurich Graduate School
University of Zurich, Winterthurerstrasse 190, 8057 Zurich, Switzerland
[3]Department of Biochemistry, University of Lausanne, Chemin des Boveresses 155, CH-1066 Epalinges, Switzerland
[4]Present address: Université de Lyon, F-69000 Lyon, France; CNRS, UMR5286, Centre de Recherche en Cancérologie de Lyon, F-69000 Lyon, France; Inserm U1052, Centre de Recherche en Cancérologie de Lyon, F-69000 Lyon, France; Université Lyon 1, F-69000 Lyon, France
*Correspondence: hottiger@vetbio.uzh.ch
DOI 10.1016/j.molcel.2012.02.016

SUMMARY

Caspase 1 is part of the inflammasome, which is assembled upon pathogen recognition, while caspases 3 and/or 7 are mediators of apoptotic and nonapoptotic functions. PARP1 cleavage is a hallmark of apoptosis yet not essential, suggesting it has another physiological role. Here we show that after LPS stimulation, caspase 7 is activated by caspase 1, translocates to the nucleus, and cleaves PARP1 at the promoters of a subset of NF-κB target genes negatively regulated by PARP1. Mutating the PARP1 cleavage site D214 renders PARP1 uncleavable and inhibits PARP1 release from chromatin and chromatin decondensation, thereby restraining the expression of cleavage-dependent NF-κB target genes. These findings propose an apoptosis-independent regulatory role for caspase 7-mediated PARP1 cleavage in proinflammatory gene expression and provide insight into inflammasome signaling.

INTRODUCTION

The nuclear factor kappaB (NF-κB) signal transduction pathway is induced in response to a wide range of stimuli and regulates the cellular response to stress, inflammation, infections, and cytokines (Mankan et al., 2009). The transcription factor activity of NF-κB can be regulated by reversible posttranslational modification of NF-κB itself (e.g., acetylation), by the recruitment of cofactors (e.g., CBP/p300), or by the modification of chromatin structure (Lomvardas and Thanos, 2002; Natoli, 2006; Ramirez-Carrozzi et al., 2009).

Caspases are highly conserved cysteine-dependent aspartate-specific proteases. The human caspase family consists of 12 members that can be grouped into inflammatory and apoptotic caspases (Chowdhury et al., 2008). Caspase 1 is the prototypical member of the inflammatory caspases that mediate the maturation of inflammatory cytokines like proIL-1β and proIL-18 (Ghayur et al., 1997; Martinon et al., 2004; Thornberry et al., 1992). Caspase-1 is activated within a cytoplasmic multiprotein complex named the inflammasome, which consists of a receptor, an adaptor (e.g., ASC), and caspase 1 (Schroder and Tschopp, 2010). Genetic studies in mice suggest at least four inflammasomes with distinct receptors detecting different PAMPs (*p*athogen-*a*ssociated *m*olecular *p*atterns) and DAMPs (*d*anger-*a*ssociated *m*olecular *p*atterns).

Active caspase 3 and 7 cleave a large set of substrates, which ultimately results in apoptosis or necrosis (Kuida et al., 1996; Malireddi et al., 2010). Whereas caspase 3 knockout mice die prematurely (Kuida et al., 1996), caspase 7 knockout mice show no phenotypic abnormalities (Lakhani et al., 2006). Caspase 3/7 double-knockout mice suffer from early perinatal lethality (Lakhani et al., 2006). Accumulating evidence also suggests nonredundant roles and nonapoptotic functions for caspase 3 and caspase 7 in different cellular processes such as cell proliferation, cell-cycle regulation, and cell differentiation and inflammation (Algeciras-Schimnich et al., 2002; Denis et al., 1998; Lamkanfi et al., 2008).

Poly(ADP-ribose) polymerase 1 (PARP1, recently renamed ARTD1 [Hottiger et al., 2010]) is a nuclear chromatin-associated multifunctional enzyme found in most eukaryotes apart from yeast and catalyzes the polymerization of ADP-ribose units from donor NAD^+ molecules (Hassa et al., 2006; Kim et al., 2005). During apoptosis, PARP1 is cleaved by caspases 3 and 7, yielding two enzymatically inactive fragments (24 and 89 kDa) (D'Amours et al., 2001). Interestingly, PARP1 knockin mice, which harbor a mutated caspase cleavage site (D214N), develop normally, indicating that cleavage of PARP1 is not required during apoptosis (Pétrilli et al., 2004). This observation raises the fundamental question why such an elaborate mechanism for selective degradation of a subset of cellular proteins exists, when eventually all the cellular components need to be destroyed. Important regulatory functions other than apoptosis that are mediated by PARP1 cleavage could explain the development of this intricate mechanism.

Although historically studied in the context of genotoxic stress signaling, PARP1 has more recently been linked to the regulation of chromatin structure, transcription, and chromosome

Please cite this article in press as: Erener et al., Inflammasome-Activated Caspase 7 Cleaves PARP1 to Enhance the Expression of a Subset of NF-κB Target Genes, Molecular Cell (2012), doi:10.1016/j.molcel.2012.02.016

organization (Kraus and Lis, 2003; Krishnakumar and Kraus, 2010). Based on the analysis of gene expression profiles in PARP1 knockout or siRNA treated cells, genes can be classified as PARP1-independent or PARP1-dependent (Frizzell et al., 2009), although the molecular basis that determines PARP1 dependency is not yet understood. Furthermore, PARP1-dependent genes can be regulated positively or negatively by PARP1 (Carrillo et al., 2004; Krishnakumar et al., 2008). Earlier studies from our laboratory provide evidence that in mouse lung fibroblasts (MLFs) the stimulus-dependent transcriptional activation of transiently transfected reporter plasmids containing the NF-κB sites of the *iNOS* and *MIP2* genes depends on PARP1 (Hassa et al., 2006; Hassa and Hottiger, 1999). Further studies revealed that the stimulus-induced gene expression of the *iNOS* (NF-κB) reporter plasmid containing the *nos-2* promoter was severely reduced in the presence of noncleavable (D214N) PARP1, while the presence of a cleavable PARP1 (WT or enzymatically inactive) was beneficial (Pétrilli et al., 2004). This observation was confirmed for endogenous *nos-2* and strongly suggests that PARP1 is most likely processed upon stimulation and that cleavage of PARP1 at D214 is beneficial for full transcriptional activation of certain NF-κB target genes. Here, we elucidate the cellular signaling mechanism that leads to PARP1 cleavage under inflammatory conditions and the consequence of this cleavage event for proinflammatory gene expression.

RESULTS

Induction of a Subset of NF-κB Target Genes Is Compromised in Peritoneal Macrophages Isolated from D214N PARP1 Mice

To investigate the regulatory function of PARP1 cleavage for NF-κB-dependent gene expression at the molecular level during inflammation, peritoneal macrophages expressing either WT or noncleavable D214N PARP1 were stimulated for 1 hr with LPS. Gene expression analysis by customized NF-κB microarrays (Jayne et al., 2009) identified ten genes that were less stimulated by LPS in D214N PARP1 cells as compared to WT cells (data not shown). Real-time RT-PCR revealed that the LPS-induced expression of *CSF2*, *IL-6*, and *LIF* was indeed dependent on PARP1 cleavage (reduced in D214N) (Figure 1A). IL-6 levels were also reduced at the protein level in LPS-induced D214N cells (Figure S1A). Interestingly, the three genes were highly expressed in *PARP1* −/− macrophages, indicating a repressory function of PARP1 for these genes (Carrillo et al., 2004) (data not shown). IP-10 was also negatively regulated by PARP1 (PARP1-dependent), but in contrast to the other three genes comparably induced in WT and D214N PARP1 cells (Figure 1A) and was therefore included as a control gene, which is not expressed in a PARP1 cleavage-dependent manner. Together, these data show that only a subset of PARP1-dependent genes was additionally regulated by PARP1 cleavage.

PARP1 Cleavage at D214 Regulates the LPS-Induced Expression of NF-κB Target Genes Also in Human THP1 Cells

To further investigate the physiological relevance of LPS-induced PARP1 cleavage, we expressed WT or noncleavable D214N PARP1 in human THP1 cells depleted of endogenous PARP1 (Figure S1B). LPS stimulation (1 hr) of THP1 cells complemented with noncleavable D214N PARP1 (as compared to THP1 cells complemented with WT *PARP1*) resulted in significantly reduced *IL-6* gene induction, while *IP-10* induction was not affected (Figure 1B), and thus implied that PARP1 cleavage is important for the transcriptional activation of *IL-6* and confirmed the results obtained with primary cells.

Since PARP1 cleavage is considered a hallmark of apoptosis, we tested whether LPS treatment of THP1 cells would induce cell death under the tested conditions by two independent methods. While the control treatment with camptothecin (CPT) induced a significant increase of dead cells, LPS stimulation did not induce any detectable increase in cell death for the indicated time period as measured by staining with ethidium homodimer and calcein or LDH release (Figures 1C and 1D). Moreover, treatment of complemented THP1 cells with CPT induced an 89 kDa cleavage fragment in WT-complemented cells, but not in cells expressing D214N PARP1, confirming that the mutant D214N PARP1 was indeed protected from caspase cleavage (Figure 1E).

The PARP1 D214N Mutation Does Not Affect NF-κB Function or Biochemical Properties of PARP1

The observation that *CSF2* and *IL-6* induction were both abolished upon knockdown of the large NF-κB subunit p65 (Figures S1C and S1D) suggested that stimulus-induced expression of these genes is mainly dependent on p65 signaling. Therefore, we performed ChIP experiments with an antibody against p65 to investigate whether the reduced gene induction in D214N PARP1 cells was due to hampered recruitment of p65 to target DNA sequences. p65 recruitment to the promoters of *CSF2*, *IL-6*, and *IP-10*, but not to the promoter of the control gene *Prolactin*, occurred as soon as 30 min after LPS stimulation of peritoneal macrophages isolated from WT and D214N animals (Figure 2A). After 1 hr, p65 dissociated from the *IL-6* and *IP-10* promoters and exhibited a comparable distribution in WT and D214N cells (Figure 2A). These results clearly suggested that the differential expression of the studied NF-κB target genes was not due to differential p65 recruitment.

In order to exclude that the above-described expression changes were due to altered biochemical properties of D214N PARP1, additional analyses were performed. The enzymatic activity of WT and D214N PARP1 was induced by DNA to the same extent in vitro (Figure 2B). Since the stimulation by DNA is known to induce a conformational change that brings the N-terminal DNA-binding domain to the C-terminal catalytic domain of PARP1 proteins (Messner et al., 2010), the D214N mutation is unlikely to alter the overall configuration of PARP1. We have previously described that PARP1 can bind and be acetylated by p300 (Hassa et al., 2005). Acetylation of PARP1 by p300 revealed that D214N and WT PARP1 can be acetylated in vitro to the same extent (Figure 2C), implicating that complex formation with other proteins was not affected. Complex formation between p65 and PARP1 was also not affected by the D214N mutation in vivo as well as in vitro (Figures 2D and 2E).

These results furthermore implied that the reduced induction of gene expression observed in D214N cells was neither due to

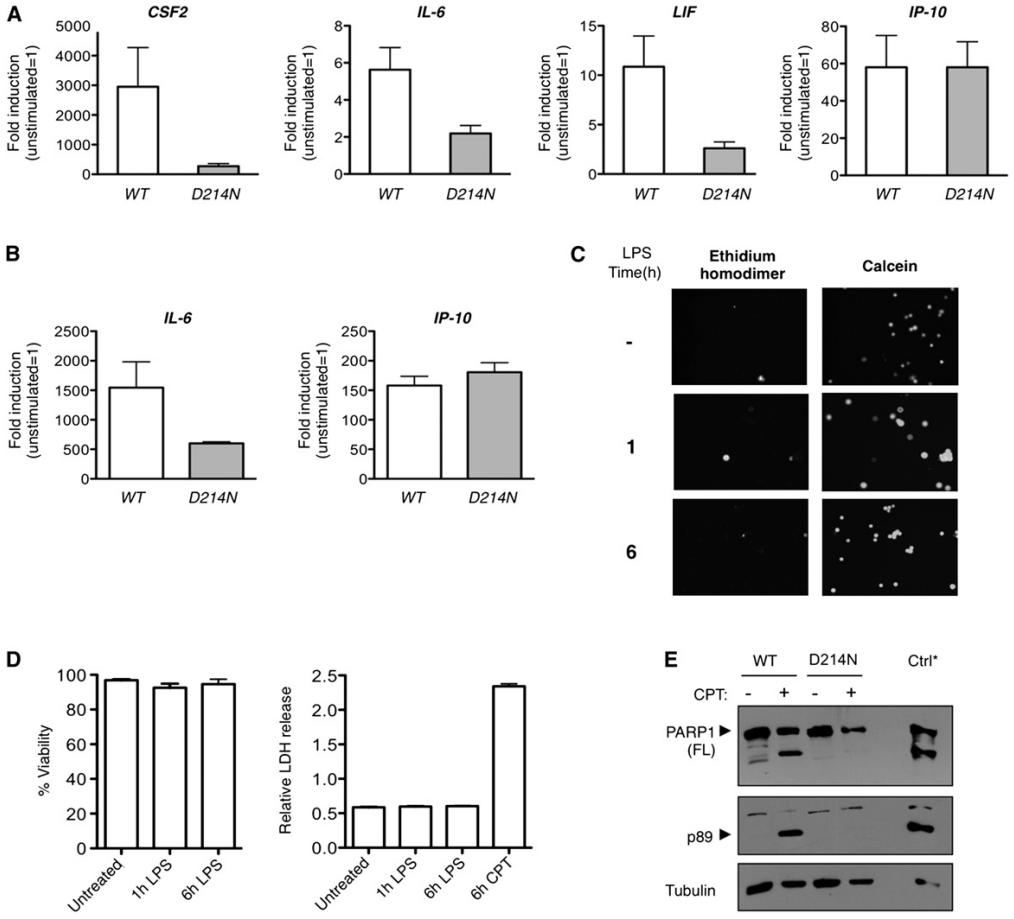

Figure 1. PARP1 Cleavage at D214 Regulates Expression of a Subset of NF-κB Target Genes

(A) LPS-stimulated induction of *CSF2, IL-6*, *LIF*, and *IP-10* expression in peritoneal macrophages isolated from WT and D214N PARP1 mice. Cells were stimulated with LPS for 1 hr and mRNA levels were determined by real-time RT-PCR analysis. Samples were normalized to *Rps12* expression levels and expressed as fold increase relative to unstimulated mRNA levels. Data are means ± SEM of at least four independent representative experiments.

(B) Induction of *IL-6* and *IP-10* expression in stably complemented THP1 cells. Cells were stimulated with LPS for 1 hr and mRNA levels were determined by real-time RT-PCR analysis. Samples were normalized to *Rpl28* expression levels and expressed as fold increase relative to unstimulated mRNA levels. Data are means ± SD, n = 2.

(C and D) LPS stimulation does not affect cell viability. THP1 macrophages were stimulated with LPS for the indicated times and (C) stained with calcein and ethidium homodimer and analyzed by immunofluorescence microscopy (n = 3–7, mean ± SEM) or (D) assayed for LDH release as indicated in the experimental procedures (n = 3, mean ± SEM).

(E) THP1 cells were stimulated with camptothethcin (CPT; 10 μM for 6 hr), total cell extracts were prepared and proteins were analyzed by western blot. Ctrl* is the sample treated with etoposide for 16 hr.

hampered NF-κB signaling nor caused by altered biochemical properties of D214N PARP1.

PARP1 Is Cleaved by Caspases after LPS Induction

To confirm that PARP1 cleavage indeed occurs upon LPS induction, the presence of the enzymatically inactive, C-terminal, large PARP1 fragment (p89; resulting from cleavage at D214) was assessed in stimulated bone marrow-derived macrophages (BMDM) from wild-type mice. PARP1 cleavage was distinctly observed after 2 hr of LPS treatment (Figure 2F) and similarly detected in THP1 cells (Figures S2A and S2B). The observation that PARP1 cleavage affected transcript levels already after 1 hr of LPS induction (Figure 1A) suggested that the cleaved PARP1 fragments might be immediately degraded by the proteasomal machinery and thus rendered undetectable for western blot analysis at early time points. Upon inhibition of the proteasome activity by MG132 and stimulation of the cells with LPS, the p89 fragment could be consistently detected already at the 1 hr time point, and the cleaved PARP1 fragment was exclusively found in the nuclear fraction (Figures S2C and S2D). MG132

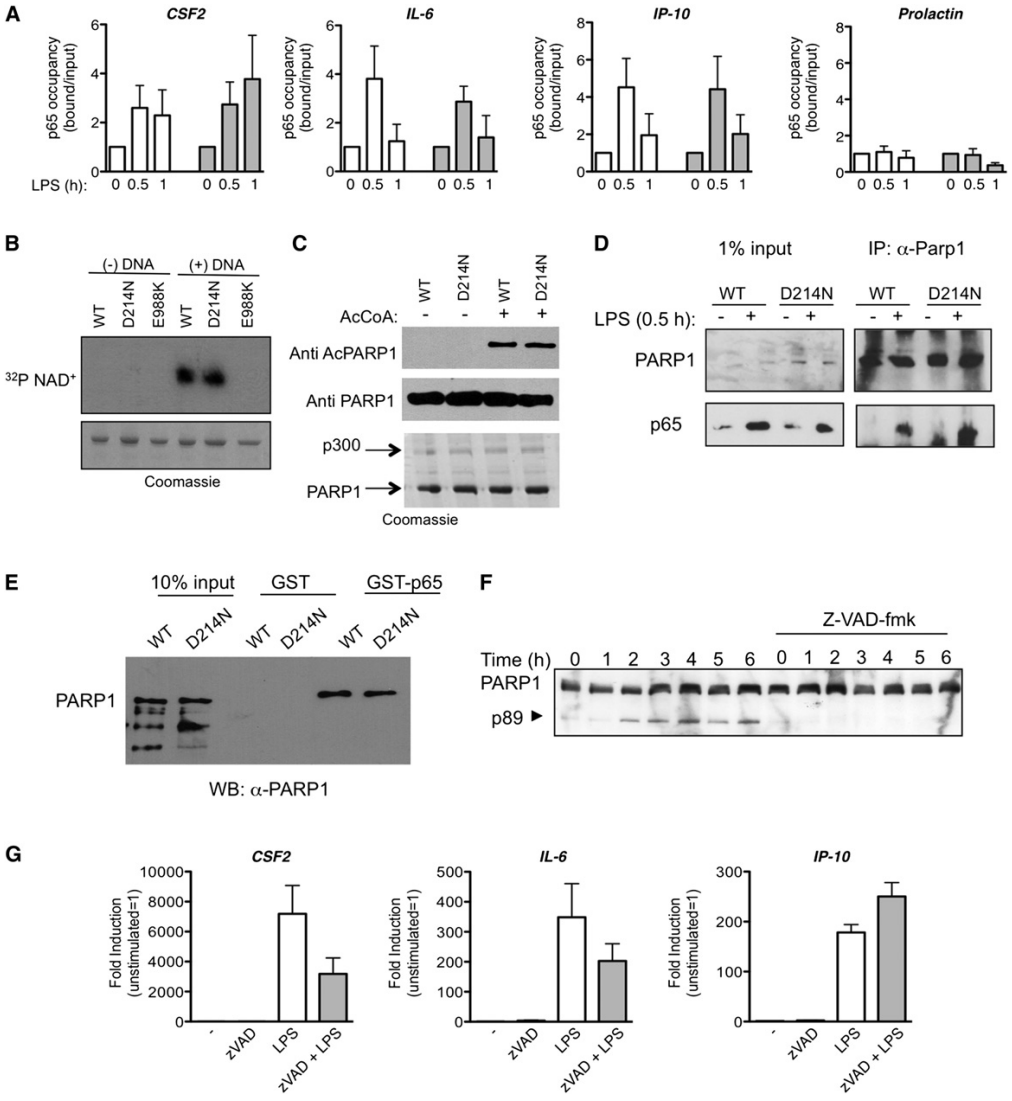

Figure 2. Characterization of WT and D214N PARP1

(A) ChIP analysis of p65 recruitment upon LPS stimulation on the target promoters. WT (white bars) and D214N (gray bars) PARP1 peritoneal macrophages were stimulated with LPS for the indicated times. p65 was immunoprecipitated, and the occupancy on the indicated promoters was measured by qRT-PCR. Data are represented as bound/input and normalized to values corresponding to unstimulated conditions. Unstimulated levels were arbitrarily set as 1. Prolactin promoter was assessed as negative control. Data represent means from 3–4 independent experiments ± SEM.

(B) Enzymatic activity of recombinant PARP1 proteins. WT, D214N, and E988K PARP1 baculovirus generated proteins were incubated with or without DNA for 5 min, and ribosylation was analyzed by autoradiography.

(C) Acetylation of WT and D214N PARP1 (AcCoA=Acetyl coenzyme A).

(D) PARP1 interaction with p65 after LPS stimulation in WT and D214N peritoneal macrophages. Cells were stimulated with LPS and then fractionated. Nuclear extracts were subjected to western blotting.

(E) Interaction of PARP1 fragments with GST-p65. GST-p65 recombinant protein purified from insect cells was incubated with full-length WT and D214N PARP1 proteins. Interaction was analyzed by western blot.

(F) Bone marrow-derived macrophages from wild-type mice were stimulated with LPS for different times in the presence or absence of Z-VAD-fmk (50 μM). Total cell extracts were prepared, and PARP1 cleavage was analyzed by western blot.

(G) Gene expression profiles of *CSF2, IL-6*, and *IP-10* in Raw 264.7 cells. Cells were treated with LPS (1 μg/ml) and/or Z-VAD-fmk (10 μM) for 4 hr and mRNA levels were determined by real-time RT-PCR analysis. Samples were normalized to *Rps12* expression levels and expressed as fold increase relative to unstimulated mRNA levels. Data are means ± SEM of three independent experiments.

alone had no effect on PARP1 cleavage (Figures S2C and S2D) and did not induce apoptosis under the tested conditions (Figure S2E). These results suggested that PARP1 is cleaved upon LPS stimulation and that the C-terminal p89 cleavage fragment is subject to proteasomal degradation and reduced to levels below the detection limit for western blot analysis at early time points after LPS treatment.

Moreover, the caspase inhibitor Z-VAD abrogated LPS-dependent PARP1 cleavage as shown by western blot analysis (Figure 2F). Z-VAD treatment also reduced LPS induced *CSF2* and *IL-6* transcription but not *IP-10* transcription in Raw 264.7 cells (Figure 2G), although LPS-induced nuclear translocation of NF-κB was not affected (Figure S3A). These data strongly suggested that Z-VAD treatment per se did not affect LPS signaling and that caspases were responsible for the cleavage of PARP1.

Caspase 7 Cleaves PARP1 at D214 In Vitro and Enhances NF-κB-Dependent Gene Induction In Vivo

In order to identify which of the caspases 1–10 cleaves PARP1 upon LPS stimulation, purified recombinant WT and D214N PARP1 were incubated with active human caspases (caspase 1–10; expressed and purified with a baculovirus expression system). Western blot analysis with an antibody directed against the catalytic domain of PARP1 confirmed that PARP1 is predominantly cleaved at D214 by caspase 3 and 7 and to a lesser extent by caspases 1, 6, 8, 9, and 10 (Figure 3A).

Since PARP1 is localized in the nucleus, we investigated whether the homologous and highly similar caspases 3 and 7 translocate to the nucleus upon LPS induction. THP1 monocytes were stimulated with LPS for 1.5 or 3.5 hr, and cytoplasmic and nuclear fractions were prepared. Western blot analysis with an antibody that detects only the activated caspase 7 resulting from cleavage at D198 (p19) revealed that a minor but detectable amount of active caspase 7 translocated to the nucleus after stimulation (Figure 3B). Although we could observe caspase 3 activation upon LPS stimulation, we were unable to detect caspase 3 in the nucleus under our experimental conditions and in our cell lines (Figure S3B), suggesting that caspase 7 is mainly responsible for the observed PARP1 cleavage in vivo.

To confirm that caspase 7 has a functional role in LPS-dependent NF-κB gene induction, we transfected peritoneal macrophages and THP1 cells with *caspase 7* or *caspase 3* (as a control) siRNAs and confirmed siRNA specificity by western blot and quantitative RT-PCR (Figures S4A and S4B and data not shown). LPS-induction of *CSF2* and *LIF* was reduced in macrophages transfected with *caspase 7* siRNA, while it was increased or not affected in cells transfected with *caspase 3* siRNA (Figure 3C; similar for THP1 cells in Figure S4C). The control gene *IP-10* was not affected (Figure 3C), indicating that mainly caspase 7 was responsible for the cleavage of PARP1 and the induction of PARP1-cleavage-dependent NF-κB target genes. The strongly reduced IL-6 protein levels secreted by LPS-treated peritoneal macrophages of *caspase 7* −/− mice, as compared to cells from WT animals, supported the above observation for *IL-6* gene expression at the protein level (Figure 3D).

To confirm that this LPS-dependent role of caspase 7 on NF-κB is linked to PARP1 cleavage, THP1 cells expressing WT or D214N PARP1 were transiently transfected with mock or *caspase 7* siRNA and stimulated 1 hr with LPS. Indeed, real-time RT-PCR analysis revealed that caspase 7 knockdown led to a 50% reduction of *IL-6* gene induction in WT PARP1-expressing THP1 cells, whereas no significant increase was observed upon caspase 7 knockdown in D214N PARP1-expressing THP1 cells (Figure 3E). Since the caspase 7 knockdown did not affect nuclear translocation of the large subunit of NF-κB p65 (Figure S4D), we concluded that caspase 7 has a proinflammatory role in NF-κB-mediated gene induction that is mainly mediated by PARP1 cleavage at D214.

Caspase 7 Is a Target of the NLRP3 Inflammasome

The proinflammatory effects seen for caspase 7 encouraged us to test the link between PARP1 cleavage, inflammatory caspase 1, and caspase 7. Peritoneal macrophages isolated from WT, *caspase 1* −/−, and *caspase 7* −/− mice were stimulated with LPS for different times ranging from 1 hr to 16 hr. LPS treatment of WT cells induced PARP1, caspase 1, and caspase 7 cleavage (Figure 4A). In WT cells, PARP1 cleavage was visible as early as 1 hr after stimulation, but it was not observed in *caspase 7* −/− cells, confirming the proposed role for caspase 7 in cleaving PARP1 upon LPS stimulation in vivo (Figure 4A). Similarly, PARP1 and caspase 7 cleavage was not detected in *caspase 1* −/− cells (Figure 4A). In *caspase 7* −/− cell extracts, LPS-dependent caspase 1 activation was not affected, providing evidence that caspase 1 is upstream of caspase 7 activation, not vice versa.

Based on these findings, we further investigated caspase 1, inflammasome formation, and caspase 7 activation. Caspase 7 was not required for inflammasome formation and IL-1β maturation in response to classical inflammasome activators (Figures S5A and S5B). Remarkably, IL-1β levels in WT and D214N macrophages were comparable (Figure S5C), suggesting that observed changes in IL-1β serum levels after LPS treatment in mice are the result of a more complex response in vivo (Pétrilli et al., 2004). Next, we tested whether the essential inflammasome adaptor protein ASC is required to activate caspase 1 in response to LPS stimulation. Indeed, in peritoneal macrophages lacking ASC, LPS-dependent caspase 1 activation, caspase 7 activation, and PARP1 cleavage were abolished (Figure S5D). Moreover, IL-6 protein release upon LPS stimulation of *ASC* −/− cells was reduced (Figure 4B). LPS dependent caspase 1 activation and caspase 7 activation were also abolished in BMDMs lacking the NLRP3 inflammasome component *NLRP3* (Figure 4C). The NLRP3 inflammasome can be activated by exposure to bacterial products as well as danger signals (Mariathasan et al., 2004; Pétrilli et al., 2007; Tschopp and Schroder, 2010). In WT macrophages, LPS stimulation induced intracellular caspase 1 maturation (XT), whereas a typical NLRP3 inflammasome inducer like monosodium urate (MSU) led to release of active caspase 1 into the cell culture media (Figure 4D). Western blot analysis also confirmed that caspase 1 and 7 were similarly activated in WT and D214 PARP1 cell lines (Figure 4E). We thus concluded that the transcriptional effects caused by the PARP1 D214N mutation were not caused by altered caspase 7 activation.

These results indicate that LPS-dependent caspase 7 activation is mediated by the NLRP3 inflammasome and highlight

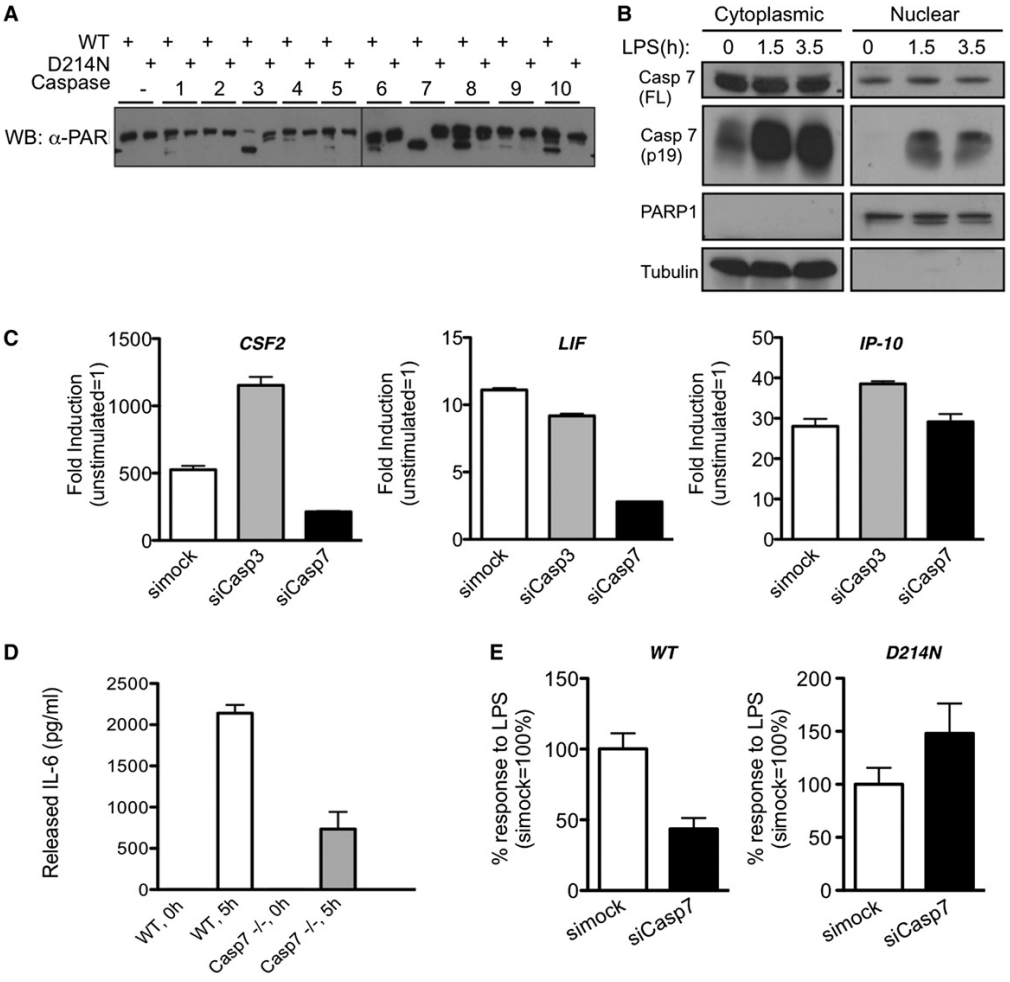

Figure 3. Caspase 7 Cleaves PARP1 at D214 In Vitro and Controls NF-κB Gene Induction

(A) Screening of caspase family members (1–10) for PARP1 cleavage at D214 in vitro. Recombinant PARP1 WT or D214N mutant recombinant proteins were incubated with active caspases (1–10) for 20 min at 30°C in a caspase cleavage buffer. Reaction products were analyzed by SDS gel followed by western blot using PARP1 antibody.

(B) THP1 cells were stimulated with LPS for the indicated times. Cells were then fractionated, and cytoplasmic and nuclear extracts were subjected to western blotting.

(C) *CSF2, LIF*, and *IP10* fold induction upon LPS stimulation of caspase 3 and 7 knockdown macrophages. Cells were stimulated with LPS for 1 hr and gene expression was analyzed by real-time RT-PCR. Samples were normalized to *Rps12* and expressed as fold increase relative to unstimulated mRNA levels. Data are means ± SD, n = 2.

(D) IL-6 protein levels released by IP macrophages were determined by ELISA after 5 hr of LPS induction (IL-6 could not be detected in uninduced peritoneal macrophages). Values represent means ± SD of two measurements.

(E) *IL-6* expression is significantly reduced in siCasp7-treated THP1 cells. Changes in gene expression upon LPS stimulation were expressed as fold response. Fold response was set arbitrarily as 100% in simock transfected cells. Data are means ± SD, n = 2.

a role for activated intracellular caspase 1 that is also supported by other recent observations (Malireddi et al., 2010).

LPS Induces PARP1 Dissociation from the *CSF2*, *IL-6*, and *IP-10* Transcription Start Site upon Recruitment of Caspase 7

To elucidate the chromatin association of PARP1 after LPS stimulation at the transcriptional start site (TSS) of the indicated genes, ChIP experiments with antibodies that recognize the C-terminal part of PARP1 (p89) were performed. PARP1 was associated with the TSS of the three indicated genes under unstimulated conditions (Figure 5A). Stimulation with LPS for 2 hr or more lead to reduced PARP1 occupancy on the *CSF2* and *IL-6* promoters, while PARP1 dissociation could not be detected at earlier time points (Figure 5A). The chromatin association of PARP1 was lost immediately after LPS stimulation at the TSS

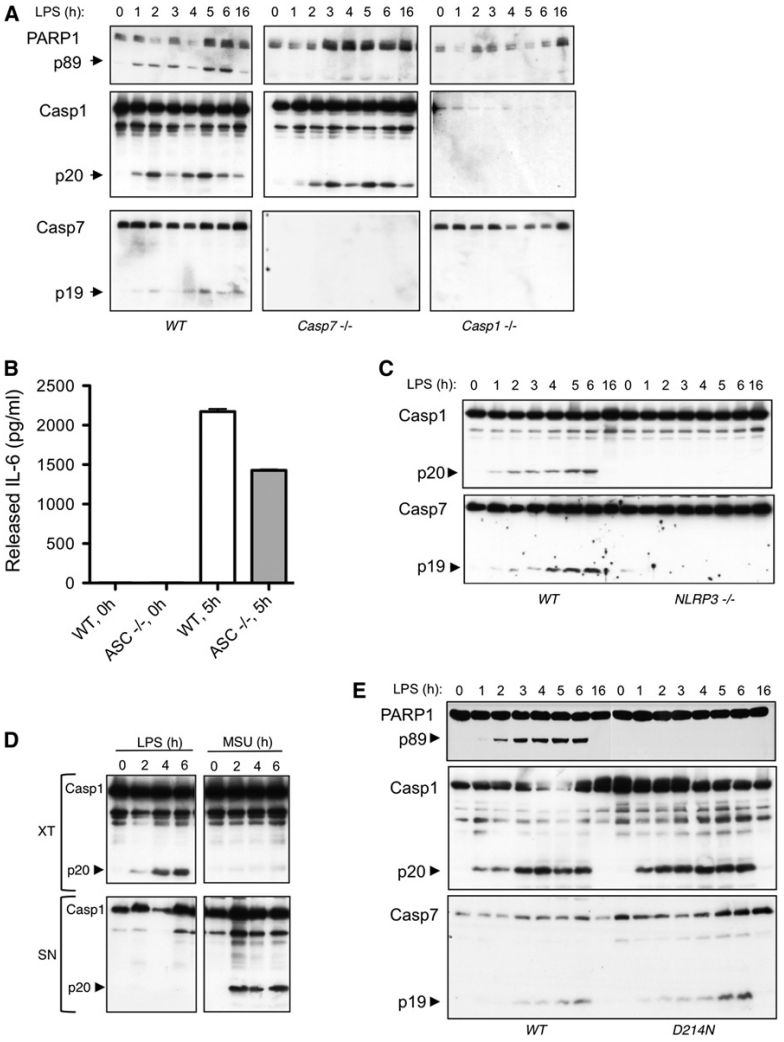

Figure 4. Caspase 7 Is a Target of the NLRP3 Inflammasome

(A) PARP1 cleavage upon LPS stimulation is mediated by caspase 1 and caspase 7. Peritoneal macrophages from wild-type, *caspase 1* −/−, and *caspase 7* −/− mice were stimulated for the indicated times with LPS, total cell extracts were prepared, and PARP1 cleavage and caspase 1 and caspase 7 activation were analyzed by western blot.

(B) In IP macrophages lacking the essential inflammasome adaptor ASC, IL-6 protein levels upon LPS stimulation were strongly reduced as determined by ELISA (means ± SEM).

(C) BMDM cells from wild-type and *NLRP3* −/− mice were stimulated for the indicated times with LPS, total cell extracts were prepared, and PARP1 cleavage and caspase 1 and caspase 7 activation were analyzed by western blot.

(D) Peritoneal macrophages from wild-type mice were stimulated for the indicated times with LPS or MSU. Total cell extracts (XT) or the culture media (SN) were analyzed by western blot.

(E) Uncleavable PARP1 (D214N) does not interfere with caspase activation by LPS. Peritoneal macrophages from wild-type and D214N PARP1 mice were stimulated for the indicated time with LPS, total cell extracts were prepared, and PARP1 cleavage and caspase 1 and caspase 7 activation were analyzed by western blot.

of *IP-10* (Figure 5A), indicating differences in the chromatin dissociation of PARP1 for different NF-κB target genes. Stimulation of Raw 264.7 macrophages for 2 hr in presence of Z-VAD inhibited the chromatin dissociation of PARP1 from the *CSF2* and *IL-6* (but not *IP-10)* promoters and thus implied that the release of PARP1 at these sites is dependent on caspase activity (Figure 5B). In agreement with this finding, we could detect a small but distinct caspase 7 recruitment to the promoter of the cleavage-dependent gene *IL-6,* but not to the promoter of *IP-10* (Figures 5C and S5E).

Next we compared chromatin association of PARP1 in THP1 cells complemented with N-terminally myc-tagged WT or D214N PARP1. The uncleaved or enzymatically inactive p24 PARP1 cleavage fragment was immunoprecipitated with an anti-myc antibody (Figure S1B). Already, after 1 hr of LPS stimulation, myc-PARP1 chromatin association was reduced at the TSS of *IL-6* in THP1 cells complemented with WT PARP1 (Figure 5D). In contrast, the myc-tagged PARP1 was still detectable in cells complemented with noncleavable D214N PARP1 (Figure 5D). Interestingly, PARP1 seemed even enriched at the *IL-6* TSS upon LPS stimulation of these cells. This was not observed for the TSS of *H2B*, which served as a control gene not regulated by PARP1. Together, these data suggested that PARP1 is associated with chromatin and that upon LPS stimulation and recruitment of caspase 7 both the N-terminal (myc-tagged) and the C-terminal PARP1 fragments dissociate from chromatin at the TSS (Figures 5B and 5D).

LPS-Induced PARP1 Chromatin Dissociation Leads to Chromatin Decondensation

Previous studies have shown that PARP1 can regulate nucleosome compaction and the accessibility of DNA in chromatin (Gottschalk et al., 2009; Timinszky et al., 2009). To gain more insight into the functional consequences of PARP1 cleavage and dissociation at the chromatin level, we performed a chromatin accessibility assay for *CSF2,* as a representative PARP1 cleavage-dependent gene. Chromatin from unstimulated or 1 hr LPS-stimulated cells were isolated, digested with MNase, and subsequently analyzed by CHART-PCR. The chromatin at the TSS of *CSF2* became more accessible upon LPS stimulation (Figure 5E). This effect on chromatin accessibility was more

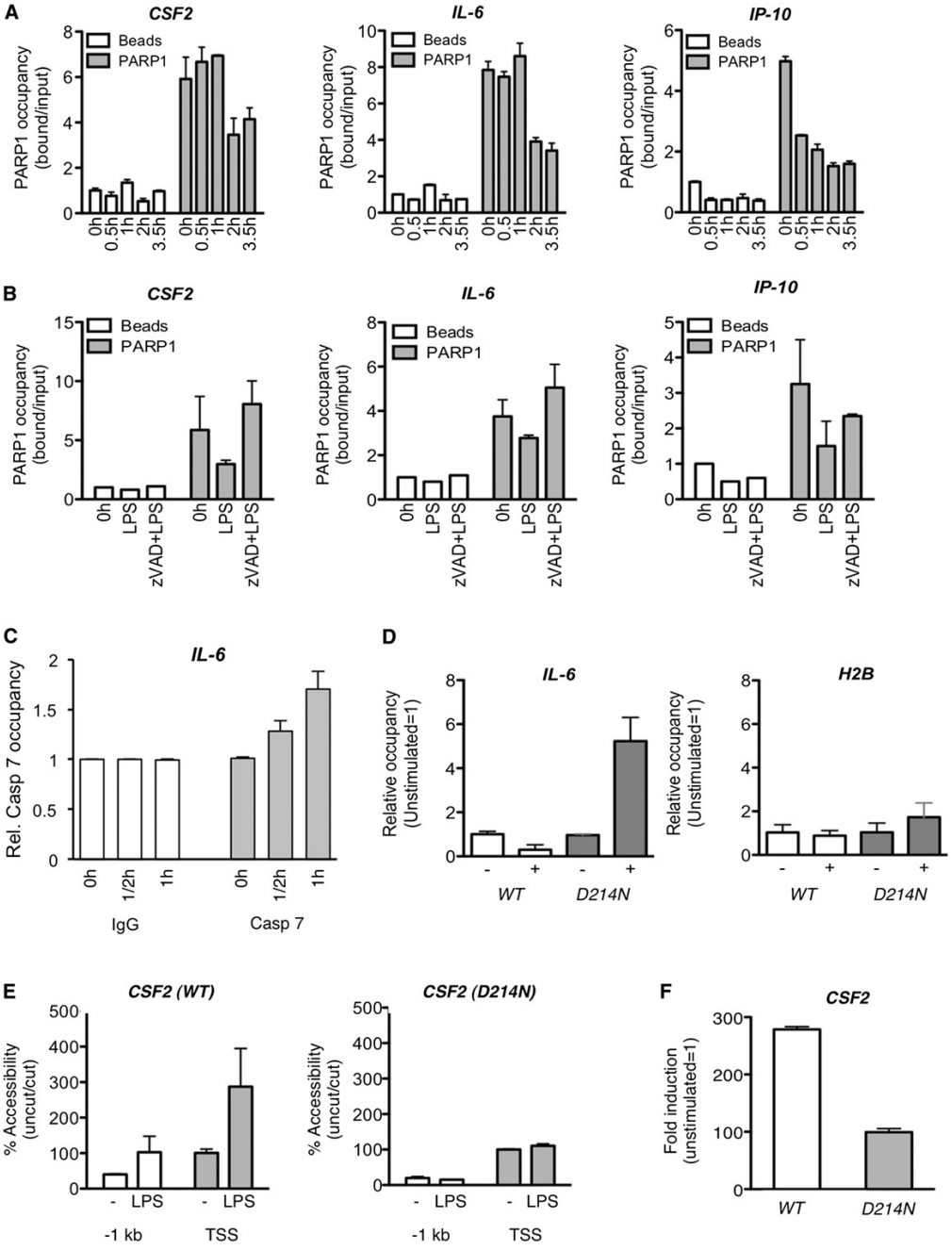

Figure 5. PARP1 Cleavage Regulates the Expression of *IL-6* in THP1 Cells

(A) Kinetics of PARP1 occupancy upon LPS stimulation on the target promoters by ChIP analysis. Raw 264.7 cells were stimulated with LPS for different times. PARP1 was immunoprecipitated with a PARP1 antibody, and the occupancy on the indicated promoters was measured by real-time RT-PCR. Results are normalized to values corresponding to the beads control (0 hr time point), and the means ± SEM are shown.

(B) Effect of Z-VAD-fmk on PARP1 occupancy on the target promoters after LPS stimulation. Raw 264.7 cells were treated for 2 hr with LPS and Z-VAD-fmk. The same analysis was performed as in (A). Results are from two independent experiments, ± SD.

(C) Kinetics of caspase 7 occupancy at the *IL-6* promoter. Values are represented as bound/input and were normalized to the IgG control. The mean ± SD of two RT-PCR quantifications is shown, and two independent experiments were performed.

pronounced around the TSS than 1 kb upstream of this site (Figure 5E). Interestingly, analysis of the corresponding site in cells isolated from D214N PARP1 mice revealed that the extent of chromatin decompaction was significantly reduced upon LPS stimulation (Figure 5E), which correlated with the observed gene expression levels for *CSF2* upon LPS stimulation (Figure 5F). Together, these data provided strong evidence that PARP1 cleavage decreased chromatin compaction at the TSS in vivo and enhanced LPS induction of defined NF-κB target genes.

DISCUSSION

The results presented here demonstrate that (1) upon LPS stimulation and after activation of the NLRP3 inflammasome and of caspase 1, caspase 7 translocates to the nucleus; (2) caspase 7 is recruited to the transcription start site of specific NF-κB target genes; (3) caspase 7 cleaves mainly PARP1 at D214; and (4) release of the PARP1 cleavage fragments leads to subsequent chromatin decondensation and enhanced gene expression. Our conclusions are based on several observations: (1) on differential gene expression in mouse primary cells and human THP1 cells genetically complemented with WT or noncleavable D214N PARP1; (2) on different mouse models lacking caspase 7 or individual components of the NLRP3 inflammasome; (3) on differential chromatin accessibilities based on MNase experiments; and (4) on ChIP experiments for p65, caspase 7, and PARP1. These results may have broad implications for the regulation of the inflammatory response, since several NF-κB target genes involved in inflammation are regulated by PARP1 cleavage.

Nuclear Translocation of Caspase 7 upon LPS Stimulation

Our experiments show that LPS-activated caspase 7 and PARP1 cleavage stimulated the expression of PARP1 negatively regulated NF-κB target genes in the tested cells. This tight regulation could be achieved by LPS-induced activation of a very distinct cytoplasmic complex containing caspase 7 and/or the induction of a posttranslational modification, which would allow caspase 7 to translocate to the nucleus and to be recruited to the TSS, where mainly PARP1 seems processed. However, the protein responsible for recruiting caspase 7 is currently not known. An LPS-induced factor that translocates to the nucleus could function as a carrier or regulator for caspase 7, since caspase 7 lacks a classical NLS. Such a mechanism could also cause alternative shuttling and targeting of caspase 7 and thus explain the biologically different functions of the highly similar caspases 3 and 7.

Different Kinetics of PARP1 Release from NF-κB Target Genes

Chromatin dissociation and the release of the p89 PARP1 fragment (Figure 5A) was only observed after 2 hr of LPS stimulation for *CSF-2* and *IL-6*, while the p89 fragment dissociated within minutes from the promoter of the control gene *IP-10* (Figure 5A). The observation that PARP1 can dissociate from some NF-κB target genes either within minutes and even in the presence of Z-VAD (*IP-10)* or only 2 hr after LPS induction (*CSF-2, IL-6*) hints at different mechanisms that mediate release of PARP1: fast, PARP1 cleavage-independent (observed for *IP-10*) and slow, PARP1 cleavage-dependent chromatin release.

PARP1 (C- and N-terminal fragments) was released from the chromatin of a subset of genes in a caspase-dependent manner (Figure 5), but a certain amount of PARP1 remained associated with the promoters (Figure 5A). This observation implies that transcriptional initiation does not require full dissociation of PARP1. The functional relevance of this residual PARP1 is currently not understood.

Caspases 3 and 7 Have Distinct Functions Independent of Apoptosis

Caspases are important effectors of programmed cell death and their function in apoptosis has been extensively studied (Thornberry and Lazebnik, 1998). For example, the activations of the NLRP3 and NLRC4 inflammasomes and of caspase 7 was described upon induction of pyroptosis (Malireddi et al., 2010). Similarly, the infection of macrophages with *L. pneumophila* results in cell death due to the NLRC4/IPAF inflammasome and to activation of caspase 7 (Akhter et al., 2009). During apoptosis, caspases also cleave PARP1 (Germain et al., 1999). To our knowledge, there are currently no publications describing the activation of the NLRP3, caspase 1, caspase 7 signaling axis independent of any type of programmed cell death.

Upon LPS stimulation, we did not detect ADP-ribose polymer formation (sign of genotoxic stress signaling) with the available antibodies against ADP-ribose polymers, and the amount of activated caspases 3/7 during LPS treatment was very low compared to apoptotic conditions. It is therefore likely that the herein described processing of PARP1 by caspases 1/7 represents a direct mechanism of chromatin regulation. However, we cannot exclude that active caspase 7 is cleaving additional proteins important for other cellular processes during LPS stimulation or that other caspases are also able to cleave PARP1 upon LPS stimulation (e.g., caspase 6, 8, 9, or 10) (Figure 3A). Reports documenting functions of caspases in nonapoptotic cellular processes are accumulating. For example, stimulation of microglia with various inflammogens activates caspase 8

(D) ChIP analysis of PARP1 occupancy upon LPS stimulation on the target promoters in WT and D214N *PARP1*-complemented THP1 cells. Cells were stimulated with LPS for 1 hr. PARP1 was immunoprecipitated with a myc antibody, and the occupancy on the indicated promoters was measured by real-time RT-PCR. Results are corrected for the input controls and expressed as relative occupancy, unstimulated levels being set arbitrarily as 1. H2B promoter was assessed as negative control. Data are means ± SD, n = 2.

(E) Chromatin accessibility was assessed by real-time PCR (CHART-PCR). Nuclei from unstimulated and LPS-stimulated BMDMs were incubated with MNase. (−1) kb upstream promoter and TSS of *CSF2* were analyzed. Results are expressed as uncut over cut genomic DNA and normalized to unstimulated levels. Unstimulated uncut/cut genomic DNA level around TSS was arbitrarily set as 100. Data are from a pool of six mice, and means ± SD are shown (n = 2).

(F) After stimulation of BMDMs with LPS for 1 hr, mRNA levels were determined by real-time RT-PCR analysis. Samples were normalized to *Rps12* expression levels and expressed as fold increase relative to unstimulated mRNA levels. Data are means ± SEM, three independent mice groups where each group contains two mice, n = 6.

and caspase 3/7 without triggering cell death in vitro or in vivo, providing another example for a nonapoptotic function (Burguillos et al., 2011). The results presented here are also in agreement with the recently published finding that caspase 7 (but not caspase 3) is a downstream target of caspase 1, which provides evidence for distinct activation mechanisms for caspase 3 and 7 in response to microbial stimuli and bacterial infection (Lamkanfi et al., 2008). Interestingly, PARP1 cleavage was also observed in extracts of differentiating cells, implicating PARP1 cleavage in other cellular processes and emphasizing its physiological relevance (Fujita et al., 2008).

PARP1 Cleavage-Dependent Regulation of NF-κB Target Gene Expression Is Not Due to Altered p65 Recruitment

At present, the molecular basis of the PARP1 and PARP1 cleavage dependency leading to differential NF-κB transcriptional activation is not understood. The observation that the recruitment of p65 to the promoters of *CSF2, IL-6*, and *IP-10* was comparable in WT and D214N PARP1 cells underlines the notion that these genes have an inherent competence to respond to NF-κB (Smale, 2011). PARP1 may thus be involved in maintaining and fine-tuning the extent of the NF-κB response, likely due to a stimulation of RNA polymerase II-dependent transcription.

The changes in gene expression (mRNA and protein levels) could also be influenced at the posttranscriptional level, but so far PARP1 has not been implicated in such a regulatory mechanism. Although poly-ADP-ribose regulates stress responses and microRNA activity in the cytoplasm, PARP1 was neither detected in stress granules nor involved in any kind of regulation (Leung et al., 2011). Together, we think that our data on PARP1 cleavage and chromatin association, chromatin decondensation, and mRNA levels are all in agreement and do not hint at a posttranscriptional effect of PARP1 cleavage on mRNA stability.

It also remains to be determined if PARP1 positively regulated genes respond similarly to caspase-induced PARP1 cleavage. Our previous findings provide evidence that PARP1 is present as a chromatin regulator in different biochemically induced NF-κB complexes and is required for at least a subset of NF-κB gene expression (Hassa et al., 2008). Such a differential NF-κB-specific promoter regulation has been described for other transcriptional cofactors, such as CARM1 (Covic et al., 2005), or as the result of sumoylation of PARP1 (Messner et al., 2009). PARP1 association in different regulatory complexes or PARP1 posttranslational modification may thus result in differential susceptibility to caspase cleavage and thereby limit the regulatory function of PARP1 cleavage to a specific subset of NF-κB target genes.

In this study we explored the signaling and molecular mechanism by which PARP1 cleavage contributes to NF-κB-dependent transcriptional regulation. We provide evidence that LPS-activated nonapoptotic PARP1 cleavage by caspase 7 releases PARP1 from chromatin, reduces chromatin compaction, and enhances the expression of a subset of NF-κB-dependent genes. Mutation of the PARP1 cleavage site (D214) or absence of activated caspase 7 abolishes LPS-stimulated PARP1 cleavage, prevents release of PARP1 from chromatin, maintains chromatin compaction, and compromises the induction of a subset of PARP1 negatively regulated NF-κB target genes. These results functionally link the NLRP3 inflammasome-activated caspase 7 to inflammation and transcription.

EXPERIMENTAL PROCEDURES

A brief description of the experimental procedures is given below. A more detailed delineation of the methods is provided in the supplemental material. All experiments shown and discussed were performed at least twice and one representative result is shown.

Mice and Cell Isolation

WT and transgenic mice were maintained in a specific pathogen-free facility and were from the same genetic background (C57BL/6). For the generation of bone marrow macrophages, 6- to 8-week-old mice were sacrificed, and the cells were isolated as described elsewhere (Pétrilli et al., 2007). Cells were plated in 10 cm uncharged plastic plates (Petri dish) and incubated for full differentiation in RPMI medium supplemented with 10% FCS, 100 units/ml penicillin/streptomycin (GIBCO), 1× nonessential amino acids (GIBCO), 1 mM sodium pyruvate (GIBCO), 50 μM β-mercaptoethanol (GIBCO), and 20% L929 conditioned medium for 10 days in a humidified incubator (with 5% CO2 at 37°C). After 10 days, cells were counted and seeded in 6-well tissue culture plates. After 16 hr, cells were stimulated with 10 μg/ml LPS for 1 hr and harvested for RNA extraction.

For the isolation of peritoneal macrophages, 8- to 10-week-old mice were i.p injected with 1 ml of 10% Brewer thioglycollate medium for 3 days. Mice were sacrificed, and cells were collected as described previously (Pétrilli et al., 2004). Briefly, cells were collected in RPMI medium by abdominal lavage, washed with PBS, and seeded at a cell density of 1×10^6 cells/ml in tissue culture plates in full-RPMI medium containing 10% FCS, 100 units/ml penicillin/streptomycin (GIBCO), 1× nonessential amino acids (GIBCO), and 1mM sodium pyruvate (GIBCO). Cells were cultured in full-RPMI medium. Animal experiments were performed according to the regulations of the cantonal veterinary office.

RNA Extraction and Gene Expression Analysis by Real-Time RT-PCR

Unless stated otherwise, subconfluent (50%) cells were stimulated with 10 μg/ml LPS for 1 hr. Total RNA was isolated using kits according to the manufacturers' recommendation (Macherey-Nagel and Ambion). RNA was reverse-transcribed (kit from Applied Biosystems) and real-time PCR was performed using the Rotor-Gene 3000 (Corbett Life Science/QIAGEN) and TaqMan assays or SYBR Green (primers listed in Tables S1 and S2).

Transient Transfections

THP1 cells were primed with PMA (10 ng/ml) for 24 hr and transfected with 30 pmol siRNA oligos (QIAGEN) with 4 μl Lipofectamine RNAiMAX reagent (Invitrogen) according to the manufacturer's protocol. Transfection into HEK293 cells was described elsewhere (Hassa et al., 2005).

Chromatin Immunoprecipitation

Cells were crosslinked with 1% formaldehyde (Calbiochem) or with formaldehyde and dimethyl 3,3′-DTBP (Kurdistani and Grunstein, 2003). Chromatin was fragmented with the Bioruptor (Diagenode), incubated with specific antibodies, and collected with Protein A Agarose/salmon sperm DNA (Millipore). DNA was extracted and measured by real-time PCR using SYBR Green (see above). Primers are listed in Table S3.

Chromatin Accessibility by Real-Time PCR

Accessibility of DNA to MNase was analyzed by real-time PCR (CHART-PCR) as described elsewhere (Rao et al., 2001). The genomic DNA was isolated using a mammalian Genomic DNA miniprep kit (Sigma). Primers used in real-time PCR analysis are listed in Table S3.

SUPPLEMENTAL INFORMATION

Supplemental Information includes five figures, three tables, Supplemental Experimental Procedures, and Supplemental References and can be found with this article online at doi:10.1016/j.molcel.2012.02.016.

ACKNOWLEDGMENTS

We thank Zhao-Qi Wang for PARP1 D214N mice and Peter Vandernabele for providing caspase 1 antibody. We are grateful to Monika Fey, Mareike Hesse, Florian Freimoser, and all the members of the Institute of Veterinary Biochemistry and Molecular Biology (University of Zurich, Switzerland) and group Tschopp for helpful advice and discussions. This work was supported by a Marie Curie Fellowship to V.P. and in part by Swiss National Science Foundation Grants 31003A-122421 and 310030B-138667 and support from the Kanton of Zurich to M.O.H. S.E. and V.P. designed the experiments; S.E., V.P., R.C., R.M., I.K., R.S., and P.O.H. performed experiments; J.T. and M.O.H. designed and supervised the study. S.E. and M.O.H. wrote the manuscript. J.T. passed away shortly before the submission of the manuscript. All the authors read and corrected the manuscript.

Received: June 30, 2011
Revised: December 1, 2011
Accepted: February 28, 2012
Published online: March 29, 2012

REFERENCES

Akhter, A., Gavrilin, M.A., Frantz, L., Washington, S., Ditty, C., Limoli, D., Day, C., Sarkar, A., Newland, C., Butchar, J., et al. (2009). Caspase-7 activation by the Nlrc4/Ipaf inflammasome restricts Legionella pneumophila infection. PLoS Pathog. *5*, e1000361.

Algeciras-Schimnich, A., Barnhart, B.C., and Peter, M.E. (2002). Apoptosis-independent functions of killer caspases. Curr. Opin. Cell Biol. *14*, 721–726.

Burguillos, M.A., Deierborg, T., Kavanagh, E., Persson, A., Hajji, N., Garcia-Quintanilla, A., Cano, J., Brundin, P., Englund, E., Venero, J.L., and Joseph, B. (2011). Caspase signalling controls microglia activation and neurotoxicity. Nature *472*, 319–324.

Carrillo, A., Monreal, Y., Ramírez, P., Marin, L., Parrilla, P., Oliver, F.J., and Yélamos, J. (2004). Transcription regulation of TNF-alpha-early response genes by poly(ADP-ribose) polymerase-1 in murine heart endothelial cells. Nucleic Acids Res. *32*, 757–766.

Chowdhury, I., Tharakan, B., and Bhat, G.K. (2008). Caspases - an update. Comp. Biochem. Physiol. B Biochem. Mol. Biol. *151*, 10–27.

Covic, M., Hassa, P.O., Saccani, S., Buerki, C., Meier, N.I., Lombardi, C., Imhof, R., Bedford, M.T., Natoli, G., and Hottiger, M.O. (2005). Arginine methyltransferase CARM1 is a promoter-specific regulator of NF-kappaB-dependent gene expression. EMBO J. *24*, 85–96.

D'Amours, D., Sallmann, F.R., Dixit, V.M., and Poirier, G.G. (2001). Gain-of-function of poly(ADP-ribose) polymerase-1 upon cleavage by apoptotic proteases: implications for apoptosis. J. Cell Sci. *114*, 3771–3778.

Denis, F., Rhéaume, E., Aouad, S.M., Alam, A., Sékaly, R.P., and Cohen, L.Y. (1998). The role of caspases in T cell development and the control of immune responses. Cell. Mol. Life Sci. *54*, 1005–1019.

Frizzell, K.M., Gamble, M.J., Berrocal, J.G., Zhang, T., Krishnakumar, R., Cen, Y., Sauve, A.A., and Kraus, W.L. (2009). Global analysis of transcriptional regulation by poly(ADP-ribose) polymerase-1 and poly(ADP-ribose) glycohydrolase in MCF-7 human breast cancer cells. J. Biol. Chem. *284*, 33926–33938.

Fujita, J., Crane, A.M., Souza, M.K., Dejosez, M., Kyba, M., Flavell, R.A., Thomson, J.A., and Zwaka, T.P. (2008). Caspase activity mediates the differentiation of embryonic stem cells. Cell Stem Cell *2*, 595–601.

Germain, M., Affar, E.B., D'Amours, D., Dixit, V.M., Salvesen, G.S., and Poirier, G.G. (1999). Cleavage of automodified poly(ADP-ribose) polymerase during apoptosis. Evidence for involvement of caspase-7. J. Biol. Chem. *274*, 28379–28384.

Ghayur, T., Banerjee, S., Hugunin, M., Butler, D., Herzog, L., Carter, A., Quintal, L., Sekut, L., Talanian, R., Paskind, M., et al. (1997). Caspase-1 processes IFN-gamma-inducing factor and regulates LPS-induced IFN-gamma production. Nature *386*, 619–623.

Gottschalk, A.J., Timinszky, G., Kong, S.E., Jin, J., Cai, Y., Swanson, S.K., Washburn, M.P., Florens, L., Ladurner, A.G., Conaway, J.W., and Conaway, R.C. (2009). Poly(ADP-ribosyl)ation directs recruitment and activation of an ATP-dependent chromatin remodeler. Proc. Natl. Acad. Sci. USA *106*, 13770–13774.

Hassa, P.O., and Hottiger, M.O. (1999). A role of poly (ADP-ribose) polymerase in NF-kappaB transcriptional activation. Biol. Chem. *380*, 953–959.

Hassa, P.O., Haenni, S.S., Buerki, C., Meier, N.I., Lane, W.S., Owen, H., Gersbach, M., Imhof, R., and Hottiger, M.O. (2005). Acetylation of poly(ADP-ribose) polymerase-1 by p300/CREB-binding protein regulates coactivation of NF-kappaB-dependent transcription. J. Biol. Chem. *280*, 40450–40464.

Hassa, P.O., Haenni, S.S., Elser, M., and Hottiger, M.O. (2006). Nuclear ADP-ribosylation reactions in mammalian cells: where are we today and where are we going? Microbiol. Mol. Biol. Rev. *70*, 789–829.

Hassa, P.O., Covic, M., Bedford, M.T., and Hottiger, M.O. (2008). Protein arginine methyltransferase 1 coactivates NF-kappaB-dependent gene expression synergistically with CARM1 and PARP1. J. Mol. Biol. *377*, 668–678.

Hottiger, M.O., Hassa, P.O., Lüscher, B., Schüler, H., and Koch-Nolte, F. (2010). Toward a unified nomenclature for mammalian ADP-ribosyltransferases. Trends Biochem. Sci. *35*, 208–219.

Jayne, S., Rothgiesser, K.M., and Hottiger, M.O. (2009). CARM1 but not its enzymatic activity is required for transcriptional coactivation of NF-kappaB-dependent gene expression. J. Mol. Biol. *394*, 485–495.

Kim, M.Y., Zhang, T., and Kraus, W.L. (2005). Poly(ADP-ribosyl)ation by PARP-1: 'PAR-laying' NAD+ into a nuclear signal. Genes Dev. *19*, 1951–1967.

Kraus, W.L., and Lis, J.T. (2003). PARP goes transcription. Cell *113*, 677–683.

Krishnakumar, R., and Kraus, W.L. (2010). The PARP side of the nucleus: molecular actions, physiological outcomes, and clinical targets. Mol. Cell *39*, 8–24.

Krishnakumar, R., Gamble, M.J., Frizzell, K.M., Berrocal, J.G., Kininis, M., and Kraus, W.L. (2008). Reciprocal binding of PARP-1 and histone H1 at promoters specifies transcriptional outcomes. Science *319*, 819–821.

Kuida, K., Zheng, T.S., Na, S., Kuan, C., Yang, D., Karasuyama, H., Rakic, P., and Flavell, R.A. (1996). Decreased apoptosis in the brain and premature lethality in CPP32-deficient mice. Nature *384*, 368–372.

Kurdistani, S.K., and Grunstein, M. (2003). In vivo protein-protein and protein-DNA crosslinking for genomewide binding microarray. Methods *31*, 90–95.

Lakhani, S.A., Masud, A., Kuida, K., Porter, G.A., Jr., Booth, C.J., Mehal, W.Z., Inayat, I., and Flavell, R.A. (2006). Caspases 3 and 7: key mediators of mitochondrial events of apoptosis. Science *311*, 847–851.

Lamkanfi, M., Kanneganti, T.-D., Van Damme, P., Vanden Berghe, T., Vanoverberghe, I., Vandekerckhove, J., Vandenabeele, P., Gevaert, K., and Núñez, G. (2008). Targeted peptidecentric proteomics reveals caspase-7 as a substrate of the caspase-1 inflammasomes. Mol. Cell. Proteomics *7*, 2350–2363.

Leung, A.K., Vyas, S., Rood, J.E., Bhutkar, A., Sharp, P.A., and Chang, P. (2011). Poly(ADP-ribose) regulates stress responses and microRNA activity in the cytoplasm. Mol. Cell *42*, 489–499.

Lomvardas, S., and Thanos, D. (2002). Modifying gene expression programs by altering core promoter chromatin architecture. Cell *110*, 261–271.

Malireddi, R.K., Ippagunta, S., Lamkanfi, M., and Kanneganti, T.D. (2010). Cutting edge: proteolytic inactivation of poly(ADP-ribose) polymerase 1 by the Nlrp3 and Nlrc4 inflammasomes. J. Immunol. *185*, 3127–3130.

Mankan, A.K., Lawless, M.W., Gray, S.G., Kelleher, D., and McManus, R. (2009). NF-kappaB regulation: the nuclear response. J. Cell. Mol. Med. *13*, 631–643.

Mariathasan, S., Newton, K., Monack, D.M., Vucic, D., French, D.M., Lee, W.P., Roose-Girma, M., Erickson, S., and Dixit, V.M. (2004). Differential activation of the inflammasome by caspase-1 adaptors ASC and Ipaf. Nature *430*, 213–218.

Martinon, F., Agostini, L., Meylan, E., and Tschopp, J. (2004). Identification of bacterial muramyl dipeptide as activator of the NALP3/cryopyrin inflammasome. Curr. Biol. *14*, 1929–1934.

Messner, S., Schuermann, D., Altmeyer, M., Kassner, I., Schmidt, D., Schär, P., Müller, S., and Hottiger, M.O. (2009). Sumoylation of poly(ADP-ribose) polymerase 1 inhibits its acetylation and restrains transcriptional coactivator function. FASEB J. *23*, 3978–3989.

Messner, S., Altmeyer, M., Zhao, H., Pozivil, A., Roschitzki, B., Gehrig, P., Rutishauser, D., Huang, D., Caflisch, A., and Hottiger, M.O. (2010). PARP1 ADP-ribosylates lysine residues of the core histone tails. Nucleic Acids Res. *38*, 6350–6362.

Natoli, G. (2006). Tuning up inflammation: how DNA sequence and chromatin organization control the induction of inflammatory genes by NF-kappaB. FEBS Lett. *580*, 2843–2849.

Pétrilli, V., Herceg, Z., Hassa, P.O., Patel, N.S.A., Di Paola, R., Cortes, U., Dugo, L., Filipe, H.-M., Thiemermann, C., Hottiger, M.O., et al. (2004). Noncleavable poly(ADP-ribose) polymerase-1 regulates the inflammation response in mice. J. Clin. Invest. *114*, 1072–1081.

Pétrilli, V., Papin, S., Dostert, C., Mayor, A., Martinon, F., and Tschopp, J. (2007). Activation of the NALP3 inflammasome is triggered by low intracellular potassium concentration. Cell Death Differ. *14*, 1583–1589.

Ramirez-Carrozzi, V.R., Braas, D., Bhatt, D.M., Cheng, C.S., Hong, C., Doty, K.R., Black, J.C., Hoffmann, A., Carey, M., and Smale, S.T. (2009). A unifying model for the selective regulation of inducible transcription by CpG islands and nucleosome remodeling. Cell *138*, 114–128.

Rao, S., Procko, E., and Shannon, M.F. (2001). Chromatin remodeling, measured by a novel real-time polymerase chain reaction assay, across the proximal promoter region of the IL-2 gene. J. Immunol. *167*, 4494–4503.

Schroder, K., and Tschopp, J. (2010). The inflammasomes. Cell *140*, 821–832.

Smale, S.T. (2011). Hierarchies of NF-κB target-gene regulation. Nat. Immunol. *12*, 689–694.

Thornberry, N.A., and Lazebnik, Y. (1998). Caspases: enemies within. Science *281*, 1312–1316.

Thornberry, N.A., Bull, H.G., Calaycay, J.R., Chapman, K.T., Howard, A.D., Kostura, M.J., Miller, D.K., Molineaux, S.M., Weidner, J.R., Aunins, J., et al. (1992). A novel heterodimeric cysteine protease is required for interleukin-1 beta processing in monocytes. Nature *356*, 768–774.

Timinszky, G., Till, S., Hassa, P.O., Hothorn, M., Kustatscher, G., Nijmeijer, B., Colombelli, J., Altmeyer, M., Stelzer, E.H., Scheffzek, K., et al. (2009). A macrodomain-containing histone rearranges chromatin upon sensing PARP1 activation. Nat. Struct. Mol. Biol. *16*, 923–929.

Tschopp, J., and Schroder, K. (2010). NLRP3 inflammasome activation: The convergence of multiple signalling pathways on ROS production? Nat. Rev. Immunol. *10*, 210–215.

Molecular Cell, Volume *46*
Supplemental Information

Inflammasome-Activated Caspase 7 Cleaves PARP1 to Enhance the Expression of a Subset of NF-κB Target Genes

Süheda Erener, Virginie Petrilli, Ingrid Kassner, Roberta Minotti, Rosa Castillo, Raffaella Santoro, Paul O. Hassa, Jürg Tschopp, and Michael O. Hottiger

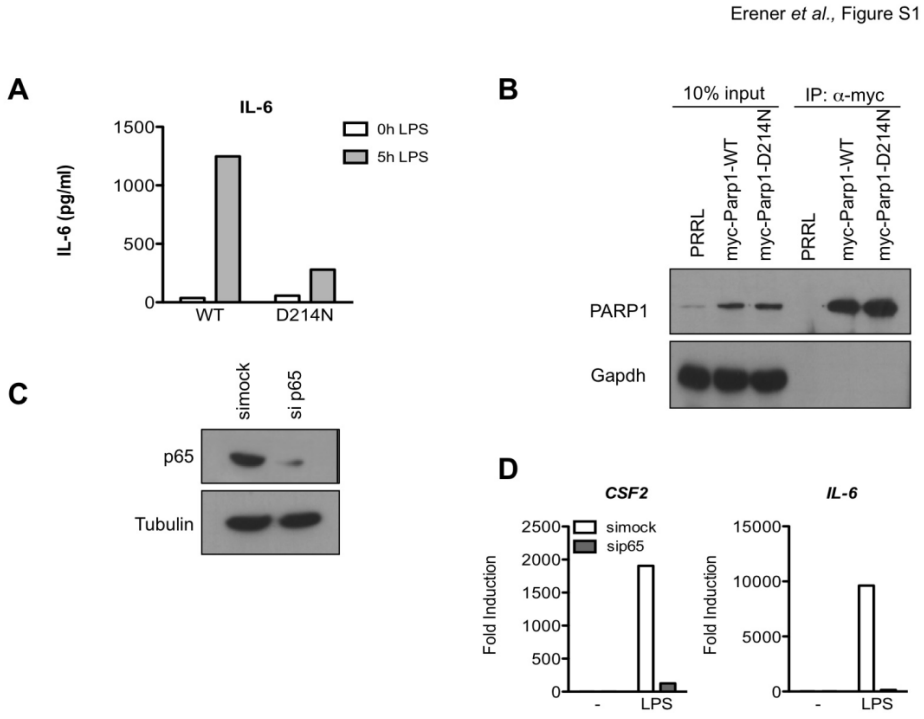

Figure S1. Genetic Complementation of THP1 Cells

(A) IL-6 levels in the supernatant of IP macrophages were determined by ELISA before and after 5h of LPS induction.

(B) Stable complementation of THP1 PARP1 knockdown cells either with PRRL-empty vector, myc-tagged WT PARP1 or uncleavable PARP1 D214N mutant. Total cell extracts were prepared and proteins were immunoprecipitated with a myc antibody and analyzed by western blot using PARP1 antibody. Gapdh was used as loading control.

(C and D) p65 knock-down abolishes LPS induced gene induction. THP1 cells were transiently transfected with the p65 siRNA oligos and (C) analyzed by western blot or (D) real-time RT-PCR analysis was performed after one hour LPS stimulation. Samples were normalized to *Rpl28* and expressed as fold increase relative to unstimulated mRNA levels.

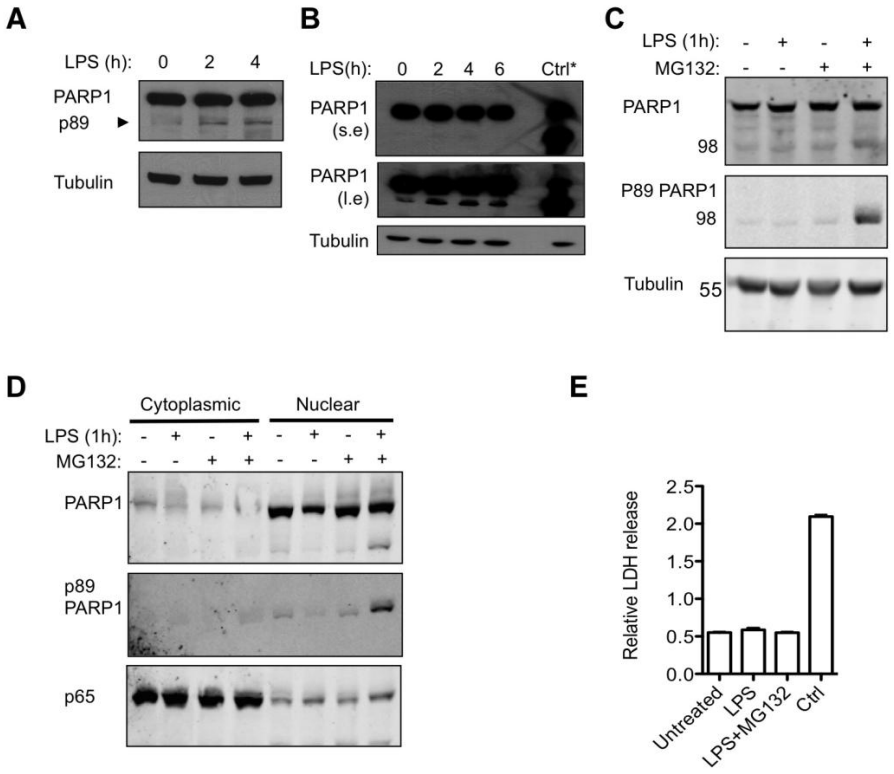

Figure S2. LPS Stimulation Induces PARP1 Cleavage and Inhibition of Caspase Activity Does Not Affect LPS Induced p65 Shuttling to Nucleus

(A) PARP1 cleavage profile in LPS treated THP1 macrophages. Total cell extracts were prepared and analyzed by western blot using indicated antibodies.

(B) THP1 monocytes were stimulated with LPS for different times, total cell extracts were prepared from and analyzed by western blot using antibodies against the full-length and cleaved C-terminal fragment of PARP1 (p89) and Tubulin as loading control. A short and long exposure (s.e and l.e, respectively) of the same blot are shown. Ctrl* is the sample treated with Etoposide for 16 hours.

(C) Total cell extracts were prepared and proteins were analyzed by western blot

using the indicated antibodies.

(D) Cells were fractionated and cytoplasmic and nuclear extracts were subjected to western blotting with the indicated antibodies.

(E) Cells were assayed for LDH release as indicated in the experimental procedures. Camptothethcin (CPT) was assessed as positive control. n=3, ± SEM.

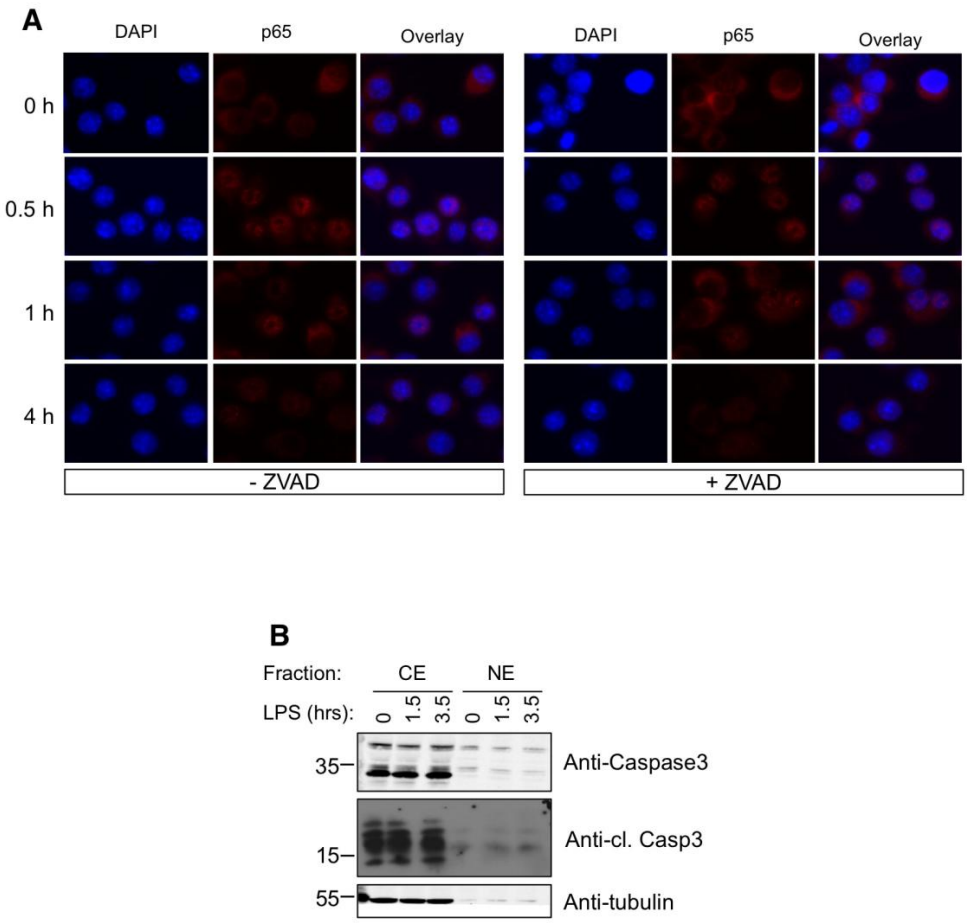

Figure S3. PARP1 Cleavage at D214 Occurs after One Hour of LPS Stimulation

(A) Raw 264.7 cells were stimulated with LPS in the presence or absence of z-VAD-fmk (10 μM) for the indicated times. Cells were fixed, incubated with p65 antibody and DAPI and analyzed by immunofluroscence microscopy.

(B) THP1 cells were stimulated with LPS for the indicated times. Cells were then fractionated and cytoplasmic and nuclear extracts were subjected to western blotting.

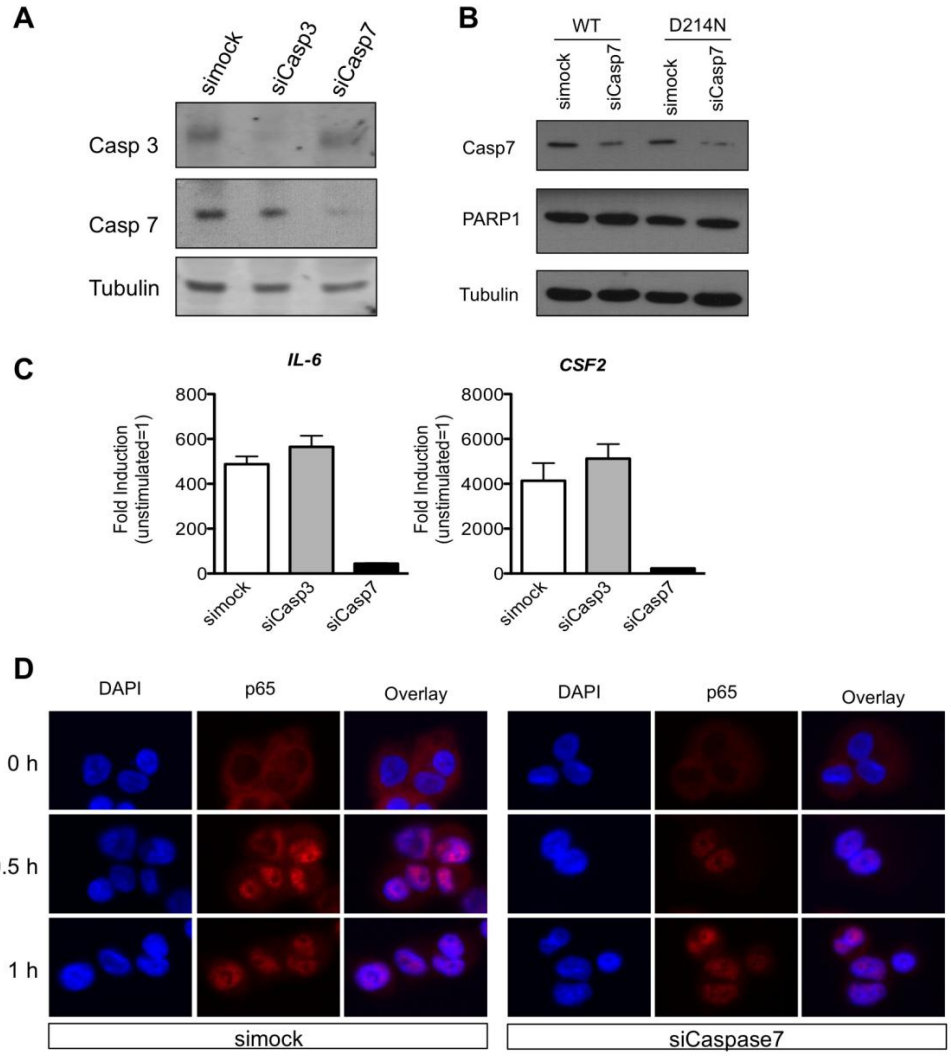

Figure S4. Caspase 3 and 7 Knock-down in IP Cells and Caspase 7 Knock-down Effect on LPS Induced p65 Shuttling to Nucleus

(A and B) IP cells were transiently transfected with the indicated siRNA oligos. (A) Knock-down efficiency was confirmed with western blot. (B) THP1 cells complemented with WT or D214N PARP1 were PMA primed, transfected with mock

or caspase 7 siRNA oligos, total cell extracts were prepared and subjected to western blotting using the indicated antibodies.

(C) Effect of caspase knockdown on LPS dependent NF-κB target gene response. THP1 cells were transiently transfected with the indicated siRNA oligos, stimulated with LPS for one hour and gene expression was analyzed by real-time RT-PCR. Samples were normalized to *Rpl28* and expressed as fold increase relative to unstimulated mRNA levels. Data are means of ± SD, n=2.

(D) THP1 cells were PMA primed, transiently transfected with the mock or caspase 7 siRNA oligos and stimulated with LPS for the indicated times. Cells were fixed, incubated with p65 antibody and DAPI and analyzed by immunofluorescence microscopy.

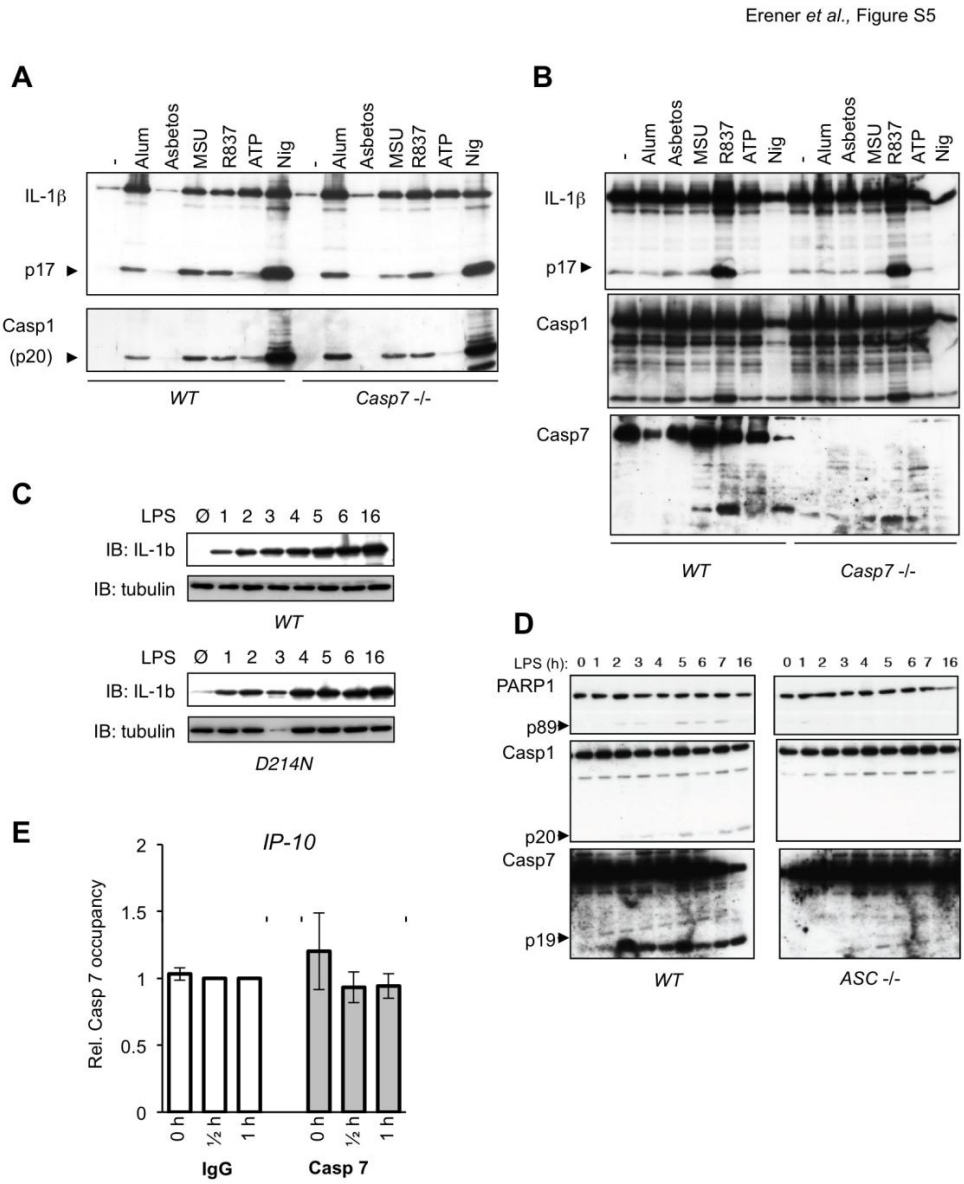

Figure S5.

(A and B) Absence of caspase 7 does not affect inflammasome activation. Peritoneal macrophages from WT and *caspase 7* -/- mice were were primed overnight with LPS then incubated with with different inflammasome activators. Cell supernatants (A) and cell extracts (B) were prepared, IL-1β secretion and caspase 1 activation was analyzed by western blot.

(C) IL-1b levels in WT and D214N PARP1 expressing macrophages after stimulation by LPS for 0-16 hours.

(D) The inflammasome adaptor protein ASC is required for LPS-dependent caspase 1 and caspase 7 activation and for PARP1 cleavage. IP cells from wild-type and *ASC* -/- mice were stimulated for the indicated times with LPS, total cell extracts were prepared and PARP1 cleavage, caspase 1 and caspase 7 activation was analyzed by western blot.

(E) As a control, the kinetics of caspase 7 occupancy at the *IP-10* promoter was determined. Cells were stimulated with LPS for different times. Caspase 7 was immunoprecipitated with a Caspase 7 antibody and the occupancy on the *IP-10* promoter was measured by real time RT-PCR. Results are normalized to values corresponding to the beads control (0h time-point).

Tables S1, S2, and S3. PCR Primers Used in This Study

The sequences of forward (F) and reverse (R) primers used for PCR are given in 5`-3`direction.

TABLE S1. SyBr Green Primers Used in Real-Time RT-PCR Analysis

Gene	Species	Sequence (F, R; 5`-3`)
CSF2	*Mus musculus*	ACATGCCTGTCACGTTGAAT TTGAGTTTGGTGAAATTGCC
IP-10	*Mus musculus*	GCACGAACTTAACCACCATCTTCC CTACCCATTGATACATACTTGATGACAC
IL-6	*Mus musculus*	ACTGACAATATGAATGTTGGGACAC ACCATCTGGCTAGGTAACAGAA
MIP2	*Mus musculus*	ACATCCCACCCACACAGTGAAAGA TCCTTCCATGAAAGCCATCCGACT
LIF	*Mus musculus*	CCATAGATGCAGCAAGGAGA CAGTCCTGAGATGAGCCTGA
RPS12	*Mus musculus*	GAAGCTGCCAAAGCCTTAGA AACTGCAACCAACCACCTTC
RPL28	*Homo Sapiens*	GCAATTCCTTCCGCTACAAC TGTTCTTGCGGATCATGTGT
IL-6	*Homo Sapiens*	GGCACTGGCAGAAAACAACC GCAAGTCTCCTCATTGAATCC

TABLE S2. Taqman Probes Used in Real-Time RT-PCR Analysis

Gene	Species	Taqman-Number
NOS-2	*Mus musculus*	Mm00440485
CALNEXIN	*Mus musculus*	Mm00500330_m1
IP-10	*Homo Sapiens*	Hs00171042_m1
CSF2	*Homo Sapiens*	Hs99999044_m1

TABLE S3. SyBr Green Primers Used in ChIP and CHART RT-PCR Analysis

Gene	Species	Sequence (F, R; 5`-3`)
IP-10	*Mus musculus*	GCAATGCCCTCGGTTTACAG GGCTGACTTTGGAGATGACTCA
IL-6	*Mus musculus*	CCCCACCCTCCAACAAAGATTTT CCCCAGTCTCATATTTATTAGGAGTCAAC
CSF2	*Mus musculus*	AATTCTGCAGCCACATCCTC GCCAGGAGATTCCACAACTC
CSF2(-1KB)	*Mus musculus*	CTTGAGACCATGCTGCCTTT GCTTCCCTGGCAAGTTCTC
NOS-2	*Mus musculus*	ATGGCCTTGCATGAGGATAC GCAGCAGCCATCAGGTATTT
NOS-2 (-1KB)	*Mus musculus*	GGGTGTTGCCTGGATAAAGA CACTTGCACACACACACAGC
Prolactin	*Mus musculus*	CCTTCATTTCTGGCCAATGT GCCTGAGAGAACCACAGCTT
IL-6	*Homo Sapiens*	CCTCACCCTCCAACAAAGAT GCCTCAGACATCTCCAGTCC
H2B	*Homo Sapiens*	TTGCATAAGCGATTCTATATAAAAGCG ATAAAGCGCCAACGAAAAGG

Supplemental Experimental Procedures

Tissue Culture

THP1 monocytic cells were grown in suspension and maintained in RPMI supplemented with 10% FCS, 1mM sodium pyruvate (Gibco), 1x non-essential amino acids (Gibco) and 100units/ml penicillin/streptomycin (Gibco), 50 μM β-mercaptoethanol (Gibco) at a cell density of 0.3 to $1.0x10^6$/mL. For differentiation into macrophages, cells were plated at a density of $1x10^6$/6-cm dish in RPMI with 10 ng/ml PMA for 18 hours to become fully differentiated macrophages before use in experiments. HEK 293 cells were maintained in DMEM supplemented with 10% FCS and 100 units/ml penicillin/streptomycin. All cells were maintained at 37°C in 5% CO_2.

Plasmids

Plasmid for the mammalian expression of human PARP1 was generated by cloning human PARP1 cDNA into XhoI cloning site of pCDNA 3 with a hemagglutinin-tag at the C-terminus. Corresponding D214N PARP1 mutant was generated by site directed mutagenesis and confirmed by sequencing. Plasmids for the mammalian expression of HDAC 1-2 were described elsewhere (Hassa et al., 2005). myc-PARP1(WT), myc-PARP1 (89 kDa), myc-PARP1 (24 kDa) were cloned into pCMV vector and the latter two constructs had a nuclear localization signal at the N-terminus.

Reagents and Antibodies

Lipopolysaccharide (LPS, 055:B5) was purchased from Sigma. Active recombinant human caspase Set IV was purchased from Biovision. Etoposide was purchased from Calbiochem. Ethidium homodimer and Calcein AM were purchased from Fluka. SyBR Green was purchased from Quantace. The following antibodies were purchased from Santa Cruz Biotechnologies: anti-RelA (sc-372), anti-PARP1 (sc-7150), anti-GAPDH (FL-335), anti-caspase 7 (sc-28295). The anti-PARP1 (89) and active-caspase 7 (9491) antibodies were from Cell Signaling. Anti-mouse caspase-1 was obtained from Peter Vandernabele. The anti-myc antibodies were either purchased from Roche (11-667-149-001) or purified from hybridoma cells. The anti-Tubulin and anti-Flag (M2) antibodies were purchased from Sigma and the anti-HA was from Covance (MMS-101P). The anti-caspase 7 from Epitomics (1032-1) antibody was

purchased was used for ChIP experiments. The p65 antibody from Enzo Lifesciences (ALX-210-574) was used for immunohistochemistry.

Generation of Recombinant Proteins

The recombinant proteins were expressed by baculovirus in Sf21 cells using either the FastBac (Invitrogen) or the BacPAK systems (Clontech). His-tagged proteins were purified over Ni^{2+}-beads (ProBond, Invitrogen) and GST-tagged proteins over L-Glutathione beads (Sigma). All purified proteins were analyzed by coomassie staining and confirmed by western blot analysis using the corresponding antibodies.

Stable PARP1 Knockdown and Complementation in THP1 Cells

Generation of viruses and transduction of cells was done as described earlier (Ariumi et al., 2005). Briefly, pRDI vector containing PARP1 shRNA (#5) was used to transduce THP1 cells. The short hairpin RNA was against 5`UTR region of PARP1 mRNA. Transduced cells were selected through puromycin resistance gene. Complementation of cells was done with pRRL-myc-PARP1 vectors containing a blasticidin resistance marker and complemented cells were subsequently selected for three weeks with 2 μg/ml blasticidin.

^{32}P- NAD Automodification

Experiment was performed as described elsewhere (Altmeyer et al., 2009).

In Vitro Translation

HA-tagged WT and D214N mutant PARP1 were *in vitro* translated using the `TNT coupled reticulocyte lysate systems` (Promega) following the manufacturer's instructions.

In Vitro PARP1 Cleavage Assay

10 pmol recombinant or 125 ng *in vitro* translated ^{35}S labeled WT or D214N PARP1 proteins were incubated for 20 minutes at 37°C with 1U of recombinant caspases in caspase cleavage buffer (50 mM Hepes pH 7.2, 50 mM NaCl, 0.1% Chaps, 10 mM EDTA, 5% Glycerol, 10 mM DTT). Proteins were subsequently resolved by SDS-PAGE and analyzed by western blot.

In Vitro Interaction and GST Pull-Down Assays

GST-p65 expressed in insect cells was immobilized on glutathione-sepharose beads (Amersham Biosciences) and incubated with recombinant PARP1 proteins (WT, D214N mutant) in binding buffer (50 mM Tris pH 8, 100 mM NaCl, 0.5% NP-40, 5

mM DTT, 1 mM PMSF) for 2 h at 4°C rolling. Glutathione beads were washed three times with precission buffer (50 mM Tris-HCl pH 7.5, 150 mM NaCl, 1mM EDTA, 1 mM DTT) and incubated with precission enzyme in 50 ul precission buffer overnight. Proteins in the supernatant were boiled, resolved on SDS-PAGE and subjected to western blot using anti-PARP1 or anti-HA antibodies.

Immune Fluorescence Microscopy

For immune fluorescence stainings, cells were grown on cover slips and fixed with icecold methanol for 10min at 4°C, followed by washing with PBS. 10% FCS in PBS was used for blocking at RT for 30min. Cells were then incubated with the primary antibody directed against RelA (C20, Santa Cruz sc-372) and the secondary antibody ($Cy^{TM}3$-conjugated AffiniPure Goat Anti-Rabbit, Jackson ImmunoResearch Laboratories). Both antibodies were used in a dilution of 1:250 in 5%FCS in PBS for 1hr at RT. Cells were mounted with Vectashield containing DAPI and analyzed by fluorescence microscopy using a Leica DMI 6000B.

Whole Cell Extract and Immunoprecipitation for Myc-PARP1

Unless stated otherwise, whole cell extracts were prepared by lyzing the cells for 15 minutes in lysis buffer (50 mM Tris pH 8, 500 mM NaCl, 1% Triton X-100, 1µg/ml pepstatin, 1µg/ml bestatin, 1µg/ml leupeptin, 2 mM PMSF) at 4°C. One milligram of whole cell extract was incubated with anti-myc antibody for 2 hours at 4°C. Immunocomplexes were collected with Protein A agarose beads (GE Healthcare) for 1 hour at 4°C and washed three times with wash buffer containing 120 mM NaCl. Immunocomplexes were analyzed by standard western blot analysis using anti-PARP1 and anti-GAPDH antibodies.

Nuclear Extract Preparation

Cells were stimulated with 10 µg/ml LPS for the indicated times, washed with PBS, harvested and washed again three times in buffer A (10 mM HEPES KOH pH7.9, 1.5 mM $MgCl_2$, 10 mM KCl, 1µg/ml pepstatin, 1µg/ml bestatin, 1µg/ml leupeptin, 2 mM PMSF, 5mM DTT). Cells were lysed with A+ buffer (Buffer A+ 0.06 % NP-40) and centrifuged for 5 minutes at 5000 rpm. Supernatant corresponding to cytoplasm was saved for western blot analysis. Pellet was washed three times with buffer A and subsequently resuspended in three volumes of Buffer C (20 mM HEPES KOH pH7.9, 0.42 M NaCl, 1.5 mM $MgCl_2$, 25% v/v glycerol, 1µg/ml pepstatin, 1µg/ml bestatin,

1μg/ml leupeptin, 2 mM PMSF, 5 mM DTT) and incubated for 15 minutes at 4°C on rotating wheels. Lysate was centrifuged for 10 minutes at 4°C at 14000 rpm with the supernatant corresponding to the nuclear fraction.150 μg cytoplasmic extracts and 50 μg nuclear extracts were boiled with Laemmli buffer, resolved on 15% SDS-PAGE and subjected to western blot using different antibodies.

Cell Viability Assay

THP1 macrophages stimulated with 10 μg/ml LPS for the indicated times were incubated with 4 μM Ethidium homodimer and 2 μM Calcein mix in PBS for 30 minutes at 37°C incubator. Ethidium homodimer positive and Calcein positive cells were visualized using Olympus BX51 microscope.

In Vitro Inflammasome Formation

Peritoneal macrophages were primed overnight with 100 ng/ml of ultra-pure LPS and stimulated as indicated asbestos (150 μg/ml), MSU (150 μg/ml), R837 (10 μg/ml), Nigericin (20μM) for 6hr except ATP 5mM 30' (Pétrilli et al., 2007).

Supplemental References

Altmeyer, M., Messner, S., Hassa, P.O., Fey, M., and Hottiger, M.O. (2009). Molecular mechanism of poly(ADP-ribosyl)ation by PARP1 and identification of lysine residues as ADP-ribose acceptor sites. Nucleic Acids Research *37*, 3723-3738.

Ariumi, Y., Turelli, P., Masutani, M., and Trono, D. (2005). DNA damage sensors ATM, ATR, DNA-PKcs, and PARP-1 are dispensable for human immunodeficiency virus type 1 integration. J Virol *79*, 2973-2978.

Hassa, P.O., Haenni, S.S., Buerki, C., Meier, N.I., Lane, W.S., Owen, H., Gersbach, M., Imhof, R., and Hottiger, M.O. (2005). Acetylation of poly(ADP-ribose) polymerase-1 by p300/CREB-binding protein regulates coactivation of NF-kappaB-dependent transcription. J Biol Chem *280*, 40450-40464.

Pétrilli, V., Papin, S., Dostert, C., Mayor, A., Martinon, F., and Tschopp, J. (2007). Activation of the NALP3 inflammasome is triggered by low intracellular potassium concentration. Cell Death Differ *14*, 1583-1589.

6. Unpublished Results

6.1. ARTD1 recruitment, release and PAR formation at laser-induced DNA lesions in live cells

As described in section 5.1, SET7/9 methylates ARTD1 at K508 and influences its H_2O_2-induced PAR formation. One mechanism to regulate ARTD1 activity *in vivo* is to alter its recruitment and affinity to damaged chromatin. Therefore, we wanted to study the effects of SET7/9-mediated methylation on ARTD1 activity in live cells. This was done in collaboration with the group of Elisa May at the Bioimaging Center in Konstanz, who have established methods for DNA damage induction with near infrared short laser pulses [222,223]. The binding characteristics of ARTD1 wildtype and the methylation deficient mutant K508R were compared in presence and absence of SET7/9. Strinkingly, both EGFP-ARTD1 wildtype and K508R are recruited less efficiently to DNA lesions induced with a 1050 nm laser, when SET7/9 is depleted (Fig. 6a and b). The K508R mutation itself had no effect on ARTD1 recruitment to DNA damage sites induced at this wavelength. Furthermore, the release of PAGFP-ARTD1 wildtype and K508R from laser-induced DNA lesions was comparable (Fig. 6c and d).

PAR formation at irradiated sites can be monitored in real-time by using the macrodomain of macroH2A fused to EGFP. This protein domain is known to bind PAR resulting in a time-dependent increase of fluorescence signal in the damaged area, when PAR is formed. Live cell microscopy showed that less PAR is formed at laser-irradiated sites in SET7/9 knockdown cells than in cells treated with a control siRNA (Fig. 6e). No differences in PAR formation were observed between ARTD1 knockdown cells complemented with ARTD1 wildtype or K508R (data not shown). These results indicate that under the tested conditions (multiphoton laser irradiation with λ = 1050 nm) ARTD1 recruitment to and activation by DNA damage is enhanced by SET7/9 independent of the methylation at K508. The data described here suggest that SET7/9 regulates ARTD1 by other mechanisms in addition to the methylation at K508. This could be achieved in several ways, e.g. (1) by methylating other chromatin-associated factors and thereby inducing chromatin changes leading to enhanced DNA damage or better access for ARTD1, (2) by methylating other proteins that in turn activate ARTD1 and (3) by methylation independent mechanisms e.g.

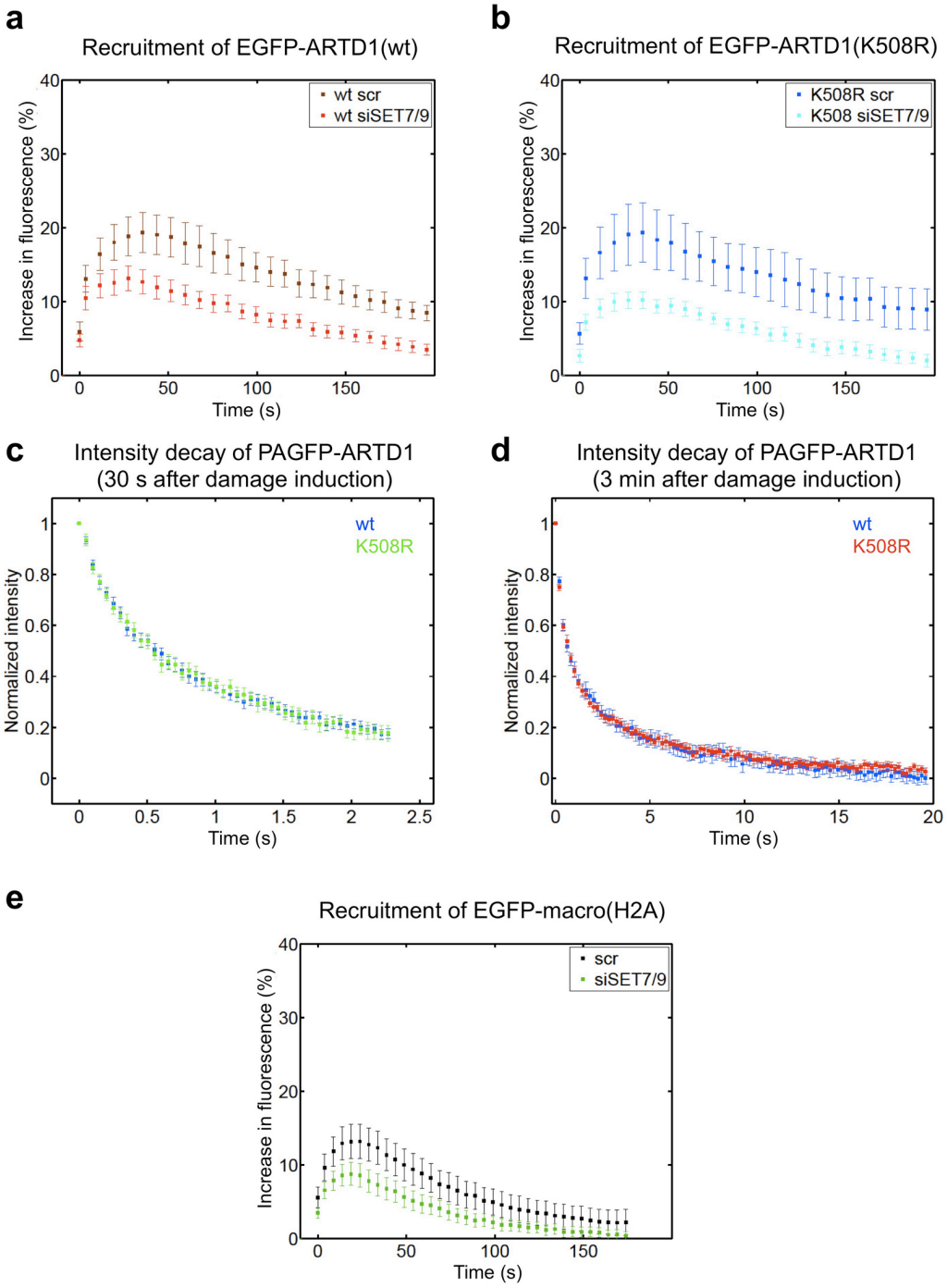

Figure 6. ARTD1 binding and PAR formation kinetics at multiphoton laser induced DNA lesions. (a and b) ARTD1 wildtype (wt) and K508R recruitment to DNA lesions induced with a 1050 nm laser was measured and analyzed as described elsewhere [223]. Briedfly, U2OS cells were transfected with siRNA directed against SET7/9 or a control siRNA (scr) using RNAiMAX according to the manufacturer's instructions. One day later, medium was changed and EGFP-ARTD1 plasmids were transfected by calcium phosphate transfection in a BES-buffered system. One-and-a-half or two days later, confocal microscopy was performed in phenol-red free DMEM and fluorescence intensity increase was measured at DNA lesions. (c and d) ARTD1 release from DNA lesions was analyzed using ARTD1 proteins fused to photoactivatable GFP. Cells were transfected with siRNA against ARTD1 and PAGFP-ARTD1 plasmids as described in (a and b). At the indicated times after DNA damage induction with a 1050 nm laser, PAGFP was photoactivated in the same area with a short laser pulse at 775 nm and fluorescence intensity decay was measured over time. (e) Recruitment of the macrodomain of macroH2A was examined as in (a and b).

direct interaction and recruitment of ARTD1. One possible factor that might influence ARTD1 in a SET7/9 methylation-dependent manner is histone H1, which was previously reported to activate ARTD1 [224].

The comparable binding dynamics and PAR formation kinetics of ARTD1 wildtype and K508R can be explained by the following possibilities: (1) Endogenous wildtype ARTD1 levels (at least in the recruitment studies with SET7/9 knockdown) might mask a methylation-dependent effect. (2) At this wavelength the methylation might not influence ARTD1 activity (compare section 8). (3) SET7/9 might methylate another lysine residue close-by if K508 is mutated. The last point is strengthened by the fact that *in vitro* methylation of ARTD1 K508R was observed at some conditions (e.g. low salt stringency).

6.2. ARTD1 demethylation

Lysine methylation is a reversible modification. Demethylation is catalyzed by proteins of the LSD and JmjC domain families. LSD1 and LSD2 were shown to demethylate other SET7/9 targets such as H3 [210,225] and E2F1 [203]. Therefore, we tried if they also remove the methyl group from monomethylated ARTD1 K508. H3 was used as a positive control. The substrate proteins were first methylated with radioactive SAM and then incubated with GST (as a negative control), LSD1 or LSD2 after residual SAM had been removed by spin-column chromatography. Incubation with LSD1 and LSD2 clearly decreased the radioactive signal of H3 as well as full-length ARTD1 and the fragment 373-524 (Fig. 7). This could indicate that both LSD1 and LSD2 are indeed able to remove the [^{14}C]-labeled methyl group from K508.

However, it has to be noted that the LSD1 and LSD2 preparations might have been contaminated by bacterial proteases as their expression in *E. coli* did not yield high amounts of full-length protein and generated many truncated products. Thus, demethylation of ARTD1 has to be studied in more detail with other LSD protein preparations and in presence of high amounts of protease inhibitors to elucidate if LSD1 and LSD2 indeed reverse the SET7/9-dependent methylation. Other demethylases from the JmjC domain family could be included in future studies.

It will also be interesting to investigate the effect of demethylase knockdown and overexpression on ARTD1 activity *in vivo*.

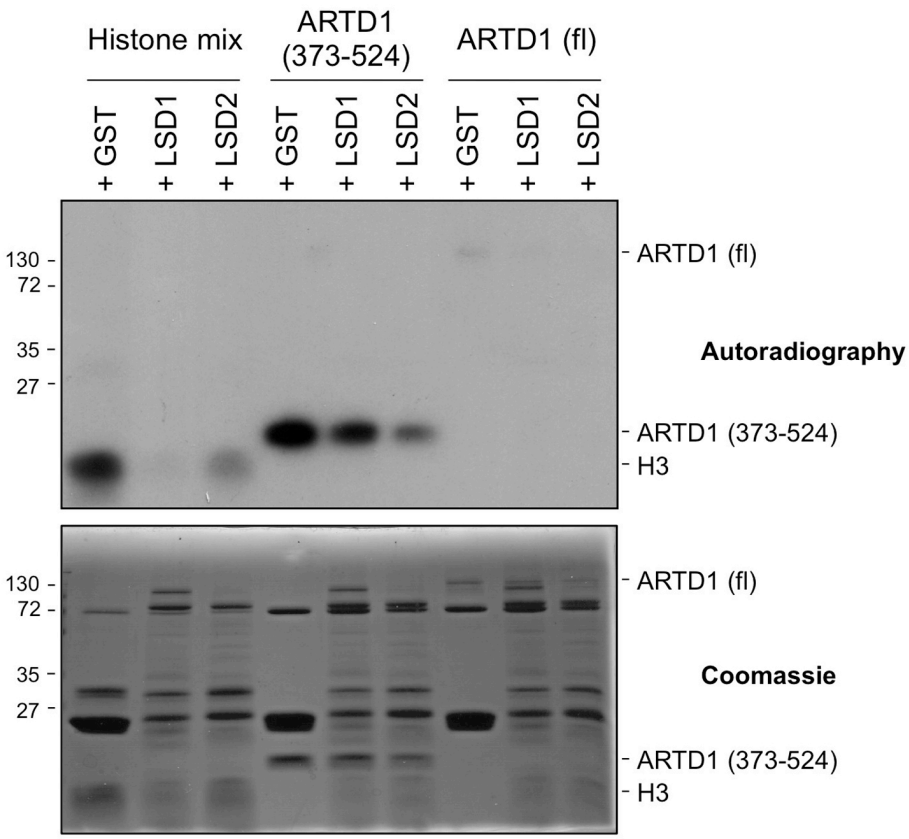

Figure 7. Demethylation of histones and ARTD1 by LSDs. His-tagged LSD1 and LSD2 were expressed in *E. coli* in presence of 10 µM riboflavin and purified by one-step nickel affinity chromatography. 1 µg ARTD1 or 2.5 µg histone mix were methylated with [^{14}C]-labeled SAM by SET7/9 as described in section 5.1. To remove residual SAM, proteins were then purified over a G-50 column (GE Healthcare) according to the manufacturer's recommendations. The same volume of 1x demethylation buffer (50 mM Tris pH8.0, 50 mM KCl, 5 mM $MgCl_2$, 5% glycerol, 1 mM DTT, 0.2mM PMSF) and LSD proteins or GST were added. Demethylation was allowed to proceed for 3 hrs at 37°C. Proteins were then separated by SDS-PAGE, stained with Coomassie and analyzed by autoradiography.

6.3. Mutation of SET7/9 target lysine residues does not change the nuclear distribution of H1.4

SET7/9 methylates the residues K121, K129, K159, K171, K177 and K192 in the C-terminal domain of H1.4 (see section 5.2). To investigate the influence of SET7/9-dependent methylation on H1.4, we mutated these residues to arginines and analyzed the nuclear distribution of N-terminally EGFP-tagged H1.4 in U2OS cells. Neither the combined mutation of the four last target residues (K4R) nor the mutation of all six residues (K6R) had an influence on the localization pattern of H1.4 in the nucleus (Fig. 8). H1.4 wildtype, K4R and K6R were preferentially localized to hetero-chromatin as described previously [28].

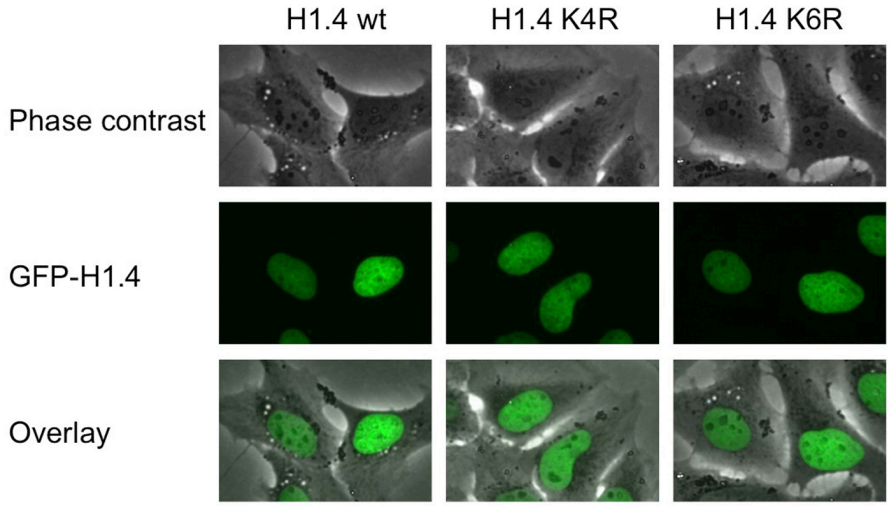

Figure 8. H1.4 distribution in the nucleus. U2OS cells were transfected with EGFP-H1.4 expression plasmids and analyzed by live cell microscopy in phenol-red free medium two days later. wt: wildtype, K4R: K159/171/172/192R mutant, K6R: K121/129/159/171/172/192R mutant

6.4. SET7/9 is modified by ARTD1

During our studies, we realized that ARTD1 was not only methylated by SET7/9 but that SET7/9 was also modified by ARTD1 in radioactive trans-ADP-ribosylation assays (Fig. 9). As ADP-ribosylation might also occur in the N-terminal GST-tag of SET7/9, the GST fusion protein was cleaved with PreScission protease and GST was removed. This revealed that SET7/9 itself and not the GST tag was modified by ARTD1. It will be exciting to see if and under which conditions ADP-ribosylation of SET7/9 occurs in cells and how this modification affects SET7/9 activity and substrate specificity.

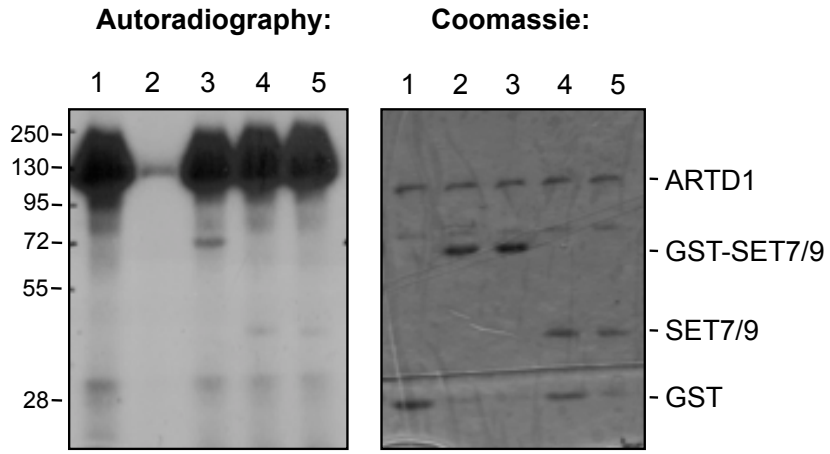

Figure 9. SET7/9 is ADP-ribosylated by ARTD1. GST and GST-SET7/9 were expressed in *E. coli* and purified using glutathione sepharose according to the manufacturer's instructions (GE Healthcare). 1 µg of each purified GST protein was incubated with recombinant ARTD1 in presence of 100 nM ^{32}P-labeled NAD^+ and 5 pmol EcoRI DNA for 15 min at 30°C. Poly-(ADP-ribosyl)ation was visualized by autoradiography and protein levels by Coomassie staining. (Lane 1: GST, Lane 2: GST-SET7/9 without EcoRI, Lane 3: GST-SET7/9, Lane 4: GST-SET7/9 cleaved by PreScission, Lane 5: SET7/9 after PreScission cleavage and removal of GST)

6.5. SET7/9 is mainly localized in the nucleus

As most cellular target proteins of SET7/9 are nuclear proteins, at least a fraction of SET7/9 has to be localized in the nucleus despite the lack of any DNA binding motifs or nuclear localization signals [185]. Interestingly, SET7/9 was mainly found in the cytoplasmic extracts of MCF7 human breast cancer cells (Fig. 10a). Cytoplasmic localization was similarly seen for other cell types such as U2OS cells, T24 human bladder carcinoma cells, HEK 293T cells and mouse lung fibroblasts (data not shown). Adriamycin treatment, which induces DNA DSBs by topoisomerase II inhibition, had no effects on the observed SET7/9 distribution in MCF7 cells (Fig. 10a).

To identify the localization of SET7/9 in intact cells, we expressed a GFP-tagged version of SET7/9 in U2OS cells and performed live cell imaging under different conditions. In contrast to cell extracts, in untreated cells, GFP-SET7/9 was found in the cytosol and even more abundantly in the nucleus, but was completely absent from the nucleoli (Fig. 10b). This distribution did not change upon treatment with the DSB inducer etoposide, the inflammatory cytokine TNFα or the nuclear export inhibitor leptomycin B. We thus speculate that in living cells a decent amount of SET7/9 resides in the nucleus, but that during the preparation of nuclear extracts SET7/9 is lost from this fraction, as it is not tightly bound to the chromatin.

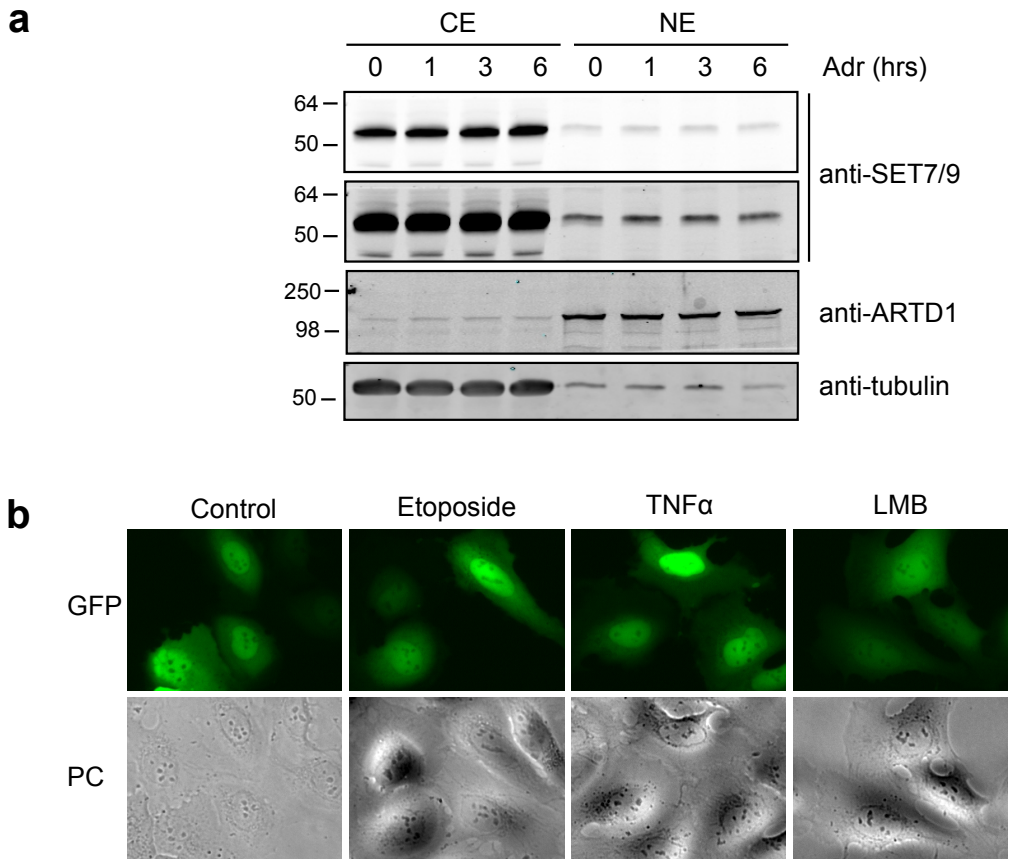

Figure 10. SET7/9 is mainly localized to the nucleus but not tightly associated with the chromatin. (a) MCF7 cells were treated with 0.5 µM Adriamycin for the indicated times and fractionated into cytoplasmic (CE) and nuclear extracts (NE). SET7/9 localization was then analyzed by Western blot (low and high exposure). Preparation of the cellular fractions was controlled by ARTD1 and tubulin. (b) U2OS cells were treated with 50 µM etoposide, 10 ng/ml TNFα or 10 ng/ml leptomycin B (LMB) for 1 hr and GFP-SET7/9 localization was visualized by live cell microscopy. PC: phase contrast. Note: The phase contrast image of the control cells looks different because it was taken in a different area of the well, the microscope settings were kept equal for all images.

6.6. Role of ARTD1 in NF-κB-dependent gene expression after DNA damage

ARTD1 plays a role as a cofactor for several transcription factors such as NF-κB [103,106,226]. NF-κB is a widely expressed, hetero-dimeric transcription factor that is activated by many inflammatory and immunological stimuli like TNFα and LPS. In unstimulated cells, it is usually sequestered in the cytosol through its interaction with one of several inhibitors of NF-κB (IκBs). Most exogenous stimuli activate NF-κB via a canonical pathway involving rapid IκB kinase (IKK) dependent phosphorylation of IκBs and their degradation by the proteasome, which allows the subsequent translocation of NF-κB to the nucleus, where it induces its target genes [227,228].

Apart from this classical stimulation by exogenous factors, NF-κB can also be triggered by endogenous stimuli like genotoxic stress [229]. NF-κB activation by these stimuli occurs through an atypical pathway with much slower kinetics and a weaker response. The exact mechanisms of NF-κB activation and the set of genes induced by DNA damage vary among different cell lines and depend on the DNA damage inducing agent and the dose applied [230,231]. Many of the genes induced by NF-κB upon DNA damage are anti-apoptotic genes (e.g. *cIAPs*, *XIAP*, *BCL-X_L*) and genes involved in cell cycle regulation (e.g. *Gadd45β*) [230,232,233]. NF-κB induction and the resulting activation of pro-survival factors is an important mechanism how malignant cells develop chemo- and radioresistance and thereby evade effective cancer treatment.

As ARTD1 was shown to act as a coactivator for NF-κB-dependent gene expression and its enzymatic activity is strongly induced upon DNA damage, it might play a role in DNA damage induced NF-κB activation. Reporter gene assays revealing that NF-κB-dependent gene expression is severely impaired in ARTD1 knockout cells treated with etoposide strengthen this hypothesis [103,111].

We investigated the functional relevance of ARTD1 in DNA damage induced NF-κB-dependent gene expression by addressing two different aspects: (i) The role of ARTD1 in DNA damage induced nuclear translocation of NF-κB (role of ARTD1 as sensor/inducer). (ii) The role of ARTD1 as transcriptional cofactor in DNA damage induced gene expression of endogenous NF-κB target genes.

6.6.1. ARTD1 is not required for DNA damage induced nuclear shuttling of NF-κB

X-radiation was used to induce DSBs in MLFs isolated from *ARTD1* wildtype (+/+) and *ARTD1* knockout (-/-) cells. This resulted in the formation of γ-H2AX foci that gradually decreased over time as a result of DSB repair. Some DNA damage independent speckles were detected by the γ-H2AX antibody in untreated cells, but these were clearly different from the ones induced upon X-radiation. The induction of γ-H2AX foci as well as the DSB repair was comparable in both cell lines (Fig. 11a). This indicated that *ARTD1* -/- cells were not more susceptible to the induction of DSBs by X-radiation and that ARTD1 was not required for the repair of these DSBs.

X-radiation also resulted in the formation of PAR in *ARTD1* +/+ cells in a dose-dependent manner. This could be inhibited by the addition of the PARP inhibitor DAM-TIQ-A. ARTD1 was the enzyme responsible for PAR formation upon X-radiation, as PAR was not induced in *ARTD1* -/- cells (Fig. 11b).

In order to address the aspect, if ARTD1 is required for the translocation of NF-κB to the nucleus after DNA damage, the shuttling of NF-κB subunit RelA was compared in *ARTD1* -/- and +/+ cells (Fig. 11c). The inflammatory cytokine TNFα induced a fast and robust nuclear translocation of RelA in all cells. X-radiation on the other hand induced a much weaker response that developed over a much longer time. Only a fraction of RelA shuttled to the nucleus and this was seen in only about 25% of the cells. NF-κB shuttling was equal in both cells lines, suggesting that ARTD1 is not required for the observed redistribution of RelA upon X-radiation or TNFα treatment.

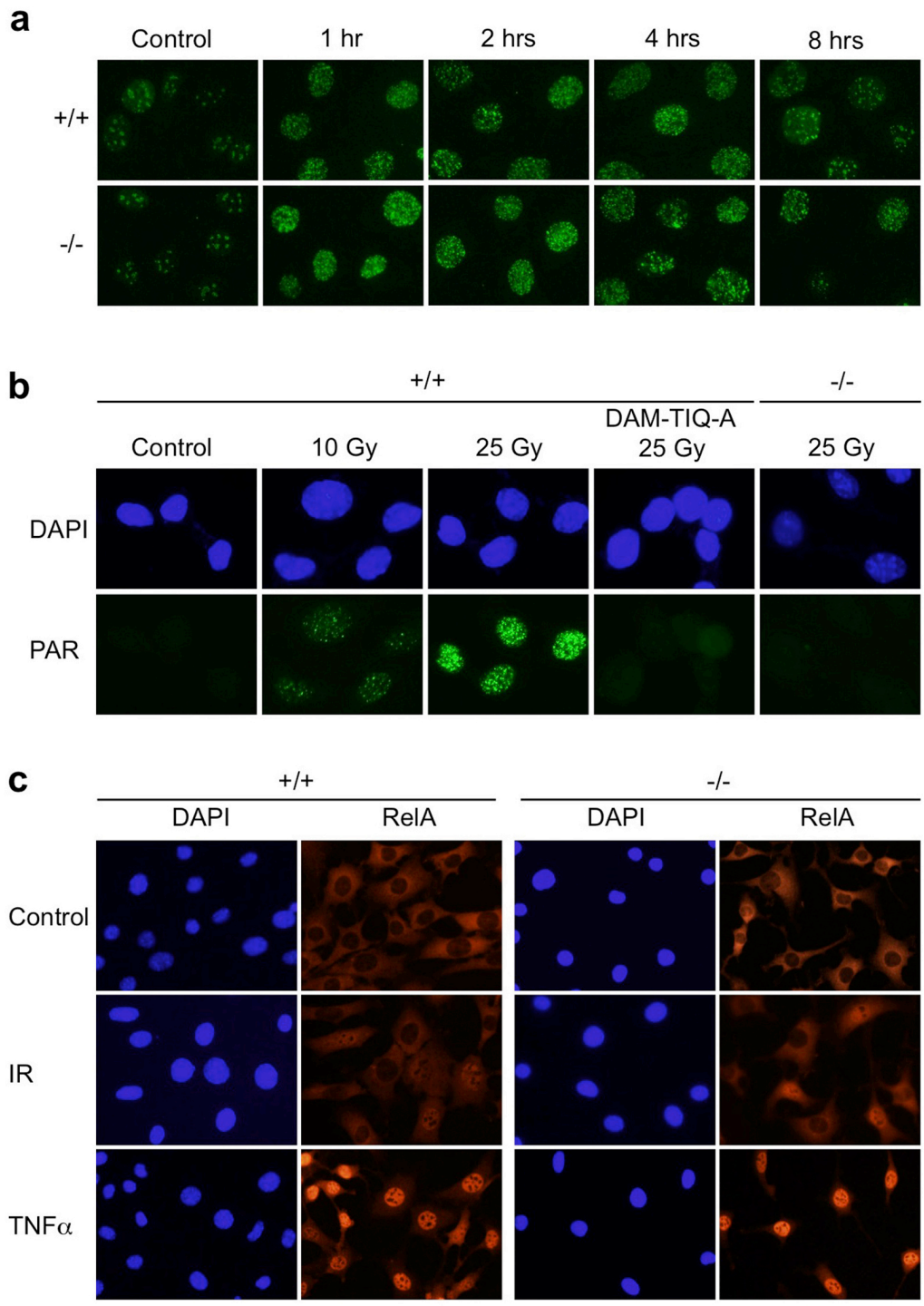

Figure 11. DNA damage induced RelA shuttling to the nucleus is not impaired in ARTD1 knockout cells. (a) MLFs isolated from ARTD1 wildtype (+/+) and ARTD1 knockout (-/-) mice were X-radiated with 3 Gy and afterwards allowed to recover for the indicated times. DSBs were then visualized by immunofluorescence staining of γ-H2AX. (b) ARTD1 +/+ and -/- MLFs were X-radiated with the indicated dose, fixed 5 min later and PAR formation was detected by immunofluorescence microscopy. Cells were preincubated with 10 µM DAM-TIQ-A for 2 hrs to inhibit ARTD1 activity. (c) ARTD1 +/+ and -/- MLFs were treated with 30 ng/ml murine TNFα for 20 min or X-radiated (IR) and fixed after 3 hrs. NF-κB shuttling was then analyzed by immunofluorescence staining of the RelA subunit. DAPI was used to stain the DNA.

6.6.2. DNA damage induced NF-κB-dependent gene expression is impaired in ARTD1 knockout cells

ARTD1 could also play a role in NF-κB signaling after it has been activated and shuttled to the nucleus for example as a transcriptional cofactor of NF-κB or by changing the local chromatin architecture. To investigate this possibility, NF-κB-dependent gene expression was analyzed in *ARTD1* +/+ cells after stimulation with different DNA damage inducing agents and compared to the response in *ARTD1* -/- cells.

IκBα was used as a target gene that is usually activated upon NF-κB activation by a negative feedback loop independent from the stimulus. The ribosomal gene *RPS12* was used as a negative control whose expression should not change after the treatments. Gene expression analysis of *IκBα* and several anti-apoptotic and cell-cycle regulatory genes (*GADD45β*, *cIAP1*, *XIAP*, *BCL-X_L*) in *ARTD1* +/+ MLFs confirmed that genotoxic stress induces the expression of endogenous NF-κB target genes. As expected, the response to DNA damage was much weaker than the one to TNFα treatment (induction: 3-4 versus 20 fold) and occurred at later time points (4-6 hours instead of 1 hour)(Fig. 12). Although *ARTD1* -/- and *ARTD1* +/+ cells were treated in parallel, the expression of *IκBα* and other NF-κB-dependent target genes was impaired in cells lacking ARTD1. Since ARTD1 is not required for the nuclear shuttling of NF-κB after DNA damage in MLFs, these results suggest that ARTD1 rather regulates downstream events (such as transcription initiation).

ARTD1 -/- cells were then complemented with human and mouse ARTD1 (Fig. 13a) to verify if the impaired PAR formation and NF-κB-dependent gene expression are indeed caused by the absence of ARTD1 and not by unspecific variation between the two cell lines due to clonal selection. Complementation with human and mouse ARTD1 restored PAR formation upon X-radiation but NF-κB-dependent gene expression was not reconstituted (Fig. 13b and c).

This result can be explained by two scenarios: Either the gene expression differences between *ARTD1* +/+ and -/- cells are generated by cell line variations apart from the ARTD1 deficiency or the expression levels of ARTD1 in the complemented cells are not high enough to restore NF-κB-dependent gene expression. Although the complemented cells were maintained under selection pressure by the antibiotic blasticidine, they had a high cell-to-cell variability in ARTD1 protein expression. While some cells expressed very high levels of ARTD1, in others ARTD1 expression

was almost not detectable. It is thus possible that the amount of cells expressing the correct levels of ARTD1 was not high enough to detect an effect on the expression of NF-κB target genes.

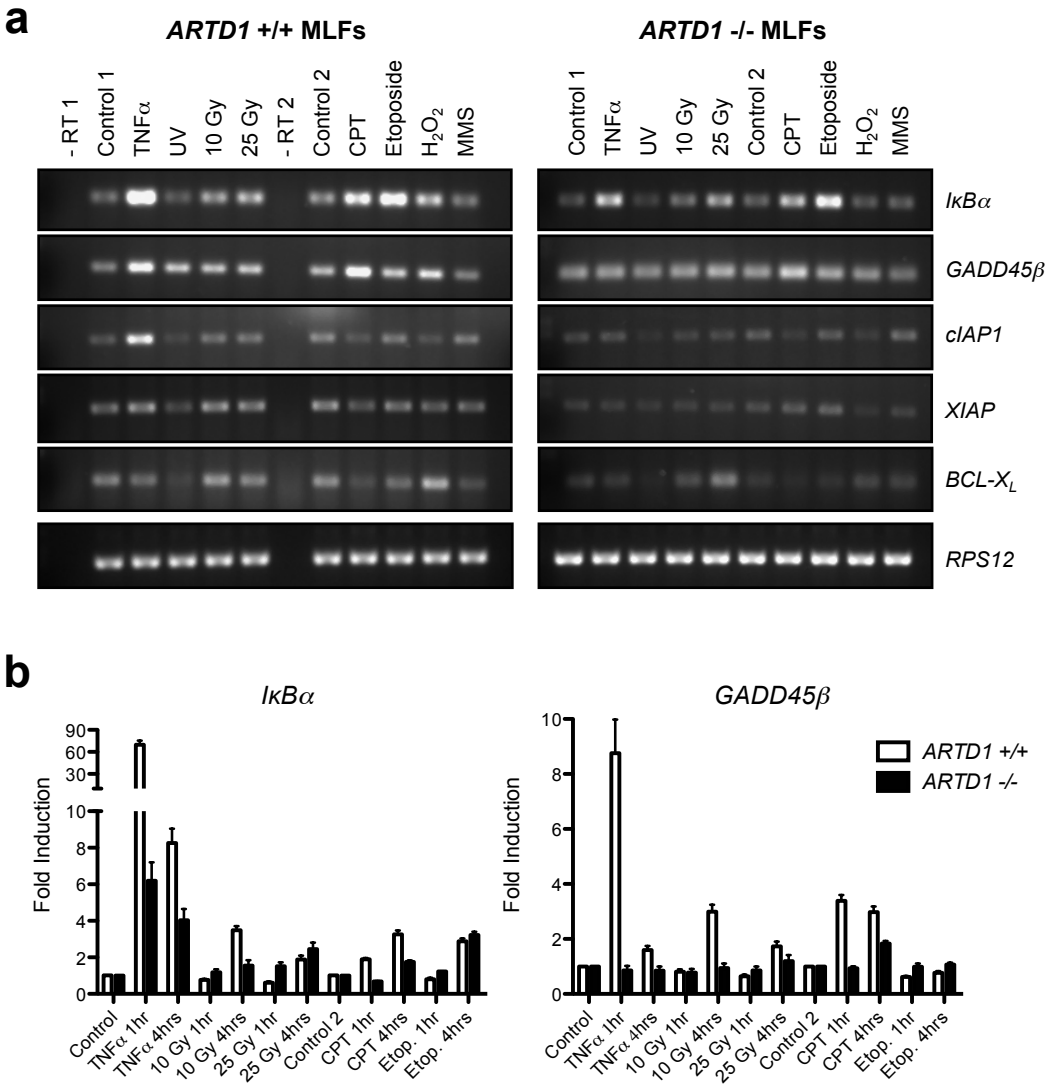

Figure 12. DNA damage induced expression of endogenous NF-κB target genes is impaired in *ARTD1* -/- MLFs. *ARTD1* +/+ and -/- MLFs were treated with 30 ng/ml mTNFα, 50 J/m^2, 10 and 25 Gy X-IR, 15 μM CPT, 50 μM etoposide, 0.5 mM H_2O_2 or 0.5 mM MMS in FCS-free medium and harvested after 1 and 4 hrs. Total RNA was then extracted and reverse transcribed with poly-A primers. (a) Gene expression was analyzed by conventional RT-PCR and agarose gel electrophoresis. Ribosomal gene *RPS12* was used as control gene. PCR reactions omitting reverse transcriptase (-RT) were used as negative controls. (b) Expression of *IκBα* and *GADD45β* was analyzed by real-time RT-PCR. Values were normalized with the expression of *RPS12*. The mean ± SEM of technical duplicates are shown as fold inductions to the expression in untreated cells.

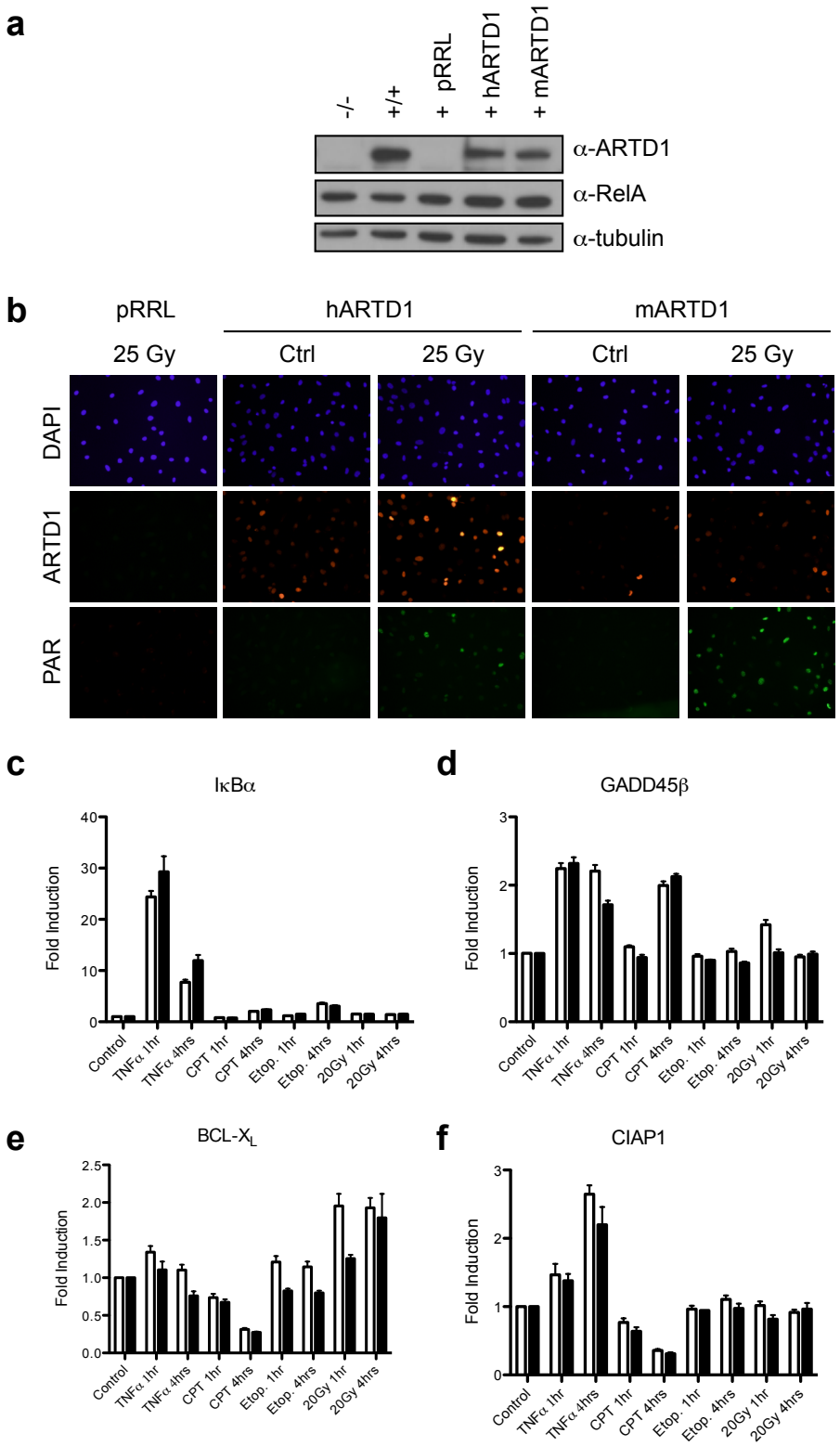

Figure 13. ARTD1 complementation does not restore NF-κB-dependent gene expression in *ARTD1* -/- cells. (a) Whole cells extracts of *ARTD1* -/- and +/+ cells as well as *ARTD1* -/- cells complemented with an emty vector (+ pRRL), hARTD1 or mARTD1 were analyzed by Western blot using antibodies directed against ARTD1, RelA and tubulin. (b) Immunofluorescence images of complemented cells showing ARTD1 expression levels and PAR generation upon X-radiation. (c-f) Complemented cells were treated as indicated and expression of *IκBα* (c), *GADD45β* (d), *BCL-X$_L$* (e) and *cIAP1* (f) was analyzed by real-time RT-PCR (compare Fig. 12). Open bars: + pRRL, solid bars: + hARTD1.

6.6.3. Discussion

While it is widely accepted that ARTD1 is involved the regulation of NF-κB target gene expression upon DNA damage, the underlying mechanisms are still under debate. This has been investigated in many studies with partially contradictory results. Our results suggest that ARTD1 is not required for the nuclear translocation of NF-κB, but might regulate downstream events during the activation of NF-κB-dependent genes. In agreement with this, B. Durkacz *et al.* show that IκBα degradation and nuclear translocation of NF-κB subunits p50 and RelA (measured by immunoblotting of nuclear extracts) are not affected by the PARP inhibitor AG14361 or in *ARTD1* -/- mouse embryonic fibroblasts, but that IR-induced DNA binding and target gene activation of NF-κB are disturbed [149]. Another study from this group suggests that PARP inhibitor AG-014699 radio-sensitizes cells in an NF-κB-dependent manner by preventing ARTD1 downstream signaling to NF-κB [150]. Also in this study, NF-κB shuttling after IR was not affected by ARTD1 inhibition or knockdown.

In contrast to our results, C. Scheidereit and colleagues suggest a model in which ARTD1 and its enzymatic activity are required for the formation of a nucleoplasmic signalosome that promotes the SUMOylation of IKK subunit NEMO [234]. Modified NEMO then translocates to the cytoplasm where it induces the activation of NF-κB [235]. This implies a role of ARTD1 upstream of NF-κB translocation to the nucleus. The discrepancy between the described study and our own results can be addressed in several ways. First of all, the dosage of the genotoxic agents used in this study was extremely high (80 Gy or 100 μM etoposide) which might induce other signaling pathways than the stimuli we applied (maximum 25 Gy or 50 μM etoposide). Furthermore, the results are mainly based on differences between *ARTD1* -/- and +/+ cells, which could potentially differ in more parameters than the ARTD1 deficiency. And finally, the conclusions are also based on the application of the first generation PARP inhibitor 3-AB, which is known to inhibit many cellular targets apart from ARTD1 [236,237]. Due to this lack in specificity, it is very well possible that 3-AB influences NF-κB activation via ARTD1 independent mechanisms.

6.7. Phosphorylation of ARTD1 by AMPK

AMPK is a key player in the regulation of energy metabolism. It is activated by a rise in the AMP/ATP ratio within the cell and influences the cellular energy homeostasis by phosphorylating many downstream targets. It was shown that ARTD1 is phosphorylated by AMPK *in vitro* and that this phosphorylation is stimulated by the addition of AMP [140]. In cells, ARTD1 and AMPK were shown to physically interact and overexpression of a constitutively active form of AMPK lead to increased ARTD1 automodification [140]. This positive regulation of ARTD1 activity could be a direct effect of ARTD1 phosphorylation by AMPK or an indirect effect as AMPK activation also increases cellular NAD^+ levels [238].

We were interested to determine where ARTD1 is phosphorylated by AMPK and if the phosphorylation has a direct effect on ARTD1 activity *in vitro*. In order to identify the phosphorylation site in ARTD1, ARTD1 and fragments covering the whole protein were subjected to an *in vitro* kinase assay with AMPK (Fig. 14a). The assay confirmed that ARTD1 is phosphorylated by AMPK. The phosphorylation increased upon addition of AMP. ARTD1(1-373) was strongly phosphorylated, indicating that AMPK phosphorylates ARTD1 in its DBD. ARTD1(373-525) was also modified by AMPK, but as ARTD1(373-1014) was not phosphorylated, this site is probably not accessible for AMPK in the context of the whole protein. In an attempt to identify the sub-domain of the DBD that is phosphorylated by AMPK, ARTD1 deletion mutants lacking either the ZFI (aa 1-111), the ZFII (aa 117-201) or the ZBDIII (aa 279-333) were *in vitro* modified with AMPK (Fig. 14b). Deletion of either one of the two zinc fingers of ARTD1 almost completely abolished its phosphorylation by AMPK. Interestingly, the deletion of the ZBDIII had the opposite effect and markedly increased the phosphorylation efficiency. These data suggest that AMPK phosphorylates ARTD1 in its first 279 aa and that this phosphorylation requires the presence of two intact zinc fingers. Furthermore, it seems that the ZBDIII has an inhibitory effect on the phosphorylation maybe by limiting the access of AMPK to its phosphorylation site(s) in ARTD1.

The localization of the AMPK target site within the DBD of ARTD1 prompted us to investigate if the phosphorylation was influenced by the presence of DNA, but pre-incubation of ARTD1 with an annealed double-stranded oligomer had no effect on its phosphorylation by AMPK (Fig. 14c).

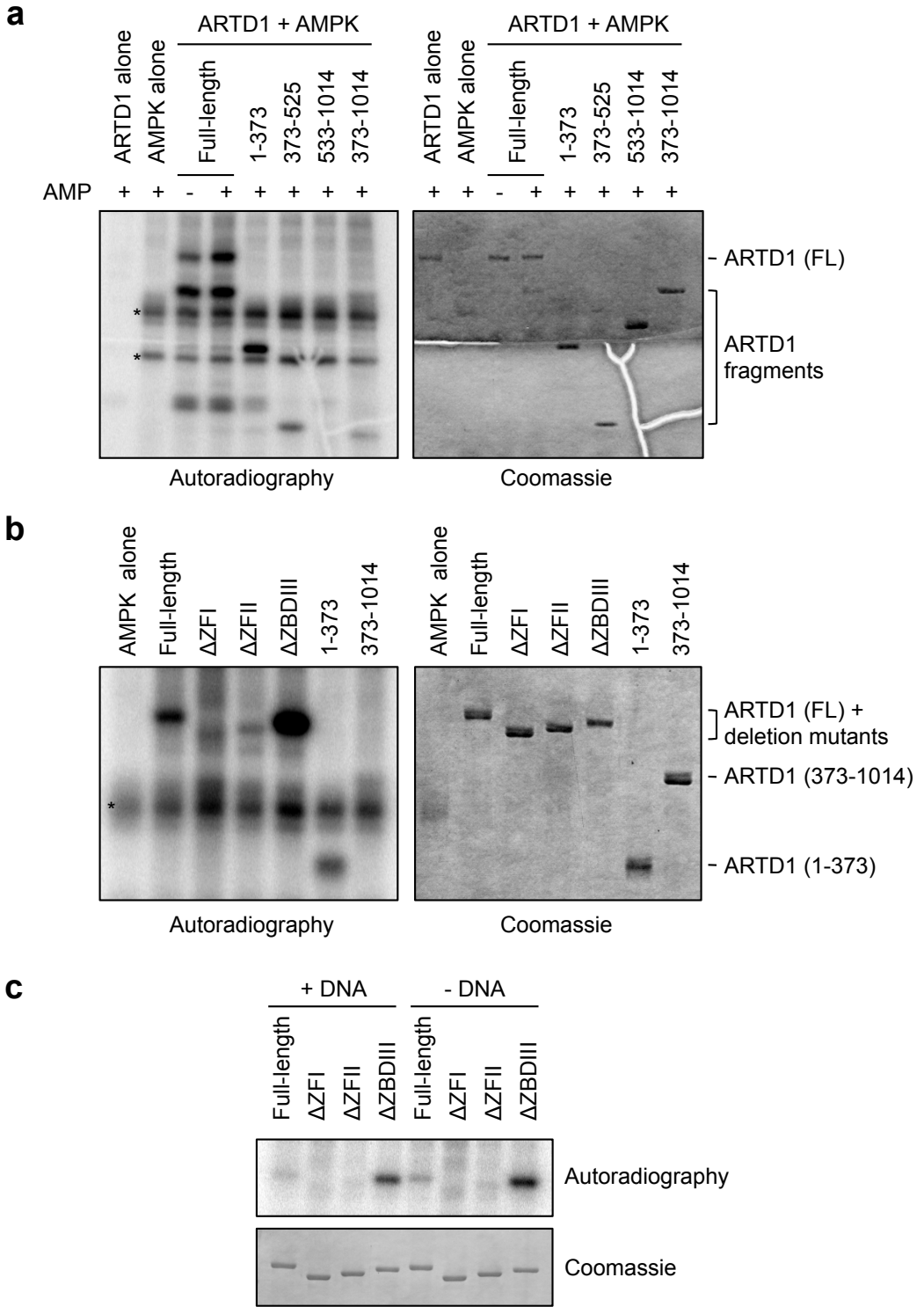

Figure 14. AMPK phosphorylates ARTD1 in its DNA binding domain. (a) Recombinant ARTD1 full-length and fragments covering the whole protein were incubated with AMPK in an *in vitro* phosphorylation assay with ^{32}P-γ-ATP. AMP was used to stimulate AMPK activity. The asterisk indicates AMPK autophosphorylation. (b) ARTD1 full-length and DBD sub-domain deletion mutants were phosphorylated as in (a). ΔZFI: ARTD1 lacking aa 1-111, ΔZFII: ARTD1 lacking aa 117-201, ΔZBDIII: ARTD1 lacking aa 279-333. (c) ARTD1 phosphorylation by AMPK as in (b) but ARTD1 proteins were preincubated with and without 5 pmol activating DNA for 15 min on ice.

The phosphorylation of ARTD1 introduces a negative charge into its DBD and might thus change its interaction with DNA by electrostatic repulsion. This in turn could affect its DNA-dependent enzymatic activity. This hypothesis was tested by first phosphorylating ARTD1 with AMPK and then inducing auto-ADP-ribosylation. Pre-incubation of ARTD1 with AMPK and ATP had no influence on its PARylation activity at different NAD^+ concentrations (Fig. 15a). ARTD1 was purified from insect cells and might therefore be post-translationally modified already. To rule out that a pre-existing phosphorylation of ARTD1 might mask an effect of the *in vitro* phosphorylation by AMPK, a new batch of ARTD1 was purified including a dephosphorylation step with calf intestinal alkaline phosphatase (CIP). Pre-incubation with CIP had no effect on the PARylation activity of ARTD1 (Fig. 15b). ARTD1 mono-ADP-ribosylation at very low NAD^+ concentrations (10 nM) was also not influenced by AMPK-dependent phosphorylation (Fig. 15c).

We therefore conclude that ARTD1 phosphorylation by AMPK has no influence on ARTD1 activity under the conditions tested. It is possible, however, that an effect on ARTD1 automodification was missed due to insufficient *in vitro* phosphorylation efficiency.

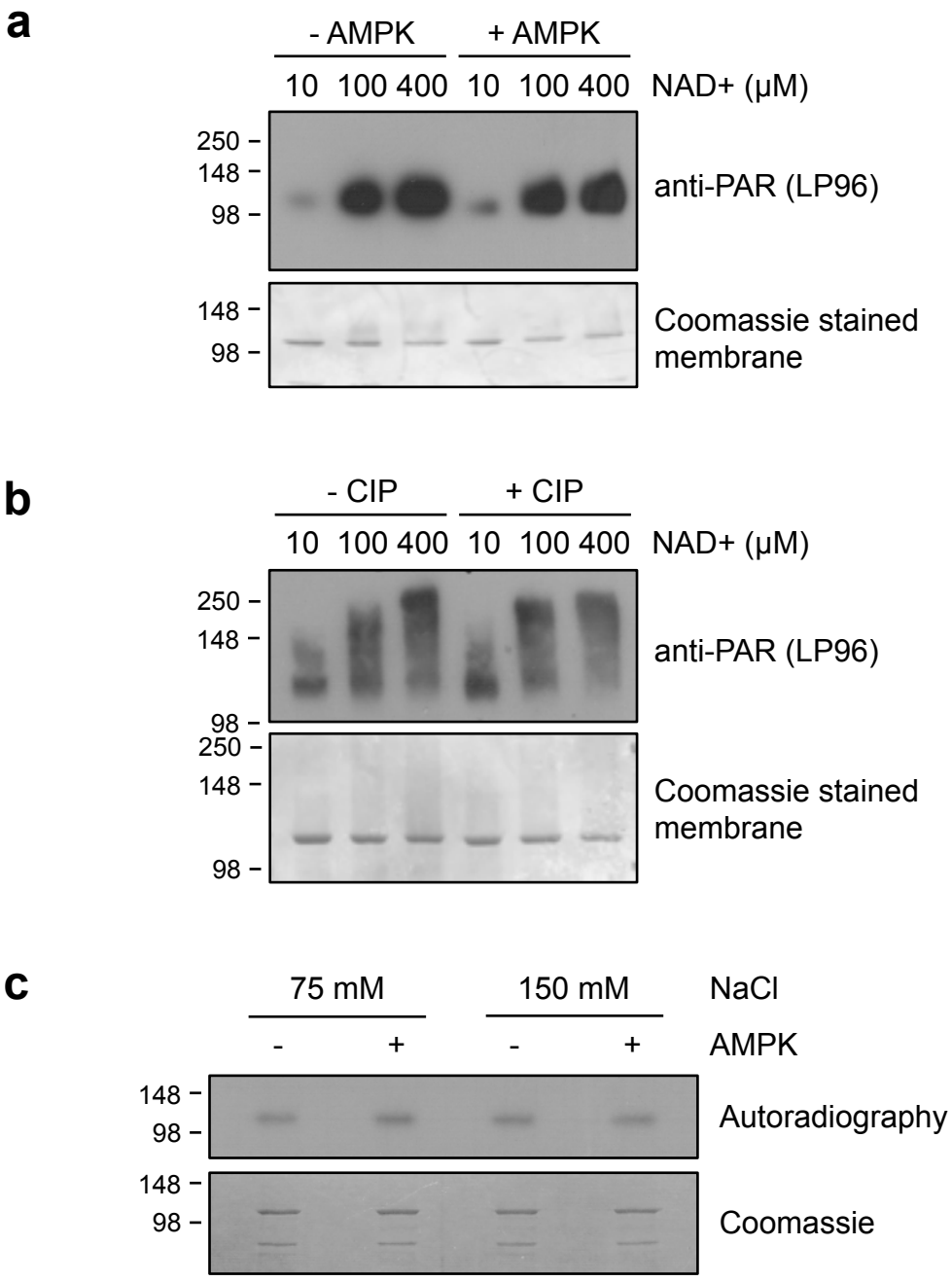

Figure 15. ARTD1 activity does not change upon phosphorylation by AMPK. (a) ARTD1 was *in vitro* phosphorylated with AMPK, purified by nickel affinity chromatography and *in vitro* PARylation was performed on the nickel beads by addition of activating DNA and the indicated concentrations of cold NAD^+. Automodification was analyzed by immunoblotting with a PAR-specific antibody (LP96). (b) Automodification activity of recombinant ARTD1 that was treated with and without CIP during purification was examined in an *in vitro* PARylation assay in solution [89] followed by immunoblotting. (c) ARTD1 activity after phosphorylation by AMPK was assessed as in (a) but with 10 nM ^{32}P-labeled NAD^+. Mono-ADP-ribosylation of ARTD1 was visualized by autoradiography.

6.8. Growth defect in cells complemented with ARTD1 E988K

The catalytic glutamate E988 in ARTD1 is important for its ability to synthesize ADP-ribose polymers. The ARTD1 mutant E988K thus displays only weak monoART activity, but is not able to attach further ADP-ribose units to the initially transferred ADP-ribose molecules. Complementation of MLFs isolated from *ARTD1* -/- mice with ARTD1 E988K induced a severe growth defect although ARTD1 deficient cells (complemented with an empty vector) or cells complemented with wildtype ARTD1 grew normally (Table 2). The doubling time of E988K complemented cells was 2-3 times longer than the one of wildtype complemented cells.

	Growth rate in 48 hrs		**Doubling time (hrs)**	
	$1x10^5$	$5x10^5$	$1x10^5$	$5x10^5$
pRRL	2.85	3.21	31.77	28.53
ARTD1 wt	2.65	3.52	34.14	26.44
ARTD1 E988K	1.46	1.625	87.92	68.53

Table 2. Proliferation of *ARTD1 -/-* cells complemented with wildtype (wt) ARTD1 or the E998K mutant. *ARTD1 -/-* MLFs were complemented with an empty vector (pRRL), hARTD1 wt or hARTD1 E988K. To determine proliferation rates and duplication times, $1x10^5$ and $5x10^5$ cells were seeded, grown in presence of 5 µg/ml blasticidine for 48 hrs and then harvested and counted using a Neubauer hemocytometer.

The reduced proliferation rates were not caused by cell cycle defects as E988K cells displayed similar cell cycle profiles as cells complemented with an empty vector or wildtype ARTD1 in early as well as in later passages (Fig. 16b and c). E988K cells were also not positive for senescense-associated β-galactosidase activity (Fig. 16d) indicating that E988K expression did not induce senescence. The negative effect of ARTD1 E988K on cell growth was further emphasized by the finding that E988K expression levels at later passages were much lower than wildtype expression levels (Fig. 16a) concomitant with the recovery of normal proliferation rates. This suggested that silencing of the E988K construct e.g. by epigenetic mechanisms conferred a growth advantage to the outgrowing clones.

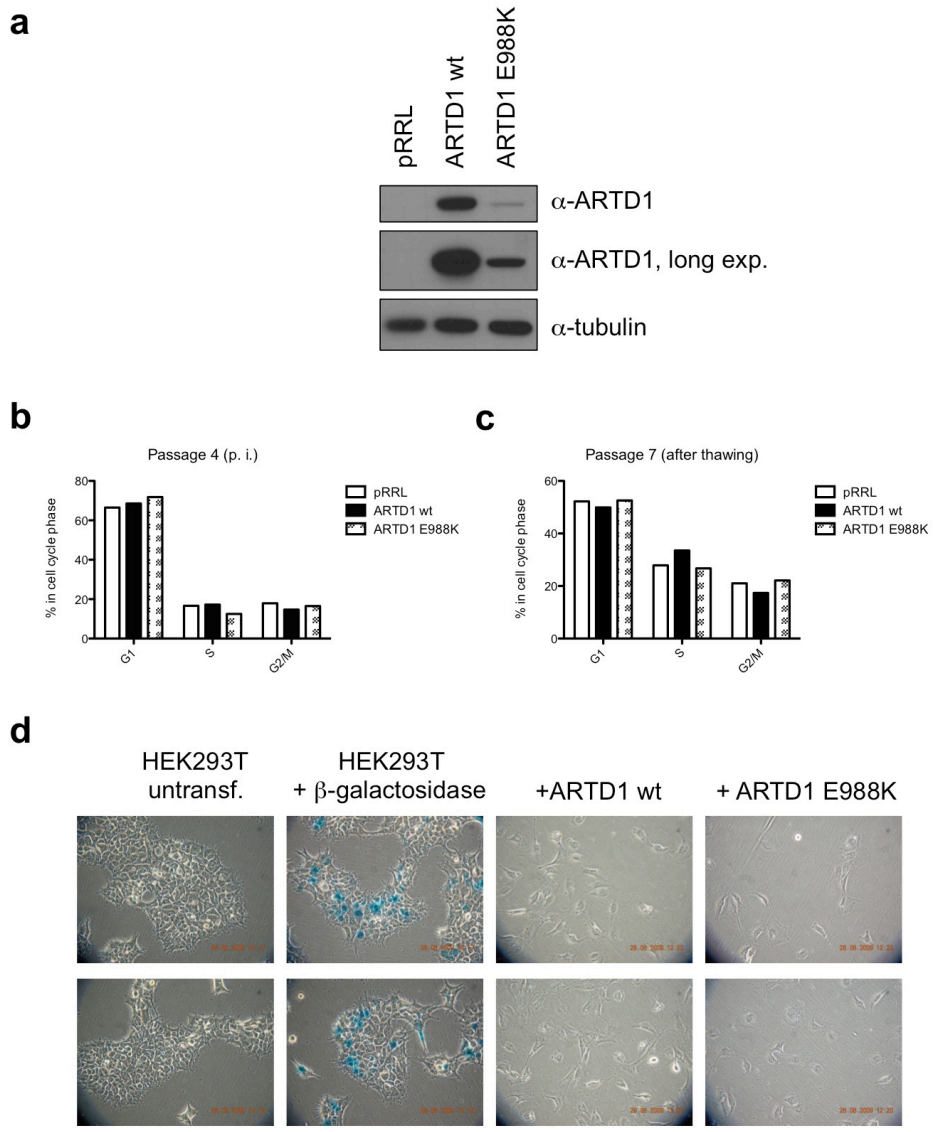

Figure 16. Characterization of E988K complemented cells. (a) Protein expression levels of ARTD1 in ARTD1 complemented stable cell lines (compare Table 1) were analyzed by Western blot. (b) Cell cycle profiles of ARTD1 complemented cells (passage 4 post transduction) were analyzed by flow cytometry. Cells were fixed, RNA was digested and DNA content was determined by propidium iodide staining and flow cytometry. (c) Same as in (b), but the experiment was performed with cells that were frozen and thawed after the transduction (passage 7 after thawing). (d) Senescence-associated β-galactosidase activity was analyzed by acidic β-galactosidase staining [239]. Briefly, cells were fixed with 0.2% glutaraldehyde in PBS for 5 min and then stained with 1 mg/ml X-gal at pH 6.0 and 37°C for 24 hrs. HEK293T cells overexpressing β-galactosidase were used as positive control. Representative light-microscopy images are shown.

The phenomenon that mutations interfering with the enzymatic activity of ARTD1 cause prolonged doubling times has been reported previously [240,241]. Cells completely lacking ARTD1 grow normally indicating that ARTD1-dependent PAR formation *per se* is not required for cell proliferation. This suggests that the

unprocessive ARTD1 protein itself disturbs normal cell growth. It is possible that E988K binds to certain DNA structures e.g. nick and DSBs, but unlike wildtype ARTD1, it cannot dissociate upon activation and thus blocks the access for other factors such as ARTD2 and proteins of the transcription and DNA repair machinery. This dominant-negative effect was also seen for the ARTD1 DBD alone whose overexpression in cells markedly inhibited PAR formation, induced hypersensitivity to alkylating agents and in some studies also reduced cell growth [242-245]. The hypothesis is challenged by the fact that ARTD1 inhibition by small-molecule inhibitors is compatible with normal cell growth in most cell lines. This inhibition, however, is reversible in most cases and thus might have other effects than the irreversible inactivation of ARTD1's PAR activity by certain mutations. The exact mechanisms of cell growth inhibition by unprocessive ARTD1 and its cellular targets have to be elucidated in future studies.

6.9. Materials and methods

6.9.1. Mouse cell lines and complementations

MLFs were isolated from *ARTD1* +/+ and -/- mice and immortalized using the 3T3 protocol [246]. Established MLF cell lines were grown in Dulbecco's Modified Eagle medium supplemented with 10% (v/v) fetal calf serum, penicillin/streptomycin and 1X Non Essential Amino Acids (Gibco). Lentivirus production in HEK293T cells and transduction of MLFs was performed as described elsewhere [247]. Briefly, HEK 293T cells were pretreated with 25 µM chloroquine for 5 min and transfected with 3.5 µg envelope plasmid, 6.5 µg packaging plasmid and 10 µg transfer vector (pRRL backbone) using the calcium phosphate method. Medium was replaced 6 hrs later and virus was harvested 40 hrs post transfection.

For transductions, 1 x 10^5 MLFs were seeded in sixwell plates and one day later, cells were incubated with the virus in presence of 4 µg/ml polybrene overnight. Selection was started with 5 µg/ml blasticidine two days after the transduction and stable cell lines were maintained in presence of the antibiotic.

6.9.2. Live cell microscopy and immunofluorescence

Images were taken with an Olympus BX51 microscope or a Leica DMI6000 B inverted microscope. For immunofluorescence analysis, cells were fixed with 4%

paraformaldehyde in PBS for 15 min at RT. Samples were then blocked with 2% BSA in PBS with 0.1% Triton and afterwards incubated with the indicated antibodies in blocking solution. For anti-PAR immunofluorescence staining, cells were fixed in methanol:acetic acid 3:1 for 5 min on ice. Blocking and antibody incubation were then performed in 5% milk in PBS-T (0.05% Tween-20). Mounting was done in Vectashield with DAPI (Vector Labs).

6.9.3. Gene expression analysis by conventional and real-time RT-PCR

Total RNA was extracted using the NucleoSpin® RNA II kit (Macherey Nagel). 1 – 2 µg total RNA were reverse transcribed with the High Capacity cDNA Reverse Transcription kit (Applied Biosystems). For conventional RT-PCR, 150 ng cDNA were amplified with 0.6 u GoTaq® DNA Polymerase (Promega) using 0.4 µM primers in a 25 µl reaction. Real-time PCR was performed in duplicates in a Rotor-Gene 3000A thermal cycler (Corbett Research) using the SensiMix SYBR & Fluorescein kit (Bioline). 10 ng cDNA were used in each reaction and a standard curve ranging from 0.05 to 50 ng cDNA was done to calculate primer efficiencies. Statistical analysis was performed with REST© software, version 2 [248].

6.9.4. In vitro *phosphorylation assay*

1 µg recombinant ARTD1 was incubated with 100 ng active AMPK (A1/B1/G2, SignalChem) in presence of 10 µM ATP spiked with 1µCi ^{32}P-γ-ATP (Hartmann Analytic) in kinase buffer (20 mM HEPES pH7.5, 5 mM $MgCl_2$, 0.01% Brij-35, 0.4 mM DTT, 300 µM AMP, 1 mM NaF, 0.1 mM NaV_3O_4, 20 mM β-glycerophosphate) for 15 min at 30°C. Reactions were stopped by addition of 5X SDS-sample buffer, denatured at 95°C for 5 min and separated by SDS-PAGE. Gels were stained with Coomassie, dried and autoradiographed.

For sequential phosphorylation/ADP-ribosylation assays, CIPped ARTD1 was phosphorylated as described above but using 20 µM cold ATP, bound to nickel affinity resin after phosphorylation, washed and modified in PAR buffer (50 mM Tris pH8.0, 150 mM NaCl, 4 mM $MgCl_2$, 5 pmol activating DNA, 1 mg/ml pepstatin, 1 mg/ml bestatin, 1 mg/ml leupeptin) after addition of hot or cold NAD^+ as indicated.

DISCUSSION AND PERSPECTIVES

7. Summary of results

We have investigated the influence of the KMT SET7/9 on the two chromatin-associated proteins ARTD1 and linker histone H1. *In vitro* methylation assays demonstrated that SET7/9 specifically methylates ARTD1, but not ARTD2, another member of the ARTD family. Using *in silico* analysis and mass spectrometry, K508 of ARTD1 was identified as the target site for SET7/9-dependent methylation. This was confirmed by site-directed mutagenesis of this residue to arginine. Interestingly, K508 is located close to confirmed acetylation and PARylation sites within the AMD of ARTD1 [89,142]. This prompted us to investigate the reciprocal influence of ARTD1 methylation and other post-translational modifications within this region. While methylation of ARTD1 did not interfere with its automodification, ARTD1 PARylation strongly inhibited its subsequent methylation by SET7/9. In contrast, we did not observe differences in p300-dependent acetylation of methylated and unmethylated ARTD1.

Using a newly generated antibody directed against the monomethylated lysine residue K508 in ARTD1, we were able to detect ARTD1 K508 methylation in U2OS cells overexpressing wildtype SET7/9, but not after overexpression of the enzymatically inactive mutant H297A. Interestingly, we found that PAR formation after H_2O_2 treatment was decreased after SET7/9 knockdown, while we could see enhanced H_2O_2–induced PAR formation after overexpression of wildtype but not H297A SET7/9. Reduced ARTD1 activity in nuclear extracts from SET7/9 knockdown cells was also observed in radioactive PARylation assays.

In radioactive PARylation assays, we observed that ARTD1 activity was higher in nuclear extracts of cells complemented with wildtype ARTD1 compared to cell lines complemented with methylation deficient ARTD1 mutants. This effect was reduced in presence of exogenous ARTD1-activating DNA. These results indicate that SET7/9-dependent methylation of K508 is important for ARTD1 activity in cells, especially under conditions where ARTD1 is only weakly activated. We then monitored ARTD1 recruitment to locally induced DNA lesions by live cell microscopy and found that ARTD1 K508R is recruited less efficiently to DNA

damage sites induced with a 775 nm laser than the wildtype protein. This difference was not observed at 1050 nm.

Finally, we observed that H1 is also monomethylated by SET7/9 at several lysine residues in its CTD. We used deletion and cluster mutation strategies to identify six KAK motifs in H1 that are methylated by SET7/9 at the last lysine residue (K121, K129, K159, K171, K177 and K192). The addition of plasmid DNA completely abolished SET7/9-dependent methylation of H1. Furthermore, we found that ARTD1-dependent PARylation of H1 and H3 prevents their subsequent methylation by SET7/9. In a histone mix, H3 is the preferred target for ARTD1 as well as for SET7/9, but prior PARylation of the histones can shift the substrate specificity of SET7/9 from H3 to H1.

8. ARTD1 regulation by SET7/9-dependent methylation

The addition of a methyl group to lysine residues of target proteins can affect the protein function by different mechanisms. While methylation does not change the positive charge of the lysine residue, it increases the size and hydrophobicity of the side chain and might thus directly influence the enzymatic activity if the target site lies in or close to the catalytic center or if the methylation induces or inhibits intramolecular interactions. *In vivo*, methylation can also indirectly regulate the function of a protein by inducing or inhibiting the interaction with other proteins or partner molecules, by changing its subcellular localization or by influencing its stability.

In the presented work, it was discovered that SET7/9 methylates ARTD1 at a specific lysine residue in its AMD (K508) and that this modification increases ARTD1 activity *in vitro* and *in vivo*. This positive effect on the enzymatic activity of ARTD1 was mainly observed at sub-optimal conditions i.e. at non-saturating DNA (compare Fig. 4B and C in section 5.1) or low NAD^+ concentrations (100 nM, data not shown). These results indicate that SET7/9-dependent methylation lowers the activation threshold for ARTD1 by weak triggers rather than being an absolute requirement for its activity. We thus became interested in the mechanism by which methylation at K508 sensitizes ARTD1 for stimulation by low DNA damage. To address this question we analyzed the nuclear distribution of ARTD1 as a function of its methylation. The affinity of ARTD1 for undamaged chromatin did not change upon

SET7/9 knockdown. However, ARTD1 wildtype was recruited more efficiently to laser-induced DNA damage than ARTD1 K508R at 775 nm, but not at 1050 nm (Fig. 1D and S1D in section 5.1).

These different observations at 775 and 1050 nm wavelengths can be explained in two ways: (1) Fewer DSBs are formed at 1050 nm than at 775 nm and thus overall less ARTD1 protein is recruited to the laser damaged site. At this wavelength, the sensitivity of the system might thus not be high enough to detect differences between ARTD1 wildtype and K508R. (2) It is known that the setup at 1050 nm selectively produces DNA strand breaks while multiphoton absorption at 775 nm generates UV photo products (cyclobutane-pyrimidine dimers and 6-4 photoproducts) and oxidative base damage in addition to DNA strand breaks [222]. Thus, it is possible that ARTD1 methylation regulates its recruitment to specific types of DNA damage that are only induced at 775 but not at 1050 nm. Several lines of evidence indicate that ARTD1-dependent PAR formation is triggered by UV damage or exposure to reactive oxygen species (although the exact molecular structures responsible for ARTD1 activation by these stresses remain to be determined) and that ARTD1 modulates the induction of cell death upon these stresses [249-251]. Therefore, it will be interesting to see if methylation sensitizes ARTD1 for the activation by these types of DNA damage.

This could be further investigated by *in vitro* PARylation assays in which DNA structures containing different types of lesions with protected ends are used to activate methylated and unmethylated ARTD1. Another approach to test this hypothesis would be to directly measure the affinity of unmethylated and methylated ARTD1 to different DNA structures e.g. by DNA-pulldown assays, by microplate capture assays with immobilized DNA probes or by surface plasmon resonance spectroscopy.

If SET7/9-dependent monomethylation indeed increases the response of ARTD1 to certain types of stress, it might also influence the cellular fate induced by these stresses. In fact, SET7/9 has been previously implicated in the modulation of cell cycle regulation and apoptosis in response to diverse stresses such as treatment with the inflammatory cytokine TNFα or DNA intercalator doxorubicin by methylating different factors e.g. p53, E2F1 and pRb [195,201-203]. ARTD1 methylation might thus be an additional level of cell fate regulation by SET7/9 in response to particular stresses. However, the role of SET7/9 at least in p53-induced cell cycle arrest and apoptosis after topoisomerase inhibitor treatment was not confirmed in SET7/9 knockout mice [187,196]. A detailed characterization of SET7/9 knockout mice and

derived cell lines will elucidate if and how SET7/9 might influence the sensitivity to other cellular insults such as UV irradiation or reactive oxygen species. In this respect, it is also important to note that SAH, which is generated as a byproduct of methylation reactions, is a potent inhibitor of all methyltransferases [252,253]. To prevent accumulation of SAH and resynthesize SAM, SAH is cleaved by the enzyme SAH hydrolase, which requires NAD^+ as essential cofactor. Thus, it is very likely that cellular stresses that influence nutrient supply and energy consumption (and thereby indirectly the cellular SAM/SAH ratio critical for the methylation potential) will also influence the methylation processes within a cell [254]. As ARTD1 is a NAD^+-consuming enzyme, this might create a feedback loop between ARTD1 methylation and ARTD1 activity. ARTD1 might not be methylated under conditions that do not favor methylation i.e. when NAD^+ levels and hence SAM/SAH ratio are low. As a result, ARTD1 would only be activated by high genotoxic stress at these conditions in order to preserve the cellular NAD^+ levels. Methylation might thus be a fine-tuning mechanism to facilitate ARTD1 activation when NAD^+ levels are high enough.

The results described here provide first insights for the regulation of ARTD1 enzymatic activity by SET7/9-dependent methylation. We show that SET7/9 methylates ARTD1 in its AMD, but neither in its DBD nor in its catalytic and NAD^+-binding domain (Fig. 2B in section 5.1), which would have supported an involvement in substrate or activator binding. The catalytic mechanism of ARTD1 is little understood. It is known that the DBD of ARTD1 interacts with its catalytic domain in a DNA-dependent manner and that this interaction increases the affinity of ARTD1 for its co-substrate NAD^+ [89]. Furthermore, several studies suggest that ARTD1 acts as a catalytic dimer [89,255,256]. It is thus tempting to speculate that the methylation at K508 enhances the dimerization or intramolecular interactions of ARTD1 and thereby modulates its activity.

In vivo, the methylation of ARTD1 might alternatively influence its function by promoting the interaction with other proteins. HP1 proteins are known to interact with ARTD1 [257] and contain a chromodomain, which binds trimethylated H3K9. However, it is unlikely that this domain also recognizes monomethylated ARTD1, as both the methyl state and the sequence context of this site are quite different from H3K9. Yet, the list of protein domains specifically recognizing individual protein modifications or their combinations is constantly increasing and it is very well

possible that future work will identify interaction partners of ARTD1 that are dependent on the methylation of K508.

Finally, it remains to be determined if ARTD1 is constitutively methylated *in vivo* or if it is only methylated in response to certain conditions. We have tried to tackle this question by treating cells with different stimuli (LPS, TNFα, etoposide, UV irradiation, H_2O_2), using different cell types in varying differentiation stages and by analyzing cells in different cell cycle phases (data not shown). So far, ARTD1 methylation could only be detected in cells overexpressing SET7/9 (Fig. 2E and F in section 5.1) and none of the treatments or cell cycle phases led to specific differences. It could be that endogenous K508 methylation levels are very low and cannot be detected by the generated antibody. Alternatively, SET7/9-dependent monomethylation of ARTD1 might be the rate-limiting step for further methylation events *in vivo* and therefore mainly di- or trimethylated ARTD1 exists under physiological conditions, which might not be recognized by the antibody developed against monomethylated ARTD1. ARTD1 monomethylation at K508 was also found in several mass spectrometric studies with breast cancer samples and Jurkat T cells cited on PhosphoSitePlus® [258], but there is no information about control tissues or non-cancerous cell lines.

9. Putative functions of H1 methylation by SET7/9

SET7/9 was first isolated as a mono-methyltransferase for H3K4 [182,183]. In the course of our studies, we found that SET7/9 is also capable of methylating linker histones. We identified six KAK sites in the CTD of H1.4, which are methylated at the last lysine residue in *in vitro* methylation assays with recombinant SET7/9 (Fig. 17). However, the *in vivo* function and biological relevance of this modification are still unclear. This is partially due to the lack of specific antibodies recognizing the mono-methylated KAK motifs in H1.4. We found that the antibody generated against methylated ARTD1 showed cross-reactivity with methylated H1.4 *in vitro* (data not shown). Yet, its application for methylated linker histones *in vivo* is difficult, as it lacks specificity for H1.4 and recognizes many other potentially methylated proteins as well. We also tested other antibodies directed against methylated lysines, but faced the same limitations (data not shown).

Figure 17. Human H1.4 amino acid sequence with known post-translational modification sites. The grey box marks the central globular domain. The six newly identified KAK motifs that are methylated by SET7/9 are highlighted in red. Blue: PARylation (PAR), red: phosphorylation (P), green: methylation (me, number indicates methylation state).

One possible function of H1 methylation by SET7/9 might be the stimulation or repression of other post-translational modifications. Compared with core histones, little is known about the modifications and the corresponding modifiers of the linker histones. Interestingly, the four last KAK motifs, which displayed the strongest methylation in *in vitro* methylation assays with SET7/9 (Fig. 1E in section 5.2), are located in close proximity to well-known CDK phosphorylation sites (Fig. 17). Crosstalk between K26 dimethylation and AuroraB-mediated phosphorylation of S27 has been reported previously [259]. A similar crosstalk might exist between SET7/9-dependent H1 methylation and phosphorylation by CDKs. Two of these sites (S172 and S187) are not exclusively phosphorylated during mitosis and their phosphorylation in interphase correlated with transcription and chromatin relaxation [48].

Based on *in vitro* experiments showing that H3K4 monomethylation precludes repressive histone modifiers, H3K4 methylation by SET7/9 was linked to transcriptional activation. Several studies confirmed a positive role of SET7/9 on expression and H3K4 methylation of specific subsets of genes [184-186,260]. SET7/9 knockout mice on the other hand show no change in global H3K4 methylation levels. The same gene-specific function could hold true for H1 methylation by SET7/9. A prerequisite to test this hypothesis is the generation of an antibody specific for this modification. With such a tool one could analyze the methylation of H1 on individual genes and promoters in a SET7/9-dependent manner. Moreover, ChIP-sequencing could be used to map the global distribution of this

modification. In this context, it will also be exciting to assess the correlation between H1 methylation by SET7/9 and H1 phosphorylation at S172 and S187.

We found that SET7/9-dependent H1 methylation is inhibited in the presence of DNA (Fig. 1B in section 5.2). This can be explained by DNA-induced conformational changes of the H1 CTD and by the charge neutralization through DNA, as SET7/9 is known to prefer lysine residues in a positively charged context. Likewise, methylation may directly influence the binding of H1 to DNA and its function in chromatin compaction, especially as the six lysine residues targeted by SET7/9 all reside in the CTD of H1.4, which is important for chromatin binding [9]. We compared the nuclear distribution of wildtype GFP-H1.4 and the K6R mutant by live cell microscopy (Fig. 8) and their mobility in FRAP experiments (data not shown) but did not observe any differences under the tested conditions. However, it is possible that differences in H1.4 mobility are only detectable in cells overexpressing or lacking SET7/9 as it was also the case for ARTD1 methylation *in vivo*. We also generated H1.4 fusion proteins with photoactivatable GFP, which may be used in future studies to monitor the dynamics of H1.4 in certain nuclear regions and under specific conditions as a function of SET7/9-dependent methylation.

Genome-wide binding studies revealed that H1 resides primarily on inactive genes, while ARTD1 displays reciprocal binding to chromatin [102]. SET7/9-mediated methylation might thus regulate the exchange of H1 and ARTD1 on their target promoters during gene activation. This could be accomplished by modulating the interaction of H1 and/or ARTD1 with other chromatin binding factors that facilitate their deposition or displacement from chromatin and thereby promote alterations in chromatin structure. This hypothesis could be analyzed by identifying methylation-dependent interaction partners of H1 and ARTD1 and by mapping the global chromatin distribution of H1 and ARTD1 in a SET7/9-dependent manner e.g. by comparing SET7/9 wildtype and knockout cells.

10. Crosstalk of ARTD1 and SET7/9 on chromatin

Epigenetic modifications are DNA-sequence independent heritable changes of chromatin that regulate gene expression and thereby influence the specific phenotype of a cell. Epigenetic modifications include (1) DNA methylation, (2) histone modifications and (3) chromatin remodeling. ARTD1 and histone ADP-ribosylation

were previously suggested as components of the histone code [73,98]. The results described here provide a further line of evidence for this hypothesis. We show that ARTD1-dependent PARylation of histones influences their subsequent methylation by SET7/9 (Fig. 3 in section 5.2). Compared to phosphorylation, which strongly reduces methylation if in proximity of SET7/9 target lysine residues [191], PARylation is a much more bulky modification with more negative charges and therefore also inhibited histone methylation by SET7/9. Based on our experiments, we know that SET7/9 methylates both, H1 and H3. Yet, when both histones are present, H3 is preferably methylated over H1. Strikingly, PARylation did not merely inhibit SET7/9-dependent methylation of histones, but completely shifted its substrate-specificity from H3 to H1. These observations could be explained by sequential PARylation events, where ARTD1 modifies H3 before H1. PARylation of H3 would then inhibit its subsequent methylation by SET7/9 and its competition as a SET7/9 target with H1 (Fig. 18).

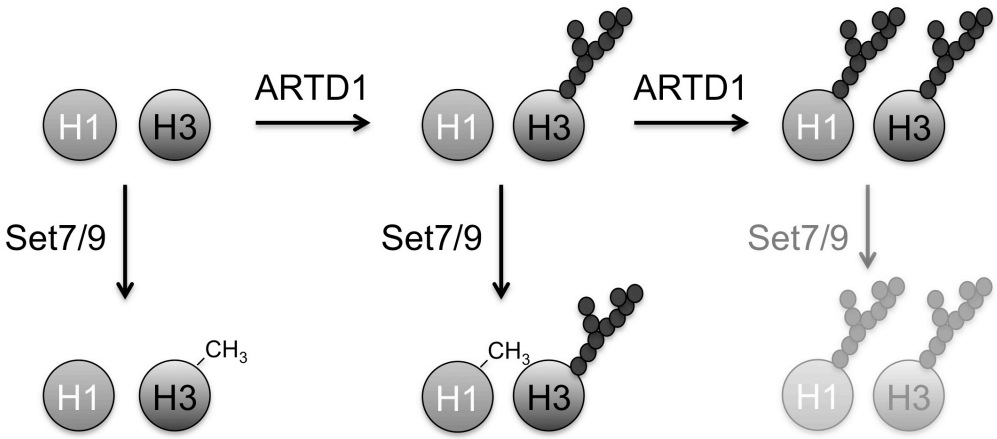

Figure 18. Crosstalk of ARTD1 and SET7/9 on histone modifications. H1 and H3 compete for methylation by SET7/9. As soon as H3 is PARylated by ARTD1, H1 becomes methylated by SET7/9. If H1 is also PARylated, none of the two histones are methylated any more. Schematic representation of our *in vitro* data.

This ARTD1-dependent regulation of the substrate specificity of another histone modifying enzyme may be an exciting mechanism to explain how ARTD1 influences chromatin-associated processes such as transcription. It is important to notice that progressive PARylation of histones also inhibited the methylation of H1, documenting that different outcomes for SET7/9-dependent histone methylation can occur depending on the extent of ARTD1 activity.

The complexity of ARTD1-dependent histone modifications is increased by the facts that (1) ARTD1 can modify all core histones and the linker histones [261] and (2) the size and quality (e.g. branching or length) of the polymers may differ under varying conditions and depending on the substrate histone. Therefore, future studies should not merely focus on the influence of ARTD1 and PARylation on other histone modifications but also on how ARTD1-dependent histone methylation itself is regulated. In this regard, it will also be interesting to investigate if SET7/9-dependent ARTD1 methylation may influence its substrate choice and trans-PARylation activities.

11. SET7/9 - a stress sensor and tumor suppressor?

While SET7/9 was first identified as a histone methyltransferase for H3K4, it is now widely accepted that its main function may be the methylation of other, non-histone proteins. SET7/9 has a unique SET domain structure and is found in many animals from zebrafish to humans. It has a broad substrate-specificity and a rather relaxed consensus motif (Fig. 19).

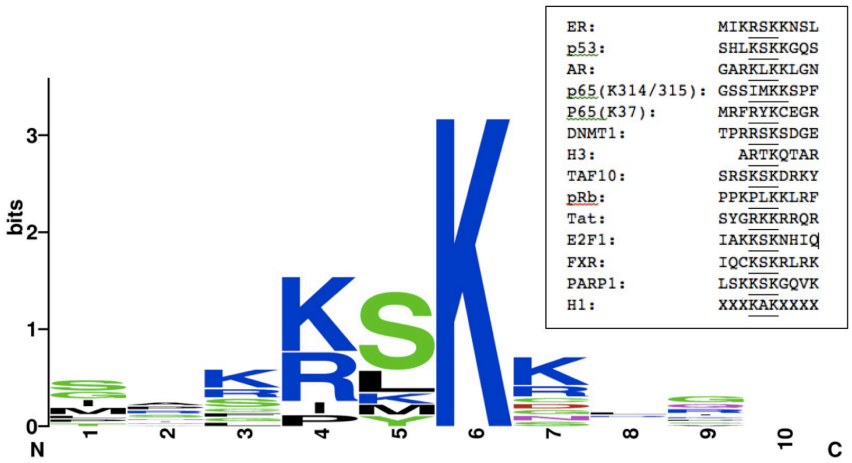

Figure 19. SET7/9 consensus motif. The only invariable residue is the lysine at position 6, which becomes methylated. The sequence logo was created using WebLogo (University of California, Berkeley [262]). SET7/9 target sequences from known substrates are displayed in the box. H3 and H1 target sequences were omitted from the logo generation for technical reasons.

Recently, Dhayalan *et al.* have published a list of 91 new SET7/9 target peptides [191]. They applied peptide-array methylation to identify an optimized target sequence for SET7/9 ([GRHKPST][K> R][S>KYA RTPN][K_{me}]). We have now identified ARTD1 and H1 as additional substrates. Thus, the list of SET7/9 target

proteins is rapidly growing, indicating that SET7/9-dependent methylation is a widely spread, relevant post-translational modification. Although the localization of SET7/9 is not confined to the nucleus, all substrates identified so far are proteins with important chromatin-associated functions related to gene expression, cell proliferation and tumor formation and progression. Yet, based on the rather mild phenotype of the available knockout mouse strains [187,196], an essential function of SET7/9 under normal, physiological conditions is very unlikely. Furthermore, although Set7/9-dependent methylation was shown to stabilize and activate several tumor suppressor proteins (e.g. p53, pRb), the knockout mice did not display any increased predisposition to tumorigenesis. Thus, SET7/9 might be only required under certain stress or pathophysiological conditions or SET7/9 loss might be compensated by other methyltransferases or unrelated mechanisms. With the help of new tools like the SET7/9 knockout cell lines and more specific chemical inhibitors of SET7/9, it will be exciting to unravel and re-evaluate the exact functions of SET7/9 during tumorigenesis and normal development.

REFERENCES

1. Campos, E.I. and Reinberg, D. (2009) Histones: annotating chromatin. *Annu. Rev. Genet.*, **43**, 559-599.
2. Arents, G. and Moudrianakis, E.N. (1995) The histone fold: a ubiquitous architectural motif utilized in DNA compaction and protein dimerization. *Proc. Natl. Acad. Sci. USA*, **92**, 11170-11174.
3. Bednar, J., Horowitz, R.A., Grigoryev, S.A., Carruthers, L.M., Hansen, J.C., Koster, A.J. and Woodcock, C.L. (1998) Nucleosomes, linker DNA, and linker histone form a unique structural motif that directs the higher-order folding and compaction of chromatin. *Proc. Natl. Acad. Sci. USA*, **95**, 14173-14178.
4. Felsenfeld, G. and Groudine, M. (2003) Controlling the double helix. *Nature*, **421**, 448-453.
5. Kepper, N., Foethke, D., Stehr, R., Wedemann, G. and Rippe, K. (2008) Nucleosome geometry and internucleosomal interactions control the chromatin fiber conformation. *Biophys. J.*, **95**, 3692-3705.
6. Kasinsky, H.E., Lewis, J.D., Dacks, J.B. and Ausio, J. (2001) Origin of H1 linker histones. *FASEB J.*, **15**, 34-42.
7. Ramakrishnan, V., Finch, J.T., Graziano, V., Lee, P.L. and Sweet, R.M. (1993) Crystal structure of globular domain of histone H5 and its implications for nucleosome binding. *Nature*, **362**, 219-223.
8. Allan, J., Hartman, P.G., Crane-Robinson, C. and Aviles, F.X. (1980) The structure of histone H1 and its location in chromatin. *Nature*, **288**, 675-679.
9. Caterino, T.L. and Hayes, J.J. (2011) Structure of the H1 C-terminal domain and function in chromatin condensationThis paper is one of a selection of papers published in a Special Issue entitled 31st Annual International Asilomar Chromatin and Chromosomes Conference, and has undergone the Journal's usual peer review process. *Biochem. Cell Biol.*, **89**, 35-44.
10. Lu, X., Hamkalo, B., Parseghian, M.H. and Hansen, J.C. (2009) Chromatin condensing functions of the linker histone C-terminal domain are mediated by specific amino acid composition and intrinsic protein disorder. *Biochemistry (Mosc).* **48**, 164-172.
11. Hansen, J.C., Lu, X., Ross, E.D. and Woody, R.W. (2006) Intrinsic protein disorder, amino acid composition, and histone terminal domains. *J. Biol. Chem.*, **281**, 1853-1856.
12. Fang, H., Clark, D.J. and Hayes, J.J. (2012) DNA and nucleosomes direct distinct folding of a linker histone H1 C-terminal domain. *Nucleic Acids Res.*, **40**, 1475-1484.
13. Lu, X. (2004) Identification of Specific Functional Subdomains within the Linker Histone H10 C-terminal Domain. *J. Biol. Chem.*, **279**, 8701-8707.
14. Roque, A., Iloro, I., Ponte, I., Arrondo, J.L. and Suau, P. (2005) DNA-induced secondary structure of the carboxyl-terminal domain of histone H1. *J. Biol. Chem.*, **280**, 32141-32147.
15. Clark, D.J., Hill, C.S., Martin, S.R. and Thomas, J.O. (1988) Alpha-helix in the carboxy-terminal domains of histones H1 and H5. *EMBO J.*, **7**, 69-75.
16. Vila, R., Ponte, I., Collado, M., Arrondo, J.L., Jimenez, M.A., Rico, M. and Suau, P. (2001) DNA-induced alpha-helical structure in the NH2-terminal domain of histone H1. *J. Biol. Chem.*, **276**, 46429-46435.
17. McBryant, S.J., Lu, X. and Hansen, J.C. (2010) Multifunctionality of the linker histones: an emerging role for protein-protein interactions. *Cell Res.*, **20**, 519-528.
18. Daujat, S., Zeissler, U., Waldmann, T., Happel, N. and Schneider, R. (2005) HP1 binds specifically to Lys26-methylated histone H1.4, whereas simultaneous Ser27 phosphorylation blocks HP1 binding. *J. Biol. Chem.*, **280**, 38090-38095.
19. Doenecke, D., Albig, W., Bouterfa, H. and Drabent, B. (1994) Organization and expression of H1 histone and H1 replacement histone genes. *J. Cell. Biochem.*, **54**, 423-431.
20. Izzo, A., Kamieniarz, K. and Schneider, R. (2008) The histone H1 family: specific members, specific functions? *Biol. Chem.*, **389**, 333-343.
21. Happel, N. and Doenecke, D. (2009) Histone H1 and its isoforms: Contribution to chromatin structure and function. *Gene*, **431**, 1-12.
22. Yamamoto, T. and Horikoshi, M. (1996) Cloning of the cDNA encoding a novel subtype of histone H1. *Gene*, **173**, 281-285.
23. Happel, N., Schulze, E. and Doenecke, D. (2005) Characterisation of human histone H1x. *Biol. Chem.*, **386**, 541-551.
24. Zlatanova, J. and Doenecke, D. (1994) Histone H1 zero: a major player in cell differentiation? *FASEB J.*, **8**, 1260-1268.

25. Doenecke, D., Albig, W., Bode, C., Drabent, B., Franke, K., Gavenis, K. and Witt, O. (1997) Histones: genetic diversity and tissue-specific gene expression. *Histochem. Cell Biol.*, **107**, 1-10.
26. Parseghian, M.H. and Hamkalo, B.A. (2001) A compendium of the histone H1 family of somatic subtypes: an elusive cast of characters and their characteristics. *Biochem. Cell Biol.*, **79**, 289-304.
27. Meergans, T., Albig, W. and Doenecke, D. (1997) Varied expression patterns of human H1 histone genes in different cell lines. *DNA Cell Biol.*, **16**, 1041-1049.
28. Th'ng, J.P., Sung, R., Ye, M. and Hendzel, M.J. (2005) H1 family histones in the nucleus. Control of binding and localization by the C-terminal domain. *J. Biol. Chem.*, **280**, 27809-27814.
29. Fan, Y., Sirotkin, A., Russell, R.G., Ayala, J. and Skoultchi, A.I. (2001) Individual somatic H1 subtypes are dispensable for mouse development even in mice lacking the H1(0) replacement subtype. *Mol. Cell. Biol.*, **21**, 7933-7943.
30. Sirotkin, A.M., Edelmann, W., Cheng, G., Klein-Szanto, A., Kucherlapati, R. and Skoultchi, A.I. (1995) Mice develop normally without the H1(0) linker histone. *Proc. Natl. Acad. Sci. USA*, **92**, 6434-6438.
31. Fan, Y., Nikitina, T., Morin-Kensicki, E.M., Zhao, J., Magnuson, T.R., Woodcock, C.L. and Skoultchi, A.I. (2003) H1 linker histones are essential for mouse development and affect nucleosome spacing in vivo. *Mol. Cell. Biol.*, **23**, 4559-4572.
32. Fan, Y., Nikitina, T., Zhao, J., Fleury, T.J., Bhattacharyya, R., Bouhassira, E.E., Stein, A., Woodcock, C.L. and Skoultchi, A.I. (2005) Histone H1 depletion in mammals alters global chromatin structure but causes specific changes in gene regulation. *Cell*, **123**, 1199-1212.
33. Mizzen, C.A. (2004) Purification and analyses of histone H1 variants and H1 posttranslational modifications. *Meth. Enzymol.*, **375**, 278-297.
34. Catez, F., Ueda, T. and Bustin, M. (2006) Determinants of histone H1 mobility and chromatin binding in living cells. *Nat. Struct. Mol. Biol*, **13**, 305-310.
35. Raghuram, N., Carrero, G., Th'ng, J. and Hendzel, M.J. (2009) Molecular dynamics of histone H1. *Biochem. Cell Biol.*, **87**, 189-206.
36. Balhorn, R., Chalkley, R. and Granner, D. (1972) Lysine-rich histone phosphorylation. A positive correlation with cell replication. *Biochemistry (Mosc)*. **11**, 1094-1098.
37. Suzuki, M. (1989) SPKK, a new nucleic acid-binding unit of protein found in histone. *EMBO J.*, **8**, 797-804.
38. Langan, T.A., Gautier, J., Lohka, M., Hollingsworth, R., Moreno, S., Nurse, P., Maller, J. and Sclafani, R.A. (1989) Mammalian growth-associated H1 histone kinase: a homolog of cdc2+/CDC28 protein kinases controlling mitotic entry in yeast and frog cells. *Mol. Cell. Biol.*, **9**, 3860-3868.
39. Paulson, J.R., Patzlaff, J.S. and Vallis, A.J. (1996) Evidence that the endogenous histone H1 phosphatase in HeLa mitotic chromosomes is protein phosphatase 1, not protein phosphatase 2A. *J. Cell Sci.*, **109 (Pt 6)**, 1437-1447.
40. Sarg, B., Helliger, W., Talasz, H., Förg, B. and Lindner, H.H. (2006) Histone H1 phosphorylation occurs site-specifically during interphase and mitosis: identification of a novel phosphorylation site on histone H1. *J. Biol. Chem.*, **281**, 6573-6580.
41. Hohmann, P., Tobey, R.A. and Gurley, L.R. (1976) Phosphorylation of distinct regions of f1 histone. Relationship to the cell cycle. *J. Biol. Chem.*, **251**, 3685-3692.
42. Boggs, B.A., Allis, C.D. and Chinault, A.C. (2000) Immunofluorescent studies of human chromosomes with antibodies against phosphorylated H1 histone. *Chromosoma*, **108**, 485-490.
43. Alexandrow, M.G. and Hamlin, J.L. (2005) Chromatin decondensation in S-phase involves recruitment of Cdk2 by Cdc45 and histone H1 phosphorylation. *J. Cell Biol.*, **168**, 875-886.
44. Baatout, S. and Derradji, H. (2006) About histone H1 phosphorylation during mitosis. *Cell Biochem. Funct.*, **24**, 93-94.
45. Green, G.R., Lee, H.J. and Poccia, D.L. (1993) Phosphorylation weakens DNA binding by peptides containing multiple "SPKK" sequences. *J. Biol. Chem.*, **268**, 11247-11255.
46. Hendzel, M.J. (2004) The C-terminal domain is the primary determinant of histone H1 binding to chromatin in vivo. *J. Biol. Chem.*, **279**, 20028-20034.
47. Roque, A., Ponte, I., Arrondo, J.L.R. and Suau, P. (2008) Phosphorylation of the carboxy-terminal domain of histone H1: effects on secondary structure and DNA condensation. *Nucleic Acids Res.*, **36**, 4719-4726.

48. Zheng, Y., John, S., Pesavento, J.J., Schultz-Norton, J.R., Schiltz, R.L., Baek, S., Nardulli, A.M., Hager, G.L., Kelleher, N.L. and Mizzen, C.A. (2010) Histone H1 phosphorylation is associated with transcription by RNA polymerases I and II. *J. Cell Biol.*, **189**, 407-415.
49. Dou, Y., Mizzen, C.A., Abrams, M., Allis, C.D. and Gorovsky, M.A. (1999) Phosphorylation of linker histone H1 regulates gene expression in vivo by mimicking H1 removal. *Mol. Cell*, **4**, 641-647.
50. Poirier, G.G., de Murcia, G., Jongstra-Bilen, J., Niedergang, C. and Mandel, P. (1982) Poly(ADP-ribosyl)ation of polynucleosomes causes relaxation of chromatin structure. *Proc. Natl. Acad. Sci. USA*, **79**, 3423-3427.
51. Aubin, R.J., Fréchette, A., de Murcia, G., Mandel, P., Lord, A., Grondin, G. and Poirier, G.G. (1983) Correlation between endogenous nucleosomal hyper(ADP-ribosyl)ation of histone H1 and the induction of chromatin relaxation. *EMBO J.*, **2**, 1685-1693.
52. Huletsky, A., de Murcia, G., Muller, S., Hengartner, M., Menard, L., Lamarre, D. and Poirier, G.G. (1989) The effect of poly(ADP-ribosyl)ation on native and H1-depleted chromatin. A role of poly(ADP-ribosyl)ation on core nucleosome structure. *J. Biol. Chem.*, **264**, 8878-8886.
53. Ogata, N., Ueda, K., Kagamiyama, H. and Hayaishi, O. (1980) ADP-ribosylation of histone H1. Identification of glutamic acid residues 2, 14, and the COOH-terminal lysine residue as modification sites. *J. Biol. Chem.*, **255**, 7616-7620.
54. Wisniewski, J.R., Zougman, A., Kruger, S. and Mann, M. (2006) Mass spectrometric mapping of linker histone H1 variants reveals multiple acetylations, methylations, and phosphorylation as well as differences between cell culture and tissue. *Mol. Cell. Proteomics*, **6**, 72-87.
55. Snijders, A.P., Pongdam, S., Lambert, S.J., Wood, C.M., Baldwin, J.P. and Dickman, M.J. (2008) Characterization of post-translational modifications of the linker histones H1 and H5 from chicken erythrocytes using mass spectrometry. *J. Proteome Res.*, **7**, 4326-4335.
56. Ohe, Y., Hayashi, H. and Iwai, K. (1986) Human spleen histone H1. Isolation and amino acid sequence of a main variant, H1b. *J. Biochem. (Tokyo)*. **100**, 359-368.
57. Kuzmichev, A., Jenuwein, T., Tempst, P. and Reinberg, D. (2004) Different EZH2-containing complexes target methylation of histone H1 or nucleosomal histone H3. *Mol. Cell*, **14**, 183-193.
58. Trojer, P., Zhang, J., Yonezawa, M., Schmidt, A., Zheng, H., Jenuwein, T. and Reinberg, D. (2009) Dynamic histone H1 isotype 4 methylation and demethylation by histone lysine methyltransferase G9a/KMT1C and the Jumonji domain-containing JMJD2/KDM4 proteins. *J. Biol. Chem.*, **284**, 8395-8405.
59. Weiss, T., Hergeth, S., Zeissler, U., Izzo, A., Tropberger, P., Zee, B.M., Dundr, M., Garcia, B.A., Daujat, S. and Schneider, R. (2010) Histone H1 variant-specific lysine methylation by G9a/KMT1C and Glp1/KMT1D. *Epigenetics Chromatin*, **3**, 7.
60. Collier, R.J. (2001) Understanding the mode of action of diphtheria toxin: a perspective on progress during the 20th century. *Toxicon*, **39**, 1793-1803.
61. Holbourn, K.P., Shone, C.C. and Acharya, K.R. (2006) A family of killer toxins. Exploring the mechanism of ADP-ribosylating toxins. *Febs J.*, **273**, 4579-4593.
62. Faraone-Mennella, M.R., Gambacorta, A., Nicolaus, B. and Farina, B. (1998) Purification and biochemical characterization of a poly(ADP-ribose) polymerase-like enzyme from the thermophilic archaeon Sulfolobus solfataricus. *Biochem. J.*, **335 (Pt 2)**, 441-447.
63. Werner, E., Sohst, S., Gropp, F., Simon, D., Wagner, H. and Kröger, H. (1984) Presence of poly (ADP-ribose) polymerase and poly (ADP-ribose) glycohydrolase in the dinoflagellate Crypthecodinium cohnii. *Eur. J. Biochem.*, **139**, 81-86.
64. Alvarez-Gonzalez, R. and Mendoza-Alvarez, H. (1995) Dissection of ADP-ribose polymer synthesis into individual steps of initiation, elongation, and branching. *Biochimie*, **77**, 403-407.
65. Hassa, P.O. (2006) Nuclear ADP-Ribosylation Reactions in Mammalian Cells: Where Are We Today and Where Are We Going? *Microbiol. Mol. Biol. Rev.*, **70**, 789-829.
66. Alvarez-Gonzalez, R. and Jacobson, M.K. (1987) Characterization of polymers of adenosine diphosphate ribose generated in vitro and in vivo. *Biochemistry (Mosc).* **26**, 3218-3224.
67. Kim, M.Y. (2005) Poly(ADP-ribosyl)ation by PARP-1: `PAR-laying' NAD+ into a nuclear signal. *Genes Dev.*, **19**, 1951-1967.
68. Koch-Nolte, F., Kernstock, S., Mueller-Dieckmann, C., Weiss, M.S. and Haag, F. (2008) Mammalian ADP-ribosyltransferases and ADP-ribosylhydrolases. *Front. Biosci.*, **13**, 6716-6729.
69. Oka, S., Kato, J. and Moss, J. (2006) Identification and characterization of a mammalian 39-kDa poly(ADP-ribose) glycohydrolase. *J. Biol. Chem.*, **281**, 705-713.

70. Koh, D.W., Lawler, A.M., Poitras, M.F., Sasaki, M., Wattler, S., Nehls, M.C., Stoger, T., Poirier, G.G., Dawson, V.L. and Dawson, T.M. (2004) Failure to degrade poly(ADP-ribose) causes increased sensitivity to cytotoxicity and early embryonic lethality. *Proc. Natl. Acad. Sci. USA*, **101**, 17699-17704.
71. Hanai, S., Kanai, M., Ohashi, S., Okamoto, K., Yamada, M., Takahashi, H. and Miwa, M. (2004) Loss of poly(ADP-ribose) glycohydrolase causes progressive neurodegeneration in Drosophila melanogaster. *Proc. Natl. Acad. Sci. USA*, **101**, 82-86.
72. Glowacki, G., Braren, R., Firner, K., Nissen, M., Kuhl, M., Reche, P., Bazan, F., Cetkovic-Cvrlje, M., Leiter, E., Haag, F. *et al.* (2002) The family of toxin-related ecto-ADP-ribosyltransferases in humans and the mouse. *Protein Sci.*, **11**, 1657-1670.
73. Hottiger, M.O. (2011) ADP-ribosylation of histones by ARTD1: An additional module of the histone code? *FEBS Lett.*
74. Pleschke, J.M., Kleczkowska, H.E., Strohm, M. and Althaus, F.R. (2000) Poly(ADP-ribose) binds to specific domains in DNA damage checkpoint proteins. *J. Biol. Chem.*, **275**, 40974-40980.
75. Ahel, I., Ahel, D., Matsusaka, T., Clark, A.J., Pines, J., Boulton, S.J. and West, S.C. (2008) Poly(ADP-ribose)-binding zinc finger motifs in DNA repair/checkpoint proteins. *Nature*, **451**, 81-85.
76. Karras, G.I., Kustatscher, G., Buhecha, H.R., Allen, M.D., Pugieux, C., Sait, F., Bycroft, M. and Ladurner, A.G. (2005) The macro domain is an ADP-ribose binding module. *EMBO J.*, **24**, 1911-1920.
77. Hottiger, M.O., Hassa, P.O., Lüscher, B., Schüler, H. and Koch-Nolte, F. (2010) Toward a unified nomenclature for mammalian ADP-ribosyltransferases. *Trends Biochem. Sci.*, 1-12.
78. Yamanaka, H., Penning, C.A., Willis, E.H., Wasson, D.B. and Carson, D.A. (1988) Characterization of human poly(ADP-ribose) polymerase with autoantibodies. *J. Biol. Chem.*, **263**, 3879-3883.
79. D'Amours, D., Desnoyers, S., D'Silva, I. and Poirier, G.G. (1999) Poly(ADP-ribosyl)ation reactions in the regulation of nuclear functions. *Biochem. J.*, **342 (Pt 2)**, 249-268.
80. Hassa, P.O. and Hottiger, M.O. (2008) The diverse biological roles of mammalian PARPS, a small but powerful family of poly-ADP-ribose polymerases. *Front. Biosci.*, **13**, 3046-3082.
81. Alvarez-Gonzalez, R. and Althaus, F.R. (1989) Poly(ADP-ribose) catabolism in mammalian cells exposed to DNA-damaging agents. *Mutat. Res.*, **218**, 67-74.
82. Citarelli, M., Teotia, S. and Lamb, R.S. (2010) Evolutionary history of the poly(ADP-ribose) polymerase gene family in eukaryotes. *BMC Evol. Biol.*, **10**, 308.
83. Johansson, M. (1999) A human poly(ADP-ribose) polymerase gene family (ADPRTL): cDNA cloning of two novel poly(ADP-ribose) polymerase homologues. *Genomics*, **57**, 442-445.
84. Ame, J.C., Rolli, V., Schreiber, V., Niedergang, C., Apiou, F., Decker, P., Muller, S., Hoger, T., Menissier-de Murcia, J. and de Murcia, G. (1999) PARP-2, A novel mammalian DNA damage-dependent poly(ADP-ribose) polymerase. *J. Biol. Chem.*, **274**, 17860-17868.
85. Kleine, H., Poreba, E., Lesniewicz, K., Hassa, P.O., Hottiger, M.O., Litchfield, D.W., Shilton, B.H. and Lüscher, B. (2008) Substrate-assisted catalysis by PARP10 limits its activity to mono-ADP-ribosylation. *Mol. Cell*, **32**, 57-69.
86. Marsischky, G.T., Wilson, B.A. and Collier, R.J. (1995) Role of glutamic acid 988 of human poly-ADP-ribose polymerase in polymer formation. Evidence for active site similarities to the ADP-ribosylating toxins. *J. Biol. Chem.*, **270**, 3247-3254.
87. Ruf, A., Rolli, V., de Murcia, G. and Schulz, G.E. (1998) The mechanism of the elongation and branching reaction of poly(ADP-ribose) polymerase as derived from crystal structures and mutagenesis. *J. Mol. Biol.*, **278**, 57-65.
88. Aguiar, R.C., Takeyama, K., He, C., Kreinbrink, K. and Shipp, M.A. (2005) B-aggressive lymphoma family proteins have unique domains that modulate transcription and exhibit poly(ADP-ribose) polymerase activity. *J. Biol. Chem.*, **280**, 33756-33765.
89. Altmeyer, M., Messner, S., Hassa, P.O., Fey, M. and Hottiger, M.O. (2009) Molecular mechanism of poly(ADP-ribosyl)ation by PARP1 and identification of lysine residues as ADP-ribose acceptor sites. *Nucleic Acids Res.*, **37**, 3723-3738.
90. Kickhoefer, V.A., Siva, A.C., Kedersha, N.L., Inman, E.M., Ruland, C., Streuli, M. and Rome, L.H. (1999) The 193-kD vault protein, VPARP, is a novel poly(ADP-ribose) polymerase. *J. Cell Biol.*, **146**, 917-928.
91. Rippmann, J.F., Damm, K. and Schnapp, A. (2002) Functional characterization of the poly(ADP-ribose) polymerase activity of tankyrase 1, a potential regulator of telomere length. *J. Mol. Biol.*, **323**, 217-224.

92. Wang, Z.Q., Auer, B., Stingl, L., Berghammer, H., Haidacher, D., Schweiger, M. and Wagner, E.F. (1995) Mice lacking ADPRT and poly(ADP-ribosyl)ation develop normally but are susceptible to skin disease. *Genes Dev.*, **9**, 509-520.
93. Masutani, M., Nozaki, T., Nishiyama, E., Shimokawa, T., Tachi, Y., Suzuki, H., Nakagama, H., Wakabayashi, K. and Sugimura, T. (1999) Function of poly(ADP-ribose) polymerase in response to DNA damage: gene-disruption study in mice. *Mol. Cell. Biochem.*, **193**, 149-152.
94. Shall, S. and de Murcia, G. (2000) Poly(ADP-ribose) polymerase-1: what have we learned from the deficient mouse model? *Mutat. Res.*, **460**, 1-15.
95. Shall, S. and Sugimura, T. (2006) What is new about ADP-ribosylation? *Bioessays*, **28**, 97-99.
96. Ménissier de Murcia, J., Ricoul, M., Tartier, L., Niedergang, C., Huber, A., Dantzer, F., Schreiber, V., Amé, J.-C., Dierich, A., LeMeur, M. *et al.* (2003) Functional interaction between PARP-1 and PARP-2 in chromosome stability and embryonic development in mouse. *EMBO J.*, **22**, 2255-2263.
97. Tulin, A., Stewart, D. and Spradling, A.C. (2002) The Drosophila heterochromatic gene encoding poly(ADP-ribose) polymerase (PARP) is required to modulate chromatin structure during development. *Genes Dev.*, **16**, 2108-2119.
98. Messner, S. and Hottiger, M.O. (2011) Histone ADP-ribosylation in DNA repair, replication and transcription. *Trends Cell Biol.*, **21**, 534-542.
99. Kim, M., Mauro, S., Gevry, N., Lis, J. and Kraus, W. (2004) NAD-dependent modulation of chromatin structure and transcription by nucleosome binding properties of PARP-1. *Cell*, **119**, 803-814.
100. Wacker, D.A., Ruhl, D.D., Balagamwala, E.H., Hope, K.M., Zhang, T. and Kraus, W.L. (2007) The DNA binding and catalytic domains of poly(ADP-ribose) polymerase 1 cooperate in the regulation of chromatin structure and transcription. *Mol. Cell. Biol.*, **27**, 7475-7485.
101. Tulin, A. and Spradling, A. (2003) Chromatin loosening by poly(ADP)-ribose polymerase (PARP) at Drosophila puff loci. *Science*, **299**, 560-562.
102. Krishnakumar, R., Gamble, M.J., Frizzell, K.M., Berrocal, J.G., Kininis, M. and Kraus, W.L. (2008) Reciprocal Binding of PARP-1 and Histone H1 at Promoters Specifies Transcriptional Outcomes. *Science*, **319**, 819-821.
103. Hassa, P.O. and Hottiger, M.O. (1999) A role of poly (ADP-ribose) polymerase in NF-kappaB transcriptional activation. *Biol. Chem.*, **380**, 953-959.
104. Oei, S.L., Griesenbeck, J., Schweiger, M. and Ziegler, M. (1998) Regulation of RNA polymerase II-dependent transcription by poly(ADP-ribosyl)ation of transcription factors. *J. Biol. Chem.*, **273**, 31644-31647.
105. Elser, M., Borsig, L., Hassa, P.O., Erener, S., Messner, S., Valovka, T., Keller, S., Gassmann, M. and Hottiger, M.O. (2008) Poly(ADP-ribose) polymerase 1 promotes tumor cell survival by coactivating hypoxia-inducible factor-1-dependent gene expression. *Mol. Cancer Res.*, **6**, 282-290.
106. Kraus, W.L. (2008) Transcriptional control by PARP-1: chromatin modulation, enhancer-binding, coregulation, and insulation. *Curr. Opin. Cell Biol.*, **20**, 294-302.
107. Oei, S.L., Griesenbeck, J., Ziegler, M. and Schweiger, M. (1998) A novel function of poly(ADP-ribosyl)ation: silencing of RNA polymerase II-dependent transcription. *Biochemistry (Mosc)*. **37**, 1465-1469.
108. Olabisi, O.A., Soto-Nieves, N., Nieves, E., Yang, T.T., Yang, X., Yu, R.Y., Suk, H.Y., Macian, F. and Chow, C.W. (2008) Regulation of transcription factor NFAT by ADP-ribosylation. *Mol. Cell. Biol.*, **28**, 2860-2871.
109. Zaniolo, K., Desnoyers, S., Leclerc, S. and Guerin, S.L. (2007) Regulation of poly(ADP-ribose) polymerase-1 (PARP-1) gene expression through the post-translational modification of Sp1: a nuclear target protein of PARP-1. *BMC Mol. Biol.*, **8**, 96.
110. Cervellera, M.N. and Sala, A. (2000) Poly(ADP-ribose) polymerase is a B-MYB coactivator. *J. Biol. Chem.*, **275**, 10692-10696.
111. Hassa, P.O., Covic, M., Hasan, S., Imhof, R. and Hottiger, M.O. (2001) The enzymatic and DNA binding activity of PARP-1 are not required for NF-kappa B coactivator function. *J. Biol. Chem.*, **276**, 45588-45597.
112. Petesch, Steven J. and Lis, John T. (2012) Activator-induced spread of poly(ADP-ribose) polymerase promotes nucleosome loss at Hsp70. *Mol. Cell*, **45**, 64-74.
113. Frizzell, K.M., Gamble, M.J., Berrocal, J.G., Zhang, T., Krishnakumar, R., Cen, Y., Sauve, A.A. and Kraus, W.L. (2009) Global analysis of transcriptional regulation by poly(ADP-ribose) polymerase-1 and poly(ADP-ribose) glycohydrolase in MCF-7 human breast cancer cells. *J. Biol. Chem.*, **284**, 33926-33938.

114. Ju, B.-G. (2006) A Topoisomerase II -Mediated dsDNA Break Required for Regulated Transcription. *Science*, **312**, 1798-1802.
115. Yu, W., Ginjala, V., Pant, V., Chernukhin, I., Whitehead, J., Docquier, F., Farrar, D., Tavoosidana, G., Mukhopadhyay, R., Kanduri, C. *et al.* (2004) Poly(ADP-ribosyl)ation regulates CTCF-dependent chromatin insulation. *Nat. Genet.*, **36**, 1105-1110.
116. Krishnakumar, R. and Kraus, W.L. (2010) The PARP side of the nucleus: Molecular actions, physiological outcomes, and clinical targets. *Mol. Cell*, **39**, 8-24.
117. Mortusewicz, O., Amé, J.-C., Schreiber, V. and Leonhardt, H. (2007) Feedback-regulated poly(ADP-ribosyl)ation by PARP-1 is required for rapid response to DNA damage in living cells. *Nucleic Acids Res.*, **35**, 7665-7675.
118. Haince, J.-F., Mcdonald, D., Rodrigue, A., Dery, U., Masson, J.-Y., Hendzel, M.J. and Poirier, G.G. (2007) PARP1-dependent kinetics of recruitment of MRE11 and NBS1 proteins to multiple DNA damage sites. *J. Biol. Chem.*, **283**, 1197-1208.
119. Masson, M., Niedergang, C., Schreiber, V., Muller, S., Menissier-de Murcia, J. and de Murcia, G. (1998) XRCC1 is specifically associated with poly(ADP-ribose) polymerase and negatively regulates its activity following DNA damage. *Mol. Cell. Biol.*, **18**, 3563-3571.
120. Caldecott, K.W., Aoufouchi, S., Johnson, P. and Shall, S. (1996) XRCC1 polypeptide interacts with DNA polymerase beta and possibly poly (ADP-ribose) polymerase, and DNA ligase III is a novel molecular 'nick-sensor' in vitro. *Nucleic Acids Res.*, **24**, 4387-4394.
121. Leppard, J.B., Dong, Z., Mackey, Z.B. and Tomkinson, A.E. (2003) Physical and functional interaction between DNA ligase IIIalpha and poly(ADP-Ribose) polymerase 1 in DNA single-strand break repair. *Mol. Cell. Biol.*, **23**, 5919-5927.
122. Dantzer, F., de La Rubia, G., Menissier-De Murcia, J., Hostomsky, Z., de Murcia, G. and Schreiber, V. (2000) Base excision repair is impaired in mammalian cells lacking Poly(ADP-ribose) polymerase-1. *Biochemistry (Mosc).* **39**, 7559-7569.
123. Ahel, D., Horejsí, Z., Wiechens, N., Polo, S.E., Garcia-Wilson, E., Ahel, I., Flynn, H., Skehel, M., West, S.C., Jackson, S.P. *et al.* (2009) Poly(ADP-ribose)-dependent regulation of DNA repair by the chromatin remodeling enzyme ALC1. *Science*, **325**, 1240-1243.
124. Timinszky, G., Till, S., Hassa, P.O., Hothorn, M., Kustatscher, G., Nijmeijer, B., Colombelli, J., Altmeyer, M., Stelzer, E.H., Scheffzek, K. *et al.* (2009) A macrodomain-containing histone rearranges chromatin upon sensing PARP1 activation. *Nat. Struct. Mol. Biol*, **16**, 923-929.
125. Le Page, F. (2003) Poly(ADP-ribose) polymerase-1 (PARP-1) is required in murine cell lines for base excision repair of oxidative DNA damage in the absence of DNA polymerase beta. *J. Biol. Chem.*, **278**, 18471-18477.
126. Pachkowski, B.F., Tano, K., Afonin, V., Elder, R.H., Takeda, S., Watanabe, M., Swenberg, J.A. and Nakamura, J. (2009) Cells deficient in PARP-1 show an accelerated accumulation of DNA single strand breaks, but not AP sites, over the PARP-1-proficient cells exposed to MMS. *Mutat. Res.*, **671**, 93-99.
127. Allinson, S.L., Dianova, I.I. and Dianov, G.L. (2003) Poly(ADP-ribose) polymerase in base excision repair: always engaged, but not essential for DNA damage processing. *Acta Biochim. Pol.*, **50**, 169-179.
128. Sanderson, R.J. and Lindahl, T. (2002) Down-regulation of DNA repair synthesis at DNA single-strand interruptions in poly(ADP-ribose) polymerase-1 deficient murine cell extracts. *DNA Repair*, **1**, 547-558.
129. Vodenicharov, M.D., Sallmann, F.R., Satoh, M.S. and Poirier, G.G. (2000) Base excision repair is efficient in cells lacking poly(ADP-ribose) polymerase 1. *Nucleic Acids Res.*, **28**, 3887-3896.
130. Berger, N.A., Sims, J.L., Catino, D.M. and Berger, S.J. (1983) Poly(ADP-ribose) polymerase mediates the suicide response to massive DNA damage: studies in normal and DNA-repair defective cells. *Princess Takamatsu Symp.*, **13**, 219-226.
131. Hassa, P.O. (2009) The molecular "Jekyll and Hyde" duality of PARP1 in cell death and cell survival. *Front. Biosci.*, **14**, 72-111.
132. David, K.K., Andrabi, S.A., Dawson, T.M. and Dawson, V.L. (2009) Parthanatos, a messenger of death. *Front. Biosci.*, **14**, 1116-1128.
133. Wang, Y., Kim, N.S., Haince, J.F., Kang, H.C., David, K.K., Andrabi, S.A., Poirier, G.G., Dawson, V.L. and Dawson, T.M. (2011) Poly(ADP-ribose) (PAR) binding to apoptosis-inducing factor is critical for PAR polymerase-1-dependent cell death (parthanatos). *Sci Signal*, **4**, ra20.

134. Kaufmann, S.H., Desnoyers, S., Ottaviano, Y., Davidson, N.E. and Poirier, G.G. (1993) Specific proteolytic cleavage of poly(ADP-ribose) polymerase: an early marker of chemotherapy-induced apoptosis. *Cancer Res.*, **53**, 3976-3985.
135. Soldani, C. and Scovassi, A.I. (2002) Poly(ADP-ribose) polymerase-1 cleavage during apoptosis: an update. *Apoptosis*, **7**, 321-328.
136. Herceg, Z. and Wang, Z.Q. (1999) Failure of poly(ADP-ribose) polymerase cleavage by caspases leads to induction of necrosis and enhanced apoptosis. *Mol. Cell. Biol.*, **19**, 5124-5133.
137. Pétrilli, V., Herceg, Z., Hassa, P.O., Patel, N.S.A., Di Paola, R., Cortes, U., Dugo, L., Filipe, H.-M., Thiemermann, C., Hottiger, M.O. *et al.* (2004) Noncleavable poly(ADP-ribose) polymerase-1 regulates the inflammation response in mice. *J. Clin. Invest.*, **114**, 1072-1081.
138. Kauppinen, T.M., Chan, W.Y., Suh, S.W., Wiggins, A.K., Huang, E.J. and Swanson, R.A. (2006) Direct phosphorylation and regulation of poly(ADP-ribose) polymerase-1 by extracellular signal-regulated kinases 1/2. *Proc. Natl. Acad. Sci. USA*, **103**, 7136-7141.
139. Zhang, S., Lin, Y., Kim, Y.S., Hande, M.P., Liu, Z.G. and Shen, H.M. (2007) c-Jun N-terminal kinase mediates hydrogen peroxide-induced cell death via sustained poly(ADP-ribose) polymerase-1 activation. *Cell Death Differ.*, **14**, 1001-1010.
140. Walker, J., Jijon, H. and Madsen, K. (2006) AMP-activated protein kinase is a positive regulator of poly(ADP-ribose) polymerase. *Biochem. Biophys. Res. Commun.*, **342**, 336-341.
141. Beckert, S., Farrahi, F., Perveen Ghani, Q., Aslam, R., Scheuenstuhl, H., Coerper, S., Konigsrainer, A., Hunt, T.K. and Hussain, M.Z. (2006) IGF-I-induced VEGF expression in HUVEC involves phosphorylation and inhibition of poly(ADP-ribose)polymerase. *Biochem. Biophys. Res. Commun.*, **341**, 67-72.
142. Hassa, P.O., Haenni, S.S., Buerki, C., Meier, N.I., Lane, W.S., Owen, H., Gersbach, M., Imhof, R. and Hottiger, M.O. (2005) Acetylation of poly(ADP-ribose) polymerase-1 by p300/CREB-binding protein regulates coactivation of NF-kappaB-dependent transcription. *J. Biol. Chem.*, **280**, 40450-40464.
143. Messner, S., Schuermann, D., Altmeyer, M., Kassner, I., Schmidt, D., Schar, P., Muller, S. and Hottiger, M.O. (2009) Sumoylation of poly(ADP-ribose) polymerase 1 inhibits its acetylation and restrains transcriptional coactivator function. *FASEB J.*, **23**, 3978-3989.
144. Martin, N., Schwamborn, K., Schreiber, V.e.r., Werner, A., Guillier, C., Zhang, X.-D., Bischof, O., Seeler, J.-S. and Dejean, A. (2009) PARP-1 transcriptional activity is regulated by sumoylation upon heat shock. *EMBO J.*, **28**, 3534-3548.
145. Bryant, H.E., Schultz, N., Thomas, H.D., Parker, K.M., Flower, D., Lopez, E., Kyle, S., Meuth, M., Curtin, N.J. and Helleday, T. (2005) Specific killing of BRCA2-deficient tumours with inhibitors of poly(ADP-ribose) polymerase. *Nature*, **434**, 913-917.
146. Farmer, H., McCabe, N., Lord, C.J., Tutt, A.N.J., Johnson, D.A., Richardson, T.B., Santarosa, M., Dillon, K.J., Hickson, I., Knights, C. *et al.* (2005) Targeting the DNA repair defect in BRCA mutant cells as a therapeutic strategy. *Nature*, **434**, 917-921.
147. Gottipati, P., Vischioni, B., Schultz, N., Solomons, J., Bryant, H.E., Djureinovic, T., Issaeva, N., Sleeth, K., Sharma, R.A. and Helleday, T. (2010) Poly(ADP-ribose) polymerase is hyperactivated in homologous recombination-defective cells. *Cancer Res.*, **70**, 5389-5398.
148. Tulin, A. (2011) Re-evaluating PARP1 inhibitor in cancer. *Nat. Biotechnol.*, **29**, 1078-1079.
149. Veuger, S.J., Hunter, J.E. and Durkacz, B.W. (2009) Ionizing radiation-induced NF-kappaB activation requires PARP-1 function to confer radioresistance. *Oncogene*, **28**, 832-842.
150. Hunter, J.E., Willmore, E., Irving, J.A., Hostomsky, Z., Veuger, S.J. and Durkacz, B.W. (2012) NF-kappaB mediates radio-sensitization by the PARP-1 inhibitor, AG-014699. *Oncogene*, **31**, 251-264.
151. Hamby, A.M., Suh, S.W., Kauppinen, T.M. and Swanson, R.A. (2007) Use of a poly(ADP-Ribose) polymerase inhibitor to suppress inflammation and neuronal death after cerebral ischemia-reperfusion. *Stroke*, **38**, 632-636.
152. Giansanti, V., Donà, F., Tillhon, M. and Scovassi, A.I. (2010) PARP inhibitors: New tools to protect from inflammation. *Biochem. Pharmacol.*, **80**, 1869-1877.
153. Javle, M. and Curtin, N.J. (2011) The role of PARP in DNA repair and its therapeutic exploitation. *Br. J. Cancer*, **105**, 1114-1122.
154. Kakimoto, Y. and Akazawa, S. (1970) Isolation and identification of N-G,N-G- and N-G,N'-G-dimethyl-arginine, N-epsilon-mono-, di-, and trimethyllysine, and glucosylgalactosyl- and galactosyl-delta-hydroxylysine from human urine. *J. Biol. Chem.*, **245**, 5751-5758.
155. Kakimoto, Y. (1971) Methylation of arginine and lysine residues of cerebral proteins. *Biochim. Biophys. Acta*, **243**, 31-37.

156. Klose, R.J. and Zhang, Y. (2007) Regulation of histone methylation by demethylimination and demethylation. *Nat. Rev. Mol. Cell Bio.*, **8**, 307-318.
157. Martin, C. and Zhang, Y. (2005) The diverse functions of histone lysine methylation. *Nat. Rev. Mol. Cell Bio.*, **6**, 838-849.
158. Jenuwein, T. and Allis, C.D. (2001) Translating the histone code. *Science*, **293**, 1074-1080.
159. Kim, J., Daniel, J., Espejo, A., Lake, A., Krishna, M., Xia, L., Zhang, Y. and Bedford, M.T. (2006) Tudor, MBT and chromo domains gauge the degree of lysine methylation. *EMBO Rep.*, **7**, 397-403.
160. Seet, B.T., Dikic, I., Zhou, M.-M. and Pawson, T. (2006) Reading protein modifications with interaction domains. *Nat. Rev. Mol. Cell Bio.*, **7**, 473-483.
161. Selhub, J. (1999) Homocysteine metabolism. *Annu. Rev. Nutr.*, **19**, 217-246.
162. Lake, A.N. and Bedford, M.T. (2007) Protein methylation and DNA repair. *Mut. Res.*, **618**, 91-101.
163. Jenuwein, T., Laible, G., Dorn, R. and Reuter, G. (1998) SET domain proteins modulate chromatin domains in eu- and heterochromatin. *Cell. Mol. Life Sci.*, **54**, 80-93.
164. Dillon, S.C., Zhang, X., Trievel, R.C. and Cheng, X. (2005) The SET-domain protein superfamily: protein lysine methyltransferases. *Genome Biol.*, **6**, 227.
165. Qian, C. and Zhou, M.-M. (2006) SET domain protein lysine methyltransferases: Structure, specificity and catalysis. *Cell. Mol. Life Sci.*, **63**, 2755-2763.
166. Feng, Q., Wang, H., Ng, H.H., Erdjument-Bromage, H., Tempst, P., Struhl, K. and Zhang, Y. (2002) Methylation of H3-lysine 79 is mediated by a new family of HMTases without a SET domain. *Curr. biol.*, **12**, 1052-1058.
167. Tschiersch, B., Hofmann, A., Krauss, V., Dorn, R., Korge, G. and Reuter, G. (1994) The protein encoded by the Drosophila position-effect variegation suppressor gene Su(var)3-9 combines domains of antagonistic regulators of homeotic gene complexes. *EMBO J.*, **13**, 3822-3831.
168. Jones, R.S. and Gelbart, W.M. (1993) The Drosophila Polycomb-group gene Enhancer of zeste contains a region with sequence similarity to trithorax. *Mol. Cell. Biol.*, **13**, 6357-6366.
169. Stassen, M.J., Bailey, D., Nelson, S., Chinwalla, V. and Harte, P.J. (1995) The Drosophila trithorax proteins contain a novel variant of the nuclear receptor type DNA binding domain and an ancient conserved motif found in other chromosomal proteins. *Mech. Dev.*, **52**, 209-223.
170. Schubert, H.L., Blumenthal, R.M. and Cheng, X. (2003) Many paths to methyltransfer: a chronicle of convergence. *Trends Biochem. Sci.*, **28**, 329-335.
171. Taylor, W.R., Xiao, B., Gamblin, S.J. and Lin, K. (2003) A knot or not a knot? SETting the record 'straight' on proteins. *Comput. Biol. Chem.*, **27**, 11-15.
172. Wilson, J.R., Jing, C., Walker, P.A., Martin, S.R., Howell, S.A., Blackburn, G.M., Gamblin, S.J. and Xiao, B. (2002) Crystal structure and functional analysis of the histone methyltransferase SET7/9. *Cell*, **111**, 105-115.
173. Trievel, R.C., Beach, B.M., Dirk, L.M., Houtz, R.L. and Hurley, J.H. (2002) Structure and catalytic mechanism of a SET domain protein methyltransferase. *Cell*, **111**, 91-103.
174. Zhang, X., Tamaru, H., Khan, S.I., Horton, J.R., Keefe, L.J., Selker, E.U. and Cheng, X. (2002) Structure of the Neurospora SET domain protein DIM-5, a histone H3 lysine methyltransferase. *Cell*, **111**, 117-127.
175. Xiao, B., Jing, C., Wilson, J.R., Walker, P.A., Vasisht, N., Kelly, G., Howell, S., Taylor, I.A., Blackburn, G.M. and Gamblin, S.J. (2003) Structure and catalytic mechanism of the human histone methyltransferase SET7/9. *Nature*, **421**, 652-656.
176. Trievel, R.C., Flynn, E.M., Houtz, R.L. and Hurley, J.H. (2003) Mechanism of multiple lysine methylation by the SET domain enzyme Rubisco LSMT. *Nat. Struct. Biol.*, **10**, 545-552.
177. Couture, J.-F., Collazo, E., Hauk, G. and Trievel, R.C. (2006) Structural basis for the methylation site specificity of SET7/9. *Nat. Struct. Mol. Biol.*, **13**, 140-146.
178. Couture, J.F., Collazo, E., Brunzelle, J.S. and Trievel, R.C. (2005) Structural and functional analysis of SET8, a histone H4 Lys-20 methyltransferase. *Genes Dev.*, **19**, 1455-1465.
179. Qian, C., Wang, X., Manzur, K., Sachchidanand, Farooq, A., Zeng, L., Wang, R. and Zhou, M.M. (2006) Structural insights of the specificity and catalysis of a viral histone H3 lysine 27 methyltransferase. *J. Mol. Biol.*, **359**, 86-96.
180. Zhang, X., Yang, Z., Khan, S.I., Horton, J.R., Tamaru, H., Selker, E.U. and Cheng, X. (2003) Structural basis for the product specificity of histone lysine methyltransferases. *Mol. Cell*, **12**, 177-185.

181. Schultz, J., Milpetz, F., Bork, P. and Ponting, C.P. (1998) SMART, a simple modular architecture research tool: identification of signaling domains. *Proc. Natl. Acad. Sci. USA*, **95**, 5857-5864.
182. Wang, H., Cao, R., Xia, L., Erdjument-Bromage, H., Borchers, C., Tempst, P. and Zhang, Y. (2001) Purification and functional characterization of a histone H3-lysine 4-specific methyltransferase. *Mol. Cell*, **8**, 1207-1217.
183. Nishioka, K., Chuikov, S., Sarma, K., Erdjument-Bromage, H., Allis, C.D., Tempst, P. and Reinberg, D. (2002) Set9, a novel histone H3 methyltransferase that facilitates transcription by precluding histone tail modifications required for heterochromatin formation. *Genes Dev.*, **16**, 479-489.
184. Li, Y., Reddy, M.A., Miao, F., Shanmugam, N., Yee, J.-K., Hawkins, D., Ren, B. and Natarajan, R. (2008) Role of the histone H3 lysine 4 methyltransferase, SET7/9, in the regulation of NF-kappaB-dependent inflammatory genes. Relevance to diabetes and inflammation. *J. Biol. Chem.*, **283**, 26771-26781.
185. Deering, T.G., Ogihara, T., Trace, A.P., Maier, B. and Mirmira, R.G. (2009) Methyltransferase Set7/9 maintains transcription and euchromatin structure at islet-enriched genes. *Diabetes*, **58**, 185-193.
186. Brasacchio, D., Okabe, J., Tikellis, C., Balcerczyk, A., George, P., Baker, E.K., Calkin, A.C., Brownlee, M., Cooper, M.E. and El-Osta, A. (2009) Hyperglycemia induces a dynamic cooperativity of histone methylase and demethylase enzymes associated with gene-activating epigenetic marks that coexist on the lysine tail. *Diabetes*, **58**, 1229-1236.
187. Lehnertz, B., Rogalski, Jason C., Schulze, Felix M., Yi, L., Lin, S., Kast, J. and Rossi, Fabio M.V. (2011) p53-dependent transcription and tumor suppression are not affected in Set7/9-deficient mice. *Mol. Cell*, **43**, 673-680.
188. Jacobs, S.A., Harp, J.M., Devarakonda, S., Kim, Y., Rastinejad, F. and Khorasanizadeh, S. (2002) The active site of the SET domain is constructed on a knot. *Nat. Struct. Biol.*, **9**, 833-838.
189. Kwon, T., Chang, J.H., Kwak, E., Lee, C.W., Joachimiak, A., Kim, Y.C., Lee, J. and Cho, Y. (2003) Mechanism of histone lysine methyl transfer revealed by the structure of SET7/9-AdoMet. *EMBO J.*, **22**, 292-303.
190. Kouskouti, A., Scheer, E., Staub, A., Tora, L. and Talianidis, I. (2004) Gene-specific modulation of TAF10 function by SET9-mediated methylation. *Mol. Cell*, **14**, 175-182.
191. Dhayalan, A., Kudithipudi, S., Rathert, P. and Jeltsch, A. (2011) Specificity analysis-based identification of new methylation targets of the SET7/9 protein lysine methyltransferase. *Chem. Biol.*, **18**, 111-120.
192. Yang, J., Huang, J., Dasgupta, M., Sears, N., Miyagi, M., Wang, B., Chance, M.R., Chen, X., Du, Y., Wang, Y. *et al.* (2010) Reversible methylation of promoter-bound STAT3 by histone-modifying enzymes. *Proc. Natl. Acad. Sci. USA*, **107**, 21499-21504.
193. Chuikov, S., Kurash, J.K., Wilson, J.R., Xiao, B., Justin, N., Ivanov, G.S., McKinney, K., Tempst, P., Prives, C., Gamblin, S.J. *et al.* (2004) Regulation of p53 activity through lysine methylation. *Nature*, **432**, 353-360.
194. Ivanov, G.S., Ivanova, T., Kurash, J., Ivanov, A., Chuikov, S., Gizatullin, F., Herrera-Medina, E.M., Rauscher, F., Reinberg, D. and Barlev, N.A. (2007) Methylation-acetylation interplay activates p53 in response to DNA damage. *Mol. Cell. Biol.*, **27**, 6756-6769.
195. Kurash, J.K., Lei, H., Shen, Q., Marston, W.L., Granda, B.W., Fan, H., Wall, D., Li, E. and Gaudet, F. (2008) Methylation of p53 by Set7/9 mediates p53 acetylation and activity in vivo. *Mol. Cell*, **29**, 392-400.
196. Campaner, S., Spreafico, F., Burgold, T., Doni, M., Rosato, U., Amati, B. and Testa, G. (2011) The methyltransferase Set7/9 (Setd7) is dispensable for the p53-mediated DNA damage response in vivo. *Mol. Cell*, **43**, 681-688.
197. Subramanian, K., Jia, D., Kapoor-Vazirani, P., Powell, D.R., Collins, R.E., Sharma, D., Peng, J., Cheng, X. and Vertino, P.M. (2008) Regulation of estrogen receptor alpha by the SET7 lysine methyltransferase. *Mol. Cell*, **30**, 336-347.
198. Estève, P.-O., Chin, H.G., Benner, J., Feehery, G.R., Samaranayake, M., Horwitz, G.A., Jacobsen, S.E. and Pradhan, S. (2009) Regulation of DNMT1 stability through SET7-mediated lysine methylation in mammalian cells. *Proc. Natl. Acad. Sci. USA*, **106**, 5076-5081.
199. Yang, X.-D., Huang, B., Li, M., Lamb, A., Kelleher, N.L. and Chen, L.-F. (2009) Negative regulation of NF-kappaB action by Set9-mediated lysine methylation of the RelA subunit. *EMBO J.*, **28**, 1055-1066.

200. Ea, C.-K. and Baltimore, D. (2009) Regulation of NF-kappaB activity through lysine monomethylation of p65. *Proc. Natl. Acad. Sci. USA*, **106**, 18972-18977.
201. Munro, S., Khaire, N., Inche, A., Carr, S. and La Thangue, N.B. (2010) Lysine methylation regulates the pRb tumour suppressor protein. *Oncogene*, **29**, 2357-2367.
202. Carr, S.M., Munro, S., Kessler, B., Oppermann, U. and Thangue, N.B.L. (2010) Interplay between lysine methylation and Cdk phosphorylation in growth control by the retinoblastoma protein. *EMBO J.*, **30**, 317-327.
203. Kontaki, H. and Talianidis, I. (2010) Lysine methylation regulates E2F1-induced cell death. *Mol. Cell*, **39**, 152-160.
204. Gaughan, L., Stockley, J., Wang, N., McCracken, S.R., Treumann, A., Armstrong, K., Shaheen, F., Watt, K., McEwan, I.J., Wang, C. *et al.* (2011) Regulation of the androgen receptor by SET9-mediated methylation. *Nucleic Acids Res.*, **39**, 1266-1279.
205. Bannister, A.J. and Kouzarides, T. (2005) Reversing histone methylation. *Nature*, **436**, 1103-1106.
206. Wang, Y., Wysocka, J., Sayegh, J., Lee, Y.H., Perlin, J.R., Leonelli, L., Sonbuchner, L.S., McDonald, C.H., Cook, R.G., Dou, Y. *et al.* (2004) Human PAD4 regulates histone arginine methylation levels via demethylimination. *Science*, **306**, 279-283.
207. Cuthbert, G.L., Daujat, S., Snowden, A.W., Erdjument-Bromage, H., Hagiwara, T., Yamada, M., Schneider, R., Gregory, P.D., Tempst, P., Bannister, A.J. *et al.* (2004) Histone deimination antagonizes arginine methylation. *Cell*, **118**, 545-553.
208. Mosammaparast, N. and Shi, Y. (2010) Reversal of histone methylation: biochemical and molecular mechanisms of histone demethylases. *Annu. Rev. Biochem.*, **79**, 155-179.
209. Shi, Y., Lan, F., Matson, C., Mulligan, P., Whetstine, J.R., Cole, P.A. and Casero, R.A. (2004) Histone demethylation mediated by the nuclear amine oxidase homolog LSD1. *Cell*, **119**, 941-953.
210. Karytinos, A., Forneris, F., Profumo, A., Ciossani, G., Battaglioli, E., Binda, C. and Mattevi, A. (2009) A novel mammalian flavin-dependent histone demethylase. *J. Biol. Chem.*, **284**, 17775-17782.
211. Tsukada, Y., Fang, J., Erdjument-Bromage, H., Warren, M.E., Borchers, C.H., Tempst, P. and Zhang, Y. (2006) Histone demethylation by a family of JmjC domain-containing proteins. *Nature*, **439**, 811-816.
212. Shi, Y.J., Matson, C., Lan, F., Iwase, S., Baba, T. and Shi, Y. (2005) Regulation of LSD1 histone demethylase activity by its associated factors. *Mol. Cell*, **19**, 857-864.
213. Lee, M.G., Wynder, C., Cooch, N. and Shiekhattar, R. (2005) An essential role for CoREST in nucleosomal histone 3 lysine 4 demethylation. *Nature*, **437**, 432-435.
214. Metzger, E., Wissmann, M., Yin, N., Muller, J.M., Schneider, R., Peters, A.H., Gunther, T., Buettner, R. and Schule, R. (2005) LSD1 demethylates repressive histone marks to promote androgen-receptor-dependent transcription. *Nature*, **437**, 436-439.
215. Huang, J., Sengupta, R., Espejo, A.B., Lee, M.G., Dorsey, J.A., Richter, M., Opravil, S., Shiekhattar, R., Bedford, M.T., Jenuwein, T. *et al.* (2007) p53 is regulated by the lysine demethylase LSD1. *Nature*, **449**, 105-108.
216. Wang, J., Hevi, S., Kurash, J.K., Lei, H., Gay, F., Bajko, J., Su, H., Sun, W., Chang, H., Xu, G. *et al.* (2009) The lysine demethylase LSD1 (KDM1) is required for maintenance of global DNA methylation. *Nat. Genet.*, **41**, 125-129.
217. Spannhoff, A., Hauser, A.-T., Heinke, R., Sippl, W. and Jung, M. (2009) The emerging therapeutic potential of histone methyltransferase and demethylase inhibitors. *ChemMedChem*, **4**, 1568-1582.
218. Greiner, D., Bonaldi, T., Eskeland, R., Roemer, E. and Imhof, A. (2005) Identification of a specific inhibitor of the histone methyltransferase SU(VAR)3-9. *Nat. Chem. Biol.*, **1**, 143-145.
219. Mori, S., Iwase, K., Iwanami, N., Tanaka, Y., Kagechika, H. and Hirano, T. (2010) Development of novel bisubstrate-type inhibitors of histone methyltransferase SET7/9. *Bioorg. Med. Chem.*, **18**, 8158-8166.
220. Lee, M.G., Wynder, C., Schmidt, D.M., McCafferty, D.G. and Shiekhattar, R. (2006) Histone H3 lysine 4 demethylation is a target of nonselective antidepressive medications. *Chem. Biol.*, **13**, 563-567.
221. Yang, M., Culhane, J.C., Szewczuk, L.M., Jalili, P., Ball, H.L., Machius, M., Cole, P.A. and Yu, H. (2007) Structural basis for the inhibition of the LSD1 histone demethylase by the antidepressant trans-2-phenylcyclopropylamine. *Biochemistry (Mosc).* **46**, 8058-8065.

222. Trautlein, D., Deibler, M., Leitenstorfer, A. and Ferrando-May, E. (2010) Specific local induction of DNA strand breaks by infrared multi-photon absorption. *Nucleic Acids Res.*, **38**, e14.
223. Clement, F.C., Kaczmarek, N., Mathieu, N., Tomas, M., Leitenstorfer, A., Ferrando-May, E. and Naegeli, H. (2011) Dissection of the xeroderma pigmentosum group C protein function by site-directed mutagenesis. *Antioxid. Redox. Signal.*, **14**, 2479-2490.
224. Kun, E., Kirsten, E., Mendeleyev, J. and Ordahl, C.P. (2004) Regulation of the enzymatic catalysis of poly(ADP-ribose) polymerase by dsDNA, polyamines, Mg2+, Ca2+, histones H1 and H3, and ATP. *Biochemistry (Mosc)*. **43**, 210-216.
225. Fang, R., Barbera, A.J., Xu, Y., Rutenberg, M., Leonor, T., Bi, Q., Lan, F., Mei, P., Yuan, G.-C. and Lian, C. (2010) Human LSD2/KDM1b/AOF1 regulates gene transcription by modulating intragenic H3K4me2 methylation. *Mol. Cell*, **39**, 222-233.
226. Hassa, P.O. and Hottiger, M.O. (2002) The functional role of poly(ADP-ribose)polymerase 1 as novel coactivator of NF-kappaB in inflammatory disorders. *Cell. Mol. Life Sci.*, **59**, 1534-1553.
227. Scheidereit, C. (2006) IkappaB kinase complexes: gateways to NF-kappaB activation and transcription. *Oncogene*, **25**, 6685-6705.
228. Solt, L.A. and May, M.J. (2008) The IkappaB kinase complex: master regulator of NF-kappaB signaling. *Immunol. Res.*, **42**, 3-18.
229. Janssens, S. and Tschopp, J. (2006) Signals from within: the DNA-damage-induced NF-kappaB response. *Cell Death Differ.*, **13**, 773-784.
230. Wu, Z.-H. and Miyamoto, S. (2007) Many faces of NF-kappaB signaling induced by genotoxic stress. *J. Mol. Med.*, **85**, 1187-1202.
231. Habraken, Y. and Piette, J. (2006) NF-kappaB activation by double-strand breaks. *Biochem. Pharmacol.*, **72**, 1132-1141.
232. Dutta, J., Fan, Y., Gupta, N., Fan, G. and Gélinas, C. (2006) Current insights into the regulation of programmed cell death by NF-kappaB. *Oncogene*, **25**, 6800-6816.
233. Rashi-Elkeles, S., Elkon, R., Weizman, N., Linhart, C., Amariglio, N., Sternberg, G., Rechavi, G., Barzilai, A., Shamir, R. and Shiloh, Y. (2006) Parallel induction of ATM-dependent pro- and antiapoptotic signals in response to ionizing radiation in murine lymphoid tissue. *Oncogene*, **25**, 1584-1592.
234. Stilmann, M., Hinz, M., Arslan, S.Ç., Zimmer, A., Schreiber, V. and Scheidereit, C. (2009) A nuclear poly(ADP-ribose)-dependent signalosome confers DNA damage-induced IκB kinase activation. *Mol. Cell*, **36**, 365-378.
235. Hinz, M., Stilmann, M., Arslan, S.Ç., Khanna, K.K., Dittmar, G. and Scheidereit, C. (2010) A cytoplasmic ATM-TRAF6-cIAP1 module links nuclear DNA damage signaling to ubiquitin-mediated NF-kappaB activation. *Mol. Cell*, **40**, 63-74.
236. Milam, K.M., Thomas, G.H. and Cleaver, J.E. (1986) Disturbances in DNA precursor metabolism associated with exposure to an inhibitor of poly(ADP-ribose) synthetase. *Exp. Cell Res.*, **165**, 260-268.
237. Eriksson, C., Busk, L. and Brittebo, E.B. (1996) 3-Aminobenzamide: effects on cytochrome P450-dependent metabolism of chemicals and on the toxicity of dichlobenil in the olfactory mucosa. *Toxicol. Appl. Pharmacol.*, **136**, 324-331.
238. Canto, C., Gerhart-Hines, Z., Feige, J.N., Lagouge, M., Noriega, L., Milne, J.C., Elliott, P.J., Puigserver, P. and Auwerx, J. (2009) AMPK regulates energy expenditure by modulating NAD+ metabolism and SIRT1 activity. *Nature*, **458**, 1056-1060.
239. Jardine, L.J. (2004) Identification of senescence in cancer cells. *Methods Mol. Med.*, **88**, 231-238.
240. Chatterjee, S., Hirschler, N.V., Petzold, S.J., Berger, S.J. and Berger, N.A. (1989) Mutant cells defective in poly(ADP-ribose) synthesis due to stable alterations in enzyme activity or substrate availability. *Exp. Cell Res.*, **184**, 1-15.
241. Yoshihara, K., Itaya, A., Hironaka, T., Sakuramoto, S., Tanaka, Y., Tsuyuki, M., Inada, Y., Kamiya, T., Ohnishi, K. and Honma, M. (1992) Poly(ADP ribose) polymerase-defective mutant cell clone of mouse L1210 cells. *Exp. Cell Res.*, **200**, 126-134.
242. Küpper, J.H., de Murcia, G. and Bürkle, A. (1990) Inhibition of poly(ADP-ribosyl)ation by overexpressing the poly(ADP-ribose) polymerase DNA-binding domain in mammalian cells. *J. Biol. Chem.*, **265**, 18721-18724.
243. Witmer, M.V., Aboul-Ela, N., Jacobson, M.K. and Stamato, T.D. (1994) Increased sensitivity to DNA-alkylating agents in CHO mutants with decreased poly(ADP-ribose) polymerase activity. *Mutat. Res.*, **314**, 249-260.

244. Schreiber, V., Hunting, D., Trucco, C., Gowans, B., Grunwald, D., De Murcia, G. and De Murcia, J.M. (1995) A dominant-negative mutant of human poly(ADP-ribose) polymerase affects cell recovery, apoptosis, and sister chromatid exchange following DNA damage. *Proc. Natl. Acad. Sci. USA*, **92**, 4753-4757.
245. Kupper, J.H., Müller, M. and Bürkle, A. (1996) Trans-dominant inhibition of poly(ADP-ribosyl)ation potentiates carcinogen induced gene amplification in SV40-transformed Chinese hamster cells. *Cancer Res.*, **56**, 2715-2717.
246. Todaro, G.J. and Green, H. (1963) Quantitative studies of the growth of mouse embryo cells in culture and their development into established lines. *J. Cell Biol.*, **17**, 299-313.
247. Zufferey, R., Nagy, D., Mandel, R.J., Naldini, L. and Trono, D. (1997) Multiply attenuated lentiviral vector achieves efficient gene delivery in vivo. *Nat. Biotechnol.*, **15**, 871-875.
248. Pfaffl, M.W., Horgan, G.W. and Dempfle, L. (2002) Relative expression software tool (REST) for group-wise comparison and statistical analysis of relative expression results in real-time PCR. *Nucleic Acids Res.*, **30**, e36.
249. Loor, G., Kondapalli, J., Schriewer, J.M., Chandel, N.S., Vanden Hoek, T.L. and Schumacker, P.T. (2010) Menadione triggers cell death through ROS-dependent mechanisms involving PARP activation without requiring apoptosis. *Free Radic. Biol. Med.*, **49**, 1925-1936.
250. Chiu, L.-Y., Ho, F.-M., Shiah, S.-G., Chang, Y. and Lin, W.-W. (2011) Oxidative stress initiates DNA damager MNNG-induced poly(ADP-ribose)polymerase-1-dependent parthanatos cell death. *Biochem. Pharmacol.*, **81**, 459-470.
251. Qin, X.-J., Liu, W., Li, Y.-N., Sun, X., Hai, C.-X., Hudson, L.G. and Liu, K.J. (2012) Poly(ADP-ribose) polymerase-1 inhibition by arsenite promotes the survival of cells with unrepaired DNA lesions induced by UV exposure. *Toxicol. Sci*.
252. Lu, S.C. and Mato, J.M. (2008) S-Adenosylmethionine in cell growth, apoptosis and liver cancer. *J. Gastroenterol. Hepatol.*, **23 Suppl 1**, S73-77.
253. Grillo, M.A. and Colombatto, S. (2008) S-adenosylmethionine and its products. *Amino Acids*, **34**, 187-193.
254. Luo, J. and Kuo, M.-H. (2009) Linking nutrient metabolism to epigenetics. *Cell Science Reviews*, 6, 49-54.
255. Mendoza-Alvarez, H. and Alvarez-Gonzalez, R. (2004) The 40 kDa carboxy-terminal domain of poly(ADP-ribose) polymerase-1 forms catalytically competent homo- and heterodimers in the absence of DNA. *J. Mol. Biol.*, **336**, 105-114.
256. Pion, E., Ullmann, G.M., Amé, J.-C., Gérard, D., de Murcia, G. and Bombarda, E. (2005) DNA-induced dimerization of poly(ADP-ribose) polymerase-1 triggers its activation. *Biochemistry (Mosc)*. **44**, 14670-14681.
257. Quenet, D., Gasser, V., Fouillen, L., Cammas, F., Sanglier-Cianferani, S., Losson, R. and Dantzer, F. (2008) The histone subcode: poly(ADP-ribose) polymerase-1 (Parp-1) and Parp-2 control cell differentiation by regulating the transcriptional intermediary factor TIF1 and the heterochromatin protein HP1 *FASEB J.*, **22**, 3853-3865.
258. Hornbeck, P.V., Kornhauser, J.M., Tkachev, S., Zhang, B., Skrzypek, E., Murray, B., Latham, V. and Sullivan, M. (2012) PhosphoSitePlus: a comprehensive resource for investigating the structure and function of experimentally determined post-translational modifications in man and mouse. *Nucleic Acids Res.*, **40**, D261-270.
259. Hergeth, S.P., Dundr, M., Tropberger, P., Zee, B.M., Garcia, B.A., Daujat, S. and Schneider, R. (2011) Isoform-specific phosphorylation of human linker histone H1.4 in mitosis by the kinase Aurora B. *J. Cell Sci.*, **124**, 1623-1628.
260. Okabe, J., Orlowski, C., Balcerczyk, A., Tikellis, C., Thomas, M.C., Cooper, M.E. and El-Osta, A. (2012) Distinguishing hyperglycemic changes by Set7 in vascular endothelial cells. *Circ. Res.*
261. Messner, S., Altmeyer, M., Zhao, H., Pozivil, A., Roschitzki, B., Gehrig, P., Rutishauser, D., Huang, D., Caflisch, A. and Hottiger, M.O. (2010) PARP1 ADP-ribosylates lysine residues of the core histone tails. *Nucleic Acids Res.*, **38**, 6350-6362.
262. Crooks, G.E., Hon, G., Chandonia, J.M. and Brenner, S.E. (2004) WebLogo: a sequence logo generator. *Genome Res.*, **14**, 1188-1190.

CURRICULUM VITAE

Personal Information

Name:	KASSNER
Surname:	Ingrid
Address:	Nötzlistrasse 1, CH-8049 Zürich
	Phone: +41-76-2706974
Email:	kassner@vetbio.uzh.ch
Date of birth:	May 11, 1983
Place of birth:	Düsseldorf, Germany
Nationality:	German

Education

May 2008 – present Doctoral Studies in Molecular Biology

- Institute of Veterinary Biochemistry and Molecular Biology, University of Zurich, Switzerland
- Ph.D. Program in Molecular Life Sciences/LSZGS
- Thesis Title: Regulation of ARTD1 by SET7/9-dependent Methylation
- Degree: Dr. sc. nat.

Aug. 2005 – Apr. 2006 Exchange year in Canada

- McMaster University, Hamilton, CA

Oct. 2002 – Oct. 2007 Academic Studies

- University of Konstanz
- Field of Study: Biology
- Degree: Diplom (October 5, 2007)

Aug. 1993 – May 2002 Secondary School

- Gymnasium Nepomucenum, Coesfeld
- Degree: Allgemeine Hochschulreife

List of Publications

I. Kassner, M. Fey, M. Tomas, E. Ferrando-May, and M. O. Hottiger. Set7/9-dependent methylation of ARTD1 at K508 enhances poly-ADP-ribose formation. *Manuscript submitted*

S. Erener, V. Pétrilli, I. Kassner, R. Minotti, R. Castillo, R. Santoro, P. O. Hassa, J. Tschopp, and M. O. Hottiger. 2012. Inflammasome-Activated Caspase 7 Cleaves PARP1 to Enhance the Expression of a Subset of NF-κB Target Genes. *Mol Cell*

S. Messner, D. Schuermann, M. Altmeyer, I. Kassner, D. Schmidt, P. Schär, S. Müller, and M. O. Hottiger. 2009. Sumoylation of poly(ADP-ribose) polymerase 1 inhibits its acetylation and restrains transcriptional coactivator function. *FASEB J*

C. Pelzer, I. Kassner, K. Matentzoglu, R. K. Singh, H. P. Wollscheid, M. Scheffner, G. Schmidtke, and M. Groettrup. 2007. UBE1L2, a novel E1 enzyme specific for ubiquitin. *J Biol Chem*

ACKNOWLEDGEMENTS

First of all, I would like to thank my supervisor, Prof. Michael O. Hottiger, for his continuous support and motivation throughout my thesis, for the tremendous amount of time he invests in running the lab and for our nice group events.

I would also like to thank my PhD thesis committee members Prof. A. Bürkle, Prof. M. Peter and Prof. P. Schär for their support during my PhD studies, the stimulating discussions and helpful suggestions during our committee meetings and all the trips to the Irchel Campus in Zürich. Furthermore, I would like to thank Prof. B. Lüscher for agreeing to review this thesis.

A big thank goes to all present and former members of the Hottiger lab and Raffa's group, who have made my PhD life much more agreeable. Thank you for many helpful discussions, for keeping up my spirits and for the nice company during lunch breaks!

Especially I would like to thank Karo and Süheda, who accompanied me during most of my PhD, helped whenever they could and shared many laughs. Special thanks goes to Moni, for her open ear to our daily concerns, her patience and encouragement, and to Marc, who was a great master student and helped me a lot with the H1 story. Furthermore, I thank Florian Freimoser for the work he spend on the manuscripts as well as on correcting my thesis. I would also like to thank the whole IVBMB and CABMM for their scientific advice, the nice working atmosphere, the institute events and coffee breaks.

I also thank my collaborators in the Functional Genomics Center Zurich (especially Peter Hunziker) and the Bioimaging Center Konstanz (especially Martin).

The most important people in my life are Jochen and my family. My parents, my sister Ruth and my brothers Norbert and Gunther had to cope with my endless questions as soon as could speak (and my lab mates know of what I am talking…). Thank you for your unconditional support, love and trust in me. Thank you, Jochen, for giving me a home in Zürich, for making the time outside the lab so valuable and for the supply of delicious food ☺. It is the greatest gift to have you around!